The influence of calcineurin inhibitors on renal medullary microcirculation: a novel approach to nephrotoxicity

Mark Christopher Kelly

A thesis in partial fulfilment of the requirements of the University of Kent and the University of Greenwich for the degree of Doctor of Philosophy

Department of Biological Sciences
Medway School of Pharmacy
Universities of Kent and Greenwich
2015

Declaration

I certify that this work has not been accepted in substance for any degree, and is not concurrently being submitted for any degree other than that of Doctor of Philosophy being studied at the Universities of Greenwich and Kent. I also declare that this work is the result of my own investigations except where otherwise identified by references and that I have not plagiarised the work of others.

September 2015

To my family

Acknowledgements

First and foremost, I would like to thank the dynamic duo of my supervisors Dr Scott Wildman and Dr Claire Peppiatt-Wildman for their invaluable guidance, advice and support throughout my PhD. It's been a hell of a ride and I have them to thank for the initial opportunity and many that have arisen from this journey!

Thank you to all my "lab chums" in the Urinary Systems Physiology Unit, at MSOP. Both past and present members have made this experience truly enjoyable and without their support, the journey from day one would not have been the same.

Last but never least, I will be forever grateful to all my family and friends for their encouragement, support and patience throughout this experience.

Abstract

The calcineurin inhibitors (CNIs), cyclosporine A (CsA) and tacrolimus (FK506), have revolutionized solid organ transplantation with their unprecedented ability to increase graft and patient survival. However, they have a plethora of unwanted side effects, of which nephrotoxicity is predominant. Renal cortical blood flow is majorly suppressed with administration of CsA and FK506, however the impact of these drugs on medullary blood flow is still unclear.
It was previously thought that renal medullary blood flow (RMBF) was regulated upstream by the larger arterioles of the cortex, however new evidence suggests that a local regulation of blood flow exist and is partially controlled through the vasoconstriction of renal pericytes on descending vasa recta (DVR) capillaries. Renal pericytes have been shown to contract and/or dilate in response to a variety of endogenous and exogenous factors suggesting they have the ability to locally regulate RMBF and respond accordingly after insult or in stress situations.

The first chapter of this thesis demonstrates the ability of CNIs to induce pericyte-mediated vasoconstriction of DVR. A significant decrease of DVR diameter likely results in decreased blood flow *in vivo* and contributes to increased ischemia. Furthermore, an alternative immunosuppressant, rapamycin, a mammalian target of rapamycin inhibitor (mTOR-i) failed to induce any significant vasoconstriction.

The following chapter investigates the use of antihypertensives in combination with CNIs and highlights a mechanism for their potential beneficial use in combating the progression of CNI-induced hypertension and nephrotoxicity.

The third results chapter sets out to establish a perfusion method for DVR *in situ*. The results demonstrate the feasibility of *in situ* perfusion within the established live kidney slice model, and also the impact of perfused CNIs on the vasoconstriction of vasa recta as defined in chapter 1. The data presented here further demonstrates how CNIs may augment the known nephrotoxic effect but, also how they may instigate medullary ischemia.

The final results chapter emphasises how the generation of reactive oxygen species (ROS) induced by CNIs could be a foremost mechanism in pericyte-mediated vasoconstriction of DVR. In addition, prevention of ROS production, rather than it's scavenging, could be an enhanced approach for the inhibition of CNI induced renal damage and nephrotoxicity.

Taken together, the data presented here suggests a role of RMBF in the pathogenesis of CNI nephrotoxicity. Given that our understanding of RMBF is only now coming to light, its role in many disease states, including CNI nephrotoxicity, may have a greater impact than previously assumed and potentially offer a novel therapeutic approach for the prevention of renal decline.

Table of Contents

Figures

Tables

Abbreviations

AA	Afferent arteriole
A.A	Arachidonic acid
ACE	Angiotensin-converting enzyme
ACEi	ACE inhibitor
Ach	Acetylcholine
ADP	Adeonsie diphospahte
AIF	Apoptosis-inducting-factor
AIN	Acute interstitial nephritis
ANG II	Angiotensin II
ANT	Adenine nucleotide translocator
ARB	ANG II receptor blockers
ARI	Angiotensin II receptor inhibitors
ATN	Acute tubular necrosis
ATP	Adenosine triphosphate
AT1	Angiotensin receptor 1
AUC	Area under the curve
AV	Arterial-venous
AVP	Vasopressin
AVR	Ascending vasa recta
AQP	Aquaporin
αSMA	α-Smooth muscle actin
Bax	BAX apoptosis regulator
BF	Blood flow
BH4	Tetrahydrobiopterin
BP	Blood pressure
Ca^{2+}	Calcium
CaCL2	Calcium Chloride
cAMP	Cyclic adenosine monophosphate
CBB	Channel blockers
CCB	Calcium channel blockers
CCD	Charged coupled device
CDCA	Chenodeoxycholate
cGMP	Cyclic guanosine monophosphate
CKD	Chronic kidney disease
CL_{ca}	Calcium activate chloride channels
Cmax	Concentration max
CNIs	Calcineurin inhibitors
COX	Cyclooxygenase
CsA	Cyclosporine A
CyD	Cyclophiln D
CYP 450	Cytochrome P450
C0	Drug trough concentration
C02	Carbon dioxide
DCT	Distal convoluted tubule
DHCL	Diltiazem hydrochloride
DHE	Dihydroethidum
DIC	Differential interference contrast
DMSO	Dimethyl sulfoxide
DVR	Descending vasa recta

E-Cadherin	Epithelial cadherin
EC	Endothelial cells
ECM	Extracellular matrix
EMT	Epithelial to mesenchymal transition
ENaC	Epithelial sodium channel
eNOS	Endothelial NOS
ER	Endoplasmic reticulum
ET	Endothelin
FAD	Flavin adenine dinucleotide
FCCP	Carbonyl cyanide-*p*-trifluoromethoxyphenylhydrazone
FDA	Food & Drugs administration
FGFR2	Fibroblast-growth-factor receptor-2
FK506	Tacrolimus
FKBP12	FK506 biding protein 12
FSFS	Focal segmental glomerulosclerosis
FSP1	Fibroblast-specific protein-1
GFR	Glomerular filtration rate
GN	Glomerulonephritis
GPX	Gluthione peroxidase
GVH	Graft versus host
GVHD	Graft-versus-host disease
H_2O_2	Hydrogen peroxide
HCT	Hydrochlorothiazide
HSP70	Heat shock protein 70
HUS	Haemolytic uremic syndrome
IB4	Isolectin B4
IMM	Inner mitochondrial membrane
IL-	Interleukin
IL-R	Interleukin receptor
iNOS	inducible NOS
K^+	Potassium
KCL	Potassium chloride
MBF	Medullary blood flow
MDR1	Multidrug resistance protein 1
MET	Mesenchymal-epithelial transition
MFs	Microfilaments
MgSO4	Magnesium sulphate
MLC	Myosin light chain
MLP	Myeloperoxidase
MMF	Mycophenolate mofetil
MMT	Mitochondrial membrane transition
MPM	Multiphoton microscopy
MPT	Mitochondrial permeability transition
MPTP	Mitochondrial permeability transition pore
MRP	Multidrug resistance protein
mTOR	Mammalian target or rapamycin
mTOr-I	mTOR inhibitor
Na^+/K^+-ATP	Sodium/potassium ATPase
NA	Noradrenaline
Na acetate	Sodium acetate
Na pyruvate	Sodium pyruvate

NCC	Sodium chloride cotransporter
NaCL	Sodium chloride
Na2HPO4	Monosodium phosphate
Na2H2PO4	Disodium phosphate
NaOH	Sodium hydroxide
NFAT	Nuclear factor of activated T cells
NF-κβ	Nuclear factor kappa beta
NG2	Neural/glial antigen 2
NaHCO3	Sodium bicarbonate
NHE3	Sodium-hydrogen exchanger type 3
NKCC2	Sodium-potassium-chloride cotransporter
NO	Nitric oxide
NODAT	New onset post transplant diabetes
NOS	Nitric oxide synthase
NSAIDS	Non-steroidal anti-inflammatory drugs
NOX	NADPH oxidase
O2	Oxygen
$O_2^{-}\cdot$	Super oxide anion
OH ·	Hydroxyl radical
OMM	Outer mitochondrial membrane
ONOO	Peroxynitrite
P-GP	P-glyoprotein
PGE_2	Prostaglandin E_2
PCI	Prostacyclin
PM	Plasma membrane
PMT	Photo-multiplier-tube
PP3C	Protein phosphatases 3
PSS	Physiological saline solution
RAAS	Renin-angiotensin-aldosterone system
RBC	Red blood cells
RBF	Renal blood flow
RBFR	Renal blood flow resistance
RMBF	Renal medullary blood flow
RMIC	Renal medullary interstitial cells
ROI	Regions of interest
ROS	Reactive oxygen species
SD	Sprague-Dawley
SHR	Spontaneously hypertensive
SNAP	S-nitroso-N-acetylpenicillamine
SNP	Single nucleotide polymorphisms
SOD	Super oxide dismutase
TAL	Thick ascending limb
tAL	Thin ascending limb
TDM	Therapeutic drug monitoring
TGF-β	Transforming growth factor beta
Ti:S	Titanium: Sapphire
TMA	Thrombotic microangiopathy
TMRE	Tetramethylrhodamine, Ethyl Ester
TMRM	Tetramethylrhodamine methyl ester
UTP	Uridine triphosphate
VDAC	Voltage-dependent anion channel

VEGF	Vascular endothelial growth factor
VOCC	Voltage operated calcium channels
VSMC	Vascular smooth muscle cell
XO	Xanthine oxidase
$\Delta\Psi m$	Mitochondrial membrane potential
$^1O_2$	Singlet Oxgyen

1. General introduction

1.1 Kidney overview

The kidney is the main organ that integrates the human urinary system with its purpose to eliminate waste, regulate blood volume and pressure, balance electrolytes and metabolites, and regulate blood pH. The highly specialised function of the kidney is reflected in its elaborate and diverse structure. Each kidney is comprised of over 15 main structures, each with their own specific function and regulatory mechanism; the primary structures can be grouped into four main assemblies which include; the renal cortex, renal pyramids, renal medulla and renal pelvis, figure 1.1.

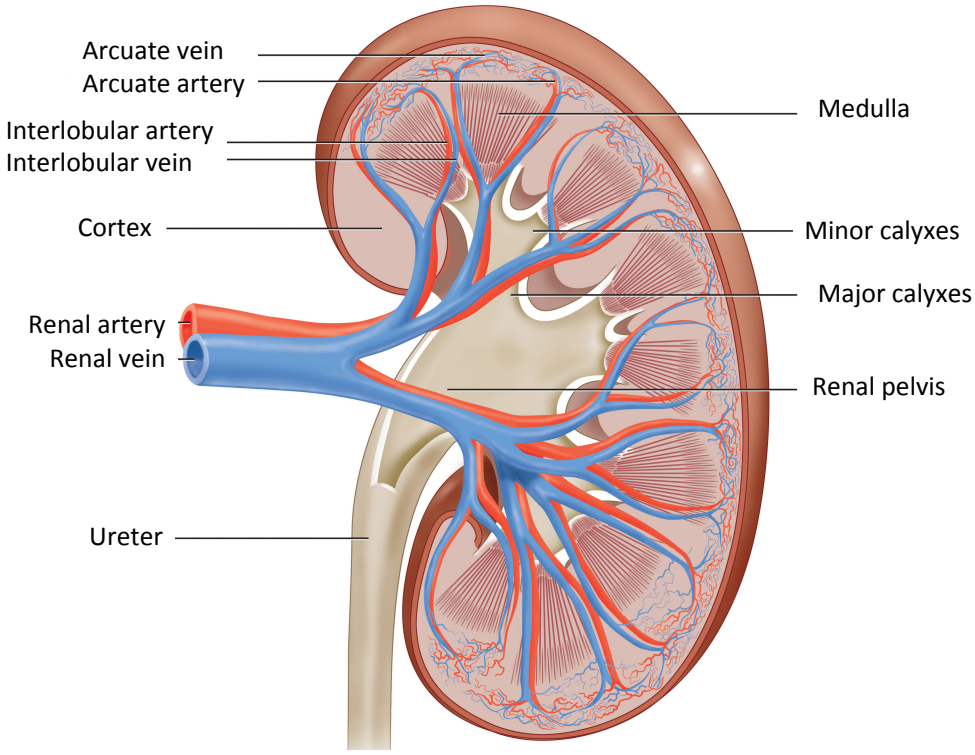

Figure 1.1 Gross anatomy of the kidney. Coronal section of the kidney showing major structures and circulation. Adapted from (Gattone 2009).

The continuous work endured by the kidney, to filter and purify blood, translates into the organ receiving approximately 25% of the cardiac output and 1200 ml of blood per minute. With this continuous filtration, approximately 1 litre of urine is produced after more than 100 litres of circulating blood has been processed per day. Urine formation arguably begins in the glomerular capillaries with dissolved metabolites and substances passing into the proximal tubule from the blood pressure force

generated in the afferent arteriole into the Bowman's capsule capillaries (Robert J Alpern 2008).

The primary functional unit within the kidney is the nephron. Each adult human kidney has approximately 1.25 million nephrons, each consisting of a glomerulus and associated tubules. The glomerulus consists of a highly organised and dense capillary network encapsulated within a porous membrane called the Bowman's capsule. Together they form the renal corpuscle. Blood enters the glomerulus *via* afferent arterioles, directed by the renal artery, where they split to from a circulatory network, of which the vasa recta are part; see 1.2. At the distal end of the glomerulus, the capillaries re-join to from the efferent arteriole from which blood leaves the glomerulus (Bonventre & Yang 2011).

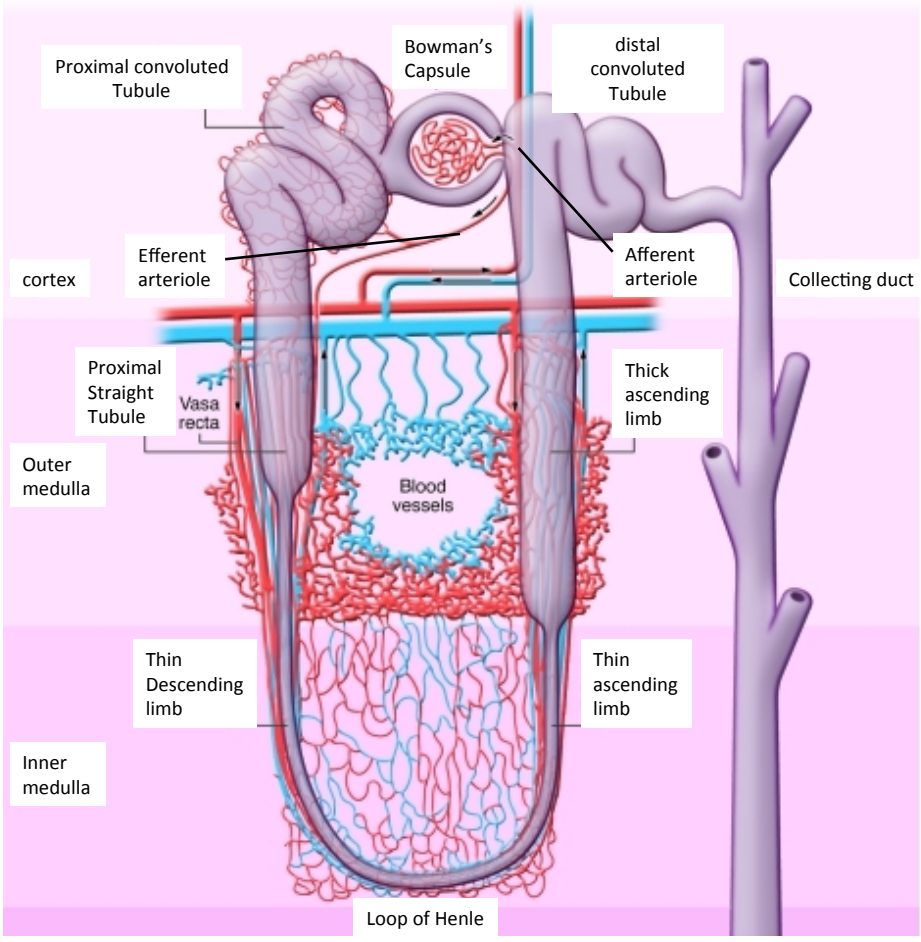

Figure 1.2 Anatomy of kidney nephron. Juxtaglomerular nephron with inner and outer medulla surrounding microcirculation. Adapted from (Bonventre & Yang 2011).

1.1.2 Vasculature compartment

Blood that enters the kidney does so at the renal hilum *via* the renal artery. The renal artery then branches to form 3 segmental arteries, which immediately branch into 5 interlobar arteries. At the junction of the renal medulla and cortex, the interlobar arteries give rise to arcuate arteries and pass along this boundary (Pallone, Z. Zhang, *et al*. 2003). Branches from arcuate arteries travel out at 90 degrees through the cortex and towards the capsule and are known as cortical radial arteries. Afferent arterioles also arise from these interlobular arteries and divide within the cortex to the glomerular capillary network. The glomerular capillaries do not drain into a vein but instead reunite to form efferent arterioles (Pallone *et al*. 2012).

The efferent arterioles then branch to various regions depending on their location. Superficallialy situated cortical efferent arterioles found in the outer two thirds of the cortex feed a plexus of peritubular capillaries. These vessels supply blood to the proximal and distal tubules and portions of the loops of Henle and the collecting ducts before joining the interlobular veins and returning to the inferior vena cava through the arcuate, interlobar, and renal veins (see Figure 1.3). The efferent arterioles in the inner third of the cortex, juxtamedullary efferent arterioles, give rise to some peritubular capillaries but also give rise to the vasa recta, small-diameter vessels that penetrate deep into the medulla after branching off from vascular bundles (Pallone *et al*. 1990). These vessels provide most of the oxygen supply to the loop of Henle, where they are adjacent, and join together to form the arcuate veins. Vasa recta and peritubular capillaries ultimately drain into the renal vein and leaves *via* the hilus (Lote 1994).

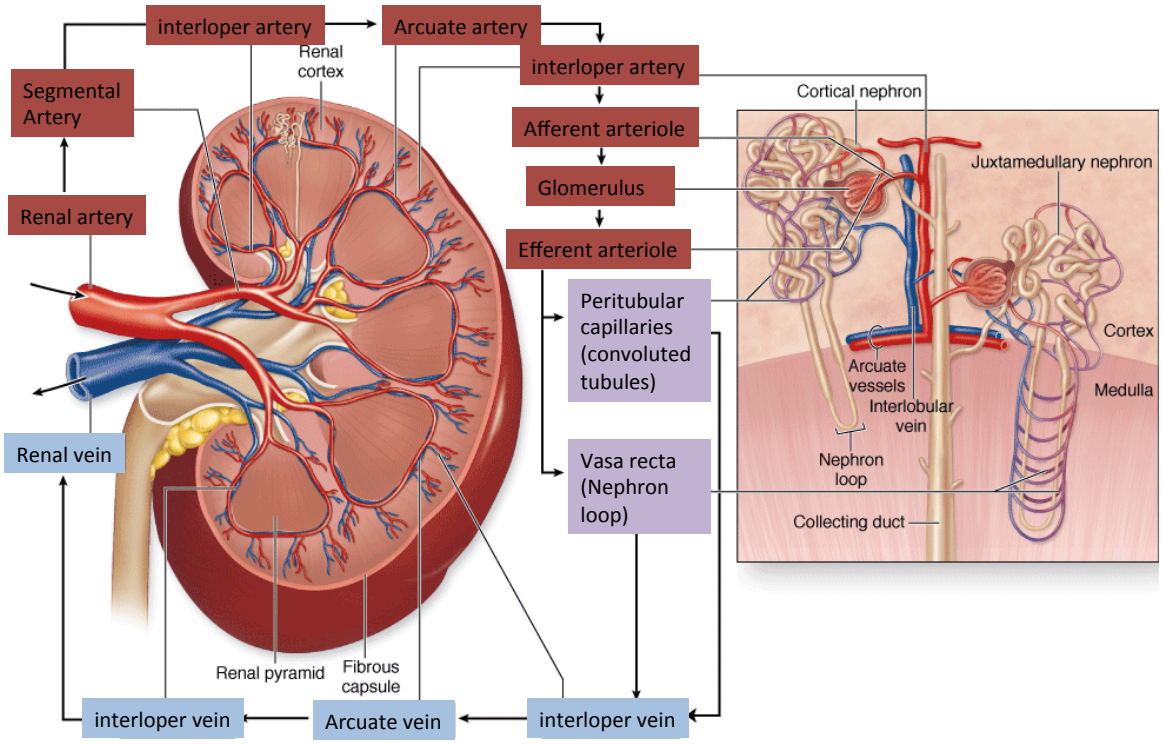

Figure 1.3 Renal blood circulation. Major blood vessels of the kidney are shown on the left. The microvascular components extending into the cortex and medulla from the interlobular vessels are shown on the right. Red boxes indicate vessels with arterial blood and blue indicate the venous return. Purple boxes are intermediate vessels. Adapted from (Mescher 2013).

1.1.3 Tubular compartment

The renal tubule is responsible for reabsorption and secretion of solutes. It includes the proximal convoluted tubule, loop of Henle (comprised of the descending limb and thin and thick ascending limbs) and distal convoluted tubule, see figure 1.2. The highly specialised epithelial cells that line the renal tubule vary considerably and consequently each of the aforementioned sections of the nephron have a specific role in absorption and secretion of solutes, water and ions (Eaton & Pooler 2009).

The proximal tubule is the first site of reabsorption. Fluid in the filtrate is reabsorbed into peritubualr capillaries and approximately 70% of all solutes and water are reabsorbed before leaving the end of the proximal tubule (Koeppen & Stanton 2013c).

The loop of Henle is an extension of the proximal tubules, which begins in the cortex, receives filtrate from the proximal convoluted tubule and its descending limb extending into the renal medulla, the ascending limb returns from the medulla to the cortex and forms the beginning of the distal convoluted tubule, see Figure 1.2. The

loop of Henle's function is primarily to concentrate urine, through increasing salt concentration in the filtrate. This is achieved *via* the countercurrent multiplier system; countercurrent flow between tubular filtrate and blood flow, within the descending and ascending limbs and vasa recta, respectively, increases the osmotic gradient between tubular fluid and interstitial space (Koeppen & Stanton 2013d).
The distal convoluted tubule is the nephrons penultimate segment, where ion exchange occurs across the epithelial cell apical and basolateral membranes to regulate potassium, sodium, calcium and pH of the filtrate. Once filtrate has exited the distal tubule, it enters the collecting ducts where principal cells are responsible for sodium reabsorption, and ultimately reaching the bladder for excretion (Koeppen & Stanton 2013e).

1.2 Renal blood flow and microcirculation

It is clear from the complexity of renal blood flow, the microvascular structures vary in the cortex and outer and inner medulla to accommodate the specialised functions and metabolic demands within each kidney region. In the cortex, afferent and efferent arterioles are the driving forces that regulate glomerular filtration. A dense peritubular capillary plexus that arise from efferent arterioles surrounds the proximal and distal convoluted tubules and function to reabsorb substantial volumes of glomerular filtrate and transport water and solutes back to the venus blood. In contrast, the medullary vasa recta capillary network serve needs that are specific to the renal medulla alone (Eaton & Pooler 2009).

The medulla is served *via* outer stripe juxtameduallary efferent arterioles which further branch to form descending vasa recta (DVR). The renal medulla has two distinct regions, outer and inner, each with their own inner and outer stripes. Each region serves distinct functions and has distinct vessel arraignments. Figure 1.4 highlights the complexity of the medullary microvasculature. Microcirculation in the outer region is characterized by a separation of capillaries into vascular bundles in which vessels run in parallel and into dense capillary plexus' of the interbundle region capillary networks that serve the inner stripe (Bankir & Derouffignac 1985). Outer medulla DVR have been well characterized and have been proven to be

experimentally valid for investigating outer medullary endothelial transport, pericyte contractility and tubule-vascular crosstalk (K. K. Evans *et al*. 2015). Inner medulla DVR however are less well understood. Although morphologically similar, limited studies have actually investigated their contribution to renal blood flow (K. K. Evans *et al*. 2015). Parallel vascular bundles and a capillary plexus at the interbundle region also serve the inner stripe of the outer medulla. The inner stripe vascular bundles include long DVR that serve the interbundle region and DVR that will penetrate beyond the inner-outer-medullary junction to the inner medulla (Pallone, Turner, *et al*. 2003). DVR that supply blood flow to the interbundle capillary plexus peel off from the periphery of the vascular bundles as they pass into the inner stripe. DVR that reside within the center of the vascular bundle cross the inner stripe of the outer medulla to reach and perfuse the inner medulla, see figure 1.4 (Pallone, Z. Z. Zhang, *et al*. 2003). Vascular bundles also contain ascending vasa recta (AVR) returning from the inner medulla. These AVR originate from the inner medulla therefore countercurrent exchange in the inner stripe involves all DVR and only AVR that drain the inner medulla and not the outer medulla stripes, figure 1.4, (Pallone *et al*. 1994). In contrast, blood that drains from the outer medullary interbundle plexus ascends directly to the cortex without rejoining vascular bundles and are not involved in countercurrent exchange (Pallone *et al*. 1990; Kriz 1981).

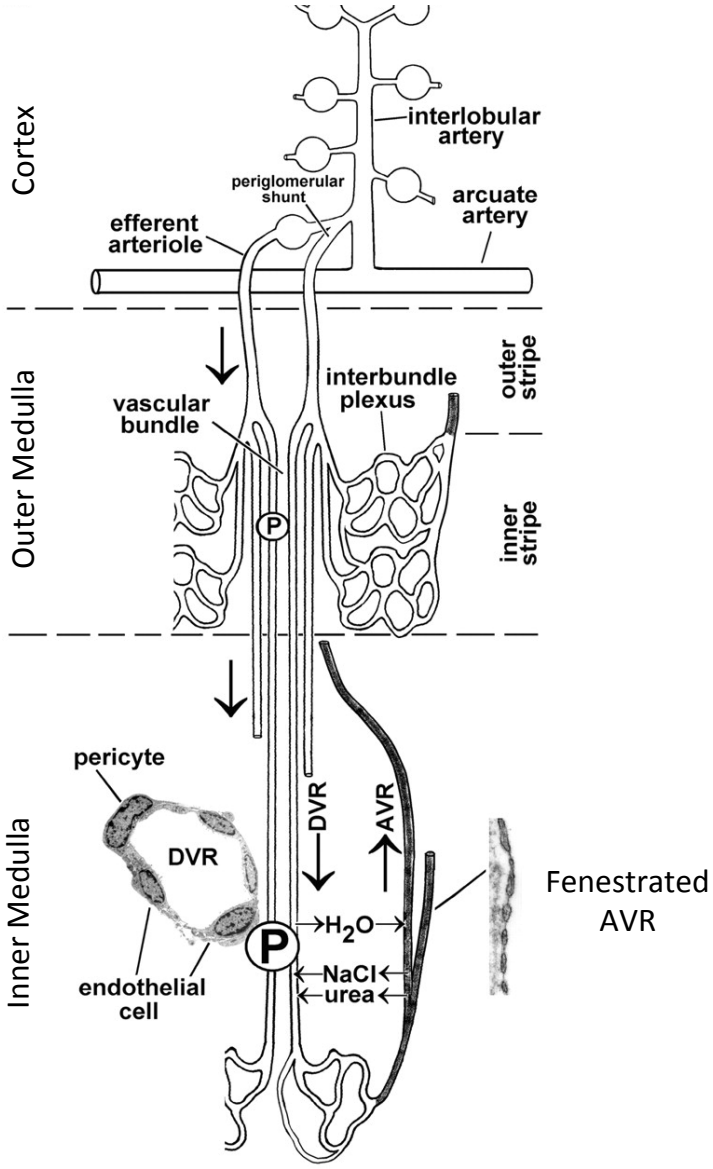

Figure 1.4 Anatomy of the medullary microcirculation. Blood is supplied to the medulla from the efferent flow out of juxtamedullary glomeruli. Efferent arterioles of juxtamedullary glomeruli give rise to bundles of descending vasa recta in the outer stripe of the outer medulla. In the inner stripe of the outer medulla, descending vasa recta and ascending vasa recta returning from the inner medulla run side by side in the vascular bundles, allowing exchange of solutes and water. The descending vasa recta from the bundle periphery supply the interbundle capillary plexus of the inner stripe, whereas those in the center supply blood to the capillaries of the inner medulla. Contractile pericytes in the walls of the descending vasa recta regulate flow. The increasing size of the circled "P" represents DVR plasma protein concentration that rises with medullary depth. DVR, descending vasa recta. AVR, ascending vasa recta. Adapted from (Pallone, Turner, *et al*. 2003).

The parallel arrangement of DVR and AVR within vascular bundles suggests they work in efficient equilibrium and that they possibly play a role in the regulation of

regional blood flow distribution throughout the medulla. For example, constriction of DVR within the bundle center should enhance perfusion of the interbundle region while constriction of DVR on the vascular bundle periphery should enhance perfusion of the inner medulla (Navar *et al*. 2011).

1.3 Medullary blood flow

The notion that medullary blood flow (MBF) may be locally regulated at the level of the DVR and AVR is not a new concept *per se*, indeed this was first suggested in the 1960's (Thurau & Deetjen 1962), however this still remains a controversial topic in the renal field. The main reason for this being that experimentally it is difficult to access the renal medulla *in vivo*, thus investigating how blood flow is regulated in this region remains an on going technical challenge.

MBF is served predominately *via* the DVR and AVR. DVR are responsible for delivery of blood from the outer stripe of the outer medulla, traversing vascular bundles in the inner stripe of the outer medulla, then ultimately to the inner medulla, figure 1.4 (Pannabecker & Dantzler 2004). DVR are approximately half the diameter of juxtamedullary efferent arterioles and range between 12-18 μM (Jamison & Kriz 1982). The DVR wall is characterised by a gradual replacement of the smooth muscle of the efferent arteriole by contractile pericyte cells. Pericyte cells are smooth muscle-like cells that surround DVR and continuous capillaries of other tissues (Shepro & Morel 1993). Pericyte density in the medulla becomes progressively irregular with increasing medullary depth but is well retained into the inner medulla (F. Park *et al*. 1997).

DVR have a continuous endothelium with tight junctions while AVR have endothelium that is highly fenestrated (Mink *et al*. 1984). The enclosing nature of pericytes around DVR and presence of smooth muscle-like properties, myofibrils similar to that of smooth muscle cells, suggest vasoconstrictor and vasorelaxant properties (Kriz 1981; Pallone & C. Cao 2007).

Efferent arterioles and DVR are the main medullary structures with sympathetic innervation, which continues when smooth muscle cells are supplemented for pericytes (Crawford *et al*. 2013), therefore it is suggestive that vascular smooth muscle cells of juxtameduallry arterioles and medullary DVR are largely accountable for the differential regulation and distribution of medullary circulation (Lemley *et al*. 1986; R. G. R. Evans *et al*. 2004; Zimerhackl *et al*. 1987).

1.3.1 Medullary countercurrent exchange

The medullary vasculature plays an important role in the generation of the countercurrent exchange mechanism, which is responsible for the gradual increase of concentrated urine whilst minimising water loss.

Through their parallel counter flow arrangement, DVR and AVR trap sodium chloride and urea deposited in the interstitium by collecting ducts and loops of Henle. Blood entering the DVR from juxtaglomerular efferent arterioles contains sodium chloride and urea at concentrations similar to that of the systemic circulation (Pallone, Z. Zhang, *et al*. 2003). As the blood flows down the DVR, an increasingly hypertonic medullary interstitium is encountered through an inward diffusion of solutes and volume efflux. On its return, blood flowing through the AVR is subsequently diluted *via* solute efflux and water volume influx (Sanjana *et al*. 1975; Sanjana *et al*. 1976).

1.3.2 Medullary gas exchange

The medullary microvasculature is also responsible for supplying oxygen and nutrients to its metabolically active surrounding tissue. However, within the medulla, the competing requirement to preserve corticomedullary osmotic gradients conflicts with this requirement. Consequently, partial pressure of oxygen in the medulla is low, between 10 and 25 mmHg, which is due to oxygen in DVR diffusing across to adjacent AVR after which blood is shunted back to the cortex, figure 1.5 (Brezis *et al*. 1991; Brezis & Rosen 1995). In contrast, the partial pressure of oxygen in the renal cortex is ~55 mmHg (Brezis & Rosen 1995).

To balance the possible insult of ischemia, the renal medulla has evolved and is able to continually adapt regional perfusion of both the outer and inner medulla through local vasodilator paracrine signalling. All paracrine signalling molecules share the ability to augment medullary blood flow therefore increase the local supply of oxygen (Pallone, Turner, *et al*. 2003). Interestingly, most vasodilators also inhibit salt reabsorption, therefore protection of potential hypoxic insult most likely involves vasodilation of the vasculature to enhance perfusion and inhibiting salt reabsorption, reducing oxygen consumption and demand (Navar *et al*. 2011).

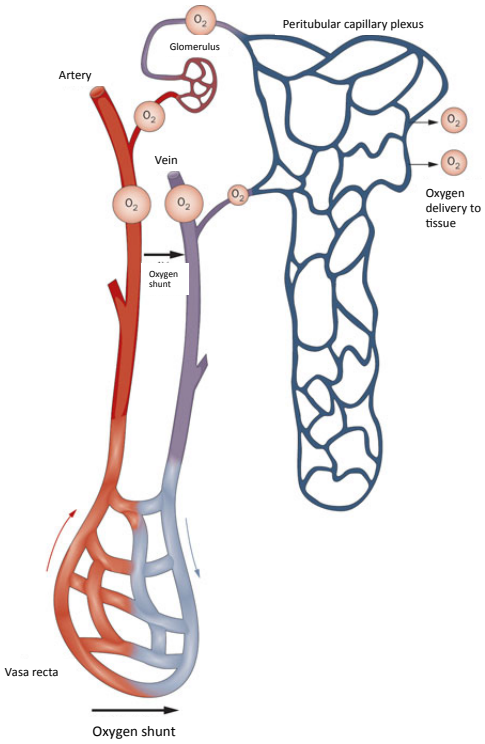

Figure 1.5 Oxygen delivery to the renal medulla. Oxygen is delivered by blood cells in the artery. Red blood cells release oxygen in the capillaries, which diffuses into the interstitium to reach target cells. Blood with low oxygen tension passes into the vein. An AV oxygen shunt present in the kidney enables oxygen to move directly from the artery to the vein. Oxygen tensions in the capillary are relatively low when blood cells reach the peritubular capillary plexus, which indicates that the kidney is ineffective in separating oxygen. The relative oxygen tensions are represented by the size of the circles surrounding the term 'O_2'. AV, arterial-to-venous Adapted from (Fry *et al*. 2014).

1.3.3 Medulla accessibility

With the renal medulla being almost completely inaccessible *in vivo* for accurate and reliable medullary blood flow measurements and its parallel positioning with glomerular circulation and juxtamedullary nephrons, efforts to study the renal medullary microcirculation has been hindered by continuous technical difficulties (Hansell 1992). Furthermore, blood flow to the inner medulla accounts for less than 1% of total renal blood flow (Cowely *et al*. 1995). Various techniques have been developed to ascertain the complexity behind medullary perfusion and although there is considerable inconsistency with the absolute values of medullary blood flow, most techniques including laser-Doppler and contrast ultrasound (Young *et al*. 1996)

are able to measure the relative changes of blood flow within the medulla (Hansell 1992; Mattson *et al*. 1993).

Laser-Doppler appears to be the most widely used and accepted method (Cowley *et al*. 1995; Hansell 1992). It relies on the Doppler shift imparted to monochromatic light by backscatter from moving red blood cells within a vessel (Pallone, Turner, *et al*. 2003). Initial experiments by Roman *et al* generated a new understanding to medullary blood flow with findings indicating papillary blood flow increased after an increase of renal perfusion pressure but interestingly the inner medulla failed to autoregulate (Roman *et al*. 1988).

This phenomenon has been heavily investigated in the past decade with several groups conforming the initial findings of impaired medullary autoregulation, while others have produced conflicting results (Cowley 1997; Navar *et al*. 1996; Majid *et al*. 1997). However in more recent years, it has become apparent, through advanced imaging techniques and our understanding of renal blood flow, that changes in medullary circulation can have a important effect on the pressure-natriuresis of the medulla and therefore effect long-term arterial pressure (Pallone *et al*. 2012; Q. Zhang *et al*. 2006).

1.4 Renal pericytes

One of the main reasons that MBF is becoming an evermore-interesting research topic is that of developing evidence favouring an intrinsic autoregulation of medullary blood flow. As mentioned, MBF regulation is still poorly understood and highly controversial, partly down to medulla inaccessibility but also due to the relatively uncharacterised contractile function of renal pericytes.

Pericytes where first identified by Rouget in the late 1800's found on the abluminal side of endothelium walls and at the time thought to be precursors of vascular smooth muscle cells (Dore-Duffy & Cleary 2011). Renal pericytes reside on DVR when smooth muscle cells of efferent arterioles become scarce. Pericyte density decreases with increasing depth of DVR into the medulla but remain present even in the inner stripe of the inner medulla (F. Park *et al*. 1997).

Pericytes are often referred to as "smooth muscle-like" cells due their expression of contractile machinery. Alpha-smooth muscle actin, myosin and fibronectin have all been shown to be expressed by pericytes and to have functional properties (Skalli *et*

al. 1989; Nehls & Drenckhahn 1991). An important point to note that distinguishes pericytes and vascular smooth muscle cells (VSMC), apart from their obvious morphological distinction of process, is their location in respect to endothelial cells (EC's). VSMC's lay outwith the basement membrane of EC's while pericytes, particularly their processes, reside within EC basement membranes (Courtoy & Boyles 1983; C. C. W. Hughes 2008).

Pericytes consist of a single cell body with multiple claw-like processes that extend from the cell body and encircle their associated microvessels, figure 1.6 (Kennedy-Lydon *et al*. 2012; Bergers 2005).

As mentioned, pericyte processes are typically enclosed within abluminal EC basement membranes, however the cell body is often exposed in basement membrane gaps. Given that pericyte processes are enclosed abluminally, this suggests possible intracellular crosstalk between pericytes and their associated underlying endothelial cell to relay signalling molecules for alterations in pericyte contractility (Kida & Duffield 2011). Furthermore, given that pericyte process are in contact with multiple EC's, it could be suggested that single pericytes are capable of linking to multiple EC's and incorporating cross-talk with parallel endothelium. This pericyte-EC crosstalk is facilitated *via* peg and socket junctions and also heterocellular gap junctions while EC-EC crosstalk is assisted *via* tight, gap and/or adherence junctions (Tell *et al*. 2006; Armulik *et al*. 2005).

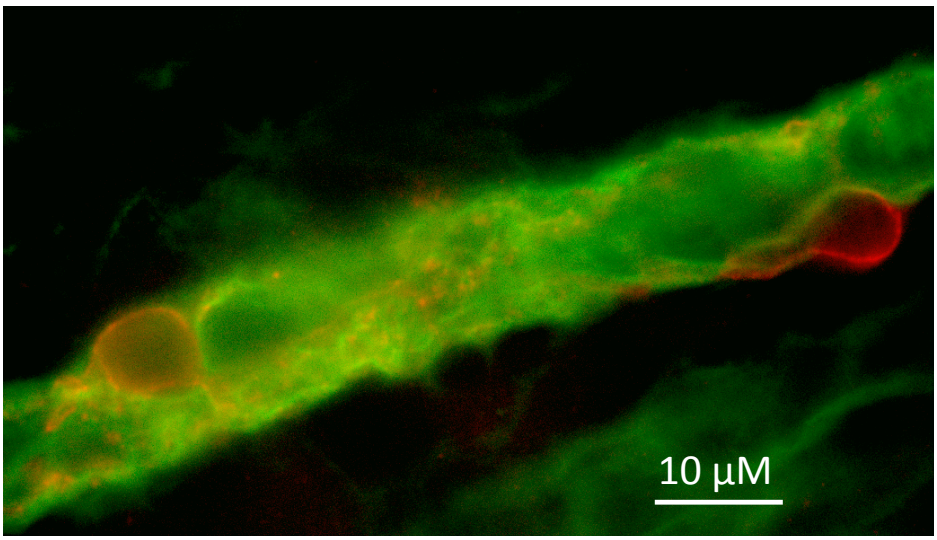

Figure 1.6 Renal pericytes envelop mouse DVR. Renal pericytes stained with anti-NG2 (red) wrap around and along DVR stained with IB4 (green).

1.4.1 Pericyte function – regulation of blood Flow

The function of renal pericytes is still debatable however given that their claw-like processes envelop microvessels, together with expression of contractile and intermediate filaments, its is thought that they play a role in regulating microvascular tone and blood flow. This therefore implies that renal pericytes may have a role in regulation of renal MBF, or at least to the extent of DVR flow regulation.

Pallone and colleagues have carried out much of the early work investigating renal pericytes and their role within the renal medulla using the isolated perfused DVR technique (Pallone 1994; Pallone *et al*. 1994; Silldorff & Pallone 2001; Edwards *et al*. 2011). Their *in vitro* technique is technically challenging, however provided clear evidence suggesting pericyte-mediated manipulation of DVR diameter. In response to various stimuli, e.g. endogenous and exogenous vasoconstrictors, angiotensin II (ANG II) and vasodilators, prostaglandin E_2 (PGE_2) and nitric oxide (NO), they were able to show that isolated perfused DVR could constrict or dilate, theoretically at pericyte locations along the vessel, therefore offering a local mechanism for the control of vessel tone and diameter of DVR (Pallone 1994; Silldorff & Pallone 2001).

Various studies have suggested that pericyte density is dependent on the functional demands of tissue, higher metabolic tissue usually requiring increased oxygen supply and nutrients, supported by studies in which differences in pericyte coverage throughout various vascular beds has been observed (Diaz-Flores *et al*. 2009; Sims 2000; Crawford *et al*. 2012). With respect to the renal medulla and DVR, its functional demand is high; therefore, tight regulation of medullary blood flow is fundamental for preservation of medullary function, in an already almost hypoxic environment. This suggests that DVR may be densely populated by pericytes to allow intricate alternations of blood flow and preserved function, which has been confirmed in a recent study undertaken by Crawford *et al* who were able to quantify pericytes within the different medullary sections (Crawford *et al*. 2012), which confirmed earlier reports of decreasing numbers of pericytes further into the inner medulla (Pallone *et al*. 1990; Armulik *et al*. 2005). This also relates to particular regional energy demands of the kidney, with the inner medulla requiring much less compared to that of the inner stripe of the outer medulla (Pallone *et al*. 2012). Interestingly, Crawford *et al* also highlighted the density of pericyte processes and suggest the network of pericyte processes facilitate communication with each other in order to tightly regulate

changes of blood flow in single DVR but also through adjacent DVR to significantly alter total MBF (Crawford *et al*. 2012).

These new findings suggested that in contrast with what was originally thought about medullary blood flow, passive and driven upstream *via* arteriolar perfusion pressure, these vasoactive segments of DVR could play a key role in the regulation of total and more importantly, regional blood flow to the renal medulla (Pallone & Silldorff 2001; Pallone *et al*. 2012; R. G. R. Evans *et al*. 2004).

1.4.2 Pericyte function- vessel stability

As well as being a possible fundamental factor in regional control of blood flow to the kidney, renal pericytes have been suggested to have other critical functions including formation, stabilization and remodelling of vascular beds (Suzuki *et al*. 2003; Hammes *et al*. 2004; Caruso *et al*. 2009). Revolutionary investigations using fate tracing, transgenic mice and renal pericyte cell line studies, have collectively suggested pericytes are involved in the pathology of various renal diseases including chronic kidney disease (CKD) *via* loss of pericytes on microvessels, their involvement in renal fibrosis *via* vessel detachment and migration and also differentiation into myofibroblasts (Y. Cao *et al*. 2013; S.L. Lin *et al*. 2011; Humphreys *et al*. 2010). Pericyte differentiation has recently been further investigated as a possible influential mechanism of renal fibrosis (Kida & Duffield 2011; S.L. Lin *et al*. 2008). These findings however are controversial due to the generally accepted mechanism of epithelial to mesenchymal transition (EMT). As its name suggests, EMT involves epithelial cells losing their cell polarity and cell adhesions to gain migratory and invasive properties of mesenchymal cells (Y. H. Liu 2004). This transition was thought to be the initial step following renal insult towards the progression of scaring and fibrosis. However, one of the first groups to challenge the role of EMT as the source of myofibroblasts in the kidney demonstrated the alpha-smooth muscle actin (αSMA) stained cells where located in the interstitium but not tubules of renal insulted mice and that αSMA positive cells where predominantly located within the perivascular region (Faulkner *et al*. 2005). This was further highlighted using *in vivo* fate tracking studies and suggested that EMT was an "*in vitro* phenomenon" and excluded EMT as the primary source of fibrogenic cells (Schrimpf & Duffield 2011; Humphreys *et al*. 2010; S.L. Lin *et al*. 2008). Furthermore, these results were replicated by two independent groups

using transgenic mice for fate tracing studies (L. Li *et al*. 2010; Koesters *et al*. 2010) casting doubt on the general acceptance of EMT as the primary source of fibrogenic cells.

1.5 Drug-induced nephrotoxicity

As the kidney receives 25% of resting cardiac output over a large endothelial surface area and filters more than 100 litres of blood per day, it is not surprising that the kidney is particularly susceptible to toxins within the blood stream (Koeppen & Stanton 2013a). Therefore, nephrotoxicity (damage to the kidney *via* drugs or toxins) is frequently seen with many common medications in clinical use today and drug-induced renal injury contributes up to 25% of all cases of acute kidney injury as a result of intrinsic renal disease (Kaufman *et al*. 1991; Nash *et al*. 2002). It is also important to note that with such a high metabolic demand involving numerous specific enzymes and cellular transport processes, glomerular, tubular and interstitial cells may be susceptible to drugs and their metabolites at higher concentrations than that of other tissues within the body (Eaton & Pooler 2009).

Several over the counter medicines and prescribed drugs have been found to be nephrotoxic by one or more common pathogenic mechanisms. These can be direct or indirect and include; altered renal haemodynamics, tubular cell toxicity, inflammation, crystal nephropathy and thrombotic microangiopathy (Schetz *et al*. 2005; Zager 1997).

Under normal homeostatic regulation, approximately 120 ml of plasma is filtered under pressure through the glomerulus per minute and corresponds to the glomerular filtration rate (GFR) (Koeppen & Stanton 2013b). The kidney is able to maintain intraglomerular pressure through regulation of afferent and efferent arterial tone.

This protective mechanism can occur in response to certain stress circumstances to prevent a fall or increase in the GFR and subsequent increased risk of renal damage. For example, volume depletion will lead to systemic circulating prostaglandins, compensating for ANG II induced vasoconstriction, causing a vasodilation of afferent arterioles to allow an increases blood flow through to the glomerulus.

Drugs that inhibit prostaglandins, non-steroidal anti-inflammatory drugs (NSAIDS), or impede angiotensin II activity, angiotensin-converting enzyme inhibitors (ACEi's)

can therefore interfere with the kidney's ability to autoregulate glomerular pressure and GFR (Palmer 2002; Schoolwerth *et al*. 2001).

1.5.1 Tubular toxicity

Due to the reabsorption function of the renal tubule, proximal tubule cells are particularly vulnerable to toxic effects of drugs due to their role in concentrating and reabsorbing glomerular filtrate and consequentially exposing them to particularly high levels of circulating toxins (Perazella 2005). Tubular cell toxicity is mediated through a variety of mechanisms including impairment of mitochondrial function, distribution of tubular transport proteins and increasing oxidative stress and/or formation of free radicals (Zager 1997; Markowitz & Perazella 2005). In addition, either direct toxic or ischemic effects of drugs may cause renal tubular epithelial cell damage, which is, observed as cellular degeneration and sloughing from proximal and distal tubular basement membranes, clinically known as acute tubular necrosis (ATN) (F. G. Silva 2004). Clinically, ATN along with tubulointerstital nephritis, are the most common presentations of drug-induced nephrotoxicity however, swelling and vacuolisation of proximal tubular cells has also be noted in patients with osmotic nephrosis (Markowitz & Perazella 2005).

Drugs can cause inflammatory changes in the glomerulus, renal tubular cells, and the surrounding interstitium, leading to fibrosis and renal scarring.

Acute interstitial nephritis (AIN), which can result from an allergic response to a suspected drug, develops in an idiosyncratic, non–dose-dependent fashion. AIN is the underlying cause for up to 3% of all cases of acute kidney injury (Rossert 2001; Perazella 2005).

1.5.2 Vascular toxicity

One of the main issues related to the mechanisms of the effects of CNI's is the putative involvement of vascular dysfunction, which can include thrombotic microangiopathy, thrombotic thrombocytopenic purpura and thrombotic vasculitis.

In drug-induced thrombotic microangiopathy, organ damage is caused by platelet thrombi in the microcirculation, as is seen in thrombotic thrombocytopenic purpura (Pisoni *et al*. 2001). Mechanisms of renal injury secondary to drug-induced thrombotic microangiopathy include an immune-mediated reaction or direct endothelial toxicity (Pisoni *et al*. 2001) however injury to the endothelial cells is

considered the central and inciting factor in the sequence of events leading to thrombotic micoangiopathy (Ruggenenti *et al*. 2001). This can be seen *in vitro* by the various compounds associated with the disease: endotoxins, viruses and immunosuppressives, all causing direct endothelial cell damage (Remuzzi 1994).

Thrombotic microangiopathy is a well-recognized serious complication of renal transplantation with occurrence either as de novo or recurrent. The latter is often in patients with previous history of hemolytic uremic syndrome (HUS), while de novo may be triggered by immunosuppressive drugs and acute antibody-mediated rejection (Noris & Remuzzi 2010).

The most commonly used immunosuppressive drugs for renal transplantation are calcineurin inhibitors of which cyclosporine and tacrolimus are the most widely used.

1.6 Calcineurin Inhibitors

It has now been over a quarter of a century since the discovery of cyclosporine (CsA) and its iconic influence on the immune system, and it is fair to say it is still the main drug used in organ transplantation in the vast majority of patients transplanted today (Calne *et al*. 1978; Powles *et al*. 1978). CsA was the first immunosuppressive drug to be discovered that allowed selective immunoregualtion of T cells without unwarranted toxicity in animal models. Before discovery, a combination of azathioprine, a less commonly used immunosuppressive in solid organ transplant, and corticosteroids were the norm for patients undergoing solid organ transplant. The combination of drugs, and azathioprines poor efficacy, resulted in a plethora of unspecific side effects and untimely led to allograft rejection and cancer development (Armstrong & Oellerich 2001).

1.6.1 Cyclosporine A

CsA was initially developed with the aim of treating immune-mediated disorders but by the mid 1970's, some 5 years after its discovery, the first experiments in animal models of transplantation indicated remarkable results. Consequently, in 1979, CsA

was used for the first time as a front line immunosuppressive in kidney transplantation in Cambridge, UK (D. Colombo & Ammirati 2011).

CsA is a lipophilic peptide that can easily cross membranes of cells such as T lymphocytes (Fahr 1993b). CsA forms a complex with a cytosolic protein called cyclophillin and ultimately inhibits calcineurin's enzymatic activity once bound with the CsA-cyclophillin complex. Calcineurin is a crucial enzyme in the transduction of signals from T-cell receptors triggering the promoters of cytokine genes (Takahashi *et al*. 1989). It is a calcium-dependent serin-threonin phosphatase, also know as protein phosphatates 3 (PP3C), that under normal active conditions dephosphorylates the nuclear factor of activated T cells (NFAT) and triggers T-cell promotion through NFAT entering the nuclease, the crucial step for activation and transcription of target genes (Takahashi *et al*. 1989; Fischer *et al*. 1989; Flanagan *et al*. 1991).

These target genes include T-cell dependent lymphokines, primarily interleukin 2, its receptor (IL-2R), tumour necrosis factor-α and granulocyte macrophage colony-stimulating factor, which are also regulated through calcineurin-dependent dephosphorylation of NFAT (Rusnak & Mertz 2000; Naesens *et al*. 2009). However, the selective immunosuppressive property of CsA is through the localization of NFAT primarily in T cells (Barbarino *et al*. 2013).

Although CsA is predominately localised to T lymphocyte NFAT, its highly lipophilic structure coupled to its highly variable pharmacokinetic profile, undoubtedly translates to dephosphorylation of substrates other than NFAT in other cells and tissues, resulting in altered transcription of genes (Rao *et al*. 1997). NFAT has 5 different isoforms, NFAT1 – NFAT5, of which NFAT5 is the only non-calcineurin dependent, adding to the susceptibility of altered NFAT other than in T lymphocytes (Su *et al*. 1995; Kung *et al*. 2001; Rao *et al*. 1997).

Some of these unwanted altered genes are thought to include: nitric oxide synthase (NOS), transforming growth factor β (TGF-β), endothelin-1, collagen I and IV and BCL-2 (Olyaei *et al*. 2001; Bobadilla & Gamba 2007; Burdmann *et al*. 2003) all of which add their own unique dynamic into the foremost side effect known of CsA; nephrotoxicity. This can be clearly seen in he classic study by Calne *et al* who demonstrated CsA was capable of nephrotoxicity in 100% of patients treated for immunosuppression in solid organ transplant (Calne *et al*. 1978).

After initial high hopes for a single drug immunosuppressive regime for renal transplantation, the first report of 34 renal transplant patients in 1979 were more than underwhelming with high incidences of lymphomas, graft dysfunction and patient mortality (D. Colombo & Ammirati 2011). After the realisation that CsA required meticulous dosing, the first trial to demonstrate the unequivocal benefit of CsA in transplant immunosuppression was in 1982. 1 year follow up of the European Multicentre Trial Group involving 232 renal transplant patients, graft survival was 72% in the CsA group compared to 52% of the control group treated with azathioprine and steroids (Group 1983). For the 10 years that followed, CsA was fundamental for preservation of renal transplantation until the discovery of tacrolimus led to a newer improved immunosuppression.

1.6.2 Tacrolimus

Tacrolimus (FK506) is a newer generation calcineurin inhibitor that was discovered in the early 1980's and was hoped to revolutionise immunosuppression with its high efficacy and reduced side effects compared to CsA, however tacrolimus still has the common side effects including cancer, nephrotoxicity and infection (Starzl *et al*. 1989; J. J. Fung *et al*. 1990).

First approved for transplantation in 1994 (Klintmalm *et al*. 1993), FK506 belongs to the macrolide drug family and has no structural similarity to CsA. Despite this, FK506 has a very similar mechanism of action to CsA through which it exerts its effects, it crosses the cell membrane and inhibits calcineurin from dephosphorylating NFAT, ultimately preventing T cell production similar to CsA (Harding *et al*. 1989; Siekierka *et al*. 1989). Similarly to CsA, FK506 binds to a cytosolic protein. FK506 binds to FKBP12 and not cyclophylin, and it is this complex, not the drug itself that is able to inhibit calcineurin (Sabatini *et al*. 1994). From this point, both calcineurin inhibitors (CNI's) have the same pharmalogical effect, albeit from a slightly altered inhibitory complex.

Upon its discovery, FK506 received a significant volume of clinical interest through its increased potency, rapid absorption, quick blood peak levels and almost complete metabolisation, less than 0.5% of parent drug excreted in the urine or faeces (Staatz & Tett 2004). It took less than 5 years after discovery to enter its first clinical trial in 1990 (J. J. Fung *et al*. 1990). FK506 received clearance from the Unites States Food and Drug Administration (FDA) in 1994 and shortly after by the Medicines Control

Agency in the UK (Randhawa *et al*. 1997; Hooks 1994). It was clear that immunopharmacology had a new key immunosuppressant.

Nevertheless, FK506 was not the perfect immunosuppressant that everyone hoped it to be. As with CsA, FK506 did not show any overwhelming side effects in animal studies. There was evidence of mild weight loss, increasing blood glucose levels and lethargy reported in rats through to primates (Ochiai *et al*. 1987; Ericzon *et al*. 1992). From these results, clinical trials looked promising and the first series of trials began with liver transplant patients. However, it was a difficult decision regarding which clinical setting to introduce this revolutionary drug. After all, the introduction of CsA had a similar dilemma. The initial results suggested FK506 was appropriate for "rescue therapy", patients currently on immunosuppressive drugs but facing re-transplantation due to organ rejection or drug toxicities (high-risk patients) (Mejia *et al*. 2014). FK506 could reverse acute rejection of grafts in almost fifty percent of CsA treated patients (Jonas *et al*. 1996). After its initial success, FK506 for first-line immunosuppressive therapy began in 1996 for liver, kidney and pancreas transplantation with the hope of both high success and low rejection rate (Webster *et al*. 2005).

Early reports were encouraging with very few major side effects and FK506 was extremely well tolerated by most patient types. After kidney transplantation, reports highlighted FK506's ability to significantly reduce or completely stop steroid administration (prednisone) in over 50% of patients, while all CsA treated patients still required steroid treatment within the study (Wallemacq & Reding 1993). 1-year survival rates also looked promising with patient and graft survival rates of 94% and 77% versus 90% and 70% of CsA treated patient's, respectively. Rejection rates were similar to CsA also, 59% and 57%, respectively, indicating a similar graft versus host (GVH) rejection rate (Shapiro *et al*. 1991).

However after the initial trials and testing success, it was becoming apparent that FK506 was also stimulating side effects similar to CsA. Given that both drugs inhibit the same molecular target, it would be reasonable to expect such side effects and ranged from mild nausea to extreme nephrotoxicity (Marti & Frey 2005). The vast array of side effects started to imply FK506 was able to modify numerous pathways *via* inhibition of systemic calcineurin. In addition, tacrolimus also had the additional side effect of new onset post transplant diabetes (NODAT) and worsening sugar control in known diabetics (Ericzon *et al*. 1992; Staatz & Tett 2004).

1.7 CNI Nephrotoxicity

CsA nephrotoxicity was first reported in the late 1970's, almost straight after its introduction into immunosuppressive regimes. Nephrotoxicity was reported in all three main compartments of the kidney: glomeruli, arterioles and tubulo-intersitium (Calne *et al*. 1978). Importantly, this side effect were not reported in initial animal experiments (Gaston 2009) and would be undeniably instrumental in future research with the development of new low-salt animal model to recreate a more representative human physiological setting.

The initial findings of nephrotoxicity were first labelled as an ambiguous phenomenon due to their absence in animal studies and the specific cause of nephrotoxicity was unclear. However, the nephrotoxicity observed was attributed to acute functional changes rather than physical changes in structure and were therefore reversible (Bennett & Pulliam 1983; Klintmalm *et al*. 1981). The functional changes later became known as acute CNI nephrotoxicity.

1.7.1 Acute CNI nephrotoxicity

1.7.1.1 Vascular, tubular & interstitial Nephrotoxicity

Acute nephrotoxicity is associated with a reversible, dose-dependent reduction of glomerular filtration rate (GFR) and plasma flow attributed by both the direct toxic effect on renal vasculature and overall systemic vasoconstrictive effects of CNI's (Dieperink *et al*. 1985). Calne and colleagues who were the early investigators of CsA nephrotoxicity, first noted nephrotoxicity with patients treated at what currently would be considered a high clinical dose of CsA, 25 mg/kg (Calne *et al*. 1978). Follow up studies using a slightly lower dosing regime, 17 mg/kg, revealed not only an improved GFR and blood pressure (BP) but a much higher percentage of one year predicated graft survival rate, over 90% compared to 60% previously (Calne *et al*. 1978).

These reversible functional changes were first hypothesised to originate from direct vasoconstriction of afferent arterioles and nonspecific vasoconstriction of efferent arterioles, resulting in a decrease of GFR and prolonged systemic exposure to CsA. Murray *et al* first observed this hypothesis and confirmed CsA was able to induce strong vasoconstriction of afferent arterioles, resulting in a rise of serum creatine and induced arterial hypertension in a conscious rat model (Murray *et al*. 1985). Renal vascular resistance and blood flow in both arterioles were then further investigated

by others including English *et al* who were able to directly measure the luminal diameter of afferent arterioles of rats treated with CsA to unequivocally highlight the importance of these vascular parameters in the acute functional impairment associated with CsA use (English *et al*. 1987). The degree of CNI induced vasoconstriction can be seen in figure 1.7.

From this initial study and the numerous that followed (Diederich *et al*. 1994; Kon *et al*. 1990; Morris *et al*. 2000), it was becoming clear that vascular dysfunction was a predominate factor in CsA nephrotoxicity, but the key question still to be answered was how CsA was able to induce vascular dysfunction and associated nephrotoxicity. It was postulated that this may be due to the fact that CsA is not T lymphocyte specific as had been previously suggested and the resulting alteration in gene expression of NOS and TGF-β for example contributed to the vascular dysfunction (Naesens *et al*. 2009), see sections 1.7.2 and 1.9.3.2 for further discussion.

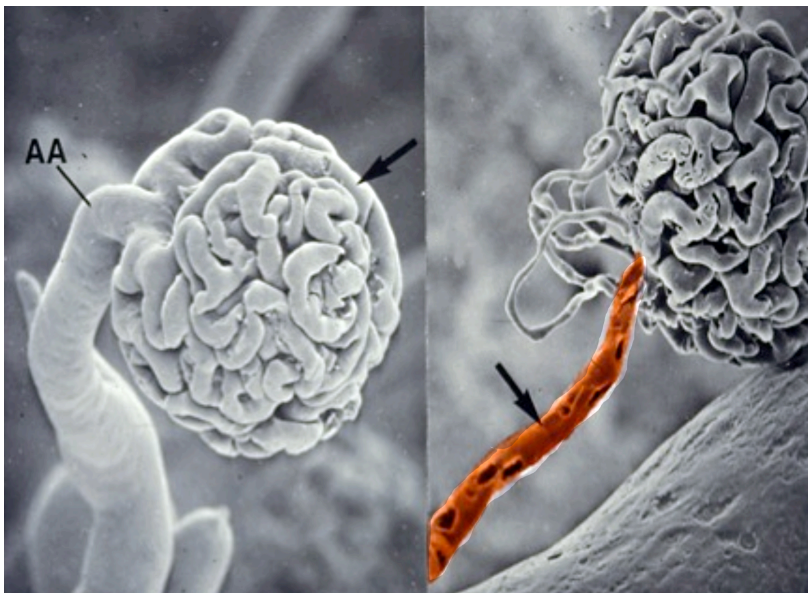

Figure 1.7 CNI induced vasoconstriction and glomerular collapse. Scanning electron micrograph of afferent arteriole (AA) and glomerular tuft from control is shown on the left panel. Right panel is a similar micrograph from CsA treated animal. Arrowhead highlights degree of vasoconstriction of AA on right panel and glomerular collapse. Adapted from (English *et al*. 1987).

1.7.2 Nitric oxide

Initial investigations for identifying specific CNI nephrotoxicity pathways focused on nitric oxide (NO) as it is one of the most potent agents able to induce vasodilation within the vascular bed (Bryan *et al*. 2009). Several groups have shown CNIs are able

to impair endothelium-dependent vasodilation mediated through NO in a range of experimental protocols. These range from single cell lines through to human *in vivo* studies investigating aorta, arteries, and afferent and efferent arterioles (Hortelano *et al*. 2000; Diederich *et al*. 1994; Navarro-Antolin *et al*. 2000).

Since CsA has also been shown to inhibit acetylcholine-induced NO production and subsequent vasodilation (Roullet *et al*. 1994), it would therefore seem logical that an increase of NO during CsA treatment would rectify the vascular dysfunction. Both animal and human studies have investigated L-arginine supplementation for preventing a decrease in systemic NO bioavailability. L-arginine is the immediate precursor to NO however investigative studies have had varying degrees of success. In rats, L-arginine was able to completely ameliorate renal dysfunction induced by CsA (Amore *et al*. 1995), however in human studies, no beneficial effect was observed with a similar supplementation protocol (X. Z. Zhang *et al*. 2001). Histopathological lesions of the renal vasculature and tubulointerstitium have also been reported to be ameliorated by L-arginine supplementation (Chander & Chopra 2005). However, contradictory studies have found elevated expression of RNA and protein levels of endothelial NOS (eNOS) in the renal cortex of rats after administration of CsA but with no increased levels of circulating or renal NO (Navarro-Antolin *et al*. 2000; Stroes *et al*. 1997).

Increased levels of NO metabolites in urine have been observed as well as an increased binding capacity of transcription factor AP-1 to the eNOS promoter, ultimately increasing NO production, after CNI administration (Stroes *et al*. 1997; Su *et al*. 1995). Interestingly, studies have shown CsA is able to increase NOS production in healthy non-transplant volunteers, but impairs basal and stimulated NO production in renal transplant patients (Morris *et al*. 2000).

Endothelial NOS is not the only NOS isoform that CNI's are able to alter. Hamalainen *et al* demonstrated inducible NOS (iNOS) was down-regulated by CsA in both epithelial and macrophage cell lines, in a NF-$_{K}\beta$ independent manner, while Dusting *et al* reported similar findings with a macrophage cell line but interestingly, also in vascular smooth muscle cells (Hamalainen *et al*. 2002; Dusting *et al*. 1999). This highlights the role of NO production in CNI therapy and direct effects on vascular smooth muscle, propagating into hypertension and nephrotoxicity.

CNIs are also known to increase free radical formation and superoxide production, thought to originate from vasoconstriction-associated hypoxia (Diederich *et al*. 1994).

Vasoconstriction-associated hypoxia stems from vasoconstriction increasing peroxynitrite while superoxide decrease NO production and bioavailability, resulting in decreased vasodilation and continuous vasoconstriction (Diederich *et al*. 1994). CsA also reduces eNOS-mediated NO production through various other pathways including protein kinase C and vascular endothelial growth factor (VEGF) (Kou, Greif & Michel 2002b; Lungu *et al*. 2004).

An interesting animal study by Zhong *et al* clearly highlighted CsA is able to induce hypoxia and produce new free radical classes exclusively within the kidney (Luntz *et al*. 2005). Interestingly, this was prevented with the addition of dietary glycine. How glycine is able to prevent CsA nephrotoxicity is still unclear, but the majority of hypothesis suggest minimisation of hypoxia-reoxygenation through a variety of pathways (Zhong *et al*. 1999; Luntz *et al*. 2005; Zhong *et al*. 1998). Suggested mechanisms include a decrease in renal sympathetic nerve firing and direct inhibition of vascular smooth muscle cell contraction (Zhong *et al*. 1999). The HEGPOL study is further investigating the beneficial effects of dietary glycine, albeit in liver transplant patients treated with CsA, and may provide a novel, cost effective, therapeutic strategy for prevention of CNI nephrotoxicity (Luntz *et al*. 2005).

Taken together, it is apparent that NO plays a vital role in vascular dysfunction and that unobstructed vasoconstriction, possibly through decreased NO bioavailability and increased free radical production, could be a foremost mechanism in CNI-induced nephrotoxicity.

1.7.3 Effect of CNIs on the production of endothelin

There is increasing evidence that CNI nephrotoxicity not only stems from decreased production of vasodilators but also from increased production and secretion of vasoconstrictor substances, predominately endothelin (ET) (Perico *et al*. 1990).

ET is a potent vasoconstrictor, with 3 isoforms, ET-1, 2 and 3, and is ubiquitously released within the kidney and vascular beds (Ramirez *et al*. 2000). It acts by binding to either of its receptors, ET_A or ET_B, and ultimately increases vasoconstriction through their coupling of corresponding G proteins, G_q and G_i, respectively (Yoshida *et al*. 1994).

The association of increased ET production and CsA nephrotoxicity was first identified by Nakahama and colleagues, who were able to display CsA stimulated ET

release from a renal epithelial cell line (Nakahama 1990). Animal studies that followed confirmed ET's role in CsA-induced vasoconstriction and was further highlighted in liver and other solid organ transplant patients with CsA immunosuppressive regimes, all resulting in an increased circulation of ET (Kon *et al*. 1990).

ET's role has been studied extensively with respect to CNI nephrotoxicity and much of the current research focuses on the use of anti-endothelial antibodies and ET_A and ET_B receptor antagonists.

Antibodies targeting ET have shown to partially reduce CNI-induced vasoconstriction and the associated decline in GFR, albeit in rat models (Perico *et al*. 1990). Contradictory to the findings of Perico *et al* with ET antibodies, Fogo and colleagues demonstrated that ET_A receptor antagonists where able to attenuate CsA-induced reduction in GFR and renal blood flow (RBF), but only when infused prior to CsA administration and not when used simultaneously or following CsA therapy (Fogo *et al*. 1990). However, Davis *et al* failed to highlight any improvement in renal function after using selective ET_A receptor antagonists or with an ET_A and ET_B receptor antagonist combination (Davis *et al*. 1994). Taken collectively, it is clear that ET does have a functioning role in CsA nephrotoxicity and possibly results in overwhelming vasoconstriction, development of hypertension and ultimately, significant reduction of renal function. Interestingly, the exact mechanism or pathway for CNI-mediated increase in ET is still not clear, as is similar to CNI nephrotoxicity in general.

1.7.4 Effect of CNIs on the production of thromboxane

Thromboxane is an additional vasoconstrictor that is associated with CNI nephrotoxicity. It acts similarly to ET, by binding to its G protein-coupled receptor, Gq, and stimulating vascular smooth muscle contraction through the PIP_2 pathway (Dorn & Becker 1993). Spurney *et al* clearly demonstrated the role for thromboxane in CNI nephrotoxicity with their results highlighting the improvement of GFR and overall vascular resistance in rats treated with a specific thromboxane A2 inhibitor while receiving CsA treatment (Spurney *et al*. 1990).

The increased production of thromboxane *via* CNI administration is thought to derive from activated platelets and macrophages within the kidney, increased lipid peroxidation, increased reactive oxygen species (ROS) production and endothelial injury (Kopp & Klotman 1990; Randhawa *et al*. 1997; Krejci *et al*. 2010). However,

clinical trials hoping to target these specific side effects have had mixed success (Grace *et al*. 1987; Perez de Hornedo *et al*. 2007). Weir *et al* piloted the use of a selective thromboxane synthase inhibitor in a cohort of renal transplant patients, which ultimately failed to protect against CsA nephrotoxicity, despite reducing urinary and systemic thromboxane metabolites (Weir *et al*. 1992). However, Smith *et al* demonstrated an improvement in renal function along with a decrease in urinary thromboxane A2 after treatment with an alternative selective thromboxane synthase inhibitor (Smith *et al*. 1993). Therefore it remains unclear to what extent thromboxane is a prerequisite in the development of CNI nephrotoxicity, especially with its origin in the arachidonic acid pathway and interrelationship with prostacyclin and prostaglandins (Parra *et al*. 1998).

1.7.5 Effect of CNIs on the production of prostaglandin & prostacyclin

Both prostaglandin and prostacyclin are vasodilatory prostanoids that are able to increase GFR and maintain the normal homeostatic gradient under hemodynamic stress conditions (Pugliese & Ciabattoni 1984). They are derived from the conversion of arachidonic acid (A.A) *via* cyclooxygenase enzymes (COX), of which three forms exist, COX-1, COX-2 and COX-3 (Berti 2013).

The foremost prostaglandin that has a role in regulating normal renal function is prostaglandin E_2 (PGE_2) (Ryffel *et al*. 1986). Along with vasodilation of blood vessels, PGE_2 also potentiates platelet aggregation and is involved in inflammation and cell growth (Vezza *et al*. 1993).

Höcherl *et al* were able to demonstrate not only a reduced production of PGE_2 after CNI administration in the rat kidney, but also a reduced expression of COX-2, suggesting a role for COX-2 expression and PGE_2 production in the development of CNI nephrotoxicity (Hocherl *et al*. 2002). Several studies have further investigated this pathway, using PGE_2 administration to overcome CNI-mediated vasoconstriction. However, only a small number of studies have demonstrated, the "protective" effect of PGE_2 administration and conversely, the protective mechanism is thought to originate from a decreased intestinal absorption of CsA rather than PGE_2's vasodilatory properties (Ryffel *et al*. 1986).

Interestingly, misoprostol is a PGE_1 analogue that has shown to have renal protective effects. PGE_1 is a vasodilatory prostaglandin with potent inhibitory platelet aggregation properties (Moran *et al*. 1990). When used in a rat model, misoprostol was shown to attenuate CsA nephrotoxicity *in vivo* (Paller 1988). In addition, when

used in humans, misoprostol was also shown to improve renal function after CsA administration, but the protective effect was attributed to a lower incidence of acute rejection rather than a protective vasodilatory effect derived from misoprostol itself (Moran *et al*. 1990). This was further confirmed by Boers *et al* who did not observe any beneficial effects of misoprostol on renal function when treating patients with CsA for rheumatoid arthritis (Boers *et al*. 1992).

Prostacyclin (PGI) is a well-known potent vasodilator that is implicated in the regulation of vessel tone along with having antiproliferative and antithrombotic properties (Berti 2013). CNIs are known to decrease PGI production and studies with PGI analogues have shown a renoprotective role against the functional changes induced by CNIs in animal models. However, clinical studies have shown conflicting results with a prostacyclin analogue, iloprost, having no effect on CsA-induced reduction of GFR in renal transplant patients (Voss *et al*. 1988; Hansen *et al*. 1996).

It is clear that CNIs have the ability to disrupt a fine balance between vasoconstriction and vasodilation, however CNIs are also involved in the generation of local vasodilatory molecules (Stroes *et al*. 1997), further adding to the already complex story. The disruption between the dynamic array of vasodilators and vasoconstrictors predominately leads to vasoconstriction, however it is still unknown which vasoconstrictor or vasodilator, if any, plays the key role in the development of nephrotoxicity. This is further complicated by the fact each vasoactive substance appears to be activated by a different independent pathway (Naesens *et al*. 2009).

1.7.6 Effect of CNIs on the renin-angiotensin-aldosterone system

As well as the significant disruption of vasoactive substances, CNI nephrotoxicity is thought to be, in part, due to the activation and overstimulation of the renin-angiotensin- aldosterone system (Naesens *et al*. 2009).

The renin-angiotensin-aldosterone system (RAAS) is a major hormonal signalling pathway that regulates BP and fluid balance within the human body.

The RAAS can be initially stimulated through a decrease in blood pressure and/or blood volume or electrical stimulation, for example, “Fight or Flight” situations (Koeppen & Stanton 2013b). Juxtaglomerular cells within the kidney secrete renin directly into the systemic circulation in response to a drop of pressure or when stimulated by macula densa cells, through activation of their prorenin. Plasma renin

then converts angiotensinogen, released by the liver, to angiotensin I (Ruester & Wolf 2006). Angiotensin I is unstable and is subsequently converted to angiotensin II (ANG II) by the angiotensin-converting enzyme (ACE), produced by endothelial cells within the lung (Remuzzi *et al*. 2005). The main functions of ANG II are to increase blood pressure and/or blood volume, although through vasopressin release. ANG II stimulates the secretion of the water retaining hormone vasopressin (AVP) from the pituitary gland and the release of adrenaline and noradrenaline (NA) as well as aldosterone from the adrenal cortex (Rüster & Wolf 2006), all aiding in its function to increase blood volume and/or pressure.

The release of adrenaline and NA augments the vasoconstrictive effect of ANG II, further increasing pressure, whereas release of aldosterone increases water reabsorption to increase blood volume.

Aldosterone acts on mineralocorticoid receptors within principal cells of the distal convoluted tubule (DCT) and the collecting duct of the nephron, where it up-regulates and activates the epithelial sodium channel (ENaC) and sodium/potassium ATPase pump (Na^+/K^+-ATPase) to create a concentration gradient, resulting in increased reabsorption of Na^+, along with water through aquaporin's (AQPs), into the blood (Harrison-Bernard 2009). AVP helps regulate this water retention by increasing the water permeability of the principal cells. AVP induces the translocation of AQP's into the apical membrane of the DCT and collecting duct epithelial cells, allowing water to move down its osmotic gradient, increasing water reabsorption from the filtrate and increasing blood volume (Koeppen & Stanton 2013c; Koeppen & Stanton 2013d). AVP also helps regulate the balance of Na^+ and K^+ electrolytes, through regulation of the sodium-potassium-chloride cotransporter (NKCC2) the thiazide-sensitive sodium-chloride cotransporter (NCC) and ENaC, while increasing water volume (Harrison-Bernard 2009).

CNIs directly and indirectly lead to the activation of the RAAS. Direct activation is through the release of renin from juxtaglomerular cells, first demonstrated by Kurtz *et al*, who found a three-fold increase of renin release after CsA administration (Kurtz *et al*. 1988). This is followed by a secondary indirect activation of RAAS instigated by renal vasculature haemodynamic changes, increased arterial vasoconstriction, and also decreased production of vasodilators and increased endothelin secretion (Kurtz *et al*. 1988). As RAAS activation leads to ANG II induced reduction of blood flow and vasoconstriction, the addition of systemic CNIs further enhances the haemodynamic

changes associated with CNI's, representing a continuous loop of damage and nephrotoxicity, this can be seen in figure 1.8. Sodium reduction, which also stimulates renin release and thus RAAS activation, enhances CNI nephrotoxicity, which coincidently is the basis for modern animal studies investigating CsA nephrotoxicity (Bennett *et al*. 1996; Bennett 1997). Recruitment of renin containing cells in afferent arterioles is also observed with the use of CsA, further increasing renin secretion and RAAS activation (D. B. Lee 1997; Lassila 2002). This dramatic increase of renin production can be seen clinically as hyperplasia of the juxtaglomerular apparatus (JGA), potent vasoconstriction of afferent arterioles and proliferation of VSMC's, all further contributing to the continuous onslaught of CNI therapy (Iijima *et al*. 2000; Bohle *et al*. 1982). Activation of RAAS, the recruitment of renin containing cells and mobilization of VSMC's is similar to other contributing side effects of CNI nephrotoxicity with the underlying mechanisms remaining ambiguous and further complicates the understanding of the pathogenesis of renal damage due to CNIs.

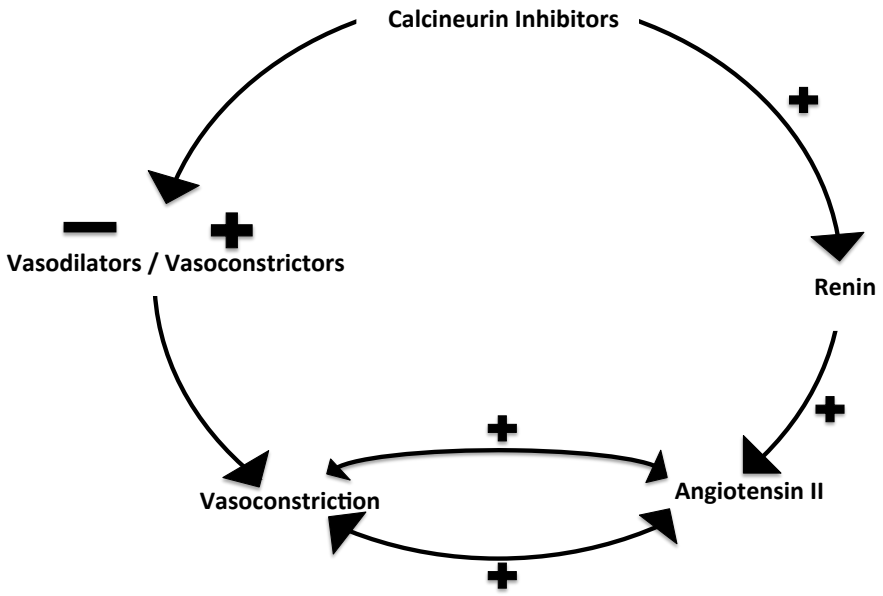

Figure 1.8 CNI and ANG II interactions to induce vasoconstriction. CNIs directly stimulate increased ANG II concentrations through increased renin release from juxtaglomerular cells, resulting in increased vasoconstriction. CNI's indirectly increase ANG II concentrations through a decrease of vasodilators and increase vasoconstrictors, resulting in increased vasoconstriction and subsequently, increased ANG II concentrations.

A general consensus was that inhibition of RAAS would potentially help alleviate the sustained vasoconstriction and reduce overall renin secretion (D. B. Lee 1997; Lassila 2002; Hiremath *et al*. 2007). This was investigated from two different perspectives: ANG II receptor inhibition and ACE inhibition.

ANG II receptor blockers (ARBs) are specific inhibitors to ANG II type I receptors (AT_1) and thus prevent ANG II from binding. Their use for CNI nephrotoxicity has been extensively investigated, both in animal studies and human trials, however the results are contradictory and vary extensively (B. K. Sun *et al*. 2005; Hannedouche *et al*. 1996). Losartan is the most common ARB to be investigated with Inigo *et al* finding RBF and vascular resistance improved with losartan treatment in patients undergoing CsA therapy but observed no improvement in GFR (Iñigo *et al*. 2001). However, Burdmann *et al* demonstrated overall renal improvement and reduction of interstitial fibrosis with losartan and CsA (Burdmann *et al*. 1995). Interestingly, out of the various studies that did show improvement with ARBs, one of the main observations that repeatedly occurred was a reduction of transforming growth factor-β (TGF-β) (Iñigo *et al*. 2001; Lassila *et al*. 2000). The influence of TGF- β is and CNI's is discussed later in this chapter.

ACE inhibitors (ACEi) are able to reduce or prevent RAAS activation through inhibited conversion of angiotensin I to ANG II, thereby preventing full ANG II conversion and activation of RAAS.

Along with ARBs, ACEi have also been extensively studied in both animal and human trials of for prevention of CNI nephrotoxicity. ACEi are particularly useful for ameliorating CsA associated hypertension, and in combination with ARBs, have been found to almost completely inhibit CsA nephrotoxicity and any of its markers in animal models (Pichler *et al*. 1995; Mervaala *et al*. 1999). However, taking human trials into consideration, the evidence is less convincing. Sennesael and colleagues compared the effects of perindopril (an ACEi) to amlodipine (a Ca^{2+} channel blocker) when both used in CsA treatment (Sennesael *et al*. 1995). Their results indicated both drugs were equally effective in lowering BP and inhibiting the functional haemodynamic changes associated with CsA. However, with such a small sample size of 10 patients, their results cannot be fully extrapolated as a concrete method for reducing CsA nephrotoxicity or associated blood pressure changes (Sennesael *et al*. 1995). Burdmann *et al* also investigated enalapril, an ACEi, along with losartan. Similar to the results with losartan by Sennesael *et al*, enalapril reduced the

production of interstitial fibrosis and improved overall renal function originating from reduced TGF-B production (Burdmann *et al*. 1995). Furthermore, most, if not all, studies were shown to have a reduced creatinine clearance, possibly through haemodynamic changes. Given that creatinine clearance is possibly the most widely used, and respected measure of renal function, especially nephrotoxicity (Bach & Lock 1987), the studies do not fair well in translation from "Bench to Bedside" and prevention of CsA nephrotoxicity.

Taken together, inhibition of RAAS, either by ARBs, ACEis or a combination of both still does not elucidate the origins of CsA nephrotoxicity, nor show whether either of these drug types can slow the progression of renal damage in a clinical setting.

1.8 Tacrolimus nephrotoxicity

The majority of early CNI nephrotoxicity research focused on CsA as it was the first available CNI but also the most widely used. However, nephrotoxicity with FK506 use was soon becoming just as routine. Similar to CsA, nephrotoxicity was present in two forms: functional and structural, with the cause of nephrotoxicity still unclear even to the present day. Animal and human studies have shown FK506 decreases GFR and increases renal vasculature resistance, increases the production of vasoconstrictors along with associated decrease of vasodilators, activates RAAS and increases stimulation of sympathetic nerve activity, which all indicate a similar nephrotoxic profile to CsA (Randhawa *et al*. 1997; Naesens *et al*. 2009).

An important study by Sigal and colleagues demonstrated the mechanisms of immunosuppression by CNI's, inhibition of calcineurin, correlated to their ability to induce nephrotoxicity (Sigal *et al*. 1991). The study involved 61 CNI analogues and highlighted an interesting point with regards to the degree of calcineurin inhibition in specific tissues, greatest in the kidney, and the specific side effects of CNI's in certain tissue, emphasizing the direct impact calcineurin inhibition has in the development of CNI nephrotoxicity. Furthermore, it is becoming apparent that the calcineurin-NFAT pathway may be fundamental in the pathogenesis of CNI nephrotoxicity especially given the pathways role in COX-2 regulation (Abraham *et al*. 2012).

The COX-2 gene promoter contains binding sites for NFAT and has been suggested to be important for COX-2 gene expression *in vitro* (Rao *et al*. 1997) and therefore, it could be postulated that inhibition of calcineurin simultaneously attenuates COX-2 expression and associated decrease of PGE_2 production, resulting in a influential

mechanism for CNI-induced renal vasoconstriction and decreased GFR (Sugimoto *et al*. 2001). Interestingly, a new CNI still in development (voclosporin) only induced renal dysfunction in a very small number of patients during a clinical trial, which was not associated with a decrease in PGE_2 (Papp *et al*. 2008). With regards to renal transplantation, voclosporin is just as potent to FK506 in respect to acute rejection, safety profile and triglyceride or magnesium levels (Ling *et al*. 2013). However, short-term results have not shown voclosporin to be of greater benefit over FK506 in respect to overall kidney function and only long-term results will truly indicate if it is of superior quality for transplantation (Ling *et al*. 2013).

Although FK506 is up to 100 times more potent than CsA (Assmann *et al*. 2001) there is extensive evidence demonstrating that it has a lower nephrotoxicity potential than CsA. Animal and human studies have shown that the vasoconstrictive effect of FK506 is weaker than CsA (Klein *et al*. 2002; Nankivell, Chapman, *et al*. 2004; Nankivell, Borrows *et al*. 2004), it also has a lower fibrogenic potential (Jain *et al*. 2000). However as with CsA, results vary considerably and conflict depending on the experimental protocol.

The group of van Groningen were unable to show FK506's lower fibrogenic potential and in fact, demonstrated a contradictory result with increased development of fibrosis with FK506 use in renal transplant patients (Groningen *et al*. 2006). Furthermore, single and multicentre studies have indicated the benefit of FK506 over CsA with regards to overall renal function, however, identical studies, single and multicentre, show conflicted results with no benefit whatsoever (Israni *et al*. 2002; Kobashigawa *et al*. 2006; Lucey *et al*. 2005). Importantly, these studies where all conducted in a non-renal transplant setting. Analysis of renal transplantation nephrotoxicity is much more difficult to extrapolate due to interference with renal allograft rejection phenomena. This being said, when FK506 and CsA had similar levels of acute rejection, equal efficacy and in the renal transplantation setting, FK506 was associated with considerably lower serum creatinine levels and/or higher GFR compared to CsA therapy and also improved graft survival (Vincenti *et al*. 2007; Webster *et al*. 2005). Studies have also highlighted conversion from CsA to FK506 for allograft dysfunction results in a significant improvement in renal function, highlighting the original role of FK506 for "rescue therapy" in high-risk patients (Garlicki *et al*. 2006). This is further demonstrated by the SYMPHONY study, a large randomized multicentre trial investigating various immunosuppressive regimens,

which exhibited improved graft function and survival with the use of low dose FK506 compared to CsA at varying doses (Ekberg *et al*. 2007).

In addition, FK506 does not present or develop influential side effects, excluding nephrotoxicity. These include lower incidences of hypercholesterolemia and hypertension, reduced hirsutism, gum hyperplasia and gingivitis, all proposing FK506 as a superior choice in immunosuppression (Mihatsch *et al*. 1998; V. W Lee & Chapman 2005). Conversely, it is associated with increased diabetes mellitus, diarrhoea and hypomagnesaemia, tremor, and glucose intolerance (Mihatsch *et al*. 1998). Intriguingly, the reasons for these different profiles are still unknown and again, only add to the complexity of CNI-mediated adverse reactions.

1.9 Chronic nephrotoxicity

1.9.1 Chronic vascular nephrotoxicity

More importantly than the acute functional changes of CNI nephrotoxicity, chronic nephrotoxicity is quintessentially the Achilles heal of modern day immunosuppression. Unlike acute CNI nephrotoxicity, which can be overcome with dosing alterations and withdrawal regimes, chronic CNI nephrotoxicity leads to a complete deterioration of the renal architecture with the almost inevitable progression to chronic kidney disease (CKD) and renal failure (Naesens *et al*. 2009).

An early study by Myers *et al* was the first to demonstrate CsA is capable of both acute functional changes but also irreversible alterations in renal architecture (Myers *et al*. 1984). The study highlighted early development of interstitial fibrosis, tubular atrophy and focal glomerular sclerosis after just 12 months of CNI therapy. It was then later discovered that vessels, tubulointerstitium and glomeruli could be irreversibly altered with CNI use and progressed with time after transplantation. Remarkably, 10 years post-transplantation, biopsy lesions suggestive of chronic CNI nephrotoxicity were seen in virtually all patients (Bennett *et al*. 1996) however it must be made clear that CNI nephrotoxicity has no specific lesions, therefore to suggest CNI nephrotoxicity alone as the only contributing factor, and that no other underlying aspects like hypertension or hyperlipidaemia may have played a role in the development of renal decline is somewhat naïve, especially as even to this day,

there is very little evidence for specific markers in CNI pathology (Nankivell, Borrows, C. L. Fung, *et al*. 2004).

As already stated, chronic use with CNIs effects all three major compartments of the kidney but importantly, all subdivisions have individual mechanisms for the development of nephrotoxicity and distinct pathologies. This is important for clinical identification of the term chronic CNI nephrotoxicity, which ironically, the term "chronic" has often been used haphazardly with no convincing evidence to suggest otherwise and only due to allograft dysfunction (Fioretto *et al*. 2011). Therefore, the term chronic CNI nephrotoxicity must be used to describe CNI-induced structural damage, often in the form of intestinal fibrosis visualized through biopsy staining (S. H. Lee *et al*. 2005; Gaston 2009; Bennett *et al*. 1996). Chronic nephrotoxicity is often associated with deteriorating hyaline changes in afferent arterioles consisting of endothelial cell swelling, hyaline deposition and smooth muscle lesions and cell necrosis (Naesens *et al*. 2009). Although very few histological markers for CNI nephrotoxicity are thought to exist, due in part to allograft rejection phenomena, key markers help distinguish between nephrotoxicity and other underlying risk factors. In renal transplantation, the arteriolar lesions are thought to be markers for chronic nephrotoxicity rather than graft rejection (Bakker *et al*. 2004). Arteriole segmental thickening resulting in a "pearl necklace" type appearance on the outer region is typical for chronic CNI use, and helps characterise against normal arteriosclerosis, which is typically characterised by hyaline deposits localised under the endothelium (Liptak & Ivanyi 2006).

Acutely, CNI nephrotoxic vascular effects are the most predominant and clinically relevant for treatment. Commonly known as acute arteriolopathy (Mittal & Kohli 2014; Naesens *et al*. 2009), these functional changes have already been discussed, but a combination of increased vasoconstrictors and reduced vasodilators, activation of RAAS, production of free radicals and sympathetic nerve activation ultimately lead to renal vasculature dysfunction and the gradual decline of GFR and overall kidney function.

Chronic vascular effects are dissimilar by the fact they cannot be overcome through medical intervention. *i.e.* removal of insult or dosing alterations.

Nodular hyaline deposits in afferent arterioles, arteriolar hyalinosis, is characterised by replacement of smooth muscle cells by protein deposits, hyaline, at the boundary

wall of afferent arterioles (Nolin & Himmelfarb 2010) and is commonly regarded as a hallmark for CNI nephrotoxicity (Mihatsch *et al*. 1998). Inevitably these deposits become larger and subsequently narrow the vascular lumen, reducing blood circulation and decrease GFR. Although regarded as irreversible, experimental and clinical studies have produced very interesting data with regards to fibrosis regression. Collins *et al* reported that complete regression of severe CsA-induced artriolopathy and remodelling of arterioles could be achieved with complete removal of CsA therapy or a severe reduction in dosage (Collins *et al*. 1992). These findings are similar to Morozumi *et al* who observed the complete regression of CsA-associated artriolopathy and remodelling of arterioles with preserved renal function after complete removal of CsA therapy or severely reduced dosage (Morozumi *et al*. 1992).

The pathogenesis of chronic CNI nephrotoxicity, specifically vascular toxicity, has been comprehensively studied over the past twenty years, however, the origins of these lesions have been difficult to extrapolate due to the lack of viable reproducible animal models. It wasn't until the laboratory of Elzinga and Rosen discovered that sodium depletion was able to exacerbate CsA nephrotoxicity and produced a quicker chronic model compared to previous methods but more importantly, sodium depletion produced histological changes that where clinically relevant with the human setting (Elizanga *et al*. 1993).

1.9.2 Calcineurin and NFAT

Mechanisms for chronic CNI nephrotoxicity are still poorly defined but are understood to be similar to acute nephrotoxicity, with a combination of factors contributing to the overall smooth muscle changes and deposition of granular protein (Chapman 2011). Interestingly, there have been studies indicating the importance of the calcineurin/NFAT pathway in smooth muscle cell regulation and differentiation. Graef *et al* were able to show early calcineurin/NFAT signalling initiates the future cross talk and stability between vessels and surrounding tissues that develop the vasculature network (Graef *et al*. 2001). It is therefore possible CNIs may be responsible for vasculature remodelling through direct inhibition of calcineurin as well as an onslaught of other contributing factors *i.e*. sustained vasoconstriction (Sieber & Baumgraass 2009).

1.9.3 Chronic interstitial nephrotoxicity

1.9.3.1 Reactive oxygen species

Histopathology, chronic tubulointerstitium CNI-induced nephrotoxicity will lead to one very apparent feature, striped interstitial fibrosis (Wang & Salahudeen 1995; Liptak & Ivanyi 2006). This often occurs in parallel with the persistent vasoconstrictive effects of CNIs and arterial narrowing, leading to subsequent renal ischemia and possible ischemic reperfusion injury and generation of free radical production and cell apoptosis (Djamali 2007; LopezOngil *et al*. 1996). Zhong *et al* have demonstrated this pathway with local ischemia of the tubular-interstitial region from CNI induced vasoconstriction, leading to the formation of ROS production (Zhong *et al*. 1998). ROS production in the development of chronic nephrotoxicity was first highlighted by Wang *et al* who observed the beneficial effect of vitamin E ROS scavenging in CsA-induced nephrotoxicity *via* lipid peroxidation (Wang & Salahudeen 1995). However, clinical trials using vitamin E as an antioxidant have had poor outcomes and furthermore, it soon became apparent that vitamin E reduces trough-levels of CsA, rather than counteracting ROS production, leaving transplant patients at substantial risk of infection or graft loss (Barany *et al*. 2001; de Vries *et al*. 2006; Wang & Salahudeen 1995).

Ischemic conditions in renal tissue is similar to other organs; vascular vasoconstriction resulting in subsequent re-oxygenation injury and formation of ROS and free radicals leading to cell injury and death *via* apoptosis (Longoni *et al*. 2001). Scavengers of ROS therefore seem a plausible target for prevention of chronic nephrotoxicity. Catalase, an enzyme capable of breaking down hydrogen peroxide (immediate precursor of the hydroxyl radical) has been indicated to reduce CsA associated cellular apoptosis (Jennings *et al*. 2007) however, CsA is capable of direct production of ROS which was exhibited *via* proximal tubular epithelial cells gathering intracellular ROS and lipid peroxidation products (Galletti *et al*. 2005). Furthermore, activation of the RAAS has also been identified as a pathway in the direct production of ROS through CNI therapy (Parra *et al*. 1998; Nishiyama *et al*. 2003).

1.9.3.2 TGF-β

Although it is unanimously understood there is no single contributing factor to the pathogenesis of chronic CNI nephrotoxicity, TGF-β appears to be a dominant cytokine that continuously presents itself through CNI-induced upregulation. TGF-β plays a major role in the generation of renal fibrosis through direct stimulation of extracellular matrix (ECM) proteins but also reducing collagenase production which limits the degradation of ECM (Wolf 2006). Renal TGF-β production has been confirmed in interstitial macrophages, fibroblasts and tubular epithelial cells, with studies suggesting the majority of TGF-β is confined to interstitial fibroblasts (Feldman *et al*. 2007; Y. H. Liu 2004). CsA also stimulates systemic production of TGF-β *via* autocrine mechanisms and upregulation of its receptors (Border & Noble 1994). Interestingly, TGF-β is upregualted by CNIs in proximal tubular cells independent of acute functional alterations and induces epithelial to mesenchymal transition (EMT) (Slattery *et al*. 2005).

1.9.3.3 Epithelial to mesenchymal transition (EMT)

EMT is currently a controversial subject with regard to chronic fibrosis; some investigators hypothesise it is the major pathway of scar forming tissue, while others have investigated exclusively to invalidate this hypothesis and believe it only as a phenomena (Slattery *et al*. 2005; Faulkner *et al*. 2005; Y. H. Liu 2004).

EMT is a multistep process in which epithelial cells lose their epithelial phenotype and acquire new characteristics features of mesenchyme including disruption of polarised epithelial cell morphology, *de novo* α-smooth muscle actin expression and reorganization, down regulation of E-cadherin resulting in the loss of cell to cell adhesion, destruction of basement membranes and increased cell migration and invasion (Thiery & Sleeman 2006). Remarkably, the exact opposite of these processes can also occur in mesenchymal-epithelial transition (MET). The complex balance between EMT and MET can be seen in figure 1.9.

Vieira and colleagues demonstrated a progressive increase in renal TGF-β production with CsA treatment resulting in development of tubulointerstitial fibrosis and Cuhaci *et al* found >70% of renal biopsies from renal transplant patients treated with CsA had extremely high levels of TGF-β staining (Vieira *et al*. 1999; Cuhaci *et al*. 1999).

Interestingly, the patients with high TGF-β had a 3 times higher rate of renal decline compared to patients with no or little TGF-β (Vieira *et al*. 1999; Cuhaci *et al*. 1999). CsA has also been shown to upregulate TGF-β expression in juxtaglomerular cells (Wolf *et al*. 1990), which could be important in chronic activation of RAAS since TGF-β expression is thought to be mediated *via* both an ANG II dependent and independent mechanism (Campistol *et al*. 1999; Wolf 2006; Iñigo *et al*. 2001; B. K. Sun *et al*. 2005). Animal studies have exhibited a significantly lower expression of TGF-β and interstitial fibrosis after administration of losartan, an AT1 antagonist (Campistol *et al*. 1999). Furosemide and hydralazine have also shown to reduce TGF-β but not associated CNI-induced arteriolopathy (Pichler *et al*. 1995), suggesting ANG II and AT1 partnership play a major role in the pathogenesis of CNI-induced arteriolopathy.

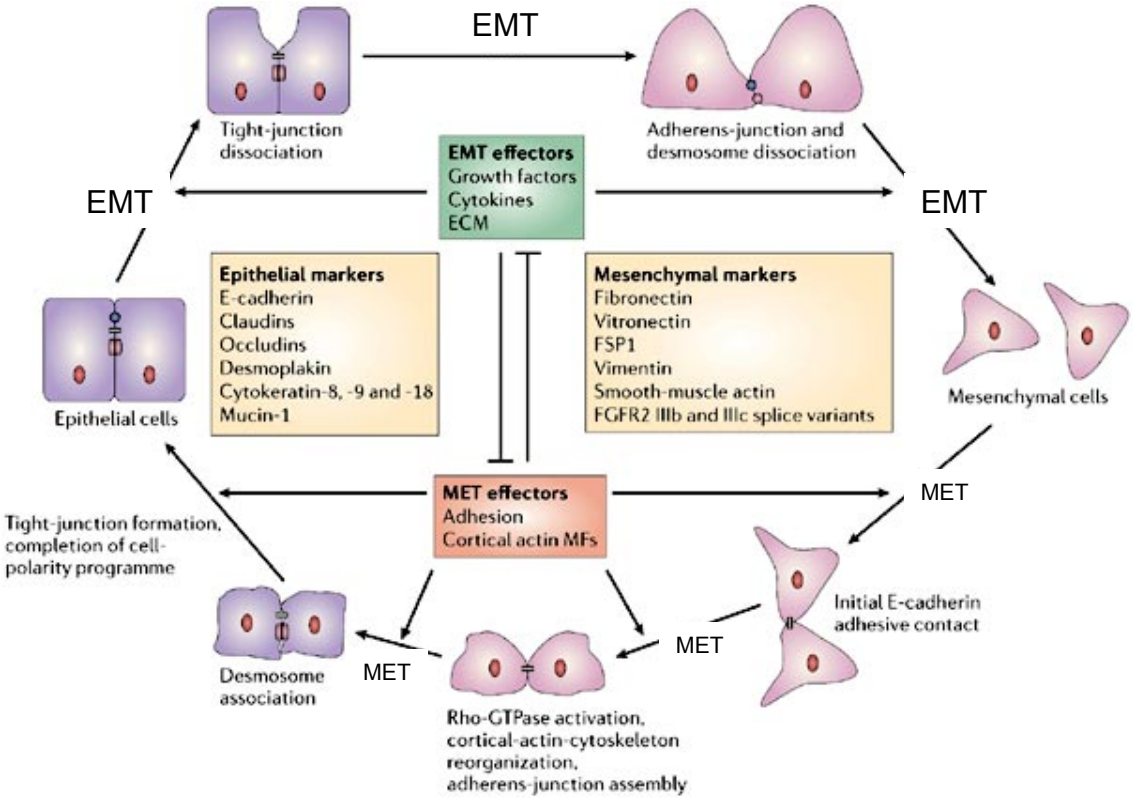

Figure 1.9 Epithelial cell transitions between EMT and MET. Cycle of events during which epithelial cells are transformed into mesenchymal cells and vice versa. The different stages during EMT and the reverse process (MET) are regulated by effectors of EMT and MET, which influence each other. Important events during the progression of EMT and MET, including the regulation of the tight junctions and the adherens junctions, are highlighted. Epithelial cell markers are highlighted in left inset while mesenchymal markers markers in right inset. E-cadherin, epithelial cadherin; ECM, extracellular matrix; FGFR2, fibroblast-growth-factor receptor-2; FSP1, fibroblast-specific protein-1; MFs, microfilaments. Adapted from (Thiery & Sleeman 2006).

1.9.4 Glomerular nephrotoxicity

Chronic glomerular nephrotoxicity is probably the most fundamental aspect of renal decline *via* nephrotoxicity. Once the glomeruli have been subject to chronic onslaught of vasoconstriction and hyaline deposition, they are unable to filter blood, process metabolites and excrete toxins (Sánchez-Lozada *et al*. 2005).

The most common form of glomerular injury is global glomerulosclerosis, and is result of CNI-induced arteriolar hyalinosis, arteriolopathy and glomerular ischemia (Perico *et al*. 1996). However, global glomerulosclerosis is not specific to chronic CNI use and its development can be associated with various underlying factors. The extent of glomerular vasoconstriction induced *via* CNIs can be seen in figure 1.7. In addition, focal segmental glomerulosclerosis is also associated with CNIs, deriving from hyperfilatraion injury connected to arteriolar hyalinosis or global glomerulosclerosis (Nankivell, Borrows, C. Fung, *et al*. 2004; Nankivell *et al*. 2004).

Arguably the most influential and well-known study investigating chronic CNI nephrotoxicity was by Nankivell *et al* (Nankivell *et al*. 2004). The authors intended to look for the progression of CsA nephrotoxicity *via* biopsy examination which was took at routine intervals; before implantation; 1, 2 and 4 weeks; after months 3, 6 and 12 then finally yearly biopsies for 10 years post transplantation. Their results proved the unequivocal progression of renal decline with 100% of patients showing lesions considered reliable of chronic CsA nephrotoxicity (Nankivell *et al*. 2004). An important note to add is that other causes of hyalinosis including hypertension, ischemic injury, dyslipidaemias, hyperglycaemia and donor hyalinosis were ruled out, therefore concluding that long-term CNI therapy was inappropriate for renal transplantation (Nankivell *et al*. 2003). Interestingly, studies were on-going at the time looking for minimal exposure to CNIs and alternative immunosuppression throughout the Nankivell *et al* study (Baboolal 2003; Chapman 2011; Olyaei *et al*. 2001).

1.9.5 Chronic tubular nephrotoxicity

Lastly, chronic tubular toxicity, toxic tubulopathy, plays a major role in the development of CNI nephrotoxicity and renal decline (Krejci *et al*. 2010).

The SEMINAL study by English and colleagues was one of the distinguished investigations to demonstrate proximal tubule necrosis is not a feature of acute CNI

nephrotoxicity in animal models but rather a consequence of chronic CNI exposure (English *et al*. 1987). However, *in vitro* studies and clinical trials suggested CNI-induced tubular injury was a subtler affair. There has been numerous studies showing increased urinary excretion of proximal tubule derived enzymes, increased excretion of magnesium, impaired urinary concentrating ability and hyperkalemia after CNI therapy (Deppe *et al*. 1997; Holzmacher *et al*. 2005; Yamauchi *et al*. 1998), suggesting a form of CNI related tubule dysfunction. *In vitro* studies have also highlighted direct dose-dependent toxic effects of CNIs on renal tubular cell lines with a variety of pathways contributing to their damage (Wilson & Hartz 1991). These include lipid peroxidation, tumour suppressor p53 expression, dysfunctional calcium signalling and reduced NO production, all recognised as tubular toxicity mechanisms (Galletti *et al*. 2005; Healy *et al*. 1998; Gordjani *et al*. 2000).

Heat shock proteins, a form of cell stress protein, have also been suggested in the development of tubular toxicity, although indirectly (Paslaru *et al*. 2000). Cavalho *et al* demonstrated only extremely high levels of CsA, 100ug/ml, caused direct tubular injury *via* heat shock protein expression but could be prevented with alterations of calcium or magnesium in the cell culture media (Carvalho da Costa *et al*. 2003).

Interestingly, chronic tubular damage leads to the development of atubular glomeruli, perfused glomeruli that are disconnected from their associated proximal tubule (Krejci *et al*. 2010). Histologically, they appear smaller and have capsular fibrosis or severely contracted within an enlarged glomerular cyst (Koesters *et al*. 2010; Krejci *et al*. 2010).

Together, these studies suggest that although acute tubular toxicity is not as widespread as vascular dysfunction, these small but important changes in tubular cell function may be relevant to cell survival and ultimately graft survival after long-term exposure to CNI's.

1.9.6 Isometric vacuolisation

Histologically, tubulopathy manifests after arteriolopathy (d'Ardenne *et al*. 1986; Mescher 2013). However it is thought to be just as significant in the development of CNI nephrotoxicity. Importantly, most tubular lesions accompanying CNI therapy are non-specific and seen in a variety of conditions and various therapies *i.e.* steroid and azathioprine administration and therefore to clinically identify CNI tubulopathy extra care must be taken (Russell *et al*. 2008).

The "typical" tubulopathy marker associated with acute CNI nephrotoxicity has historically been isometric vacuolization of the tubular cytoplasm, the tubular cells appear almost empty with large transparent vacuoles, derived from enlargement of the endoplasmic reticulum and increased lysosomes, see figure 1.10, (Sharma *et al*. 2010). Crucially, isometric vacuolization can be associated with CNI therapy without renal decline (Laftavi *et al*. 2010; Haas *et al*. 2004) and recently, studies have suggested it is not associated with the progression to chronic CNI nephrotoxicity making this historical marker possibly irrelevant (Naesens *et al*. 2007).

The possible mechanisms for CNI-induced isometric vacuolization are still unknown, and as with most CNI nephrotoxic pathways, a combination of factors plus underlying conditions is thought to contribute. The resulting ischemia through arteriolar vasoconstriction and the direct effect of CNI's on tubular epithelial cells causing endoplasmic reticulum (ER) dysfunction have been suggested to act synergistically to induce vacuolization (Mihatsch *et al*. 1986). Adding to the complexity of vacuolization, the lesion is occasionally observed in other similar renal settings other than transplantation e.g. ischemic epithelial injury and often referred to as osmotic nephrosis (Haas *et al*. 2004). Osmotic nephrosis can be distinguished from CNI tubulopathy by the varying size of vacuoles in osmotic nephrosis compared to typically isometric vacuoles in CNI-induced tubulopathy (Naesens *et al*. 2009). Therefore, it is clear that although isometric vacuolization may be an indicator for acute toxic tubulopathy, though no guarantee to be associated with CNI therapy, its relation to chronic nephrotoxicity is still uncertain and may not benefit from its identification.

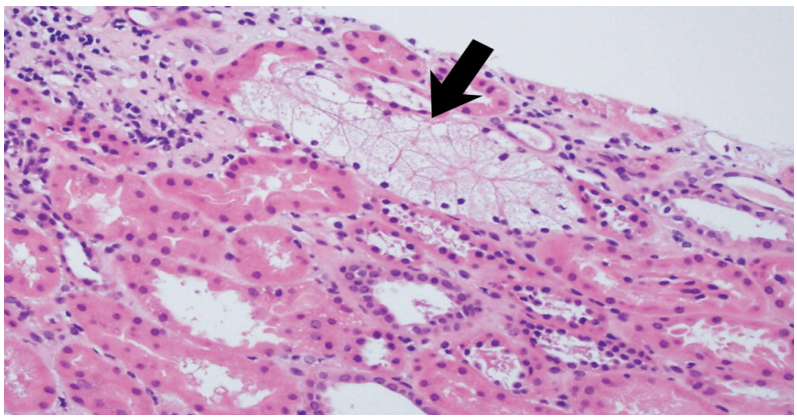

Figure 1.10 Isometric vacuolization. Renal biopsy showing focal tubular epithelial cell vacuolization (black arrow) surrounded by normal morphological tubule cells. Adapted from (Charney *et al*. 2009).

1.9.7 Inclusion bodies

Several clinical cases have noted the finding of inclusion bodies in tubular cytoplasm associated with CNI use, representing giant mitochondria and autolysomes (Mihatsch *et al*. 1986). However, these lesions are also nonspecific and often occur in ischemic injury without CNI treatment. In addition, inclusion bodies have been found in donor kidneys pre-transplantation therefore, pre-CNI administration and limit their usefulness in diagnostics of CNI nephrotoxicity (Morozumi *et al*. 1992).

1.9.8 CNI-induced apoptosis

CNI's have been shown to activate apoptosis genes and subsequently increase apoptosis in tubular cells, correlating with CNI tubular atrophy and tubulointerstitial fibrosis (Servais *et al*. 2008).

P-glycoprotein is completely inhibited by CsA and may additionally contribute to structural lesions of chronic nephrotoxicity by preventing P-glycoprotein from removing CsA within the cell therefore increasing local concentration and toxicity (Chaurk *et al*. 1995; Saeki *et al*. 1993). P-glycoprotein is a drug transporter expressed on the apical membrane of tubular epithelial cells (Saeki *et al*. 1993). Losartan has been shown to reduce the level of CNI-induced apoptosis in proximal tubule cells suggesting a role for ANG II in this pathway, further confirmed by other groups (Xiao *et al*. 2013) highlighting the role ANG II may have in the pathogenesis of chronic CNI nephrotoxicity (Thomas *et al*. 1998).

1.9.9 Electrolyte disturbances

Probably one of the most obvious markers with regards to tubular toxicity is the identification of electrolyte alterations through tubular dysfunction and identification of tubule sections most susceptible to CNI damage. Typically, CNI treatment leads to a variety of electrolyte disturbances including hyperkalemia, hypomagnesemia, hyperchloremic metabolic acidosis and hyperuricema (Heering & Grabensee 1991; Heering *et al*. 1998; Lin *et al*. 1989).

Interestingly, there is a clinical condition that has remarkable similarities to chronic CNI nephrotoxicity with regards to electrolyte disturbances. Type I Barter's syndrome patients have mutations of the Na^+-K^+-2Cl-cotransporter (NKCC2) situated in the apical membrane of tubular epithelial cells (Naesens *et al*. 2004). Commonly,

both conditions show symptoms of magnesium wasting, hyperaldosteronism, nephrocalcinosis and juxtaglomerular hyperplasia. This was further highlighted in patients receiving CSA treated with furosemide, an NKCC2 inhibitor and resulted in normalization of electrolyte regulation (Naesens *et al*. 2004).

However, not all symptoms correlate with each condition. Hyperkalemia and metabolic acidosis are not seen in Barter's syndrome but are in CNI nephrotoxicity (Stahl *et al*. 1986; Tumlin & Sands 1993).

1.9.10 CNI-Induced hyperkalaemia

It has been suggested CNI associated hyperkalaemia is multifactorial and observed in up to 40% of patients treated with CNIs (Naesens *et al*. 2009). CsA has been shown to alter the function of several transporters, increase activity of RAAS and impair tubular sensitivity to aldosterone (Fervenza *et al*. 2004; C. H. Lee & Kim 2007). Studies suggest CsA directly impairs the function of potassium secreting cells in the cortical collecting tubule *via* reduced activity of the Na^+,K^+-ATPase and associated increased chloride reabsorption (C.T. Lee *et al*. 2002). CNIs inhibit luminal potassium channels and increase chloride reabsorption *via* alterations of WNK kinases (Hoorn *et al*. 2011). There is also evidence of decreased expression of mineralorticoid receptors, seen in >75% of patents treated with CNIs, leading to hyperkalemia and metabolic acidosis *via* aldosterone resistance (Heering *et al*. 2004).

CNI-associated magnesium wasting is associated with chronic interstitial fibrosis, increased renal decline and increased rate of renal graft loss (Naesens *et al*. 2009). As well as suppressing reabsorption of magnesium from tubules, studies have insinuated CNIs reduce paracellin-1 expression in the thick ascending limb, reducing paracellular magnesium reabsorption and also indirectly openning ATP-sensitive K^+ channels, both of which could contribute to CNI-associated hyperkalemia (C. H. Lee & Kim 2007).

1.9.11 Metabolic acidosis

Metabolic acidosis is another common electrolyte disorder observed in patients treated with CNIs. Tubular acidosis is generally a mild and symptomatic condition seen in renal transplant recipients however can be classified as proximal and distal

tubular acidosis (Heering *et al*. 1998; Healy *et al*. 1998). Proximal acidosis is characterised by bicarbonate wasting due to direct toxic effects of CNIs while distal acidosis is characterised by inhibition of hydrogen ion excretion (C. H. Lee & Kim 2007).

Specific use of CsA has a predisposition to instigate distal acidosis and associated increased potassium excretion, with several studies suggesting diet as susceptibility.

Collecting ducts have two types of intercalated cells, the hydrogen ion alpha secreting or bicarbonate beta secreting intercalated cell (C. H. Lee & Kim 2007). An acid rich diet produces more alpha-intercalated cells were alkane rich diets express an increased number of beta-intercalated cells (C. H. Lee & Kim 2007). The protein hensin is crucial in mediating transformation between beta and alpha intercallted cells and it has been shown that metabolic acidosis induces the polymerization of extracellular hensin (Schwartz & Al-Awqati 2005). Generation of hensin leads to the differentiation of bicarbonate secreting beta cells into acid secreting alpha cells (Schwartz & Al-Awqati 2005).

CNIs inhibit polymerization of hensin in protein and the resulting acid secreting alpha cells will be less abundant, therefore increase the risk of metabolic acidosis (C. H. Lee & Kim 2007).

1.10 CNI Pharmacokinetics and Pharmacogenetics

1.10.1 Multidrug resistance protein

Due to CNIs having such a small therapeutic window, their pharmacokinetics plays a considerable role in their immunosuppressive viability and variability. The pharmacokinetics of CNIs are characterised by high inter-patient variability, with variability linked to genetic variation of transporters associated with CNI pharmacokinetics (Armstrong & Oellerich 2001; Barbarino *et al*. 2013). Because of this genetic predisposition, maintaining target concentrations CNI's is complicated and often results in varying dose concentration correlations, the lowest drug concentration is easier to measure rather than maximal for each individual (Fahr 1993b).

Taken orally, CNI's are absorbed from the intestine with peak concentrations typically reached within 2 hours, although intestinal absorption of CNIs is low and variable depending on several factors including digestion of food and diabetes (Fahr

1993a). CNIs are inhibitory substrates for the metabolizing cytochrome P450 3A isoenzymes, namely CYP3A4 and CYP3A5, and of the multidrug efflux transporter P-glycoprotein (MDR1 (Naesens *et al*. 2009). The variability in expression and function of these enzymes and transporter is likely to explain the variability in CNI absorption.

MDR1 is an ATP-dependent drug transporter responsible for transporting drugs from the cytoplasm to the cell surface and ultimately into the extracellular space for secretion (Cascorbi 2013). Within the kidney, MDR1 is found prominently in the brush border of proximal tubular epithelial cells (Robert J Alpern 2008). Not surprisingly, MDR1 has been shown to be upregulated with exposure to CsA and lower expression is thought to be a predisposing risk factor for development of CNI nephrotoxicity (Jette *et al*. 1996; Hauser *et al*. 2005).

CNIs distribute extensively into tissue and the cellular fraction of blood (Fahr 1993a). Erythrocytes have a high concentration of FKB12, FK506's intracellular binding protein, and explains why whole blood concentrations of FK506 are ~5 times higher than in plasma, where it is bound to albumin and lipoproteins (M. Winkler *et al*. 1994).

CNIs are mainly eliminated in bile, >90%, and have been shown to be metabolized into at least 15 metabolites (Uetrecht 2009). Interestingly, CYP3A4 is primarily involved in the metabolism of CsA whereas CYP3A5 is predominant in the metabolism of FK506 (Hesselink *et al*. 2003).

Metabolism of CNI's mainly occur in the liver and GI tract and is effectively complete with <1% of each parent drug appearing in urine or faeces (Watkins 1990).

Of recent interest, pharmacogenomics has become an area of research with regards to individual variability and identification of individual susceptibility to CNI side effects. Genetic polymorphisms in the CYP3A gene has been shown to influence CNI pharmacokinetics and the possibility of identifying those most at risk of toxicity from recessive alleles is becoming an intriguing possibility (Utecht *et al*. 2006).

1.10.2 Pharmacogentic mutations

There have been over 40 single nucleotide polymorphisms (SNPs) identified with the CYP3A4 gene, with the SNP CYP3A4*1B being most studied, an A>G transition at position 392 in the 5' regulatory region (S.-F. Zhou *et al*. 2009). Clinically, it has been suggested this allele results in reduced enzymatic activity however microsomal

studies have not been able to confirm this therefore to what extent this mutation has in predisposition of CNI nephrotoxicity remains unclear (Utecht *et al*. 2006; Barbarino *et al*. 2013). Furthermore, increased transcription of CYP3A4 has been demonstrated *in vivo* after CNI administration, suggesting a theoretical higher expression and activity (Utecht *et al*. 2006).

The role of SNP's on MDR1 function is less well-defined, with studies indicating no association of MDR1 SNP's on CsA pharmacokinetics while FK506 interaction studies are not as consistent (Qiu *et al*. 2008).

However, a recent study investigating a SNP at position 3435-T, the TT genotype, of kidney donors was associated with chronic CNI nephrotoxicity (Hauser *et al*. 2005). This SNP has been associated with an altered function of MDR1 and resulting in an increased risk of nephrotoxicity of over 40% (Hauser *et al*. 2005). The same genotype was also studied in liver transplant patients but found contradictory results, with the TT genotype group having a reduced risk of renal dysfunction and development of nephrotoxicity (Hebert *et al*. 2003). Therefore, to suggest identification of SNPs may help combat CNI toxicity is not only a touch naïve but also dangerous with risking a single SNP identification for predisposition. This being said, discovery of individuals who could be at risk through SNP's may help clinicians in choosing suitable immunosuppressive regimes with maximum efficacy and reduced chances of adverse effects.

1.11 Mammalian Target of Rapamycin Inhibitors (mTOR-i)

Although CNI minimisation protocols rely heavily on a concoction of steroids and other immunosuppressive drugs, azathioprine and mycophenolate mofetil (MMF) for example, there has been increasing interest in the use of rapamycin to fill the gap of insufficient drug combinations.

Rapamycin, clinically known as sirolimus, is a macrolide antibiotic produced by the bacterium Streptomyces hygroscopicus first discovered in the mid 1970's (Sehgal 2003). Although initially investigated as an antifungal, it soon became clear that it had potent antitumor and immunosuppressive properties (Selzner *et al*. 2010).

Its structural similarity to FK506 was suggestive to the discovery of another CNI, similar to FK506. However, unlike CsA and FK506, rapamycin does not inhibit the secretion of IL-2 through calcineurin inhibition.

Rapamycin binds to the same intracellular cytosolic protein as FK506, FKBP12, however the rapamycin-FKB12 complex does not interact with calcineurin, instead it inhibits the mammalian Target Of Rapamycin (mTOR) pathway through direct binding to mTOR complex 1 (Ballou & R. Z. Lin 2008).

mTOR is a serine/threonine protein kinase that is responsible for cell regulation, growth, proliferation and survival. It comprises of two distinct complexes, MTORC1 and MTORC2, both of which are structurally unrelated (Bracho-Valdes *et al*. 2011). Each complex has been shown to be localised to different cellular organelles and ultimately effects their function and activation. Essentially, MTORC1 is responsible for protein synthesis and monitoring of energy production and consummation while MTORC2 is responsible for regulation of cellular structure and metabolism (Bracho-Valdes *et al*. 2011). Rapamycin has a large affinity for MTORC1 which is relevant for immunosuppressive properties (Toschi *et al*. 2009). MTORC2 and rapamycin interaction is significantly more complex with the pathway and molecular interactions still remaining unclear (Toschi *et al*. 2009).

Once the rapamycin-FKB12 complex has bound to mTOR, there is subsequent inhibition of both DNA and protein synthesis which ultimately results in cell arrest in late G1 from progression to the S phase (Ballou & R. Z. Lin 2008). In IL-2 stimulated T cells, this results in inhibition of lymphocyte growth and differentiation, therefore an immunosuppressive effect (Sehgal 2003). One of the key differences between rapamycin and CNIs is their immunosuppressive properties. CNIs inhibit the transcription of IL-2 through calcineurin blockade therefore limited IL-2 production (Barbarino *et al*. 2013) whereas rapamycin inhibits the transduction pathway required for progression of cytokine stimulated T cells from G1 to S phase, consequently suppressing interleukin-driven T cell proliferation (Sehgal 2003).

Calne and colleagues conducted the first *in vivo* study using rapamycin for immunosuppression, which highlighted improved animal/allograft survival and function compared to non-immunosuppressed controls (Calne *et al*. 1989). Their initial immunosuppressive findings were further highlighted in studies using a range of animal models and eventually human trials (Sehgal 2003; Morelon *et al*. 2001; MacDonald & Grop 2001). Importantly, rapamycin does not present any acute or chronic alterations in renal blood flow or GFR (V. W. V. Lee & Chapman 2005). Kreis and colleagues, using a randomised trial, were able to demonstrate rapamycin treated patients had lower serum creatinine levels compared to those on CsA

immunosuppression suggesting an improved GFR over CsA patients (Kreis *et al*. 2000). The authors results also proved pivotal in the realisation that rapamycin did not induce obvious nephrotoxicity in the human transplant setting and only resulted in mild adverse effects.

The side effects associated with rapamycin use include myelosuppression, hyperlipidemia and anaemia, however most are mild and can typically be overcome *via* dose reductions (Sehgal 2003; V. W. V. Lee & Chapman 2005).

1.11.1 mTOR-i nephrotoxicity

Nephrotoxicity associated with rapamycin is rare and usually reported in a case-by-case basis, interestingly; most reported cases indicate development of nephrotoxicity only in preconditioned disease states. E.g. glomerulonephritis.

Fervenza *et al* investigated the use of rapamycin in chronic glomerulonephritis (GN) and moderate kidney failure. Within 6 weeks of transplantation and rapamycin therapy, over 50% of patients had developed actuate kidney failure however kidney function improved after cessation of rapamycin (Fervenza *et al*. 2004).

This is not too dissimilar to Dittrich *et al* who reported patients with chronic allograft dysfunction developed biopsy-confirmed post transplantation GN, 9 months after conversion to rapamycin from a CNI based regime. Intriguingly, kidney function stabilized in all patients after reintroduction of CNI therapy (Dittrich *et al*. 2004).

1.11.2 Acute graft rejection

Although direct rapamycin nephrotoxicity is still rare when used for immunosuppression, there has been evidence to suggest it has a limited ability to prevent acute graft rejections compared to CNI's.

The SYMPHONY study set out to investigate rejection rates of rapamycin & MMF combinations against low dose CNI & MMF treatment (Ekberg *et al*. 2007). The study suggested a cohort of patients on rapamycin & MMF had higher rejection rates without any improvement in renal function compared to those treated with CNIs & MMF. These initial findings have also been confirmed (Ekberg *et al*. 2010) suggesting that specific immunosuppressive regimes must be considered carefully to obtain the best outcome of each individual patient.

1.11.3 mTOR-i interactions

1.11.3.1 CsA & mTOR-I's

An important point to note about rapamycin therapy is its combined use with CsA. This topic remains controversial with studies indicating contradictory results and no clear option on drug combinations.

In vitro and animal studies have shown application of CsA in combination with rapamycin has a synergistic and unprecedented immunosuppressive effect (MacDonald 2003; Brook *et al*. 2005; Andoh *et al*. 1996; Podder *et al*. 2001).

This extraordinary discovery led to the possibility of a using a reduced dosage of each compound, CsA and rapamycin, while still able to maintain a safe and suitable immunosuppression condition (Brook *et al*. 2005).

Two large phase III and randomized trials investigated the use of CsA-rapamycin combination against placebo or CsA-azathioprine combination (Baboolal 2003; Kahan 2003). The results suggested that CsA-rapamycin combination significantly reduced the number of acute rejections compared to other immunosuppressive therapies. However, similar trough levels of CsA throughout the groups, along with rapamycin treated patients having the worst renal function at 1-year post transplantation, suggests that rapamycin may possibly increase the renal toxicity of CsA (Baboolal 2003; Kahan 2003). It is now therefore generally accepted that long-term use of CsA in combination with rapamycin is avoided to elude further nephrotoxicity or renal dysfunction (MacDonald 2003; Jeanmart *et al*. 2002; Cheng *et al*. 2008).

Instead, combination of both drugs for induction therapy, initial synergistic immunosuppression, then discontinuation of CsA after several months is conceivably a better option to utilize this powerful immunosuppressive combination (Lebranchu *et al*. 2009). Lebranchu and colleagues investigated this hypothesis in an open label trial with results proving positive, allowing CsA to be discontinued 3 months post transplant, an improved overall renal function and lower blood pressure compared to a continued CsA-rapamycin dosing treatment (Lebranchu *et al*. 2009).

The increased toxicity observed with combination of rapamycin and CsA is exclusively attributed to the metabolization of these compounds. Both are metabolised by cytochrome P450 CYP3A4 and MDR1 enzymes and therefore it is logical to assume some form of pharmacokinetic interaction (Naesens *et al*. 2009). Podder and colleagues were able to investigate this in great detail using a low-salt

animal model (Podder *et al*. 2001). The results implied rapamycin has the ability to potentiate CsA nephrotoxicity *via* increasing systemic and local renal concentrations of CsA *via* reduced metabolism (Podder *et al*. 2001). Importantly, the study suggested that whole blood concentrations do not correlate with local renal concentrations and care must be taken when extrapolating renal exposure to a combination of these drugs.

1.11.3.2 FK506 & mTOR-I's

Most research involving mTOR-i's and their associated interactions in immunosuppression has been done with CsA. This is most likely due to our knowledge of CsA and its unprecedented use in organ transplant since the 1970's.

However, in recent years, tacrolimus has become an ever-increasing choice for immunosuppression due to its increased potency and reduced, although still prominent, nephrotoxicity. Post transplant, tacrolimus immunosuppression now accounts for over 80% of living donors (Matas *et al*. 2015). It is therefore logical to investigate the potential side effects of mTOR-I's and a tacrolimus combination.

As with most studies involving CNI's, reports are conflicting with no clear evidence of a completely safe or detrimental combination drug regime.

Piao *et al* have reported a unfavourable effect with a combination of FK506 and rapamycin (Piao *et al*. 2014). The authors underlined the significant difference of renal injury in treatment groups of FK506 alone or in combination with rapamycin, with the latter producing increased renal and pancreatic cell injury. Interestingly, the authors also emphasised an increase in 8-hydroxy-2'-deoxyguanosine, an oxidative stress marker in the combined treatment group, indicating the role of ROS production in nephrotoxicity, similar to reports seen with CsA and rapamycin combination (Lisik *et al*. 2007).

On the other hand, Vu *et al* demonstrated a beneficial effect of combined FK506 and rapamycin in a heart allograft model (Vu *et al*. 1997). The authors reported a combination did not produce an antagonistic effect compared to either drug alone and in addition, the study also highlighted prolonged graft survival with a combined regime compared to either immunosuppressive alone (Vu *et al*. 1997).

Taken together, these early experimental studies suggest that immunosuppressive combinations run the risk of adverse effects, even if previous reports have suggested safe use.

A possible reason for such variance in side effects between groups is due to the large Interpatient and intrapatient variability of immunosuppressant's. Therefore, careful consideration must be taken to ensure each patient receives sufficient immunosuppression while having minimal a minimal exposure to the risk of adverse side effects.

1.12 Aims of the investigation

It is well known that CNIs affect the larger arterioles of the kidney and ultimately instigate nephrotoxicity through a variety of pathways, however their influence on the renal medullary microcirculation is still poorly investigated.

The initial aim of this study is to investigate the effect(s) of CNIs on medullary microcirculation, with particular focus on vasa recta diameter and pericyte contractility, with a view to inferring their effect(s) on medullary microcirculation. This is addressed in Chapter 3 using the already established live kidney slice model.

A major compilation of renal transplantation is the development of hypertension, with over 90% of recipients developing some form of systemic hypertension following surgery (Textor *et al*. 1994; Midtvedt & Hartmann 2002a). This has been historically combated with use of antihypertensives and careful monitoring of immunosuppressive drug levels. However, anecdotally it has been suggested that antihypertensives may reduce CNI-induced nephrotoxicity. The second aim of this study is to investigate the effect of combined application of antihypertensives and CNIs on vasa recta diameter and pericyte contractility, with a view to inferring their effect(s) on medullary microcirculation. This is addressed in Chapter 4.

Chapter 5 of this thesis sets out to investigate the feasibility of single vessel perfusion of *in situ* vasa recta for studying the molecular and cellular events when CNIs are luminally perfused, creating a more physiological setting for future studies (i.e. perfused vasa recta in live kidney slices). This data will aid our understanding of medulla microcirculation after CNI treatment and may identify a novel role for renal pericytes in the initiation or augmentation of CNI-induced nephrotoxicity.

Lastly, in Chapter 6, using multiphoton microscopy, the live kidney slice model is used to identify molecular signaling pathways after the tissue is treated with CNIs to help identify preliminary pathways for the prevention of nephrotoxicity. The chapter focuses on mitochondrial dysfunction and ROS production.

2. General Methodology

2.1 Animals

Animal experiments were conducted in accordance with United Kingdom Home Office Scientific Procedures Act (1986). Adult male Sprague-Dawley rats (250–300 g) were obtained from Charles River UK Ltd, Kent, UK. Animals were fed standard animal chow and housed in standard 12-hour lighting conditions. Prior to experimentation, animals were killed by cervical dislocation.

2.2 Live kidney slice model

2.2.1 Slice preparation

Kidneys were removed following cervical dislocation, promptly decapsulated, and placed in ice-cold physiological saline solution (PSS) bubbled with 95% O_2/5% CO_2 and prepared for slicing. Prior to slicing, the kidneys had any renal artery remnants removed. A single kidney was secured on the slicing block of a vibratome tissue slicer (Leica model VT1200S; Leica Microsystems (UK) Ltd, Milton Keynes, Bucks, UK), and submerged in a bath of ice-cold PSS bubbled with 95% O2/5% CO2. PSS contained (m*M*) 100 NaCl, 5 KCl, 0.24 NaH2PO4, 0.96 Na2HPO4, 10 Na acetate, 1 CaCl2, 1.2 MgSO4, 5 glucose, 25 NaHCO3, 5 Na pyruvate (Sigma-Aldrich Ltd, Poole, Dorset, UK). The pH was adjusted to 7.4 using 1 M NaOH. The outer cortical dome region (~3 mm tissue) of the kidney was removed to expose the top of the renal medulla and serial 200 μm-thick coronal kidney slices (intact cortex and medulla) were cut. Slices were collected and maintained at room temperature in a holding chamber containing PSS, and bubbled with 95% O2/5% CO2 to maintain tissue viability. Kidney slices to be used in 'live' functional experiments were maintained for up to 3 h in the holding chamber. The process can be visually understood in figure 2.0.

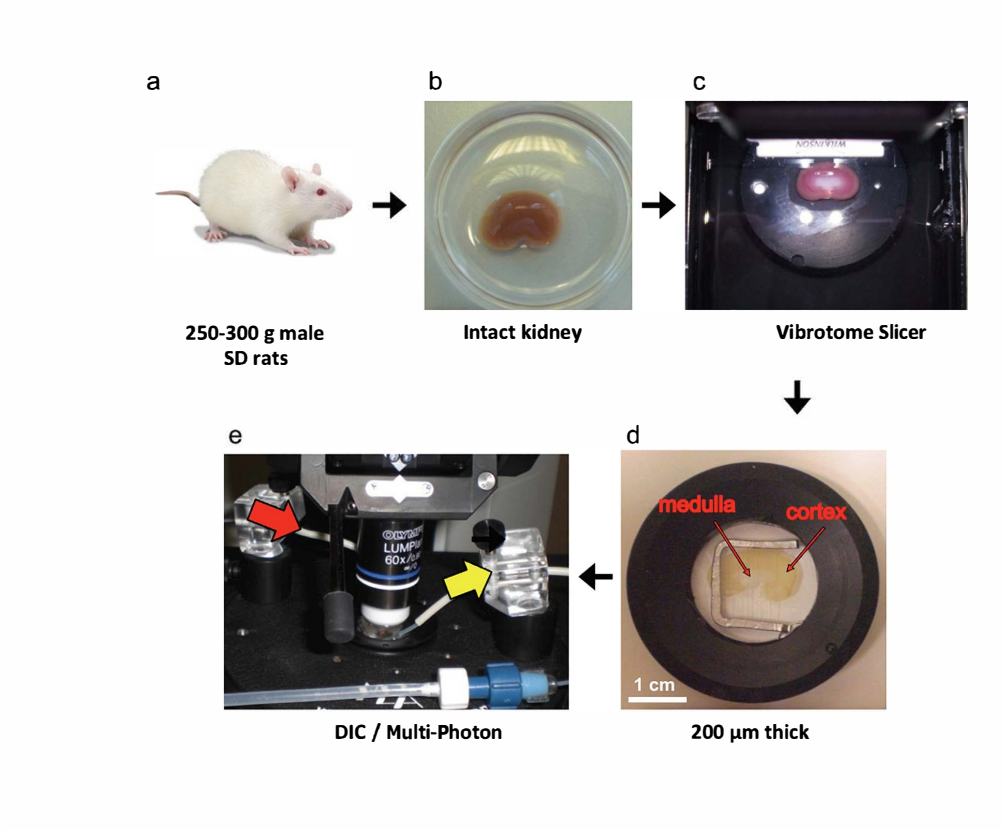

Figure 2.0 The live kidney slice model.

a) 250-300 g male Sprague-Dawley (SD) rats were killed by cervical dislocation and whole kidneys were rapidly removed (b) and secured on to the block of a vibrotome slicer, as shown in (c). Once the outer cortical dome region had been removed to expose the medulla, serial 200 µm thick slices were cut. A single kidney slice was secured in an open bath chamber using a platinum anchor, as shown in (d), which was transferred to the stage of an upright Olympus microscope (e). Kidney slices were continuously superfused with oxygenated PSS *via* inlet (red arrow) and outlet (yellow arrow) valves.

2.2.2 Live functional imaging

Live kidney slices were secured in an open-bath chamber using a purpose-built platinum slice "harp" and transferred to the stage of an upright Olympus microscope (model BX51WI; Olympus Microscopy, Southend-on-Sea, Essex, UK). Kidney slices were continuously superfused (~2.5 ml/min, 1.25 ml bath volume) with PSS, bubbled with 95% O2/5% CO2 and maintained at room temperature. Pericytes on subsurface (~50 µM below the tissue surface) vasa recta capillaries (vasa recta were defined as <10 µM in diameter) were identified by their previously established 'bump-on-a-log' morphology (Crawford *et al.* 2012) and differential interference contrast (DIC)

images were captured as a video sequence *via* a Olympus 63× water immersion objective (0.9 NA) coupled to a Rolera XR digital charged coupled device (CCD) camera (Qimaging, Surrey, Canada). Real-time video images of changes in vasa recta diameter were collected every second and recorded using Image Pro Software (Media Cybernetics Inc., Marlow, Bucks, UK).

Live kidney slices were superfused with compounds prepared in PSS All vasoactive compounds were purchased from Sigma-Aldrich Ltd and all working solutions were prepared in oxygenated PSS on the day of experimentation.

2.2.3 Slice experiments

Analysis of time-series live kidney slice experiments was carried out using the public domain software ImageJ (NIH, http://rsb.info.nih.gov.ij). For each experiment, both a pericyte site and a non-pericyte site were identified on a single vasa recta, as previously described (Crawford *et al*. 2012). The diameter of the vasa recta at both locations was measured every 5 frames for the duration of the experiment (1 frame = 1 s). Typically, kidney slices were superfused with PSS alone for 100 s to establish a baseline vessel diameter at the pericyte and non-pericyte site. Slices were then exposed to selected compounds diluted in PSS to investigate their effect on vessel diameter and were then subjected to a PSS wash. Each capillary acted as its own control; an average of the first 10 measurements was taken to represent the resting baseline diameter value (Db), and expressed as 100%, for both pericyte and non-pericyte sites. All subsequent diameter measurements (D) were calculated and expressed as a percentage of the corresponding baseline value for both pericyte and non-pericyte sites, as previously described (Crawford *et al*. 2012), figure 2.2. Percentage change in vessel diameter was calculated from actual vessel diameter measurements made throughout each experiment.

Pericyte "responders" were classed as being able to induce a % change in diameter greater than 5%. With the kidney slice model being an intact "live" tissue, pericytes are under constant regulatory tone, therefore constant changes in vessel diameter is not unusual. A vasomotin response larger than 5% upon insult is regarded as a responder to that particular stimulus.

A

$$\% \Delta \text{ Vessel Diameter} = \left(\frac{\text{Measured Diameter (D)}}{\text{Mean Baseline Diameter } (D_b)} \right) X\ 100$$

B

% Constriction or Dilation = 100%(Baseline) - %Δ Vessel Diameter

Figure 2.1 Calculation of percentage change in vessel diameter. A: an average of the first 10 measurements, 50 seconds, was taken to represent the resting vessel diameter for both pericyte and non-pericyte sites. B: Succeeding diameter measurements were expressed as a percentage of the corresponding baseline value for both pericyte and non-pericyte sites. Adapted from (Crawford *et al*. 2012).

2.3 Microperfusion of *in situ* vasa recta

Live kidney slices were transferred to the stage of an upright Scientifica microscope (model SliceScope Pro 1000; Scientifica Ltd, East Sussex, UK). Kidney slices were continuously superfused as previously described with PSS, bubbled with 95% O_2/5% CO_2 and maintained at room temperature. DIC images were captured through an Olympus 60× water immersion objective (0.9 NA). Real-time video images of changes in vasa recta diameter were collected every second by an attached Rolera XR CCD camera (Qimaging, Surrey, Canada) and recorded using Image Pro Software (Media Cybernetics Inc., Marlow, Bucks, UK).

Before perfusion, vessels were visually selected for suitability (~7-10 μm wide and ~25-50 μm below surface) and viability (long enough to withstand perfusion pressure and pipette puncture). Pericytes were identified on suitable vessels as previously described.

Glass micropipettes were prepared using borosilicate glass (1.5 mm OD, 1.17 mm ID; Harvard Apparatus) and a dual stage micropipette puller (model PC-10: Narishige

International ltd, London, UK) to produce pipettes with an inner diameter of ~3 µM and outer diameter of ~4 µM at the pipette tip.

Pipettes were filled with PSS ± selected compound after filtration using a 0.20 µM sterile syringe filter (Cole-Parmer, London, UK) before securing onto a manual micromanipulator (model LBM-7: Scientifica Ltd, East Sussex, UK). Positive pressure was applied *via* attached sphingometer adapted to a connected reservoir to avoid pipette blockage. The pipette was manually lowered into the bath (above the vessel of interest) before diagonally puncturing the vessel wall and allowing minimal pressure/flow (< 5 mmHg) into the vessel, seen in figure 2.3. For both control and experimental conditions, the perfused vessel (<5 mmHg) was allowed to stabilize for at least 5 minutes prior to an increase of pressure/flow.

After the initial stabilization period, pressure was gradually increased until chosen pressure was met (15–100 mmHg) and stable. Video images of vessels were recorded just before increase of pressure to generate a baseline for measurement later off line.

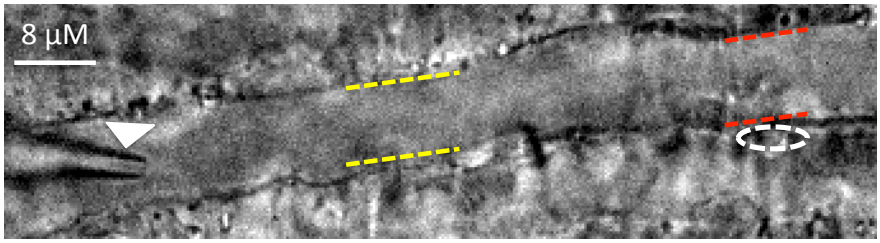

Figure 2.2 Perfusion of vasa recta capillary within the live slice model.

Perfusion pipettes (arrow head) punctured parallel vasa recta were a pericyte site (dashed red lines) was visible in conjugation with corresponding non-pericyte site (dashed yellow lines).

2.4 Multiphoton imaging on the live kidney slice

2.4.1 Imaging system

Live kidney slices were imaged using a custom built 2-photon imaging system configured by Scientifica UK, East Sussex. Additional details can be found online: http://www.scientifica.uk.com/products/multiphoton-imaging-system

The base microscope consisted of Scientifica's brightfield SliceScope Pro, fully motorised in X, Y, Z directions and DIC imaging capable through attached Olympus 60× water immersion objective (0.9 NA).

The microscope has an attached galvo scan head allowing for variable scan speeds while reducing the kidney slice exposure to laser light. The scan head consists of two back apertures, small (<9mm) and large (<20mm) and galvanometers from Cambridge Technology (8315 KL with 3 mm X and Y mirrors).

Attached to the galvo scan head is the multiphton detection unit consisting of two photo-multiplier-tube (PMT) based detector modules, containing integrated high voltage supply, active voltage divider, preamplifier and 1.25 MHz low-pass filter. The detection unit uses R9880U series detectors and is fitted with a visible 665 nm long-pass dichroic mirror and 680 nm short-pass dichroic laser blocking filter.

2.4.2 Laser

In order to excite samples, a 300-nm tunable (690 – 1040 nm) titanium/sapphire femtosecond laser (Mai-Tai HP; Newport Co Spectra-Physics, Mountain View, California) was used to excite fluorescent probes. The laser provides up to 2.5 watts of adjustable average power and a pulse width of less than 100 femtoseconds. Laser power to samples rarely increased over 60 μW.

2.5 Statistics

All data are presented as mean values ± SEM; *n* numbers are displayed as number of kidney slices and number of animals, individually indicated with brackets ( ). All experiments were performed in at least six different animals. Statistical evaluation was performed with Instat (v2.05a; GraphPad software, San Diego, CA, USA). When two groups were compared, a Student's t-test (two-tailed, paired or unpaired where appropriate) was used. A value of $P < 0.05$ was considered statistically significant.

3. The effect of calcineurin inhibitors on renal medullary vessels and tubules

3.1 Introduction

As previously mentioned, CNIs have a plethora of unwanted side effects to which there is no single proven point of cause (Naesens *et al*. 2009). The most influential side effect to have detrimental consequences on graft function is nephrotoxicity, of which there are two types, acute and chronic, as described in the general introduction (sections 1.7 & 1.9).

Although there have been countless trials targeting CNI-induced nephrotoxicity, most, if not all, have had very little success in its prevention, especially the chronic form which typically manifests as long-term structural alterations of vascular and tubular architecture (Chapman 2011).

Acute CNI nephrotoxicity is the general term used for patients presenting functional haemodynamic alterations that can be typically overcome with dose adjustments or CNI withdrawal. The classical trait of acute CNI nephrotoxicity is the reduction of glomerular filtration rate (GFR), attributed to the vasoconstriction of afferent arterioles (Tsechan 2002). Several studies in the 1980's were able to convincingly show the significant changes of vascular flow after CNI treatment and highlighted the importance of vascular dysfunction for these particular changes after CNI use (Barros *et al*. 1987; Laskow *et al*. 1988). The studies were able to show significantly reduced single nephron GFR after CNI treatment compared to controls, which corresponded to total significant GFR reduction after CNI treatment.

CNI-induced vascular dysfunction has been studied extensively *in vitro* and *in vivo* and is generally accepted to originate from an increase of vasoconstrictors and decrease in vasodilatory molecules. These include endothelin, thromboxane, prostaglandin E_2 (PGE_2) and nitric oxide (NO) (Naesens *et al*. 2009).

This was first highlighted by Murray *et al*, displaying the importance of afferent and efferent arteriole vasoconstriction and the development of acute CNI nephrotoxicity (Murray *et al*. 1985). With this in mind, it is apparent that acute CNI nephrotoxicity is clearly vascular dependent, and addressing the CNI-induced alterations in renal blood flow are the first port of call in prevention of nephrotoxicity.

Conversely, very few studies have looked at the importance of the renal microcirculation and its contribution to CNI nephrotoxicity. Watarai et el used laser

Doppler readings to investigate the effects of CNIs on the renal microcirculation of rats, while simultaneously investigating the altered production of NO in blood samples (Watarai *et al*. 2004). Their results highlighted the importance of NO generation within the microcirculation, and the effect of attenuating NO production, which they concluded as being pivotal in the development of CNI nephrotoxicity.

In addition, endothelial dysfunction is generally thought as a critical factor towards the development of vascular dysfunction in CNI nephrotoxicity. Both CNIs inhibit NO production, though no defined mechanism has been identified, and also inhibit endothelium-dependent NO-mediated renal vasodilation, through the dysregulation of eNOS (Naesens *et al*. 2009). They are also known to increase the production of free radicals and superoxide synthesis. Interestingly, both CNIs decrease eNOS-mediated NO production through various pathways including increased thromboxane A2 production, decreased vascular endothelial growth factor and decreasing cholesterol content in caveolae (Oriji & Schanz 1999.; Kou, Greif & Michel 2002a; Lungu *et al*. 2004).

Interestingly, CNIs have also been shown to impair the ability of platelets to mediate vasodilation. Platelets from CsA treated patients failed to induce vasorelaxation of pre-constricted arteries while platelets from control patients induced a significant increase in vessel diameter. Furthermore, control platelets exposed to CsA *in vitro* lost their vasorelaxation ability in a concentration and time dependent manner (Óskarsson *et al*. 1997).

Moreover, CsA has been shown to enhance platelet coagulant activity through lipid dysfunction in platelet membranes (Tomasiak *et al*. 2007). This data, along with inhibited platelet-mediated vasodilation, suggests that CNIs may have a role in thrombin generation and may contribute to the pathogenesis of the thromboembolic phenomena associated with the use of CNIs (Grace *et al*. 1987).

3.1.2 Renal microcirculation

As already highlighted (chapter 1), the renal microcirculation is regionally specific in terms of metabolic needs and demands, and therefore it would seem reasonable to assume local regional mechanisms are in place for regulation of blood flow. Regulation of renal blood flow in the cortex is well established (Robert J Alpern 2008; Young *et al*. 1996; Koeppen & Stanton 2013b; R. G. R. Evans *et al*. 2004) and is recognised that blood flow in the cortex is regulated upstream *via* pre-capillary arteriole vasoconstriction and dilation. Conversely, due to the inaccessibility of the

renal medulla *in vivo*, particularly the inner medulla, regulation of medullary blood flow (MBF) is less well understood. MBF is supplied *via* vasa recta capillaries, arsing from efferent arterioles of juxtamedullary nephrons. DVR penetrate the renal medulla in vascular bundles giving rise to the capillary plexus, wrapping around collecting ducts and loops of Henle (Pallone *et al*. 1990). Arising from this plexus are the AVR, which subsequently returns blood to the cortex, passing through the outer medullary vascular bundles, see figure 1.4. (Pallone, Turner, *et al*. 2003).

Given that until recently, it was assumed MBF was controlled upstream of the glomerulus *via* afferent arterioles, it was assumed that blood flow *via* a capillary network lacking contractile SMC's was passive (R. G. R. Evans *et al*. 2004; Kennedy-Lydon *et al*. 2012).

However in recent years, MBF has received a substantial increase in research, emphasising the importance of the renal medulla in regulation of salt and water excretion (Cowley 1997). Recent advances in technology, including laser Doppler probes and confocal microscopy, has enabled a far more detailed understanding of the regulation of MBF than what was previously acknowledged (Kneen *et al*. 1999; Hansell 1992). This has led to the now more accepted view of local regulation within the medulla, independent of total RBF, through contractile pericyte cells residing on vasa recta capillaries (Pallone & Silldorff 2001).

3.1.3 Renal pericytes

As previously discussed, renal pericytes are a specialised population of contractile cells known to reside on DVR within the medulla. Although originally discovered in 1873 by Charles Rouget, these cells were thought to function only as vessel "stabilisers" with no real function (Dore-Duffy & Cleary 2011) until recent years, in which there has been a significant rise in the number of publications focusing on the functional role of pericytes in the regulation of blood flow (Tell *et al*. 2006; Kennedy-Lydon *et al*. 2012; Peppiatt *et al*. 2006; Bandopadhyay *et al*. 2001; Crawford *et al*. 2012).

The initial studies involving pericytes and their role in MBF regulation was carried out by Pallone and colleagues who used an isolated perfused DVR technique to visualize the vasoactive properties these cells had when exposed to certain stimuli (Pallone *et al*. 1994; Pallone 1994). Although the technique was fundamental in the initial understanding of pericyte contractility, it involves the complete removal of any

surrounding architecture and loss of any stabilising remnants and as such, potential sources of endogenous vasoactive mediators.

The live kidney slice model pioneered by Crawford *et al* sought to provide an alternative model in which the surrounding architecture remained intact and facilitated investigations in the importance of tubular-vascular crosstalk within the inner medulla for regulation of blood flow (Crawford *et al*. 2012).

Crawford *et al* were able to demonstrate the viability of the live slice model by replicating results first published by Pallone and colleagues (Crawford *et al*. 2012), but also highlighted the importance of tubular-vascular crosstalk *via* extracellular nucleotides released from renal tubules (Crawford *et al*. 2011), emphasising the importance of an *in situ* vasa recta model for enhancing our understanding of MBF.

Given the established vascular component of CNI-induced nephrotoxicity and the recent evidence favouring localised regulation of MBF, the primary aim of this study was to investigate the possible effects CNIs have on the renal medullary microcirculation, with particular focus on MBF and the role of contractile pericytes, in CNI-mediated nephrotoxicity.

3.2 Methods

Intact live kidney slices were obtained as described in chapter 2: General methods. Live kidney slices were superfused with cyclosporine A (CsA), tacrolimus (FK506) or rapamycin, all purchased from Sigma-Aldrich (Dorset, UK). All working solutions were prepared in 95% O_2 / CO_2 PSS, however stocks of CsA and FK506 were made in dimethyl sulfoxide (DMSO). Final concentrations of all working solutions containing DMSO were less than 1%. A 1% DMSO control experiment was carried out to assess DMSO effects on *in situ* vasa recta. In all experiments to determine the effect on vasa recta diameter, kidney slices were superfused with 95% O_2 / CO_2 PSS for ~100 seconds (s) to establish a baseline vessel diameter at the pericyte and non-pericyte sites. Slices were then exposed to CsA or FK506 for approximately 700 s and then subjected to a PSS-wash to assess reversibility of any drug-induced alteration in vessel diameter. Similar experiments were performed with rapamycin to rule out adverse effects from similar immunosuppressant's that do not interfere with calcineurin inhibition. Analysis of video images of changes in vasa recta diameter are as described previously in chapter 2: general methods, using the free public domain

software IMAGE J (NIH; http://rsb.info.nih.gov). For each experiment, a pericyte site and non-pericyte site were identified on a single vasa recta capillary. Each non-pericyte site acted as control for subsequent pericyte site. The diameter of the vasa recta at both of these locations was measured every five seconds for the duration of the experiment. An average of the first five measurements was taken to represent the resting diameter value (*i.e.* baseline diameter) for the selected pericyte and non-pericyte sites. All subsequent diameter measurements at both sites were calculated as a percentage change of the corresponding resting diameter value.

3.2.1 Statistics

All data are presented as mean values ± SEM; *n* numbers are displayed as number of kidney slices and brackets refer to number of animals. All experiments were performed in at least six different animals. Statistical assessment was conducted with GraphPad Prisim (v5.0f; GraphPad software, San Diego, CA, USA). When two groups were compared, a Student's t-test (two-tailed, paired or unpaired where appropriate) was used. A value of $P < 0.05$ was considered significant.

3.3 Results

3.3 Effect of CsA on *in situ* vasa recta capillaries

The calcineurin inhibitor cyclosporine A was investigated for its possible role in altering vasa recta diameter *via* pericyte-mediated contraction or dilation. To test this hypothesis, live kidney slices were superfused with CsA and real time changes in subsurface vasa recta diameter was measured at pericyte and non-pericyte sites.

Superfusion (~700 s) of CsA (10 μM) resulted in a reversible constriction of vasa recta capillaries (Figure 3.0). Vasoconstriction was significantly greater at pericyte sites (12.7 ± 0.88%, n=13 (9)) compared to non-pericyte sites (2.4 ± 0.62%, n=13 (9); P<0.001) (Figure 3.0). The CsA-evoked constriction of vasa recta was reversed upon washout, and vessel diameter returned to at least 90% of the original baseline vessel diameter after 400 s washout. The success rate of experiments was classed as % of responders, described in general methods, and application of CsA resulted in ≥ 75% of pericyte constrictions.

Due to the fact the surface of the kidney slice is damaged during slicing, imaging of vasa recta are subsurface and ~50 μm deep and therefore higher concentrations of drugs than normally seen clinically or *in vivo* may be required to allow deeper tissue penetration. To determine if clinically relevant concentrations of CsA had a vasoconstrictive effect, a series of concentration response experiments were carried out using concentrations of CsA that match whole blood concentrations of CsA and the area under the curve (AUC) total drug exposure (Schiff *et al*. 2007). Clinically, concentration max (Cmax) is the concentration of CsA in whole blood after exposure that is most likely to cause CsA toxicity (Armstrong & Oellerich 2001). Therefore, the range of concentrations used in clinically relevant functional experiments should be equal to or less than Cmax.

Superfusion (~700 s) of CsA (1, 3 and 5 μM, respectively) all resulted in a reversible constriction of vasa recta capillaries (Figure 3.1). Vasoconstriction was significantly greater at all pericyte sites (5.3 ± 0.99%, 8.8 ± 1.03% and 10.2 ± 0.81%, respectively) compared to non-pericyte sites (2.4 ± 0.89%, 2.56 ± 0.65% and 2.20 ± 0.60%, respectively, n=13 (9); P<0.05, P<0.001, P<0.001), (Figure 3.1). The CsA-evoked constriction of vasa recta was reversed upon washout, and vessel diameter returned to ≥ 90% of the original baseline vessel diameter after 400 s following each concentration of CsA.

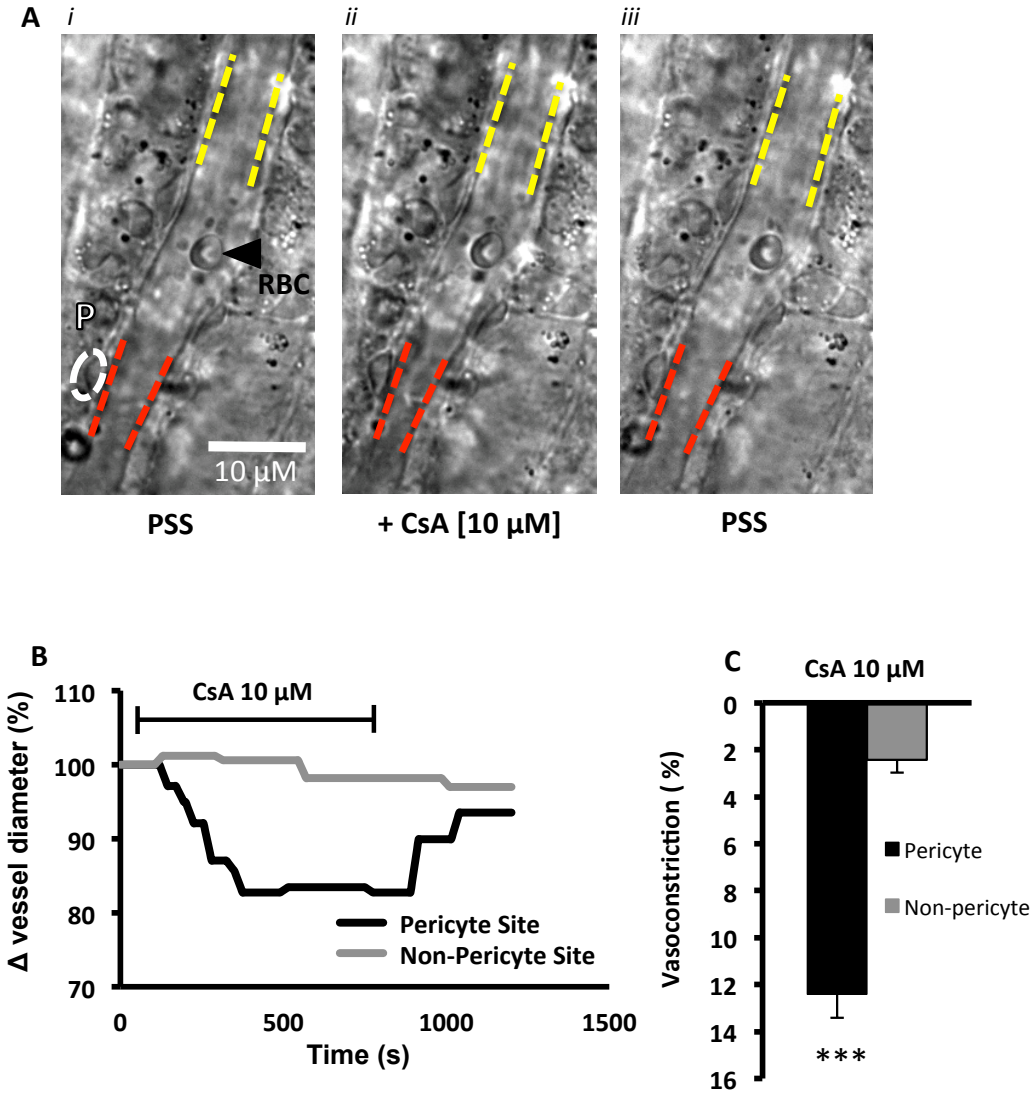

Figure 3.0 DIC imaging of CsA-induced constriction of *in situ* vasa recta capillaries mediated by pericytes.

A: Typical bright field view of vasa recta superfused with control PSS solution (i). A pericyte (P) is located on capillary walls (white oval). Red and yellow dashed lines highlight the regions where vessel diameter was measured at pericyte and non-pericyte sites, respectively. In the presence of CsA (10 µM) applied for 700 s (ii) and following washout of CsA with PSS for 400 s (iii). B: Representative trace showing the percentage change in vessel diameter at the pericyte site (black line) and non-pericyte site (grey line), in response to CsA (10 µM) exposure, respectively. C: Bar graph in shows mean data for these experiments showing CsA evoked a significantly greater constriction at pericyte sites (black bar) compared with non-pericyte sites (grey bar); ***p<0.001; n=13 (9).

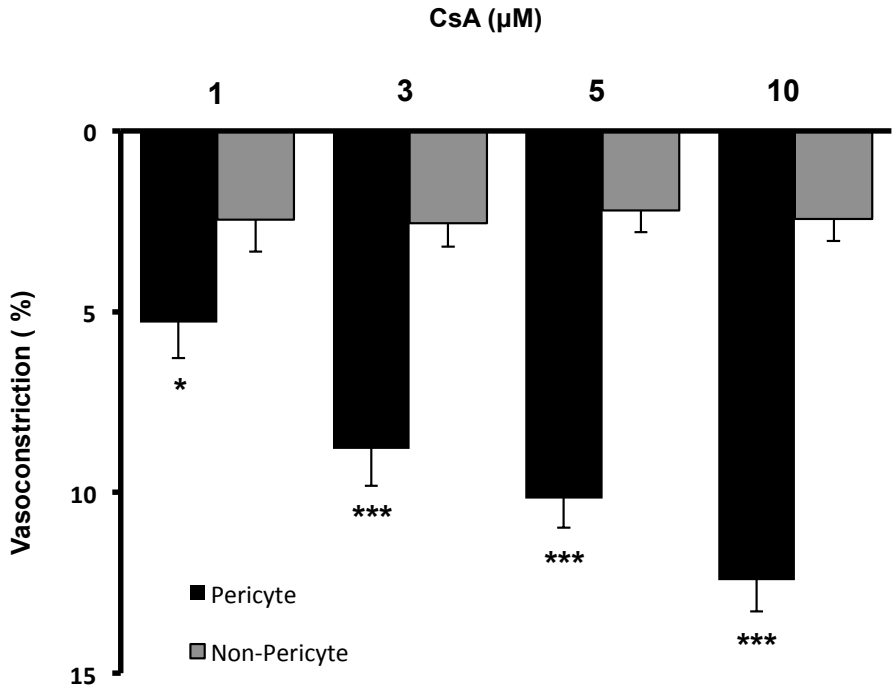

Figure 3.1 Concentration dependent effect of cyclosporine A on pericyte-mediated constriction of vasa recta. Superfusion of live kidney tissue with CsA 1-10 µM evoked a concentration dependent constriction of vasa recta at pericyte sites (black bars) compared to non-pericyte sites (grey bars). Clinically relevant values, 1-5 µM, induced significant pericyte-mediated constriction of vasa recta capillaries compared to non-pericyte sites. Values are mean ± SEM., n=13 (9). *P <0.05, *** P<0.001.

3.2 Effect of tacrolimus on *in situ* vasa recta capillary diameter

Since its first use in clinical practice, FK506 was deemed a newer generation of CNI that would be at least as effective as CsA without the unwanted side effects, particularly nephrotoxicity. However it soon become apparent that even this newer, more potent CNI, also had side effects similar to CsA including nausea, diarrhoea and nephrotoxicity (Hooks 1994; Mihatsch *et al*. 1998; Krejci *et al*. 2010; Naesens *et al*. 2007).

The ability of FK506 to alter vasa recta diameter *via* pericytes was therefore similarly investigated.

Superfusion (~700 s) of FK506 (3 µM) resulted in a reversible constriction of vasa recta capillaries (Figure 3.2). Vasoconstriction was significantly greater at pericyte sites (11.4 ± 0.65%, n=13 (9)) compared to non-pericyte sites (3.9 ± 0.69%, n=13 (9);

P<0.001), (Figure 3.2). The FK506-evoked constriction of vasa recta was reversed upon washout, and vessel diameter returned to ≥ 90% of the original baseline vessel diameter after 400 s following washout. Application of FK506 resulted in ≥ 70% of pericyte constrictions.

As FK506 is 100 times more potent than CsA with regards to immunosuppression (Kino *et al*. 1987), therapeutic drug monitoring (TDM) is essential to maintain a safe and effective therapeutic window. However, systemic concentrations do not always correlate to target organ concentrations. Ideally, systemic concentrations of FK506 would correlate to single organ concentrations, however, given that the kidney is responsible for the filtration of drugs, it is susceptible to accumulation of higher concentrations of drugs than seen in other organs. This has been observed with FK506 use and concentrations in the kidney at more than 10 times recommended therapeutic level (NA. 2002).

Therefore, to test whether clinically relevant concentrations of FK506, in whole blood, had the potential to constrict vasa recta *via* pericytes, concentrations ranging from minimal trough levels, C0, to just above Cmax were investigated.

Superfusion (~700 s) of FK506 ($8x10^{-4}$, 0.05, 0.1 and 1 μM) resulted in a reversible constriction of vasa recta capillaries. The lowest concentration of FK506, $8x10^{-4}$ μM, failed to evoke a vasoactive response (Figure 3.3). Vasoconstriction was significantly greater at pericyte sites using concentrations 1 and 0.1 μM (9.7 ± 0.49% and 8.73 ± 1.3%, respectively, n=8 (8)) compared to non-pericyte sites (2.74 ± 0.39%, and 2.22 ± 0.74%, respectively, n=8 (8); P<0.001,P<0.01 (Figure 3.3). The FK506-evoked constriction of vasa recta was reversed upon washout, and vessel diameter returned to ≥ 90% of the original baseline vessel diameter after 400 s following washout at all concentrations.

Although the response of 0.05 μM did not produce a significant constriction, there was a trend towards greater pericyte-mediated constriction (4.87 ± 0.98%) when compared to non-pericyte mediated constriction (2.24 ± 0.45%, figure 3.3).

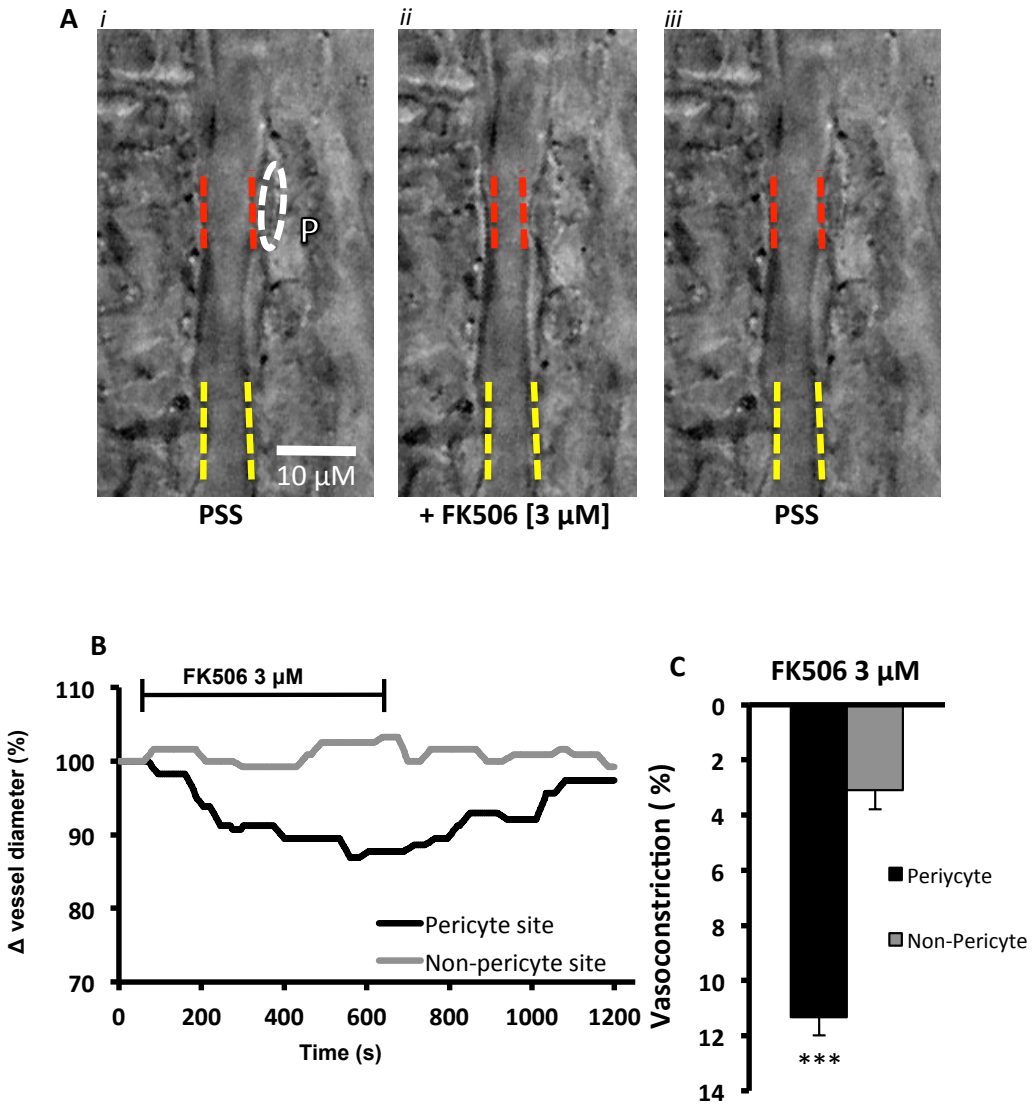

Figure 3.2 investigating the effect of FK506 on *in situ* vasa recta capillary diameter *via* pericyte constriction. A: Typical bright field view of vasa recta superfused with control PSS solution (i). A pericyte (P) is located on capillary walls (white oval). Red and yellow dashed lines highlight the regions where vessel diameter was measured at pericyte and non-pericyte sites, respectively. In the presence of FK506 (3 µM) applied for 600 s (ii) and following washout of FK506 with PSS for 400 s (iii). B: Representative trace showing the percentage change in vessel diameter at the pericyte site (black line) and non-pericyte site (grey line), in response to FK506 (3 µM) exposure, respectively. C: Bar graph in shows mean data for these experiments showing FK506 evoked a significantly greater constriction at pericyte sites (black bar) compared with non-pericyte sites (grey bar); ***p<0.001; n=13 (9).

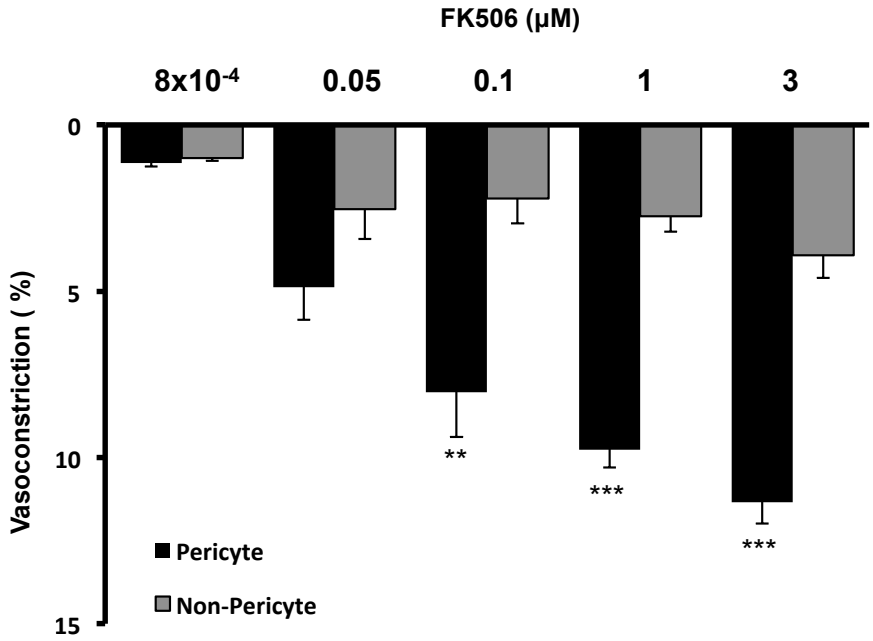

Figure 3.3 Superfusion of live kidney slices with FK506 induces a concentration dependent pericyte-mediated constriction of vasa recta. Superfusion of live kidney tissue with FK506 $8x10^{-4}$-3 μM evoked a concentration dependent constriction of vasa recta at pericyte sites (black bars) compared to non-pericyte sites (grey bars). Clinically relevant value, 0.1 μM, induced a significant pericyte-mediated constriction of vasa recta capillaries, while 0.05 μM produced a trend towards greater pericyte-mediated constriction, though not at statistically significant values. Values are mean ± S.E.M., n=8 (8), ** P <0.01, *** P<0.001.

3.3 Effect of rapamycin on *in situ* vasa recta capillaries

The effect of rapamycin was investigated in the live kidney slice model to demonstrate if it had a role in reducing vasa recta diameter specifically at pericytes on subsurface vessels.

Superfusion (~700 s) of rapamycin (1 μM) resulted in no significant constriction of vasa recta capillaries (Figure 3.4). When vasoconstriction was noted, it was not significantly greater at pericyte sites (4.30 ± 2.5%, n=9 (9)) compared to non-pericyte sites (1.31 ± 1.3%, n=9 (9); P>0.05), (Figure 3.4). Upon washout, vessel diameter continued to be stable and rarely dropped below 95% of the original baseline vessel diameter after 400 s following washout.

As with CsA and FK506, clinically relevant concentrations of rapamycin were investigated, however, given that 1 μM, almost 100 times suggested trough levels (DiJoseph *et al*. 1996), failed to evoke any significant changes in vasa recta diameter, concretions higher than clinically relevant were used. Coincidently, these high concentrations have been observed in whole blood 10 hours post drug administration in transplant patients (Jimeno *et al*. 2006; Weir & Lerma 2014).

Superfusion (~700 s) of rapamycin (0.05 and 0.1 μM) resulted in no significant constriction of vasa recta capillaries (Figure 3.4). When vasoconstriction was noted, it was not significantly greater at pericyte sites (3.30 ± 0.87% and 4.98 ± 1.30%, respectively, n=9 (9)) compared to non-pericyte sites (3.51 ± 0.50% and 4.73 ± 0.66%, respectively, n=9 (9); P>0.05), (Figure 3.4). Upon washout, vessel diameter continued to stabilise and rarely (1 out of 5 experiments) dropped below 95% of the original baseline vessel diameter after 400 s.

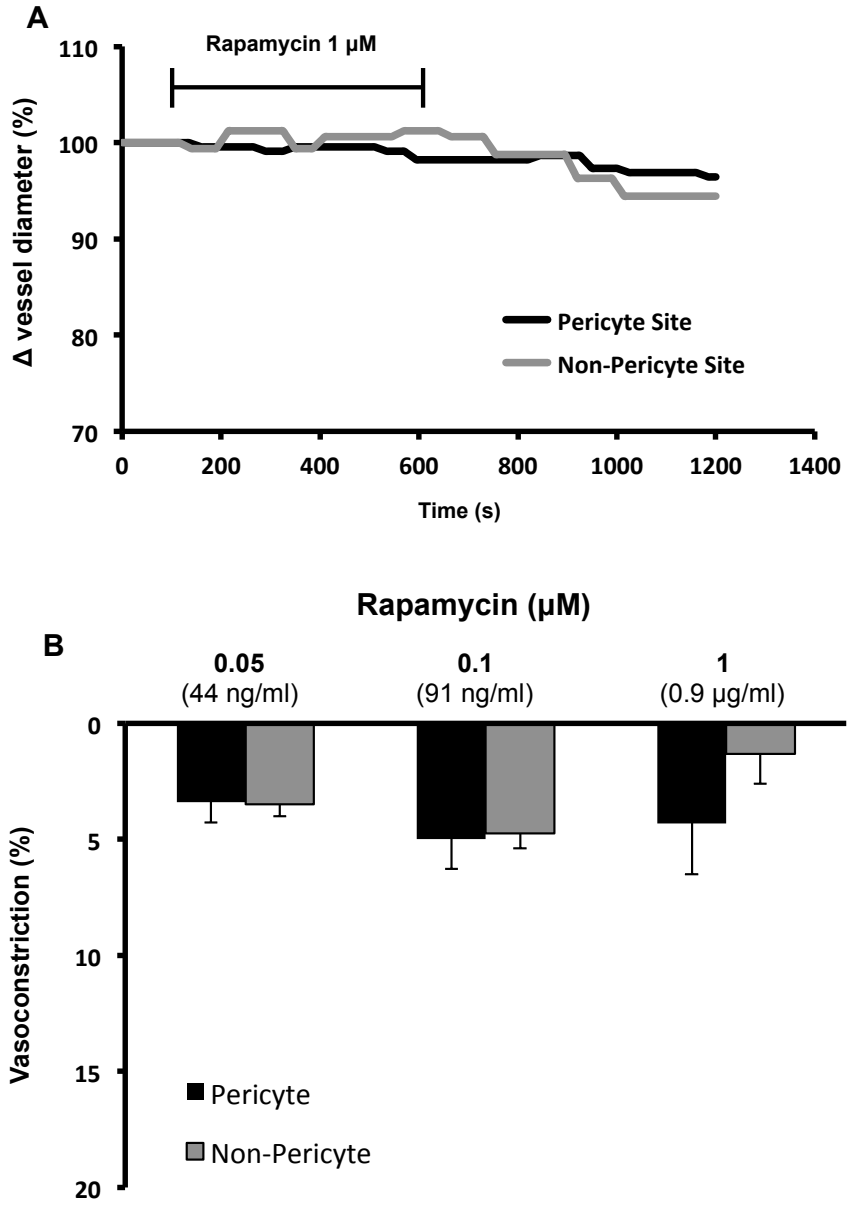

Figure 3.4 Superfusion of live kidney slices with rapamycin does not induce pericyte-mediated constriction of vasa recta. A: Representative trace of the percentage change in vessel diameter recorded over time at pericyte sites (black line) and non-pericyte sites (grey line) when live kidney slices were exposed to rapamycin (1 µM). B: Superfusion of live kidney tissue with rapamycin 0.05-1 µM did not evoke a significantly greater constriction of vasa recta at pericyte sites (black bars) compared to non-pericyte sites (grey bars). Values are mean ± S.E.M., n=8 (8).

3.5 Effect of CsA, FK506 and rapamycin on *in situ* renal tubules

One of the major advantages of the live kidney slice model is that the structural architecture is intact; therefore the vasa recta capillaries, tubules, and intrarenal innervation are all preserved (Crawford *et al*. 2012). Taken together, this allows for a more complete understanding of renal cell communication between the architecture when compared to isolated models (Burg 1972; Sendeski *et al*. 2013).

CNI nephrotoxicity is not just vascular dependent. Tubular toxicity, necrosis of tubular epithelium that form renal tubules, is a well known side effect of CNI therapy and when left untreated, can further develop into additional complications including tubular atrophy, tubulo- interstitial fibrosis and tubular acidosis (Carvalho da Costa *et al*. 2003; Wilson & Hartz 1991; Heering *et al*. 1998; Heering & Grabensee 1991).

However, most tubular toxicities are only presented histologically, in which case, the damage has already taken effect. For example, isometric vacuolisation is associated with CNI nephrotoxicity in patients with renal allografts, although seen in other disease settings (Mihatsch *et al*. 1985; Mihatsch *et al*. 1986), and identification of "giant" mitochondria post CsA therapy leads to cell apoptosis however are only presented post biopsy (Mihatsch *et al*. 1992; Servais *et al*. 2008).

With this is mind; the live kidney slice model was used to investigate the acute effects of CsA, FK506 and rapamycin on *in situ* renal tubules and potentially identify early onset events associated with CNI tubular toxicity.

Superfusion (~600 s) of CsA, FK506 and rapamycin (5, 3 and 1 μM, respectively) resulted in no significant change of *in situ* renal tubule cell size (Figure 3.5). When renal tubule diameter was measured, no significant change was also observed (1.52 ± 0.63%, 1.75 ± 0.87% and 1.08 ± 0.25%, respectively, n=9 (9) P>0.05), (Figure 3.5).

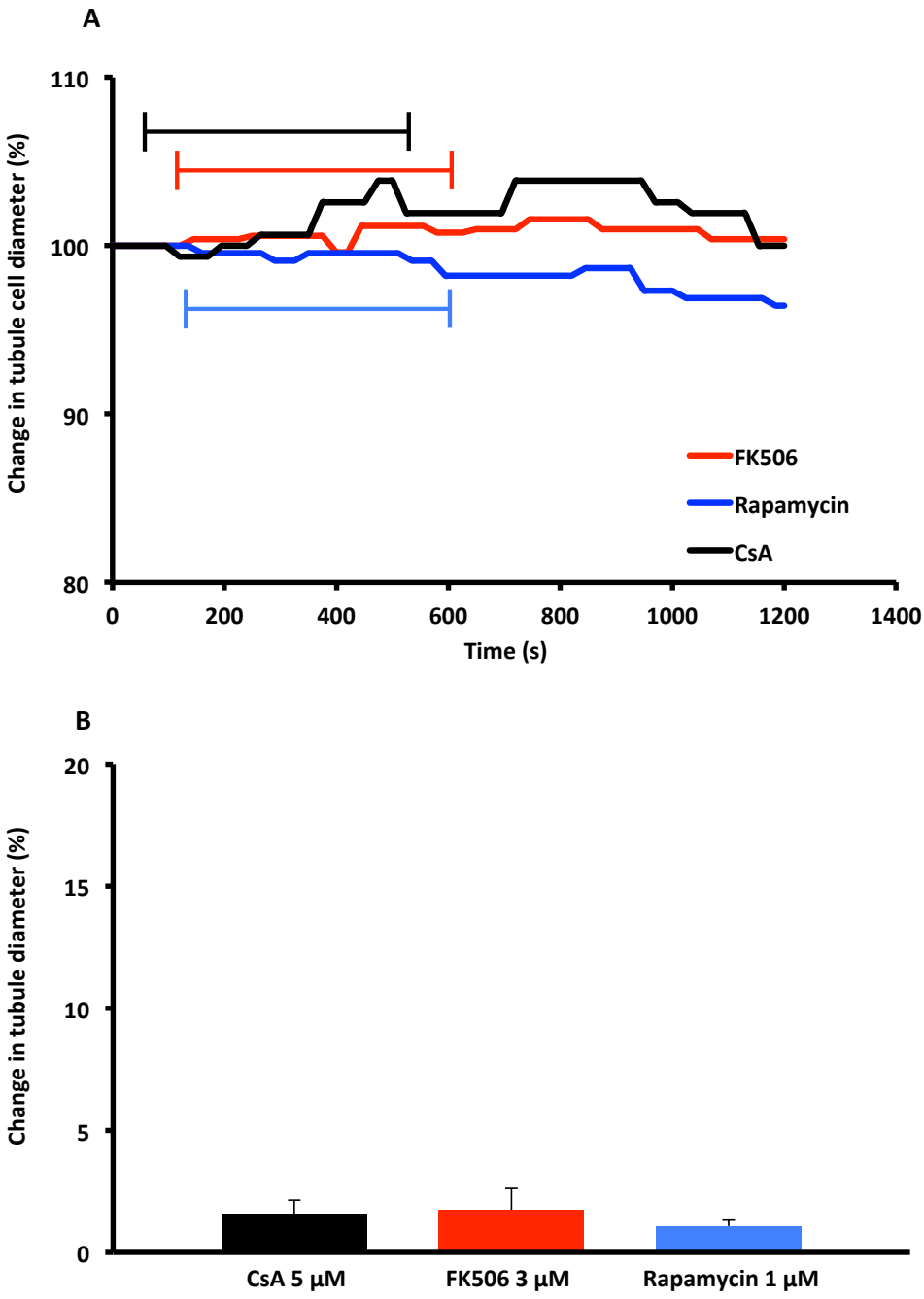

Figure 3.5 Superfusion of CNIs and rapamycin did not evoke morphological changes in renal tubules over time.

A: Representative trace of the change in cell diameter before, during and after superfusion of CsA, FK506 and rapamycin. B: Mean data for experiments investigating tubule diameter. No significant change, above or below 5%, was observed in either renal tubule cell size or renal tubule diameter. Values are mean ± S.E.M., n=10 (9).

3.6 Effect of combining CNIs with rapamycin on *in situ* vasa recta diameter

With organ rejection being one of the biggest concerns after renal transplant, sufficient immunosuppression is essential for avoiding graft-versus-host disease (GVHD) and maintaining normal function of the transplanted kidney. With the approval of rapamycin by the FDA in 1999 (Sehgal 2003), clinicians anticipated that combining rapamycin with CNIs would enhance immunosuppression and delay or prevent graft rejection (Ikeda *et al*. 1997; MacDonald 2003; McAlister *et al*. 2000).
Shortly after however, it was becoming apparent that a combination of immunosuppressive drugs, especially CsA and rapamycin, not only increased the risk of graft rejection but also nephrotoxicity, confirmed by increased rates of rejection and positive nephrotoxicity biopsies (Podder *et al*. 2001; MacDonald 2003; O'Connell *et al*. 2012).
Therefore, using the live slice model, the effect of combined immunosuppressive drugs was investigated on vasa recta capillaries at pericytes and non-pericytes.

Superfusion (~700 s) of CsA and rapamycin (3 and 1 μM, respectively) resulted in a reversible constriction of vasa recta capillaries (Figure 3.6). Vasoconstriction was significantly greater at pericyte sites (12.74 ± 0.97%) compared to non-pericyte sites (2.4 ± 0.62%, n= 9(8); P<0.001, (figure 3.6)). The CsA-rapamycin evoked constriction of vasa recta was reversed upon washout, and vessel diameter returned to ≥ 93% of the original baseline vessel diameter. Vasoconstriction at pericyte sites induced by the combination of CsA and rapamycin (12.74 ± 0.97%, n=9 (8)) was significantly greater compared to vasoconstriction at pericyte sites evoked by CsA alone (8.79 ±0.91%, n=9 (8); P<0.05), (Figure 3.6).
Superfusion (~700 s) of FK506 and rapamycin (0.1 and 1 μM, respectively) also resulted in a reversible constriction of vasa recta capillaries, (Figure 3.6). Vasoconstriction was significantly greater at pericyte sites (10.04 ± 2.01%) compared to non-pericyte sites (3.9 ± 0.69%, n= 9(8); P<0.001, (figure 3.5). The FK506-rapamycin evoked constriction of vasa recta was reversed upon washout, and vessel diameter returned to ≥ 90% of the original baseline vessel diameter. Vasoconstriction at pericyte sites induced by the combination of FK506 and rapamycin (10.04 ± 2.01%, n=9 (8)) was greater, although not significant, compared to vasoconstriction at pericyte sites evoked by FK506 alone (8.03 ±1.36%, n=9 (8); P>0.05), (Figure 3.6).

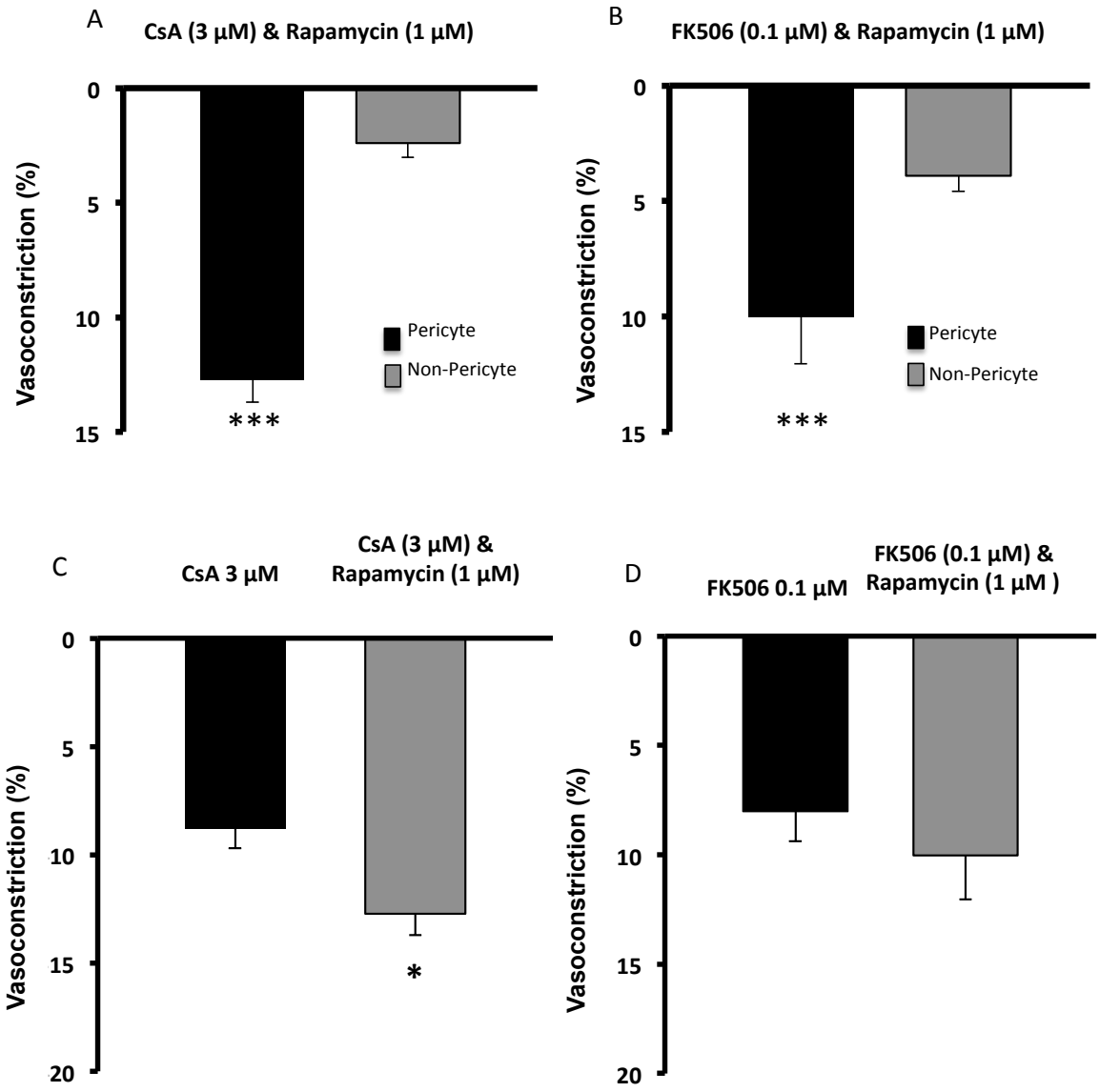

Figure 3.6 Superfusion of CNIs in combination with rapamycin induces and enhances pericyte-mediated vasoconstriction of in situ vasa recta. A: Mean data for experiments highlighting superfusion of CsA and rapamycin evokes a significantly greater constriction at pericyte sites (black bar) compared with non-pericyte sites (grey bar). Superfusion of FK506 and rapamycin (B) evokes a significantly greater constriction at pericyte sites (black bar) compared with non-pericyte sites (grey bar). C & D: Percentage change in vessel diameter in response to CsA (C) or FK506 (D) alone and in combination with rapamycin. Combining CsA and rapamycin evoked a significantly greater constriction of vasa recta at pericyte sites than when CsA was applied alone. Combining FK506 and rapamycin evoked a greater constriction compared to FK506, although not significant Data are mean ± SEM, n= 9(8); P<0.001.

3.7 Discussion

The main aim of this investigation was to establish if CNIs affect *in situ* vasa recta capillary diameter and if so, specifically *via* their action on pericytes. The experimental model used also enabled the effects of CNIs on renal tubules to be investigated and the possible role of tubular-vascular crosstalk in mediating CNI nephrotoxicity.

The main finding of this study is that both cyclosporine A and tacrolimus act specifically at renal pericytes to cause a significant, reversible, decrease in vasa recta diameter of *in situ* capillaries, at relevant clinical concentrations. Conversely, the mTOR inhibitor, rapamycin, failed to evoke any significant constriction of vasa recta *via* pericytes.

Based on previous publications using the live slice model (Crawford *et al*. 2012) that used Poiseuilles's law to estimate changes in blood flow (Landis 1933; Peppiatt *et al*. 2006), a 10% decrease of vasa recta diameter, *via* pericyte constriction, would result in an approximate 1.5 increase of renal blood flow resistance (RBFR). Given that MBF is crucial for maintenance of normal kidney function, it is conceivable that during CNI treatment, MBF may be impaired sufficiently enough that this may contribute towards CNI-mediated nephrotoxicity as a whole.

Ever since their first use for immunosuppression, CNIs have been known to be nephrotoxic in all major compartments of the kidney, however the exact molecular and cellular source of the insult has never truly been elucidated. One of the first studies to suggest renal vascular vasoconstriction as a predominant factor for the development of acute CNI nephrotoxicity was carried out in the 80's (Murray *et al*. 1985). They, along with other groups, were able to conclusively demonstrate the importance of CNIs in their ability to increase renal vascular resistance in the afferent and efferent arterioles, subsequently leading to impairment of blood flow and decreased GFR (Barros *et al*. 1987; Laskow *et al*. 1988).

The mechanisms of vascular dysfunction triggered through CNIs is however still unclear with theories ranging from direct endothelial injury to increased production of superoxide (Diederich *et al*. 1994; Voss *et al*. 1988; J. W. Park *et al*. 2011; Krejci *et al*. 2010) , although it is generally accepted that an increase in vasoconstrictors (endothelin, thromboxane and ANG II) and a decrease in vasodilators (PGE_2, NO and

prostacyclin) all contribute to the prevailing increase in vascular resistance (Naesens *et al*. 2009).

It is important to note that although this evidence is based on studies focusing on larger pre-capillary arterioles, little is known about the smaller capillaries, and in particular for this study, the effects of CNIs on vasa recta and their contractile pericytes.

Previous data has shown that all of the vasoactive substances able to effect the larger arterioles have been able to effect vasa recta diameter, *via* pericytes, either in isolation or *in situ* experimental models (Silldorff & Pallone 2001; Rhinehart & Pallone 2001a; Pallone & Silldorff 2001; Crawford *et al*. 2012; Crawford *et al*. 2013). Therefore, it appears reasonable to assume that CNIs would be able to not only decrease vascular blood flow to the larger arterioles supplying the cortex of the kidney, but also decrease blood flow to the renal medulla *via* vasa recta obtrusion through pericyte constriction. This in turn not only decreases the blood flow to an already borderline hypoxic area of the kidney (Baumgärtl *et al*. 1972; Brezis & Rosen 1995), the inner renal medulla is already subject to a reduced flow of blood therefore increasing the risk of hypoxia (R. G. Evans *et al*. 2008). In addition, this reduction of blood flow increases the risk of dysfunctional cortico-medullary osmotic gradients that are required to drive water and solute reabsorption crucial for accurate function of the kidney (Pallone, Turner, *et al*. 2003).

Taken together, the initial data presented here demonstrates for the first time the ability of renal pericytes to constrict vasa recta capillaries upon acute exposure to CNIs. This could consequently disrupt both cortical and medullary blood flow, which if left untreated, could develop into further complications including ischemia and longer term complications of fibrosis that lead to complete renal failure and total graft loss.

Chronic CNI nephrotoxicity is unfortunately outwith the realms of this experimental model. The live kidney slice is viable up to 4 hours post slicing (Crawford *et al*. 2012, unpublished data) however chronic CNI nephrotoxicity may take months to develop (Bakker *et al*. 2004; Chapman 2011). Nonetheless, it has been shown that following acute insult, renal pericytes are able to detach from their associated capillary beds, migrate to the interstitium and form the basis of fibrous scarring tissue through a variety of mechanisms (Peppiatt-Wildman 2013; Humphreys *et al*. 2010; Fligny &

Duffield 2013; Schrimpf & Duffield 2011). In addition, it has also been shown that continued vasoconstriction of pericytes "switches off" their ability to return to normal resting tension resulting in a permanent constricted state (Peppiatt *et al*. 2006; Vates *et al*. 2010; Hamilton *et al*. 2010). Together, these data highlights the possible role for pericytes contributing towards chronic CNI nephrotoxicity through either vessel detachment or continued capillary constriction.

The data presented here for the effects of CNIs on renal tubules is however, somewhat, underwhelming. It is known that CsA, and more specifically FK506, are prone to cause nephrotoxic effects through tubule dysfunction including isometric vacuolisation and tubule atrophy in the weeks following allograft transplant (Mihatsch *et al*. 1985; Mihatsch *et al*. 1986). However, with regards to acute CNI nephrotoxicity, these "specific" lesions are rarely seen or develop and only truly mature when chronic nephrotoxicity has been firmly established through biopsies. This is somewhat why acute CNI nephrotoxicity is so hard to clinically identify. For example the "specific" lesions that CNIs induce, especially in terms of kidney transplantation, far too often coincide with other injury occurrences and are often overlooked (d'Ardenne *et al*. 1986).

The data also suggests a novel mechanism for the reduced nephrotoxic side effects seen with rapamycin. Clinically, rapamycin is a considerably less nephrotoxic immunosuppressant, however it is very rarely used alone, and often used in combination with FK506 and/or steroids. It must be noted that data presented here indicates combination drug therapy by itself increases the chance of adverse drug interactions and side effects (Andoh *et al*. 1996; Brook *et al*. 2005; MacDonald 2003).
Rapamycin was first noted to have immunosuppressive effects in the late 90's when its initial use of an antifungal agent was halted and used for immunosuppression and graft survival (Sehgal 2003). Although not a CNI, rapamycin has similar immunosuppressive properties. Instead of inhibiting secretion of interleukin 2 (IL-2) *via* calcineurin, rapmycin inhibits IL-2 receptor-dependent signal transduction mechanisms *via* mTOR (V. W. V. Lee & Chapman 2005).
The main advantage of rapamycin immunosuppression is the low level of nephrotoxicity it produces, therefore seems a logical choice for the clinical setting. However, it was noted that early graft rejection rates with rapamycin alone, or in

combination with steroids, were significantly higher than that of patients treated with CNIs (Marti & Frey 2005; Dittrich *et al*. 2004; Kreis *et al*. 2000). This, along with impaired wound healing (V. W. Lee & Chapman 2005; Sehgal 2003), has reduced its use in various transplant centres, though still a highly regarded tool for transplant immunosuppression.

Given that rapamycin is a macrolide, it differs from CNIs in its structure and mode of action (Sehgal 2003). It complexes to the same binding protein as FK506, FKB12, but does not inhibit calcineurin, as is the case with FK506. Instead, the rapamycin-FKB12 complex inhibits the mammalian target of rapamycin (mTOR) which ultimately inhibits the response to IL-2 and T/B cell activation, unlike inhibition of IL-2 as is seen with FK-506 in T lymphocytes (Morelon *et al*. 2001).

Because rapamycin does not directly inhibit calcineurin, this has been the reason suggested for its reduced nephrotoxic effects (Sehgal 2003). CNI nephrotoxicity is thought to be elicited from the complete or partial inhibition of calcineurin activity (Krejci *et al*. 2010).

Calcineurin is a calcium/calmodulin dependent phosphatase that is required for dephosphorylation of the nuclear factor of activated T cells (NFAT) (Rao *et al*. 1997). Once dephosphorylated, NFAT is able to translocate to the nucleus, upregulate IL-2 transcription and therefore T cell activation (Naesens *et al*. 2009). One important note is that calcineurin and NFAT isoforms are not T cell specific and therefore suppression of the pathway can lead to various forms of toxicity, not just nephrotoxicity (E. H. Liu *et al*. 2007) and is a mechanism occurring in addition to the direct action of CNIs on pericytes.

The data presented here therefore indicates that rapamycin is unable to produce significant pericyte-mediated vasoconstriction of vasa recta and consequently would have a reduced detrimental effect on MBF compared to CNIs. Although the data presented does not completely replicate *in vivo* settings it provides evidence suggesting that in the medulla, rapamycin has less nephrotoxic side effects over CNIs.

It is now well documented that rapamycin has a significantly lower toxicity potential than either CNI, however if used in combination, the pharmacokinetic profile of each drug dramatically changes. O'Connell *et al* have demonstrated that a rapamycin and CsA combination significantly increases cytotoxicity in renal glomerular mesangial cells compared to either drug alone, and thought to be mediated through SMAD signalling (O'Connell *et al*. 2012). Podder *et al* investigated this combination *in vivo*

and was able to confirm the increased toxicity of both drugs when used in combination (Podder *et al*. 2001), however, the increase of toxicity observed was not due to SMAD signalling but pharmacokinetic interactions. Both drugs are extensively metabolised by the CYP 3A enzymes, therefore upon combined use, a coincidental increase in systolic concentrations of both drugs is undoubtedly anticipated (Picard *et al*. 2007). Interestingly, McAlister *et al* have demonstrated that a group of transplant patients (liver, kidney or pancreas) who underwent rapamycin and FK506 combination therapy, presented excellent graft function and low rejection rates without drug-induced side effects (McAlister *et al*. 2000). Therefore it is hard to deduce the extent of toxicity with combined immunosuppression, especially in the age of genetic medicine and influence of polymorphisms on single genes including CYP 3A (Barbarino *et al*. 2013).

Like CNIs, rapamycin showed no significant changes in tubule cell size or diameter, however recent evidence points towards rapamycin's ability to induce tubule dysfunction in the forms of apoptosis, tubule collapse and acute necrosis. This suggests that even though rapamycin might have less obvious toxic effects, it too could be an emerging immunosuppressant with the potential for development of nephrotoxicity (Marti & Frey 2005).

4. The effect of antihypertensive drugs in combination with CNIs on renal medulla *in situ* vasa recta

4.1 Introduction

Hypertension is the leading risk factor for premature death, stroke and development of heart disease worldwide (Joffres *et al*. 2013), therefore development of hypertension in renal transplant patients is an even greater risk factor to consider for proper function of renal allografts. This chapter set out to investigate the use of commonly prescribed antihypertensives in combination with CNIs to study their contractile effect on vasa recta pericytes and possibly identify a novel mechanism for the reduced nephrotoxicity seen in patients treated with CNIs and antihypertensives.

After successful kidney transplantation, before CNIs were introduced for first line immunosuppression, less than 50% of patients leaving hospital care would have had some form of hypertension (First *et al*. 1994). However, after CNI introduction for maintenance immunosuppression in 1983, up to 90% of all patients treated have systemic hypertension (Textor *et al*. 1994; Midtvedt & Hartmann 2002a).

Although CNIs and steroids do have a clear role in the development of pre and post-transplant hypertension, its development in the transplant population is in contrast to the general population, due to the fact donor and recipients have individual risk factors for hypertension. Some of the major risk factors associated with hypertension are highlighted in table 1.

Table1 Risk factors including pre and post-transplant of donor and recipient contributing to hypertension before and after transplant.

Pre-transplant	Donor	Recipient	Post-transplant
Pre-existing hypertension and left ventricular hypertrophy Body mass index Primary kidney disease	Elderly and female donor Hypertensive donor Use of right-sided donor kidney	Pre-existing hypertension and left ventricular hypertrophy Body mass index Corticosteroids Calcineurin inhibitors (CsA > FK506)	Prolonged ischemia time Delayed graft function Acute rejection Antibody-mediated rejection Chronic allograft nephropathy

4.1.2 Hypertension and graft function

Due to the fundamental role of the kidney in maintaining blood pressure, it is clear that hypertension is a compelling risk factor for the survival and function of any renal graft (Aparicio *et al*. 2013; Mangray & Vella 2011; Curtis *et al*. 1988; First *et al*. 1994). Moreover it has been known for some time that there is an intimate relationship between the prevalence of hypertension and the gradual demise of GFR (Cowley *et al*. 1995; Aparicio *et al*. 2013). However, the underlying mechanisms linking these parameters (GFR, hypertension and graft survival) is still poorly understood and as to whether the long-term reduction in systemic BP, improves graft function similarly remains unknown.

Modena *et al* identified a link between an increase in BP and increased rates of renal decline in transplant patients (Modena *et al*. 1991). The data obtained by Modena *et al* scrutinised the link from reciprocal of serum creatinine versus time plots in patients with clinical and histologic evidence of chronic renal transplant rejection (Modena *et al*. 1991). Furthermore, Opelz *et al* underlined the association between higher BP and kidney graft survival 1 year post transplant (Opelz *et al*. 1997). Opelz *et al* identified 29,000 patients with higher post-transplant hypertension than non-renal transplant controls, resulting in an increased risk for graft dysfunction (Opelz *et al*. 1997). Interestingly, the data produced by Opelz *et al* was followed up to investigate chronic graft dysfunction and was significantly associated with an increase in BP. The data produced by Opelz *et al* was able to undeniably conclude that post-transplant blood pressure is a highly significant predictor of long-term kidney allograft function (Opelz *et al*. 1997). Remarkably, both Modena *et al* and Opelz *et al* failed to take into account the role of CNIs in the development of hypertension and graft survival in each of the authors respective studies, even though it has been known for some time that CNIs are a significant factor in the development of transplant hypertension (First *et al*. 1994; Curtis *et al*. 1988; Textor *et al*. 1994).

4.1.3 Calcineurin inhibitors and development of hypertension

Even though both cyclosporine and tacrolimus have both been shown to induce or augment hypertension in transplant patients (Hohage *et al*. 1996; Mangray & Vella 2011; Curtis *et al*. 1988; First *et al*. 1994; Hoskova *et al*. 2014), this data and the additional risk factors discussed above, it is therefore almost impossible to asses the contribution of CNIs to the development of hypertension after renal transplant.

However, if data is compared to that collated from non-renal transplant patients, the extent to which CNI's are capable of inducing hypertension can start to be disentangled (Hoorn, *et al*. 2012; Moes *et al*. 2014; Textor *et al*. 2000; Naesens *et al*. 2009). Evidence suggests that the incidence of hypertension in patients undergoing bone marrow or heart transplant in the absence of CNI therapy is relatively uncommon, below 10%, prior to CNI therapy, but rose significantly to approximately 50% in bone marrow transplants and 80% in heart transplants after CNI induction therapy (Textor *et al*. 1994; Shiba *et al*. 2004).
Based on the above evidence it is therefore seems evident that CNIs, to a certain degree, have the capacity to induce hypertension after transplantation.

Data suggests that the hypertensive effects of CNI's could be attributed to two major models; i) vascular effects and ii) sodium retention, both will be discussed below.

4.1.3.1 Vascular effects of CNIs

CNIs have been shown to induce systemic and renal vasoconstriction (Hoorn, *et al*. 2012; Kaye *et al*. 1993), through an ANG II independent pathway (Murray *et al*. 1985). Renal vasoconstriction induced by CNIs is thought to originate from the increased production of endothelin *via* preglomerular arteries (Cavarape *et al*. 1998). This has been demonstrated directly in studies performed in rat models of CNI hypertension which utilised *in vivo* measurements of mean arterial pressure and GFR to show endothelin receptor antagonists significantly reducing CNI-induced hypertension (Perico *et al*. 1990), although it is still unclear whether endothelin contributes towards CNI hypertension through renal or systemic vasoconstriction. For example, Forslund *et al* have demonstrated that patients treated with CNIs develop hypertension independent of circulating endothelin levels. The data produced by Forslund et el was able to show rheumatoid arthritis patients receiving CsA had an increased systolic and diastolic BP 6 months after initial treatment but endothelin, as well as aldosterone and antidiuretic hormone levels remained unchanged (Forslund *et al*. 1995). Furthermore, Lanese and Conger have been able to demonstrate the direct contractile effect of CsA *via* endothelin on rat afferent and efferent arterioles of the renal microvasculature however their data suggests that endothelin is only responsible for constriction of the afferent arteriole and not efferent (Lanese & Conger 1993).

As well as increased vasoconstriction, CNI impaired vasodilation has been associated with the onset of hypertension. CsA has been shown to reduce spontaneous relaxation of resistance vessels in rat and humans and inhibit endothelium-dependent relaxation (Richards *et al*. 1989; Lassila *et al*. 2001; Vaziri *et al*. 2002.) *via* the reduction of nitric oxide (NO) (Morris *et al*. 2000). NO has also been implicated in the generation of reactive oxygen species (ROS) *via* CsA treatment (H.-W. Chen *et al*. 2002; Perez de Hornedo *et al*. 2007). The studies of Chen *et al* and Hornedo *et al* have been able to demonstrate CsA mediated production of ROS is *via* altered mitochondrial physiology and decreased production of antioxidant compounds including NAD(P)H, inducible nitric oxide synthase (iNOS), Hsp70 and dissipation of mitochondrial membrane potential (H.W. Chen *et al*. 2002; Perez de Hornedo *et al*. 2007) therefore a possible link between the up regulation of ROS and decrease of NO could be partly responsible for the vasoconstrictive effects seen with CNIs.
Data yielded from cell line studies has demonstrated that down regulation of NO after CsA treatment occurs in response to the inhibition of iNOS in VSMC's (Marumo *et al*. 1995). Tacrolimus has not been shown to induce such effect on iNOS production although in studies performed in rats, it has been shown to reduce endothelial nitric oxide synthase in aorta and also renal vasculature (Eguchi *et al*. 2013; Takeda *et al*. 1999), therefore, taken together, CNIs can be clearly demonstrated to effect systemic and local renal production of NO and possibly contribute towards the progression of hypertension.

CNIs have been shown to activate the renin-angiotensin system (RAAS) both directly, *via* juxtaglomerular cells secreting renin into the blood stream (Kurtz *et al*. 1988; Lassila 2002; Friis *et al*. 2006) and indirectly, *via* hemodynamic alterations induced by ANG II vasoconstriction (Ruester & Wolf 2006) therefore, the mechanisms for RAAS activation *via* CNIs still remains somewhat obscure. Studies performed in rats and humans investigating circulating plasma renin activity have shown contradictory results with Kurtz *et al* indicating increased levels of renin after CsA treatment (Kurtz *et al*. 1988) whereas Klein *et al* demonstrated suppressed levels of renin after CNI administration (Klein *et al*. 2002). Rats treated with CsA have been shown to have significantly higher levels of systemic and renal ANG II concentrations (Nishiyama *et al* 2003), feasibly leading to the increased production of renal ROS which was also demonstrated by Nishiyama *et el* who concluded that ROS generation induced by the

increased production of ANG II contributes to the development of CsA-induced hypertension (Nishiyama *et al*, 2003). Intriguingly, CsA has been shown to double the amount of ANG II type 1 receptor in VSMC's, that could account for the increased vasoconstrictive effects in combination with the excess production of ANG II (Avdonin *et al*. 1999).

4.1.3.2 Sodium retaining effects of CNIs

In recent years, it has become increasingly evident that CNI-induced hypertension is not completely dependent on their vasoconstrictive attributes but also their sodium retaining properties (Hoorn, *et al*. 2012; Mangray & Vella 2011; Hoorn *et al*. 2012). The definitive study to identify this effect was carried out by Curtis *et al* who investigated 15-hypertensive renal transplant patients, comparing data collected from patients having received CsA treatment, against 15 control hypertensive patients treated with azathioprine (Curtis *et al*. 1988). Using a salt variable diet in treated patients and controls, the authors were able to demonstrate the increase or decrease in BP levels after increasing dietary salt intake whereas the control patients had no such change in BP under the same salt conditions (Curtis *et al*. 1988).

Whilst the precise mechanisms underlying the CNI's-induced sodium retention are unknown, several studies have suggested that CNIs alter the expression of major sodium transporters as the reason for this physiological effect and thus these represent a novel target for the attenuation of CNI-induced sodium- retention.

Sodium reabsorption in the kidney is vital for correct homeostasis of electrolytes and water balance. There are 4 major transporters expressed along the renal tubules responsible for over 99% of total sodium reabsorption (Koeppen & Stanton 2013d). These include the sodium-hydrogen exchanger type 3 (NHE3) located on the proximal tubule, the sodium-potassium-chloride co-transporter type 2 (NKCC2) situated within the loop of Henle, the sodium chloride cotransporter (NCC) located within the distal convoluted tubule and the epithelial sodium channel (ENaC) in the collecting duct (Hoorn *et al*. 2012).

Although all of the aforementioned transporters will undoubtedly have some contribution towards the increased sodium reabsorption, it is the NCC that has received the most interest in recent years (Damiano *et al*. 2010; Hoorn *et al*. 2011; Blankenstein *et al*. 2014; Hoorn *et al*. 2012).

Various studies have focused their efforts on investigating which of the transporters is involved in the CNI-induced sodium retention and an interesting study by Hoorn *et al* investigated the possible role of WNK kinase mutations in the prevalence of hypertension while under CNI therapy (Hoorn *et al*. 2011). Their hypothesis was based on the fact that certain tubular disorders caused by CNIs have a striking similarity to Gordon syndrome, a rare from of hereditary hypertension (Hoorn *et al*. 2009). They revealed that NCC knock out mice did not develop salt sensitive hypertension after CNI treatment but mice over expressing NCC had an augmented hypertensive response to CNIs. This was extrapolated to renal transplant patents and using simple thiazide diuretics, to inhibit NCC, they were able to show a decreased expression of phosphorylated, activated form, of NCC (Hoorn *et al*. 2011). In turn, this inactive form of NCC was unable to induce levels of hypertension, *via* salt reabsorption, seen in patients treated with CNIs alone.

This simple, but ingenious, method for reducing the potential risk of CNI hypertension is a leap forward in rational for therapeutic interventions seeking to ameliorate CNI-induced hypertension (Hoorn *et al*. 2011; Hoorn *et al*. 2012; Hoorn, Walsh, McCormick, *et al*. 2012).

4.1.4 CNI-induced hypertension treatment

Following renal transplant, a complete lifestyle change is required to combat the risk or progression of hypertension and graft function or loss of function. This usually includes dietary changes, weight loss and physical exercise adjustments (Midtvedt & Hartmann 2002b).

Even having implicated many of the above significant changes, most patients require 1 or more antihypertensive medications to consistently control BP (Mangray & Vella 2011; Midtvedt & Hartmann 2002a). These include a variety of target specific drugs with the aim of combating either CNI-mediated vasoconstriction or salt retaining effects (Aparicio *et al*. 2013; Mangray & Vella 2011).

Angiotensin converting enzyme inhibitors (ACEi) and angiotensin receptor blockers (ARBs) were one of the first medications used in attempt to combat CNI induced hypertension (Aparicio *et al*. 2013). In non renal transplant patients, both drug types have been shown to slow the progression of chronic renal disease *via* a reduction in glomerular pressure (Naesens *et al*. 2009; Wolf 2006; Remuzzi *et al*. 2005) and interestingly, have also been shown to inhibit TFG-β, a growth factor upregulated by

CNIs and responsible for chronic allograft dysfunction (Lewis *et al*. 1993; Maschio *et al*. 1996). However, when used under renal transplant conditions, their effect on hypertension and chronic allograft dysfunction still remains unclear with trials suggesting both beneficial and detrimental effects thus these agents should be used with caution (Hiremath *et al*. 2007; Dudley 2001).

Calcium channel blockers (CCB) are an attractive option for clinicians trying to attenuate CNI-induced hypertension due to their vasodilatory properties (Frishman 2007; Ladefoged & Andersen 1994; Baroletti *et al*. 2003). CNIs predominantly induce vasoconstriction within the vasculature *via* their action on voltage gated calcium channels in smooth muscle cells. Blocking these channels results in a subsequent reduction in VSMC contraction and in some cases even induces vasodilation (Katz 1986). However CCBs fall into two main classes; dihydropyridines and nondihydropyridines and although both classes ultimately inhibit calcium channels, they vary considerably in their molecular targets and pharmacokinetics (Frishman 2007), which is particularly important for transplant patients already on a lifetime "cocktail" of medications and increases the risk of adverse effects through drug interactions. For example, a study by Karllova *et al* revealed the commonly used herbal medication, St Johns wort, used for its antidepressant and anti-inflammatory properties significantly reduced the systemic levels of CsA in transplant patients and put the patients at severe danger of under immunosuppression and increased risk of graft rejection (Karliova *et al*. 2000).

Diuretics, including loop diuretics, have had the least amount of attention with regards to attenuating CNI-induced hypertension over the past 30 years. Nonetheless, they have been a valuable tool for reducing salt and water retention in hypertensive transplant patients (Vergoulas 2001). Hypertension in renal transplant patients was initially thought to derive from CNI-mediated oedema and vasoconstriction (Mangray & Vella 2011), however a new mechanistic proposal has been put forward regarding the activation of NCC and increased salt reabsorption (Hoorn *et al*. 2011) as previously described, and may offer a new pharmacokinetically safe method for treating hypertension after renal transplant.

Given the vast array of risk factors for CNI-induced hypertension, coupled with the numerous amount of medications used to treat the complication, it is clear that CNI-

induced hypertension is not only inevitable in most cases, but its management remains clinically complicated. The combination of immunosuppressant's and antihypertensives must be selected with caution due to the interplay of drug interactions and possible cause for further complications.

The aim of this study was to investigate the combination of antihypertensives and CNIs to determine their effect, if any, on renal medullary vasculature and in particular focus, the effect of CNIs on pericytes in the presence of antihypertensive medications.

4.2 Methods

Intact live kidney slices were obtained as previously described in General Methods. Live kidney slices were superfused with cyclosporine A (CsA) or tacrolimus (FK506) in the presence of losartan, hydrochlorothiazide (HCT), diltiazem or isradipine, all purchased from Sigma-Aldrich (Dorset, UK). All working solutions were prepared in 95% O_2 / CO_2 PSS however stocks of CsA and FK506 were made in DMSO. The final DMSO in all working solutions was less than 1%. In all experiments to determine the affect on vasa recta diameter, kidney slices were superfused with 95% O_2 / CO_2 PSS for ~100 s to establish a baseline vessel diameter at the pericyte and non-pericyte sites. Slices were then exposed to CsA, or FK506 and an antihypertensive for approximately 700 s and then subjected to a PSS-wash to assess reversibility of any affect. In some instances, imaging experiments commenced after an incubation of the slice in the particular antihypertensive, all tissue was continually perfused with PSS bubbled with 95% O_2 / CO_2 and desired concentration of antihypertensive. Control experiments for the effect of antihypertensive alone were also carried out. Analysis of video recordings of changes in vasa recta diameter has been described previously in general methodology. Briefly, each experiment was analysed using the free public domain software IMAGE J (NIH; http://rsb.info.nih.gov). For each experiment, a pericyte site and non-pericyte site were identified on a single casa recta capillary acting as a paired control. The diameter of the vasa recta at both of these locations was measured every five frames for the duration of the experiment. An average of the first five measurements was taken to represent the resting diameter value (*i.e.* 100%) for the selected pericyte and non-pericyte sites. All subsequent diameter measurements at both sites, increase or decrease, were calculated as a percentage change of the corresponding resting diameter value.

4.2.1 Statistics

All data are presented as mean values ± SEM; *n* numbers are displayed as number of kidney slices, and were appropriate, (number of animals). All experiments were performed in at least six different animals. Statistical assessment was performed with GraphPad Prisim (v5.0f; GraphPad software, San Diego, CA, USA). When two groups were compared, a Student's t-test (two-tailed, paired or unpaired where appropriate) was used. A value of $P < 0.05$ was considered significant.

4.3 Results

4.3 Investigating the effect of losartan on CsA-mediated changes in vasa recta diameter

To determine whether the vasoconstrictive effects of CsA on *in situ* vasa recta *via* pericytes is mediated by angiotensin, the selective ANG II type I receptor inhibitor, losartan, tissue was exposed to both losartan and CsA to explore any significant losartan-mediated alterations in CsA evoked constriction of vasa recta.

Superfusion (~700 s) of CsA & losartan (5 μM / 100 nM, respectively) resulted in a reversible constriction of vasa recta capillaries *via* pericytes (Figure 4). CsA-mediated an 11.80 ± 0.60% constriction of vasa recta *via* pericytes in the presence of losartan that was not significantly different to the constriction evoked by CsA alone (12.17 ± 0.88%, n=8 (7), figure 4). Changes in vessel diameter at non-pericytes *via* CsA and losartan (5 μM / 100 nM) was not significantly different when compared to CsA alone (5 μM) alone (3.4 ± 1.1% and 2.9 ± 0.88%, respectively).

The CsA and losartan evoked constriction of vasa recta was reversed upon washout, and vessel diameter returned ≥ 92% of the original baseline vessel diameter after 500 s following washout.

Superfusion of losartan alone has previously been shown to have no significant effect on vasa recta diameter at pericyte and non pericyte sites (Crawford *et al*. 2012).

In order to investigate the possible concentration dependent effect of CsA on vasa recta pericytes, losartan was used in combination with CsA at lower concentrations to

determine if CsA dependent vasoconstriction at clinical concentrations was influenced by complete ANG II type I receptor inhibition.

Superfusion (~700 s) of CsA & losartan (1 and 3 μM / 100 nM, respectively) resulted in a reversible constriction of vasa recta capillaries *via* pericytes (Figure 4). Vasoconstriction at pericytes sites induced by CsA & losartan (1 and 3 μM / 100 nM) was not significantly attenuated by the presence of losartan (5.99 ± 0.51 % and 9.02 ± 0.48%, respectively, n=8 (7)) compared to superfusion of CsA (1 & 3 μM) alone at pericyte sites (6.8 ± 0.89% and 9.49 ± 1.03%, respectively, n=8 (7)) (Figure 4).

Similarly, changes in vessel diameter at non-pericyte sites induced by CsA and losartan (1 & 3 μM / 100 nM) was not significantly different when compared to CsA (1 & 3 μM) alone.

All CsA and losartan induced vasoconstrictions were reversed upon washout and returned to ≥ 92% original baseline diameter after 500 s following washout.

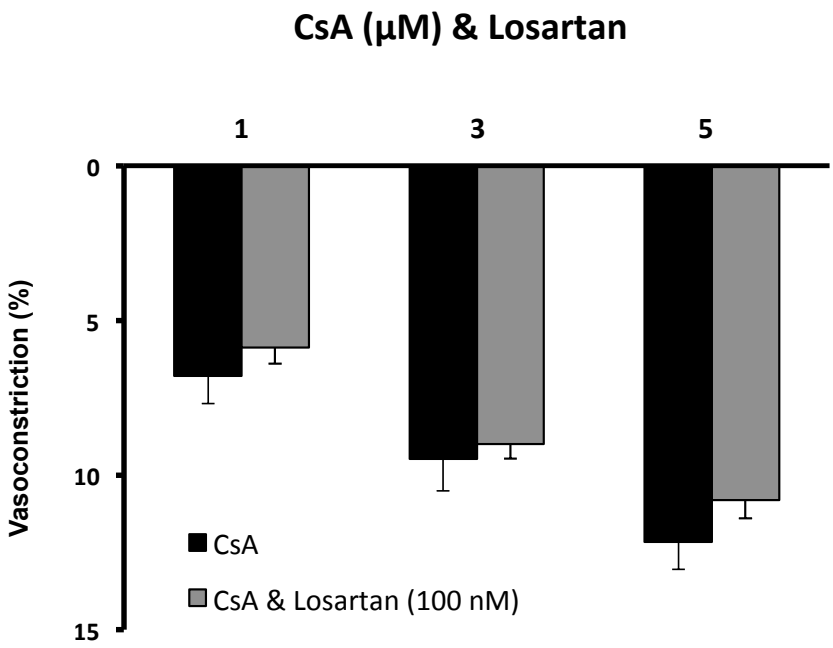

Figure 4.0 CsA-induced constriction of vasa recta is not significantly attenuated by the AT_1 receptor antagonist losartan.

Bar graph showing the mean % change in vasa recta diameter at pericyte sites when slices were superfused with CsA alone at varying concentrations (1, 3 and 5 μM; black bars) and in the presence of losartan (100 nM; Grey bars). No significant attenuation of the CsA-induced change in vessel diameter was observed when losartan was present indicating CsA-induced vasoconstriction of vasa recta by pericytes is not mediated *via* AT_1 receptors. Data are mean ± SEM, n=8 (7), $P<0.05$.

4.4 The effect of losartan on the FK506-mediated changes in vasa recta diameter

As losartan had no significant inhibitory effect on CsA mediated vasoconstriction, it was hypothesised that it would similarly have no inhibitory effect on FK506-mediated vasoconstriction.

Superfusion (~700 s) of FK506 & losartan (1 μM / 100 nM, respectively) resulted in a reversible constriction of vasa recta capillaries *via* pericytes (Figure 4.1). Vasoconstriction induced by FK506 and losartan was not significantly attenuated at pericyte sites compared to superfusion of FK506 alone at pericyte sites (10.99 ± 0.13 and 11.31 ± 0.74%, respectively, n=7 (7), figure 4.1). Vasoconstriction at non-pericytes *via* FK506 and losartan (1 μM / 100 nM) was not significantly different when compared to FK506 alone (1 μM) alone (2.78 ± 1.1% and 1.67 ± 0.78%, respectively).

The FK506 and losartan evoked constriction of vasa recta was reversed upon washout, and vessel diameter returned to ≥ 95% of the original baseline vessel diameter after 500 s following washout.

As with CsA experimentation, FK506 was investigated for concentrations dependent effects in combination with losartan.

Superfusion (~700 s) of FK506 & losartan (0.05 and 0.1 μM / 100 nM, respectively) resulted in a reversible constriction of vasa recta capillaries *via* pericytes (Figure 4.1). Vasoconstriction induced by FK506 & losartan (0.05 and 0.1 μM / 100 nM) was not significantly attenuated at pericyte sites (5.11 ± 0.98% and 8.00 ± 0.6%, respectively, n=7 (7)) compared to superfusion of FK506 (0.05 & 0.1 μM) alone at pericyte sites (5.2 ± 0.59% and 8.71 ± 1.11%, respectively, n=7 (7), figure 4.1).

Similarly, vasoconstriction at non-pericyte sites induced by FK506 and losartan (0.05 & 0.1 μM / 100 nM) was not significantly different when compared to FK506 (0.05 & 0.1 μM) alone. All FK506 and losartan induced vasoconstrictions were reversed upon washout and returned to ≥ 95% original baseline diameter after 500 s following washout.

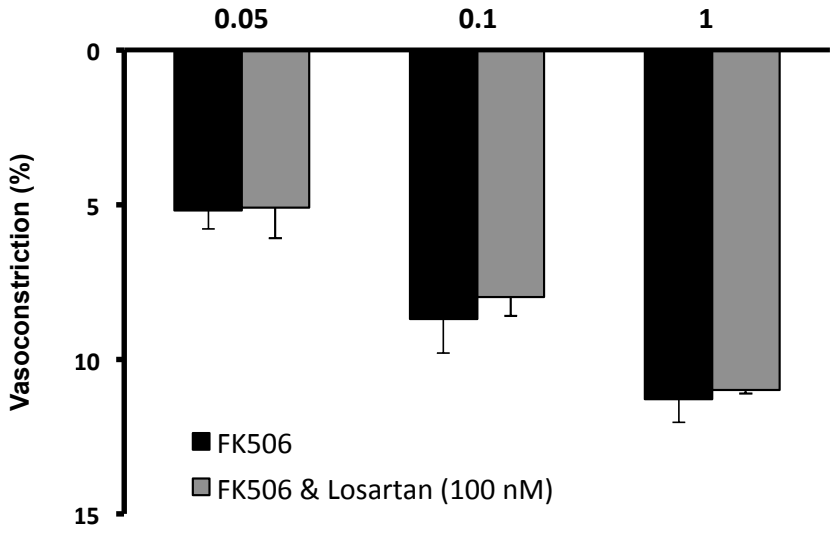

Figure 4.1 FK506-induced constriction of vasa recta is not significantly attenuated by the AT_1 receptor antagonist losartan.

Bar graph showing the mean % change in vasa recta diameter at pericyte sites when slices were superfused with FK506 alone at varying concentrations (0.05, 0.1 and 1 µM; black bars) and in the presence of losartan (100 nM; Grey bars). No significant attenuation of the FK506-induced change in vessel diameter was observed when losartan was present indicating FK506-induced vasoconstriction of vasa recta by pericytes is not mediated *via* AT_1 receptors. Data are mean ± SEM, n=7 (7), P>0.05.

4.5 The effect of hydrochlorothiazide in combination with CNIs on *in situ* vasa recta

Recently, it has been shown that FK506 upregualtes the expression the sodium chloride co-transporter (NCC) to induce hypertension (Hoorn *et al*. 2011), which suggests that CNI-induced hypertension may not be exclusively dependent on vascular dysfunction but may also be the result of altered sodium handling. Given the close apposition of tubules and vessels in the medulla and the established role for pericytes in mediating tubular-vascular cross talk (Crawford *et al*. 2012) it is feasible that CNI-mediated alterations in sodium handling may also impact upon vessel diameter due to pericyte mediated tubular-vascular cross talk. The thiazide diuretic, hydrochlorothiazide (HCT), was used in conjugation with CNIs to study the possible

role of NCC up-regulation and to what extent inhibiting NCC had on pericyte contraction in the presence of CNI's.

4.5.1 Effect of hydrochlorothiazide on *in situ* vasa recta

To determine the effects of HCT on vasa recta diameter, live tissue slice were superfused (~700 s) with HCT (1 μM) and resulted in no significant constriction of vasa recta capillaries (Figure 4.2). When a change in diameter was observed, it was not significantly greater at pericyte sites (1.70 ± 0.9%,) compared to non-pericyte sites (1.64 ± 1.3%, n=9 (9); P>0.05) (Figure 4.2). Upon washout, vessel diameter continued to be stable and rarely dropped below 97% of the original baseline vessel diameter after 400 s following washout.

To investigate if HCT had any effects in a concentration dependent manner, increasing concentrations of HCT was applied to the live kidney slice. The aim of this approach being to increase NCC inhibition, and eventually complete inhibition of the co-transporter, given that 5 μM is higher than has been clinically observed in whole blood (Swaisland 1991). HCT is not therapeutically monitored therefore concentrations between individuals will vary considerably. Furthermore, low doses of HCT range from 1.5–2.5 mg and high doses from 12.5-25 mg and are dispensed with degree of established hypertension (Tziomalos *et al*. 2013).

Superfusion (~700 s) of HCT (3 & 5 μM) resulted in no significant constriction of vasa recta capillaries (Figure 4.2). When changes in vasa recta diameter were noted, it was not significantly greater at pericyte sites (0.77 ± 2.34% and 0.43 ± 0.89%, respectively) compared to non-pericyte sites (0.42 ± 0.61% and 0.59 ± 0.46%, respectively, n=9 (9); P>0.05) (Figure 4.2). Upon washout, vessel diameter continued to stabilise and rarely dropped below 98% of the original baseline vessel diameter after 400 s, and up to 1000 s, following washout.

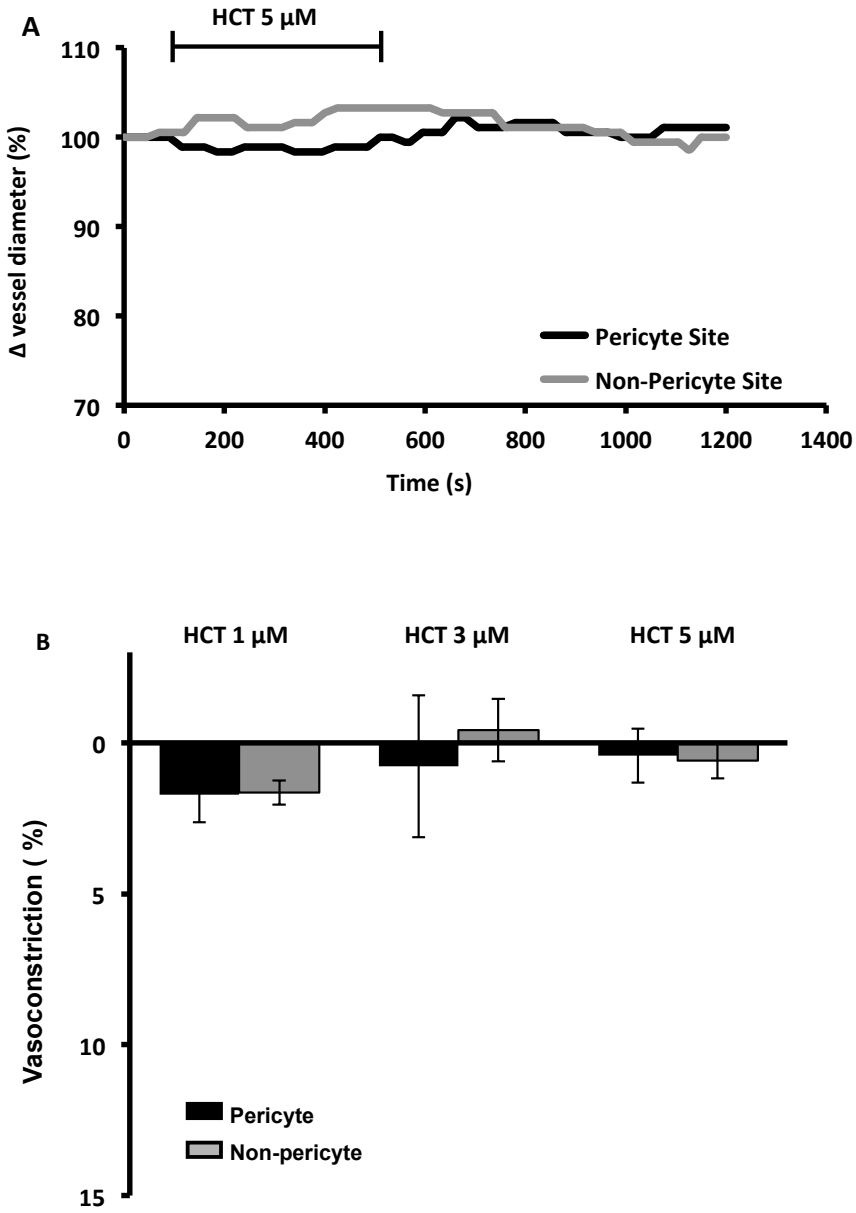

Figure 4.2 Superfusion of live kidney tissue with hydrochlorothiazide does not induce significant pericyte-mediated constriction of vasa recta. A: Representative trace of the % change in vessel diameter recorded over time at pericyte sites (black line) and non-pericyte sites (grey line) when live kidney slices were exposed to HCT (5 µM). B: Bar graph showing mean data for experiments in which live tissue was superfused with HCT (1, 3 and 5 µM). HCT does not evoke a significantly greater constriction of vasa recta at pericyte sites (black bars) compared to non-pericyte sites (grey bars). Data are mean ± SEM, n=9 (9), P>0.05.

4.5.2 Effect of exposing live kidney tissue to both HCT and FK506

Given that HCT had no significant effect on vasa recta diameter alone, the effect of combining HCT and FK506 was investigated. Referring back to the work by Hoorn *et al* (Hoorn *et al*. 2011), they were able to demonstrate in NCC knockout mice the significant reduction in blood pressure after being treated with FK506 compared to wild type mice treated with FK506. Interestingly, Melnikov *et al* have also shown similar effects with the use of CsA (Melnikov *et al*. 2011) suggesting that CNIs cause some form of salt sensitive hypertension *via* upregulation of the NCC. With this in mind, the effect of FK506 in combination with HCT was used to explore the potential role of pericytes and HCT in the progression of CNI-induced hypertension.

Superfusion (~700 s) of FK506 and HCT (3 & 1 μM, respectively) resulted in a significantly reduced reversible constriction of vasa recta capillaries when compared to that evoked following exposure of kidney slices to FK506 alone (Figure 4.3). Vasoconstriction induced by FK506 and HCT was significantly reduced at pericyte sites (5.10 ± 1.79%) compared to vasoconstriction induced by FK506 alone at pericyte sites (12.64 ± 0.65%, n= 9(9); P<0.01, (Figure 4.3). The FK506 and HCT evoked constriction of vasa recta was reversed upon washout, and vessel diameter returned to ≥ 98% of the original baseline vessel diameter after 400 s following washout. Vasoconstriction at pericyte sites induced by the combination of FK506 and HCT (3 & 1 μM, respectively) (5.10 ± 1.79%) was not significantly greater compared to non-pericyte sites (3.79 ±0.91%, n=9 (9), figure 4.3).

Given that HCT was able to attenuate FK506-medaited vasoconstriction and HCT concentrations vary considerably between individuals, increasing concentrations of HCT to theoretically completely inhibit NCC, in the presence of FK506 was investigated.

Superfusion (~700 s) of FK506 (3 μM) and HCT (3 & 5 μM) resulted in an increased attenuation of FK506-mediateed vasoconstriction of vasa recta capillaries when compared to FK506 alone (Figure 4.3). Vasoconstriction induced by FK506 (3 μM) and HCT (3 & 5 μM) was significantly reduced at pericyte sites (3.12 ± 0.93% and 3.25 ± 1.17%, respectively) compared to vasoconstriction induced by FK506 alone at

pericyte sites (12.64 ± 0.65%, n= 9(9); P<0.001, (Figure 4.3). The FK506 and HCT evoked constriction of vasa recta, at all concentrations, was reversed upon washout, and vessel diameter returned to ≥ 95% of the original baseline vessel diameter after 400 s following washout. Vasoconstriction at pericyte sites induced by the combination of FK506 (3 μM) and HCT (3 & 5 μM) (3.12 ± 0.93% and 3.25 ± 1.17%, respectively) was not significantly greater compared to non-pericyte sites (1.99 ±0.51% and 3.3 ± 1.17%, respectively. n=9 (9), figure 4.3).

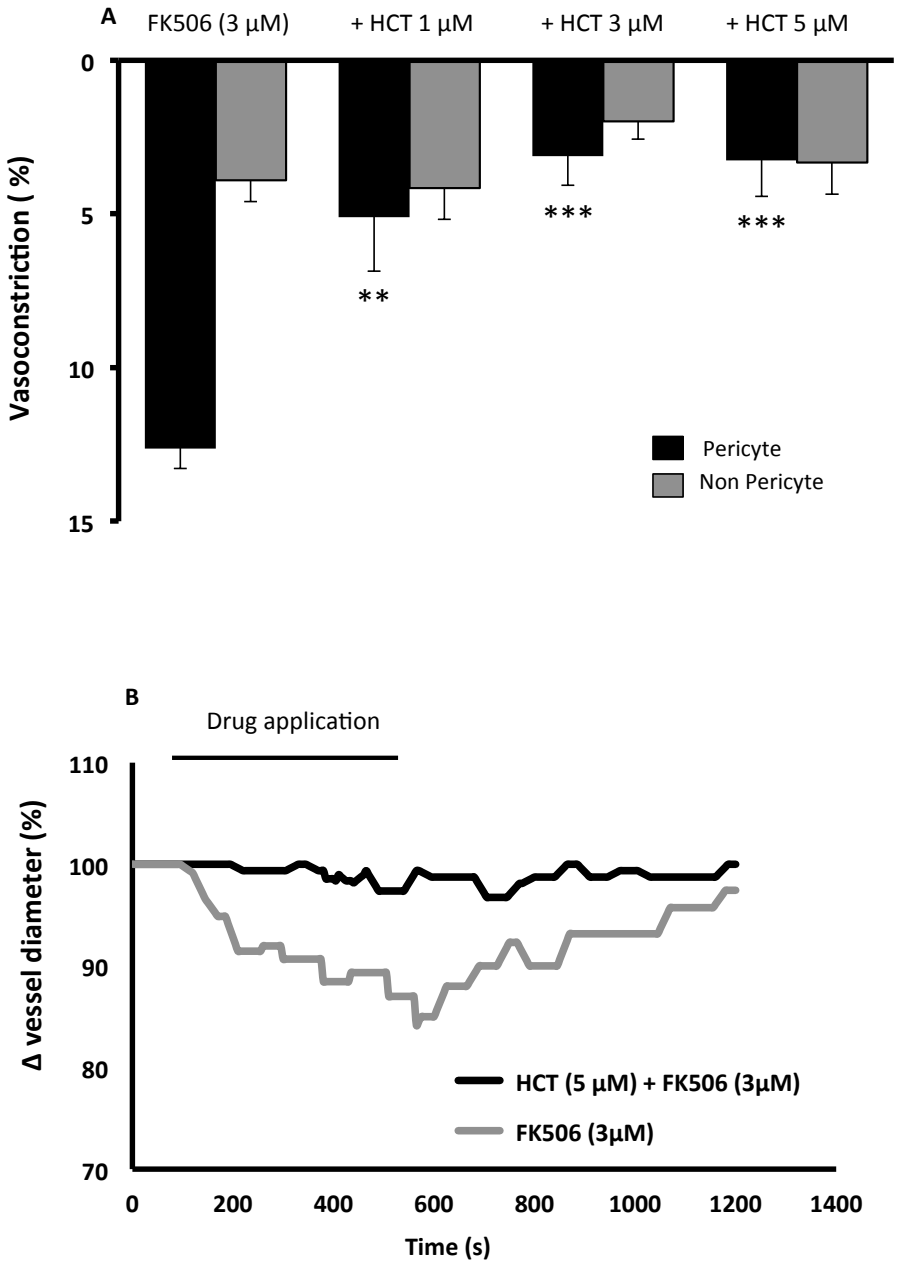

Figure 4.3 Hydrochlorothiazide attenuates the FK506 evoked vasoconstriction of *in situ* vasa recta by pericytes. A*:* Bar graph showing mean % change in vessel diameter at pericytes (black bars) in response to superfusion of tissue with FK506 alone (3 µM) and in the presence of HCT (1, 3 and 5 µM). Live tissue was pretreated with HCT for 10 minutes prior to onset of imaging. B: Representative trace of the % change in vessel diameter recorded over time at pericyte sites when exposed to FK506 (3 µM) alone (grey line) and in the presence of FK506 (3 µM) and HCT (5 µM) (black line). Data are mean ± SEM, n=9 (9). **P<0.01, ***P<0.001.

4.5.3 Effect of exposing live kidney tissue to both HCT and CsA

Superfusion (~700 s) of CsA and HCT (1 & 1 μM, respectively) resulted in an attenuation of CsA-mediated vasoconstriction of vasa recta capillaries when compared to CsA alone (Figure 4.4). Vasoconstriction induced by CsA and HCT was significantly reduced at pericyte sites (4.57 ± 1.97%) compared to vasoconstriction induced by CsA alone at pericyte sites (8.23 ± 0.44%, n= 9(9); $P<0.05$, (Figure 4.4). The CsA and HCT evoked constriction of vasa recta was reversed upon washout, and vessel diameter returned to ≥ 95% of the original baseline vessel diameter after 400 s following washout. Vasoconstriction at pericyte sites induced by the combination of CsA and HCT (1 & 1 μM, respectively) (4.57 ± 1.97%) was not significantly greater compared to non-pericyte sites (2.71 ± 0.91%, n=9 (9); $P<0.05$), figure 4.4.

As with FK506, increasing the concentrations of HCT, to completely inhibit NCC, in the presence of CsA was investigated.

Superfusion (~700 s) of CsA (1 μM) and HCT (3 & 5 μM) resulted in an increased attenuation of CsA-mediated vasoconstriction of vasa recta capillaries when compared to CsA alone (Figure 4.4). Vasoconstriction induced by CsA (1 μM) and HCT (3 & 5 μM) was significantly reduced at pericyte sites (3.83 ± 0.84% and 3.41 ± 1.32%, respectively) compared to vasoconstriction induced by CsA alone at pericyte sites (8.23 ± 0.44%, n= 9(9); $P<0.01$, (Figure 4.4). The CsA and HCT evoked constriction of vasa recta, at all concentrations, was reversed upon washout, and vessel diameter returned to ≥ 95% of the original baseline vessel diameter after 400 s following washout. Vasoconstriction at pericyte sites induced by the combination of CsA (1 μM) and HCT (3 & 5 μM) (3.83 ± 0.84% and 3.41 ± 1.32%, respectively) was not significantly greater compared to non-pericyte sites (2.33 ± 0.92% and 3.58 ± 1.98%, respectively. n=9 (9); $P>0.05$), figure 4.4.

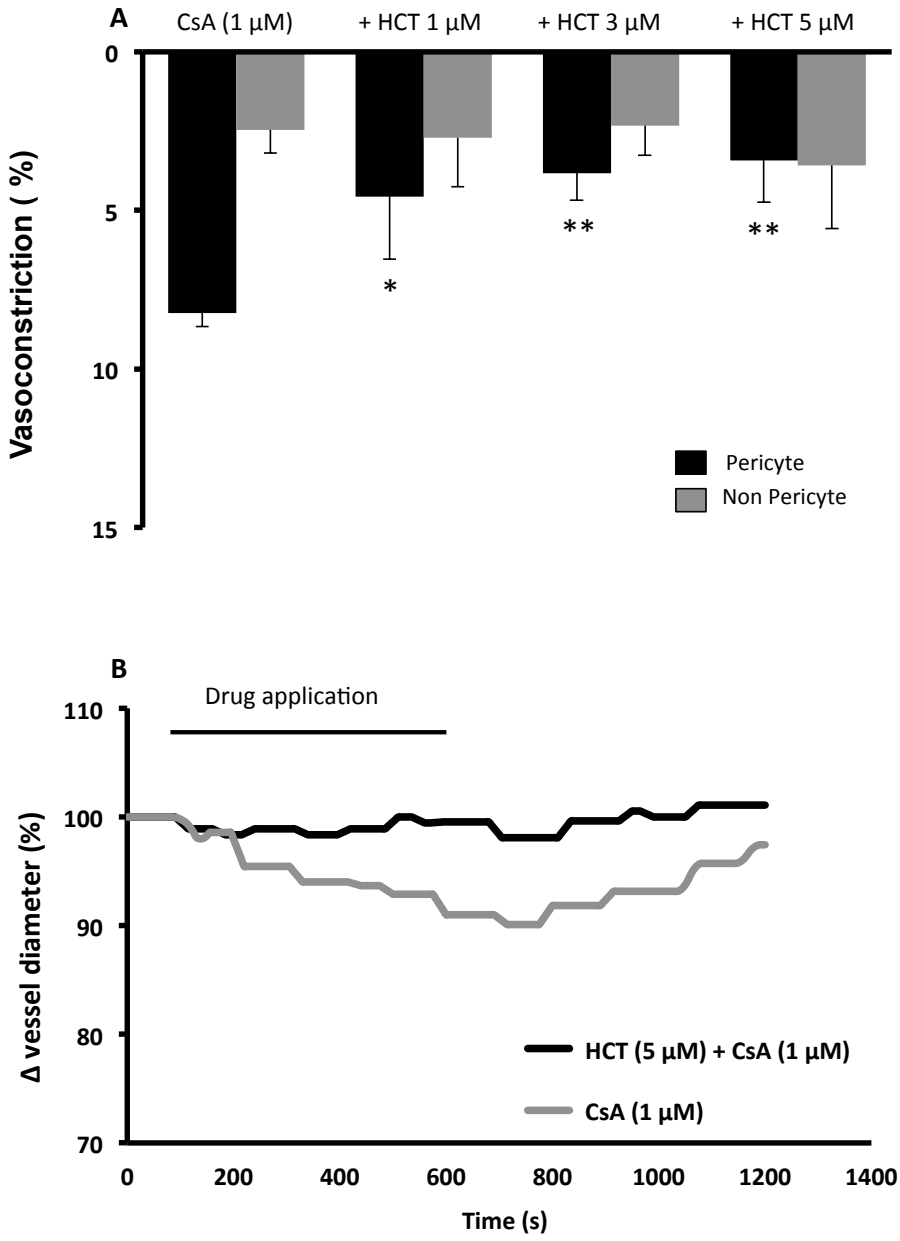

Figure 4.4 Hydrochlorothiazide attenuates the CsA-evoked vasoconstriction of *in situ* vasa recta by pericytes. A: Bar graph showing mean % change in vessel diameter at pericytes (black bars) and non pericyte sites (grey bars) in response to superfusion of tissue with CsA alone (1 µM) and in the presence of HCT (1, 3 and 5 µM). Live tissue was pretreated with HCT for 10 minutes prior to onset of imaging. B: Representative trace of the % change in vessel diameter recorded over time at pericyte sites when exposed to CsA (1 µM) alone (grey line) and in the presence of CsA (1 µM) and HCT (5 µM) (black line). Data are mean ± SEM, n=9 (9). *P<0.05, **P<0.01.

4.6 The effect of diltiazem in combination with CNIs on *in situ* vasa recta

Given that much of the literature suggests the prominent role of vasoconstriction is an important factor in CNI-induced hypertension, although new insights *via* salt sensitivity are emerging (Melnikov *et al*. 2011; Hoorn, Walsh, McCormick, *et al*. 2012), inducing some form of vasodilation is an attractive proposition to combat the onset of CNI-mediated hypertension. The most commonly used medications to combat CNI-induced renal vasoconstriction are calcium channel blockers (CCB's) (Ladefoged & Andersen 1994; Baroletti *et al*. 2003). Although CCBs fall into two major classes; dihydropyridines and nondihydropyridines, they both work to inhibit voltage-gated calcium channels from opening and preventing contraction in various types of contractile cells. Given the fact that in addition to VSMCs, pericytes are also described as smooth muscle "like" cells since they contain similar contractile proteins (Shepro & Morel 1993; S. W. Smith *et al*. 2012) therefore the effect of superfusing live kidney tissue with a combination of CCBs with CNIs was investigated to assess the possible contribution of calcium channel regulation in the pericyte-mediated contraction of vasa recta induced by CNIs.

4.6.1 Effect of diltiazem on *in situ* vasa recta diameter

Given that diltiazem has already been used clinically to treat CNI-induced hypertension and also used to investigate calcium responses in isolated pericyte experiments (Kumana *et al*. 2003; Becker *et al*. 1996; Ingsathit *et al*. 2006; Z. Zhang *et al*. 2004; Z. Zhang *et al*. 2002), it was reasonable to investigate this drug in the live kidney slice preparation to explore its potential for attenuation of CNI-mediated vasoconstriction. Superfusion (~700 s) of diltiazem alone (100 & 400 nM) resulted in no significant change of vasa recta capillary diameter (Figure 4.5). When a change in diameter was observed at 100 and 400 nM, it was not significantly greater at pericyte sites (1.67 ± 0.44% and 0.86 ± 1.56%, respectively) compared to non-pericyte sites (1.94 ± 0.83% and 1.41 ± 1.01%, respectively n=10 (9); P>0.05) (Figure 4.5). Upon washout, vessel diameter continued to be stable and rarely dropped below 96% of the original baseline vessel diameter after 400 s, and up to 1000 s, following washout of diltiazem. Although diltiazem has been thought to stick to perfusion lines, perfusion using wider tubing and slower perfusion rates (personal communication with Pallone lab), no residue was observed or seen to effect subsequent experiments.

4.6.2 Effect of diltiazem on *in situ* vasa recta diameter in combination with CsA

Diltiazem had no effect on vasa recta diameter when superfused alone whereas CsA significantly reduces vasa recta diameter *via* pericyte constriction. Diltiazem has been shown to reduce hypertension in patients treated with CNI's (Kothari *et al*. 2004) *via* a reduced dosing regime of CsA and subsequently reduced renal and systemic vasoconstriction but more notably, also reduce tubular and vascular CNI nephrotoxicity (Becker *et al*. 1996; Gokce *et al*. 2012). Therefore, to investigate the role of calcium channel activation on the established effect of CNI-mediated vasoconstriction of vasa recta *via* pericytes, live tissue was exposed to a combination of diltiazem and CsA and changes in vessel diameter were investigated.

Superfusion (~700 s) of CsA (3 μM) and diltiazem (100 & 400 nM) resulted in an attenuation of CsA-mediated vasoconstriction of vasa recta capillaries when compared to CsA alone (Figure 4.5). Vasoconstriction induced by CsA (3 μM) and diltiazem (100 & 400 nM) was significantly reduced at pericyte sites (5.21 ± 1.34% and 4.13 ± 1.10%, respectively) compared to vasoconstriction induced by CsA alone at pericyte sites (9.98 ± 0.98%, n= 10 (9); $P<0.01$, $P<0.001$, (Figure 4.5). The CsA and diltiazem evoked constriction of vasa recta, at all concentrations, was reversed upon washout, and vessel diameter returned to ≥ 95% of the original baseline vessel diameter after 400 s following washout. Vasoconstriction at non-pericyte sites induced by the combination of CsA (3 μM) and diltiazem (100 & 400 nM) (5.21 ± 1.34% and 4.13 ± 1.10%, respectively) was not significantly greater compared to vasoconstriction induced by CsA alone at non-pericyte sites (2.42 ± 1.95% and 3.4 ± 1.12%, respectively n=10 (9); $P>0.05$), (Figure 4.5).

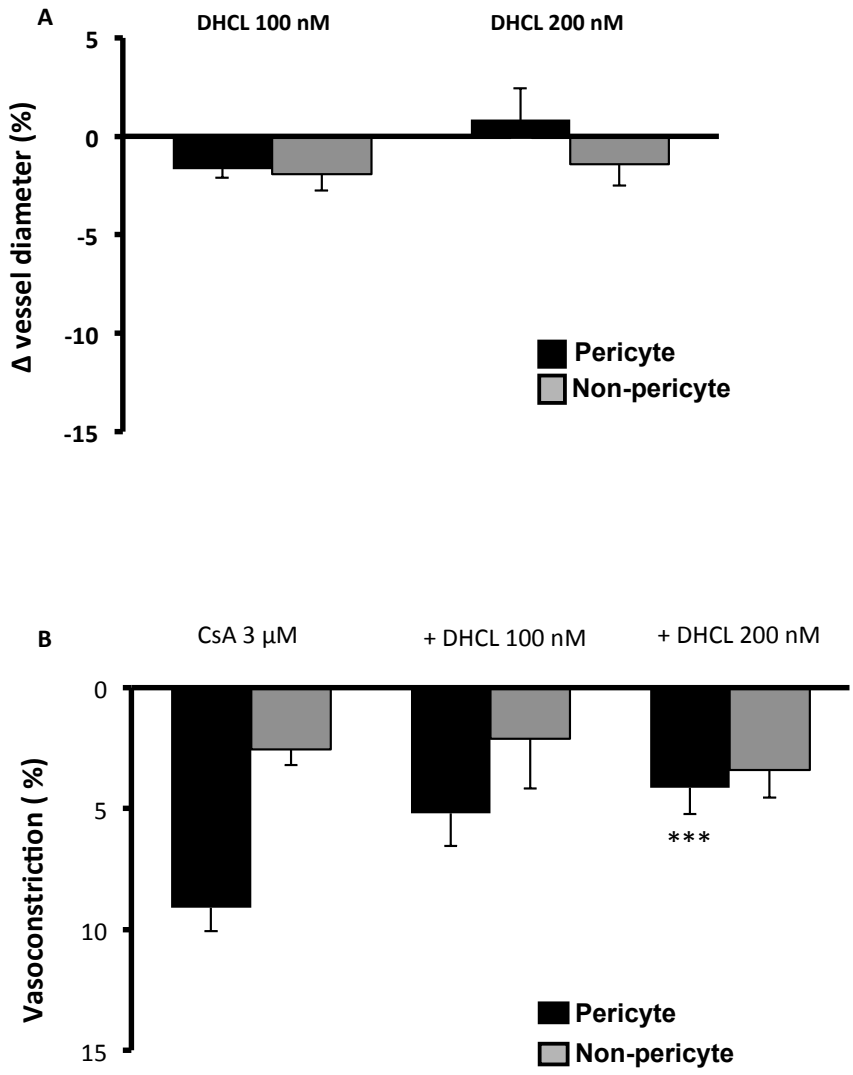

Figure 4.5 Diltiazem hydrochloride attenuates the CsA evoked vasoconstriction of *in situ* vasa recta by pericytes. A: Superfusion of live kidney tissue with diltiazem alone (100 & 400 nM) on to live kidney slices failed to evoke any significant change in vessel diameter at pericyte sites (black bars) compared to non-pericyte sites (grey bars). B: Superfusion of diltiazem (100 & 400 nM) and CsA (3 µM) significantly attenuated the pericyte-mediated vasoconstriction compared to CsA alone. Data are mean ± SEM., n=10 (9), **P<0.01, ***P<0.001.

4.6.3 Effect of diltiazem on *in situ* vasa recta in combination with FK506

Superfusion (~700 s) of FK506 (1 μM) and diltiazem (100 & 400 nM) resulted in an attenuation of FK506-mediated vasoconstriction of vasa recta capillaries when compared to FK506 alone (Figure 4.6). Vasoconstriction induced by FK506 (1 μM) and diltiazem (100 & 400 nM) was significantly reduced at pericyte sites (6.22 ± 1.65% and 3.83 ± 1.56%, respectively) compared to vasoconstriction induced by FK506 alone at pericyte sites (12.85 ± 0.85%, n= 10 (9); P<0.01, P<0.001, (Figure 4.6). The FK506 and diltiazem evoked constriction of vasa recta, at all concentrations, was reversed upon washout, and vessel diameter returned to ≥ 95% of the original baseline vessel diameter after 400 s following washout. Vasoconstriction at non-pericyte sites induced by the combination of FK506 (1 μM) and diltiazem (100 & 400 nM) (6.22 ± 1.65% and 3.83 ± 1.56%, respectively) was not significantly greater compared to vasoconstriction induced by FK506 alone at non-pericyte sites (4.55 ± 2.52% and 3.22 ± 1.25%, respectively n=10 (9), (Figure 4.6)).

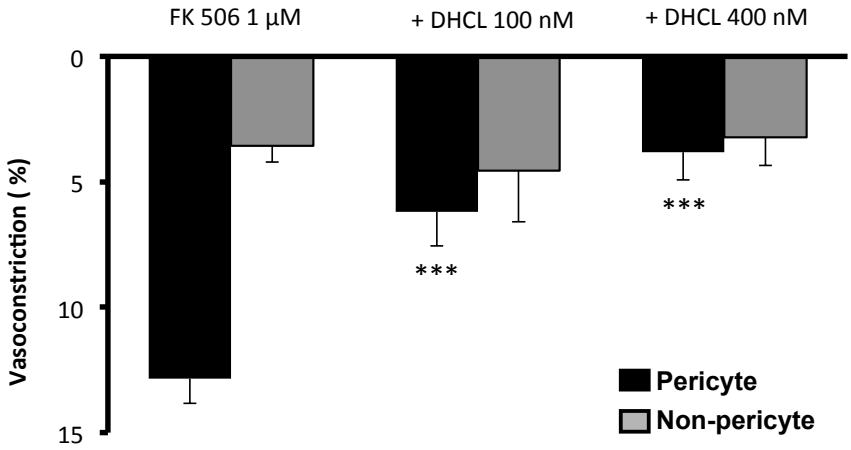

Figure 4.6 Diltiazem hydrochloride attenuates the FK506 evoked vasoconstriction of *in situ* vasa recta by pericytes. Superfusion of live kidney tissue with diltiazem (100 & 400 nM) and FK506 (1 μM) significantly attenuated the pericyte-mediated vasoconstriction compared to CsA alone. Data are mean ± SEM., n=10 (9), ***P<0.001

4.7 The effect of isradipine in combination with CNIs on *in situ* vasa recta

Given that CCBs are grouped into two major classes, and each class having subtle differences in terms of specificity, for example dyhydropyridines work better for cardiac muscle inhibition, it is interesting that both classes have been used to treat CNI-induced hypertension (Aparicio *et al*. 2013). An important point to mention is the use of nondyhydropyridines in combination with CNI's greatly increases the serum levels of CNIs soon after combination therapy (Åsberg *et al*. 1999; Xue *et al*. 2010). This has detrimental clinical consequences, requiring further therapeutic drug monitoring (TDM) and an increased strain on already weakened clinical resources (Ekser *et al*. 2015).

However, as diltiazem, a nondyhydropyridine, has already been used clinically to treat CNI-induced hypertension (Xue *et al*. 2010; Kumana *et al*. 2003), it is clear that combination therapy with these types of antihypertensive drugs are efficacious. In addition, previous results within this chapter have shown diltiazem to inhibit CNI-induced pericyte vasoconstriction. Therefore, the combination of dyhydropyridines with CNIs to investigate pericyte-mediated constriction of vasa recta should be investigated, especially as dyhydropyridines have been shown to significantly reduce CNI hypertension compared to angiotensin converting enzyme inhibitors (ACEi's) (Midtvedt, Hartmann, Holdaas, *et al*. 2001; Midtvedt, Hartmann, Foss, *et al*. 2001).

4.7.1 Effect of isradipine on *in situ* vasa recta diameter

Superfusion (~700 s) of live tissue with isradipine alone (27 & 270 nM) resulted in no significant change of vasa recta capillary diameter (Figure 4.7). When a change in vessel diameter was observed at 27 and 270 nM, it was not significantly greater at pericyte sites (1.23 ± 0.88% and 2.36 ± 1.23%, respectively) compared to non-pericyte sites (0.98 ± 0.65% and 0.56 ± 0.95%, respectively n=10 (9); P>0.05), (Figure 4.7). Upon washout, vessel diameter continued to be stable and rarely dropped below 95% of the original baseline vessel diameter after 400 s following washout.

4.7.2 Effect of combining CsA and isradipine on *in situ* vasa recta diameter

Isradipine had no effect on vasa recta diameter when superfused alone. In contrast, it is clear that CNIs are able to induce vasoconstriction of vasa recta *via* pericytes. Isradipine has been shown to reduce CNI-induced hypertension (van Riemsdijk *et al*. 2000) but intriguingly, a randomised study has shown the beneficial effects of dyhydropyridines over ACE inhibitors for improving GFR both actually and chronically (Midtvedt, Hartmann, Foss, *et al*. 2001). This is particularly interesting, as ACEi's or AGI II receptor inhibitors have been previously thought as first line drug choices for CNI-induced hypertension (Aparicio *et al*. 2013). Therefore, to consider the role dyhydropyridines have in calcium channel inhibition and reduced pericyte constriction *via* CNIs, a combination of isradipine and CsA was investigated.

Superfusion (~700 s) of CsA (3 μM) and isradipine (27 & 270 nM) resulted in a significantly reduced reversible constriction of vasa recta capillaries when compared to CsA alone (Figure 4.7). Vasoconstriction induced by of CsA (3 μM) and isradipine (27 & 270 nM) was significantly reduced at pericyte sites (6.98 ± 0.85% and 7.33 ± 0.93%, respectively) compared to vasoconstriction induced by CsA alone at pericyte sites (11.23 ± 1.28%, n= 10 (9); $P<0.05$, (Figure 4.7). The CsA and isradipine evoked constriction of vasa recta, at both concentrations, was reversed upon washout, and vessel diameter returned to ≥ 95% of the original baseline vessel diameter following washout. Vasoconstriction at pericyte sites induced by the combination of CsA (3 μM) and isradipine (27 & 270 nM) (6.98 ± 0.85% and 7.33 ± 0.93%, respectively) was significantly greater compared to vasoconstriction at non-pericyte sites (3.4 ±0.85% and 2.8 ± 0.54%, respectively n=10 (9); $P<0.01$), (Figure 4.7).

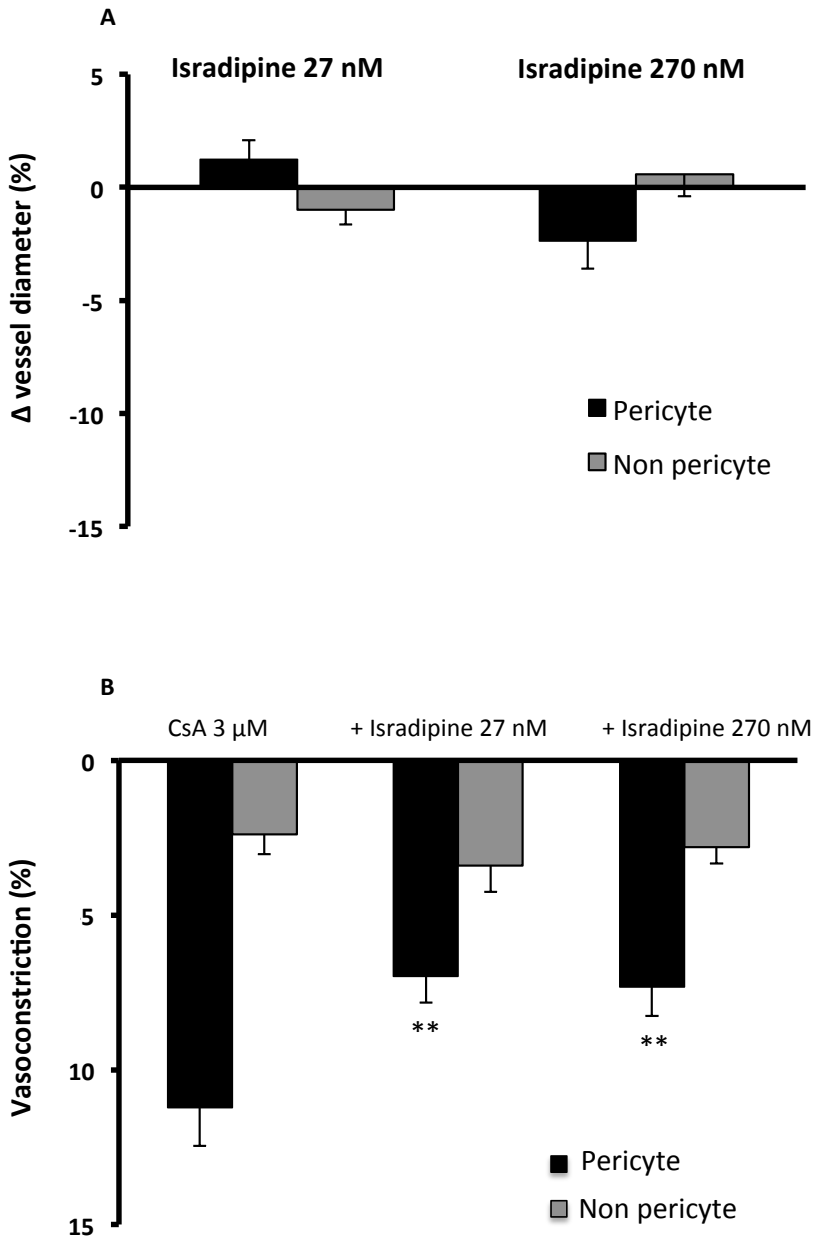

Figure 4.7 Isradipine attenuates the CsA evoked vasoconstriction of *in situ* vasa recta by pericytes. A: Superfusion of Isradipine alone (27 & 270 nM) on to live kidney slices failed to evoke any significant change in vessel diameter at pericyte sites (black bars) compared to non-pericyte sites (grey bars). B: Superfusion of Isradipine (27 and 270 nM) and CsA (3 µM) significantly attenuated the pericyte-mediated vasoconstriction compared to CsA alone. Data are mean ± SEM., n=10 (9), *P<0.05.

4.7.3 Effect of combining FK506 and isradipine on *in situ* vasa recta diameter

Superfusion (~700 s) of FK506 (1 μM) and isradipine (27 & 270 nM) resulted in a significantly reduced reversible constriction of vasa recta capillaries when compared to FK506 alone (Figure 4.8). Vasoconstriction induced by FK506 (1 μM) and isradipine (27 & 270 nM) was significantly reduced at pericyte sites (7.28 ± 0.55 and 5.62 ± 1.43%, respectively) compared to vasoconstriction induced by FK506 alone at pericyte sites (12.99 ± 2.48%, n= 10 (9); P<0.05, (Figure 4.8). The FK506 and isradipine evoked constriction of vasa recta, at both concentrations, was reversed upon washout, and vessel diameter returned to ≥ 95% of the original baseline vessel diameter after 400 s following washout. Vasoconstriction at pericyte sites induced by the combination of FK506 (1 μM) and isradipine (27 & 270 nM) (7.28 ± 0.55 and 5.62 ± 1.43%, respectively) was significantly greater compared to vasoconstriction at non-pericyte sites (3.98 ±0.42% and 3.52 ± 0.96%, respectively n=10 (9); P<0.05), (Figure 4.8).

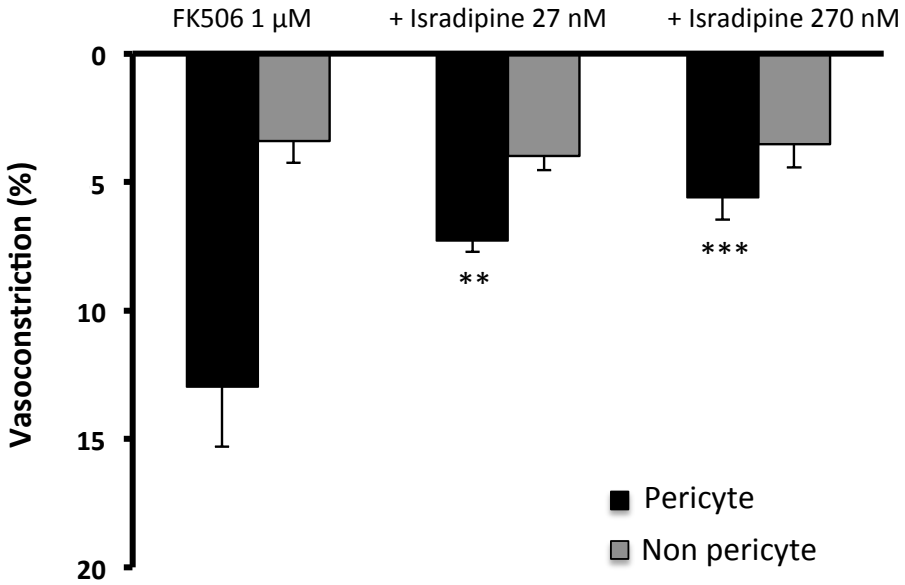

Figure 4.8 Isradipine attenuates the FK506 evoked vasoconstriction of *in situ* vasa recta by pericytes. Superfusion of Isradipine (27 and 270 nM) and FK506 (1 μM) significantly attenuated the pericyte-mediated vasoconstriction compared to FK506 alone. Data are mean ± SEM n=10 (9), **P<0.01, ***P<0.001.

4.8 Discussion

The main aim of this study was to determine whether antihypertensive medication impacts upon the previously known effects of CNIs on vasa recta diameter. Previously established experiments have shown pericytes are key in mediating effects of CNIs on vasa recta diameter, as seen in chapter 3. Data yielded here demonstrates that certain antihypertensives may also act *via* pericytes to attenuate the CNI-mediated vasoconstriction of vasa recta by pericytes. Thus it is possible that these antihypertensives ameliorate CNI-induced hypertension.

The main findings from this investigation have revealed the potential role pericytes have in contribution to CNI-induced hypertension through reduction of RMBF and how the use of selective antihypertensives, particularly CCBs and diuretics, could reduce the risk for the onset of CNI-induced hypertension in renal transplant patients.

It is now well established that CNIs lead to the activation of the RAAS, and as a result, leads to a rise in systemic blood pressure leading to hypertension due to local and systemic vasoconstriction. The mechanism through which CNIs activate the RAAS is still debatable with CNIs being shown to activate RAAS directly, through stimulation of juxtaglomerular cells to increase the release of renin (Kurtz *et al*. 1988) but also through indirect activation, of which, two mechanisms have been proposed. Firstly, researchers have shown that CNIs decrease the levels of circulating vasodilators, NO for example, and simultaneously increase the levels of vasoconstrictors, endothelin and adenosine (Ruester & Wolf 2006). These simultaneous alterations ultimately result in increased vasoconstriction and therefore increase blood pressure and associated hypertension. Secondly, it has been suggested that increased vasoconstriction results in reduced renal blood flow, through ANG II-mediated vasoconstriction, which results in altered hemodynamics seen with CNI use. This latter mechanism increases arteriole vasoconstriction and represents a malicious circle of damage through increased renal vasoconstriction with limited vasodilation (Naesens *et al*. 2009). This can be seen in figure 1.8 of chapter 1 (general introduction). In addition to direct activation of ANG II, CsA use has been shown to recruit renin containing cells to the afferent arterioles (Iijima *et al*. 2000) and interestingly, also suggested to intensify ANG II vasoconstriction through alterations of calcium signalling, increased channel sensitivity and release of internal calcium

stores, in smooth muscle cells (Lassila 2002). It therefore appears the dominant effect of CNIs on the RAAS is through increased vasoconstriction *via* increased ANG II release or augmented contractile responses to ANG II.

As previously mentioned, the use for ARBs and ACEi's for treatment of hypertension and reducing the progression of chronic kidney failure in the general population has been well accepted (Krause *et al*. 2011). However, their use for lowering hypertension in transplant patients has not been as successful compared to their non-transplant counterparts. There have been several indications for this observation; ACEi's and ARBs can induce a decrease in GFR (Curtis *et al*. 1993) and have the potential to mask any early signs of acute rejection, of which a decrease in GFR being one of these indications. Secondly, ACEi's and ARBs can exacerbate the degree of hyperkalaemia (Mangray & Vella 2011), a common metabolic abnormality after renal transplant that can be associated with delayed graft function and CNI nephrotoxicity (Palmer 2002). Lastly, ACEi's and ARBs can induce anaemia in transplant patients (Vlahakos *et al*. 1991), exacerbated with the use of CsA (Gaston *et al*. 1994) and result in an increase of up to 50% chance of thrombotic complications (Mangray & Vella 2011).

A systematic review of all recent trials, which included the selection criteria of antihypertensive treatment in renal transplant patients, has been performed by Hiremath *et al* (Hiremath *et al*. 2007). The review focuses on clinical trials, which have 2 main outcomes; overall kidney function and corresponding blood pressure. The analysis suggested that ARB or ACEi use significantly reduced GFR and proteinuria compared to non-treated matched controls. Disappointingly, due to lack of sufficient timing of trials, lack of randomized trials and insufficient patient numbers, the review had no outcomes for patient or graft survival, which ultimately is the end goal for any transplant patient.

Given that the protective mechanism of ARBs and ACEi's involves a reduction in glomerular pressure, it is disappointing to suggest they have little clinically proven benefits with the use of CNIs, especially with the known affects of CNIs and local ANG II release (Lassila 2002; D. B. Lee 1997). Nonetheless, ARBs and ACEi's do have beneficial effects for reduction of hypertension as can be clearly demonstrated with the wealth of literature surrounding their use (Frishman 2007; Tziomalos *et al*. 2013; Lewis *et al*. 1993; Duarte & Cooper-DeHoff 2010; Zachariah *et al*. 1993) however

when used in the renal transplant setting, their effectiveness is drastically reduced compared to that of non-transplant patients.

Previous data by Crawford *et al* has shown the considerable vasoconstrictive effects of ANG II on pericyte-mediated vasoconstriction of vasa recta (Crawford *et al*. 2012). Additionally, the authors have also shown that ARBs, namely losartan, completely abolishes ANG II induced vasoconstriction of DVR (Crawford *et al*. 2012), this in turn could suggest a role for pericyte contraction in contribution towards hypertension in response to increased renal and systemic ANG II concentrations. Although RMBF may only contribute to 1% of the total renal blood flow (Cowley *et al*. 1995), studies have shown that dysregulation of blood flow in this sensitive region can result in renal decline without changes in cortical blood flow being observed (Mattson *et al*. 1992). Therefore, dysfunction of RMBF may have a major impact on long-term control of blood pressure regulation and urine concentration capabilities of the kidneys due to dysfunction of the cortical–medullary countercurrent gradient.

With what is known in the literature, it is disappointing to note the results seen in this chapter regarding ARBs. Losartan failed to significantly reduce the pericyte-mediated vasoconstriction of vasa recta induced by CNIs. As such, the results suggest CNI-induced vasoconstriction of vasa recta *via* pericytes may be through another mechanism other than ANG II. As mentioned, data has been previously shown the substantial vasoconstrictive effects ANG II has on the live slice model and how ARB's are able to completely abolish such effects (Crawford *et al*. 2012), therefore, CNI-meditated vasoconstriction of vasa recta might not necessarily involve direct activation of AT1 receptors or an increase in local concentrations of ANG II. The vasoconstriction observed could stem from the decrease of vasodilators or the increase of endothelin 1, both of which are seen in CNI-induced hypertension (Naesens *et al*. 2009), importantly, both these mechanisms have been shown to alter vasa recta diameter in the live slice model (Crawford *et al*. 2012). Therefore, it is reasonable to suggest CNI-induced vasoconstriction of vasa recta is not exclusively dependent on ANG II or the RAAS. In addition, the use of ARBs and ACEi's within the transplant setting has not been shown to have significant benefits in reducing CNI induced hypertension (Naesens *et al*. 2009), further highlighting their lack of effectiveness for prevention of hypertension. Regardless of which vasoconstrictor agents are involved, evidence here indicates a clear role for pericytes in CNI-mediated vasoconstriction of vasa recta and in turn, reduction of medullary blood flow.

An interesting observation from this chapter was the hydrochlorothiazide-mediated reduction in CNI-mediated vasoconstriction of vasa recta specifically *via* pericytes.

The initial rational for this experiment was due to the recent works of Hoorn *et al* and Melnikov *et al* (Hoorn *et al*. 2011; Melnikov *et al*. 2011) who demonstrated that CNIs induced a form of salt-sensitive hypertension through non vascular mechanisms. After treatment with CNIs, the sodium-chloride-cotransporter, a major sodium and chloride reabsorbing cotransporter in the distal convoluted tubule, was significantly upregulated. This in turn suggests that CNIs have a salt-retaining effect and may regulate NCC function. The role of NCC in hypertension was further highlighted with the use of a NCC knock out mouse, which failed to develop hypertension after being treated with CNIs (Hoorn *et al*. 2011). This further highlights a role for NCC and sodium retention in development of CNI-induced hypertension.

Hydrochlorothiazide is a thiazide diuretic used to treat hypertension and edema. It works by inhibiting sodium reabsorption through the NCC in the distal convoluted tubule, therefore inducing natruesis and subsequent water loss (A. D. A. Hughes 2004; Duarte & Cooper-DeHoff 2010). Given that CNIs are able to acutely increase expression of the NCC (Blankenstein *et al*. 2014) and hydrochlorothiazide is used to inhibit NCC-mediated sodium retention, if used together, this drug combination can provide an inexpensive and more importantly, safe regime to reduce the risk of CNI-induced hypertension (Hoorn *et al*. 2011).

Despite this possible mechanism for HCT in reducing CNI-induced hypertension, it does not explain the observation that hydrochlorothiazide inhibited CNI-induced vasoconstriction of vasa recta *via* pericytes in live tissue slices. Interestingly, thiazides have been shown to have direct vasodilatory effects (Duarte & Cooper-DeHoff 2010) which could be the mechanism for the above observation. This is in addition to HCT also being found to attenuate vasoconstriction of known vasoconstrictive agents, ANG II and noradrelinnie (Colas *et al*. 2000) in an endothelium NO derived manner (Colas *et al*. 2000).

Of particular interest, Zhu *et al* revealed that thiazides inhibited ANG II-induced vasoconstriction of aorta through calcium desensitization of VSMC's, while still observing the same increase of calcium, mediated by inhibition of the Rho-Rho kinase pathway (Zhu *et al*. 2005). Under normal conditions, Rho and Rho kinase are responsible in phosphorylation of myosin light chain (MLC), resulting in increased

myosin II ATPase activity and muscle contraction (Fukata *et al*. 2001) but also inhibiting MLC phosphatase, leading to increased MLC phosphorylation and muscle contraction (Fukata *et al*. 2001). Edwards *et al* demonstrated that use of MLC kinase inhibitors were highly effective in reducing calcium dependent chloride currents in DVR pericytes (Vates *et al*. 2010). However, hydrochlorothiazide also increases the reabsorption of calcium into cells (Lajeunesse *et al*. 1994), which can open calcium-activated chloride (CL_{Ca}) channels (Hamilton *et al*. 2010). This, in combination with high intracellular chloride concentrations of pericytes enables chloride to exit the cell producing increased depolarization and increased activation of voltage operated calcium channels (VOCC) (Kawamura *et al*. 2002), VOCCs being the main channel responsible for muscle contractions . Taken together, along with data produced here, it could be speculated that the use of hydrochlorothiazide on the live slice model inhibits Rho and Rho kinase activity, in turn, decreases MLC phosphorylation and attenuating the contractile effects of CNIs acting through pericytes. Although only a speculation, the preliminary data presented here warrants the further investigation of diuretics and their interaction with CNIs to elude additional pathways for the prevention of CNI-induced hypertension.

The other group of antihypertensives used in this chapter belong to the class of calcium channel blockers (CBBs). They work by inhibiting the opening of calcium channels, and depending on which type of Ca^{2+} channels are expressed, inhibit the contraction of specific muscle fibres. Most CBBs block L-type voltage operated calcium channels (VOCC), which are responsible for contraction of skeletal, smooth and cardiac muscle through membrane depolarisation (Hamilton *et al*. 2010). Although CCBs can be classed as dihydropyridines and nondihydropyridines, their mechanism of actions are similar in the end point by inhibiting calcium ion flow. Their affinity for particular muscle types can differ drastically, with non-dihydropyridines having higher affinity for cardiac muscle (Mangray & Vella 2011).
The results from this chapter indicated that diltiazem and isradipine, a nondihydropyridine and dihydropyridine, respectively, are able to significantly reduce pericyte-mediated vasoconstriction of vasa recta induced by CNIs, with diltiazem able to attenuate both CsA and FK506-mediated vasoconstriction to a greater degree compared to that of isradipine.

The classic randomized trial carried out by Midvedt *et al* highlighted the use of CCBs against ACEi's in transplant patients for the protection of graft function and improved GFR (Midtvedt & Hartmann 2002a). Unfortunately the trial failed to measure GFR as an outcome and also showed no significant improvement in blood pressure when the two groups were compared (Midtvedt, Hartmann, Foss, *et al*. 2001).

Nonetheless, CCBs are typically thought as first-line medications for the treatment of hypertension after renal transplant (Mangray & Vella 2011) and a Meta analysis carried out some 20 years ago investigated the use of CCBs in combination with CNIs for the protection of long-term kidney grafts (Ladefoged & Andersen 1994). The published results were conflicting, with the randomised open studies involving CCB treatment having reduced rates of delayed graft function but no effect on rates of rejection and graft survival, in addition to no significant evidence in improved graft function over time. Interestingly, blood pressure was reduced in most cases treated with CCBs, although not considered statically significant (Ladefoged & Andersen 1994) and could originate from the reduced dosage of CNIs needed for immunosuppression while on CCBs due to pharmacokinetic interactions (Ladefoged & Andersen 1994).

How CCBs are able to inhibit CNI-induced pericyte mediated vasoconstriction of vasa recta is still unknown, however it can be suggested this mechanism is through blocking of VOCCs. Zhang *et al* have shown constriction of descending vasa recta *via* pericytes is mediated by voltage gated calcium entry (Z. Zhang *et al*. 2002) and as such their results indicate that pericyte contraction is stimulated through opening of VOCCs, depolarisation of the membrane, and contraction of pericytes which would fit with the observations that CCBs attenuate CNI-mediated vasoconstriction in studies demonstrated here. The same group of authors further highlighted evidence of voltage operated calcium entry into vasa recta with the use of the L-type channel blocker, diltiazem, showing reduced vasoconstriction when treated with a high potassium saline solution (Z. Zhang *et al*. 2002). Given that CNIs have been shown to increase intracellular calcium signalling in contractile myocytes (Frapier *et al*. 2001), it is likely that they also increase calcium levels in renal pericytes to induce DVR vasoconstriction. Delineating this possible mechanism could prove to be a valuable insight into the pathways of pericyte-mediated contraction and further calcium imaging studies may facilitate a better understanding of the mechanisms involved.

Data presented here, along with data presented by Zhang *et al* (Z. Zhang *et al*. 2002), suggests a role for calcium entry *via* VOCCs and the subsequent constriction of pericytes in CNI-induced pericyte constriction of vasa recta.

The data also suggests both types of CCBs are able to inhibit CNI-induced pericyte vasoconstriction, which is clinically important when considering pharmacokinetic interactions of CCB's and CNIs. Nondihydropyridines are potent inhibitors of CYP P450 C3A4 enzymes, which if used in conjunction with CNIs, cause plasma levels of CNIs to increase significantly shortly after administration (Kovarik *et al*. 2005). Therefore, ensuring a careful choice of CCB, to be used in conjunction with CNIs may help to reduce pericyte-mediated constriction of vasa recta and reduce risk of CNI-induced hypertension.

Following personal communication with the Burdyga lab, it was suggested that a high K^+ depolarisation experiment following application of CNI's and either CCB, particularly isradipine, should be performed to clearly identify the washable preparation of CCB's in PSS. It has been suggested that CCB's are particularly "sticky" to inorganic polypropylene tubing and therefore their inhibitory actions on Ca^{2+} channels can last much longer than assumed. However, given personal communication with the Pallone lab and ability of ANG-II to induce vasoconstriction after CCB and CNI washout, although ANG-II induced vasoconstriction is not from direct membrane depolarisation, the ability of Ca^{2+} washout should be investigated further. As previously shown by the Pallone lab, high K^+ bath solution was able to induce isolated perfused DVR vasoconstriction, through direct pericyte membrane depolarisation (Z. Zhang *et al*. 2002) and inhibited with the incubation of diltiazem. Although not demonstrated in their paper (Z. Zhang *et al*. 2002), the group have informed our lab that the depolarisation was repeatable after diltiazem washout. The same experimental approach in the presence of CNI's would be able to clearly identify a possible mode of action of CNI's on pericyte and EC membrane depolarization and a molecular pathway for CNI-induced pericyte vasoconstriction. This could be further investigated with the use of fluorescent probes and Ca^{2+} imaging techniques to identify a possible novel mechanism of CNI-induced vasoconstriction and help ascertain therapeutic strategies for prevention of RMBF dysfunction with the use of CNI's.

5. Perfusion of *in situ* vasa recta for delineating CNI Nephrotoxicity

5.1 Introduction

The live kidney slice model, first described by Crawford *et al* (Crawford *et al*. 2012), gave a novel approach for investigating the role of renal pericytes in physiological settings. Importantly, the initial studies revealed the importance of pericyte-mediated tubular vascular crosstalk between vascular and tubular sections of the nephron. This has been further highlighted by other groups (O'Connor & Cowley 2012; Dickhout *et al*. 2002; Tasnim & Zink 2012) and emphasises the role of pericytes in the regulation and coordination of tubular and vascular function within the medulla. Conversely, it is near impossible to understand the *in vivo* setting of the medulla due to its inaccessibility. With the development of the *in situ* live slice model by Crawford *et al* (Crawford *et al*. 2012), the role of pericytes in control of vasa recta diameter while being in constant contact and communication with surrounding tissue enabled a better understanding of the molecular and cellular events occurring physiologically. Nonetheless, the live slice model lacks single vessel perfusion and in turn, the entire tissue is subjected to drug insult *via* superfusion. This would not be seen physiologically or *in vivo* and only drug exposure *via* the blood stream would be expected. With this in mind, the aim of this chapter was to develop a model for single vessel perfusion in the live kidney slice for investigating the cellular mechanisms involved when vasoactive agents and CNIs where luminally perfused in vasa recta.

5.1.2 Initial pericyte studies

Pallone and colleagues carried out much of the early work characterising renal pericytes and their role of blood flow regulation (Pallone *et al*. 1994; Pallone 1994; Pallone 1991). The initial observations that pericytes could contract under the influence of certain endogenous vasoactive mediators led to the notion that pericytes are responsible for regulating medullary blood flow (MBF) through control of vasa recta diameter (Pallone & Silldorff 2001). The experiments carried out by the Pallone laboratory included the use of the isolated perfused DVR technique. This involves the removal of medulla segments from an intact kidney, microdissection of DVR from medulla strips, complete removal of any surrounding tissue (intact DVR with

pericytes attached) and superficially "gluing" the vessel to a submerged perfusion bath (Pallone *et al*. 1994) as seen in figure 5.0.

To carry out perfusion, they adapted a technique used for isolated tubule perfusion first described by Burg (Burg 1972). A concentric pipette arrangement was set up (a single perfusion pipette within a larger holding pipette) to allow the sealing of single DVR (within the holding pipette) and constant perfusion (*via* the perfusion pipette) (Pallone 1994). At the opposite end of the vessel, a collecting pipette was situated and researchers were able to collect perfused liquid or block flow with an adapted seal (Pallone *et al*. 1994; Sendeski *et al*. 2012). The concentric pipette system can be seen in Figure 5.0.

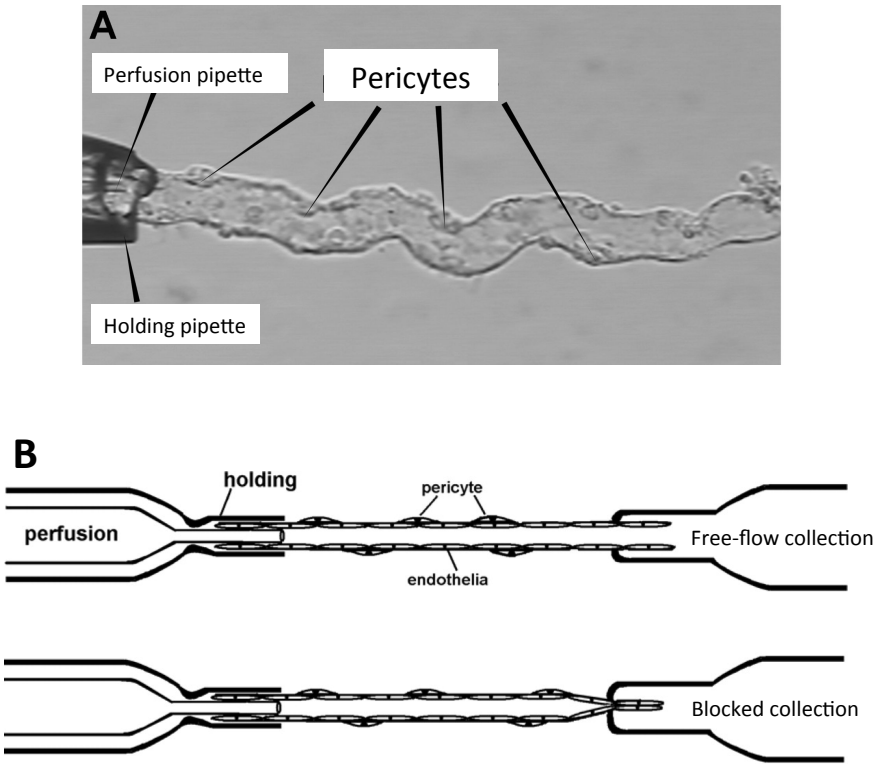

Figure 5.0 Setup of concentric pipettes to enable perfusion of isolated DVR.

A: A holding pipette seal around an isolated DVR with perfusion pipette inside to allow free flow vessel perfusion. B: Adaptation of collection pipettes to allow either free flow perfusion or blocked perfusion (Increased vessel pressure). Figures adapted from (Z. Zhang & Pallone 2004; Sendeski *et al*. 2012).

The obvious advantage of the isolated DVR technique was that for the first time, an understanding of the inner renal medulla microcirculation was able to be visualised, in real time, and not through computer modelling or laser Doppler recordings of changes in regional flow. As previously mentioned, the inner medulla is practically inaccessible *in vivo*, therefore, *in vitro* experiments are currently the only dependable way for visualisation and relatively accurate interpretation of its physiology (Pallone, Z. Zhang, *et al*. 2003). The main disadvantage of the isolated DVR technique is that the experimental preparation is void of any surrounding architecture that would normally be found *in vivo*. For example, the DVR is stripped of any supporting tissue like interstitial cells but also completely removed from surrounding tubules and additional vasa recta.

Given that it is now known pericytes are able to communicate with other neighbouring pericytes and cell types (Q. Zhang *et al*. 2006; Z. Zhang *et al*. 2014; Burdyga & Borysova 2014; Özen *et al*. 2014), but also respond to stimuli from supporting structures and tubules (Crawford *et al*. 2011; Crawford *et al*. 2012; Silldorff & Pallone 2001; O'Connor & Cowley 2012), complete removal of the surrounding structures found *in vivo* means the model does not ideally replicate the *in vivo* setting.

An example for cross communication has been shown in a study carried out by Dickhout *et al* who demonstrated a role for NO production in tubules being able to impair ANG II-mediated vasoconstriction of vasa recta (Dickhout *et al*. 2002). This has highlighted a role for pericytes acting as mediators of tubular vascular cross-talk and possibly responsible for pathological conditions such as ischemia reperfusion injury, previously thought to have no identified single cause (Yamagishi & Imaizumi 2005; Dalkara *et al*. 2011; Tasnim & Zink 2012). CNI nephrotoxicity similarly has no single identified cause and could provide a novel role for pericytes as mediators or augmenters of the initial insult for nephrotoxicity.

5.1.3 Tubular-vascular cross-talk

Within the medulla, tubular and vascular structures often run in parallel with each other, suggesting there could be potential for communication between arrangements, as seen in figure 5.1. It has been suggested that pericytes act as cellular messengers between tubules and vessels in response to release of local mediators and are able to respond to endogenous stimuli released from both structures to inform function of

the other (Crawford *et al*. 2011; Crawford *et al*. 2013; Crawford *et al*. 2012). Subsequently, pericytes would be able to alter MBF *via* vasa recta diameter and prevent or augment certain pathological conditions. A recent review of renal pericytes (Kennedy-Lydon *et al*. 2012) reviewed possible cross-talk pathways and the majority of these can be seen in figure 5.1. An important cross-talk pathway highlighted in figure 5.1 and involved in CNI-nephrotoxicity is the production of endothelin (ET-1). CNIs have been shown to increase the production of ET-1 (Nakahama 1990; Roullet *et al*. 1994; Naesens *et al*. 2009) and ET-1 has also been shown to constrict vasa recta pericytes (Silldorff & Pallone 2001; Crawford *et al*. 2012). ET-1 is synthesised by collecting duct epithelial cells and endothelial cells and upon release, ET-1 acts locally (de Nucci *et al*. 1988). Taken together, coupled with the close proximity of collecting ducts, vasa recta and thick ascending limbs, it is reasonable to suggest that CNIs activate ET-1 release from collecting ducts and endothelial cells, which would inevitably cause significant reduction of vasa recta diameter *via* its action at pericytes and therefore impede MBF.

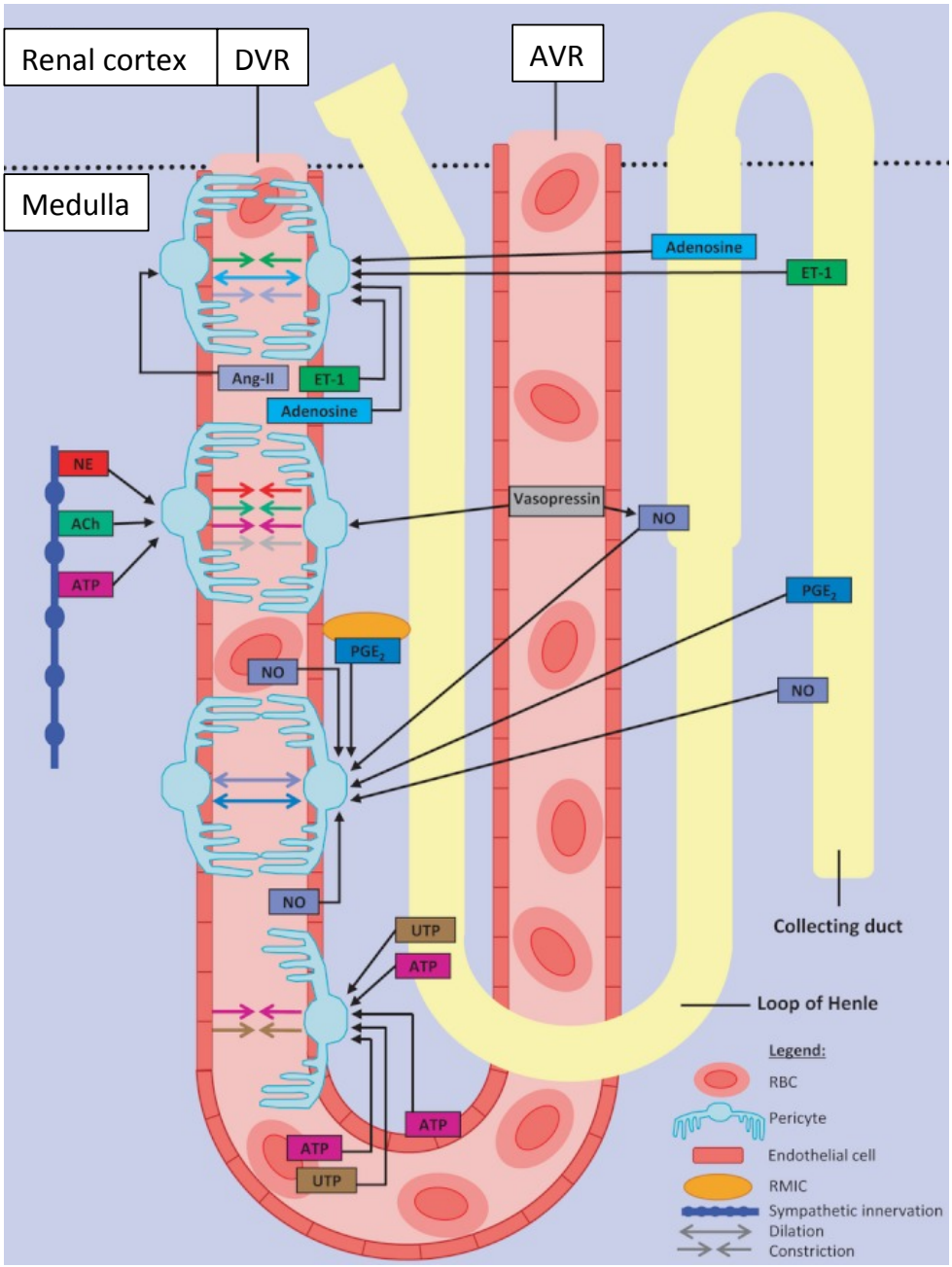

Figure 5.1 Schematic diagram showing possible mechanisms involved in pericyte-mediated regulation of descending vasa recta (DVR) diameter. Various endogenous vasoactive mediators are released from neighboring tubular epithelium, vascular endothelium, red blood cells (RBC) and interstitial cells of the renal medulla. These compounds signal to pericytes on DVR capillaries to cause pericyte-mediated vasoconstriction (Endothelin-1 (ET-1), prostaglandin E_2 (PGE_2), nitric oxide (NO), adenosine, uridine triphosphate (UTP), adenosine triphosphate (ATP), acetylcholine (Ach) and circulating hormones: angiotensin (Ang II), vasopressin, noradrenaline (NA) or vasodilation; (Nitric oxide (NO) and Prostaglandin E_2 (PGE_2). Figure adapted from (Kennedy-Lydon *et al*. 2012).

5.1.4 Experimental model advances

As previously stated, the isolated DVR technique was at the forefront of renal research when it first characterised the role of pericytes in regulation of vasa recta diameter and subsequently MBF (Pallone *et al*. 1994). However, some twenty years have gone by since its first publication and the technique is still used to this day, confirming its influential role in the understanding of pericyte physiology.

Although modifications have made the technique more advanced, with simultaneous fluorescence imaging and patch clamp recordings of pericytes (Sendeski *et al*. 2013; Sendeski *et al*. 2012; Q. Zhang *et al*. 2006), the fundamental experimental setup remains the same, *i.e.* isolation of DVR from supporting structures.

It is clear the role for surrounding tissues in understanding renal pericyte physiology is becoming increasingly significant, therefore an experimental model with intact surrounding tissue would be advantageous.

The live kidney slice model, first established by Crawford *et al* (Crawford *et al*. 2012), is a novel model for investigating *in situ* renal pericytes and their contribution to vasa recta vasoconstriction under certain pathological conditions.

Unlike *in vitro* isolated DVR, the live slice model enables complete *in situ* tissue to be investigated by taking transverse sections of a whole "live" kidney to leave all surrounding and supporting structures intact. The obvious advantage of this model over the isolated DVR is that mechanisms and pathways involved in vascular and tubular physiology can be investigated together, and even in combination through vascular and tubular stimulation (Crawford *et al*. 2013). This model has been shown to highlight the importance of tubular-vascular cross-talk with relation to tubular injury and disease (Crawford *et al*. 2011; Crawford *et al*. 2013). Although the kidney slice model has been beneficial in our understanding of pericytes in particular disease settings, nephrotoxicity for example (Peppiatt-Wildman *et al*. 2013, unpublished data), the central disadvantage of the model is the lack of perfusion within vascular or tubular structures. Although technically challenging, perfusion of structures within the slice would offer a more accurate physiological setting to assess intraluminal-signalling pathways involved in pericyte regulation of vasa recta.

Recent experiments by O'Connor *et al* have tried to overcome the lack of perfusion within vascular or tubular structures in their own experimental model (O'Connor & Cowley 2012). Similar to isolated DVR, their model encompasses isolation of medulla

strips consisting of vasa recta and adjacent tubules. They are then able to perfuse vessels while having tubular structures intact, and in close proximity. The model has highlighted, again, the role of tubular vascular cross-talk for pericyte regulation of vasa recta diameter under pathological conditions (O'Connor & Cowley 2012), and provides a novel methodology for investigations into renal medulla physiology.

However, their model is similar to the isolated DVR as it requires stripping away segments of medulla to find specific areas of *in vitro* vasa recta and adjacent tubules (O'Connor & Cowley 2012). This not only subjects the tissue to vigorous physical damage, but also increases the risk of molecular damage through ROS generation, release of ATP and NO due to shear stress and cell apoptosis.

Given that there is no currently known model that encompasses both intact *in situ* tissue (vasa recta and surrounding structures) and luminal perfusion of vascular or tubular structures, is the already acknowledged live slice model an experimental technique that could be enhanced *via* luminal perfusion to further our understanding of pericyte physiology?

The aim of this study was to establish the feasibility of *in situ* vasa recta perfusion in the live kidney slice model to aid the investigation of the role pericytes in regulation of vasa recta diameter when vasa recta are perfused with CNIs under physiological conditions and pressures.

5.2 Methods

Intact live kidney slices were obtained as described in chapter 2: General Methods. Live kidney slices were continually superfused with 95% O_2 / CO_2 PSS and individual vasa recta perfused. Luminal perfusion of vasa recta is also described in chapter 2: General Methods. In brief, in experiments to determine the effect on luminal perfusion on vasa recta diameter, a controlled perfusion experiment with PSS was carried out to determine the effect of luminal perfusion alone on vasa recta diameter. The perfusion was carried out at a set pressure, 25 mmHg *via* attached sphygmomanometer, see general methods for details. Following initial control experiments, individual vasa recta were perfused with a range of vasoactive substances known to affect vasa recta diameter when superfused, ANG II, ET-1, PGE_2 and NO. Similar experiments were performed with cyclosporine A, tacrolimus and rapamycin to investigate their action on vasa recta once perfused luminally and compared to the effects of superfusion. Video recording analysis of changes in vasa recta diameter has been described previously in chapter 2: General Methods. In brief, each experiment was analysed using the free public domain software IMAGE J (NIH; http://rsb.info.nih.gov). For each perfusion experiment, a pericyte site and non-pericyte site were identified on a single vasa recta capillary acting as a paired control. The diameter of the vasa recta at both of these locations was measured every five frames for the duration of the experiment. An average of the first five measurements was taken to represent the resting perfusion diameter value (*i.e.* 100%) for the selected pericyte and non-pericyte sites. All subsequent diameter measurements at both sites were calculated as a percentage change of the corresponding resting diameter value.

5.2.1 Statistics

All data are presented as mean values ± SEM; *n* numbers are displayed as number of kidney slices, and where appropriate, (number of animals). All experiments were performed in at least six different animals. Statistical assessment was performed with GraphPad Prism (v5.0f; GraphPad software, San Diego, CA, USA). When two groups were compared, a Student's t-test (two-tailed, paired or unpaired where appropriate) was used. A value of $P < 0.05$ was considered significant.

5.3 Results

5.3 Determining the effect luminal perfusion pressure has on flow rate

After initial practicality studies to investigate vessel stability and feasibility of single vessel perfusion *via* observational studies of perfused PSS alone in single vasa recta, it was apparent that *in situ* vasa recta were able to be luminally perfused for constant periods of time at set pressures. Given the fact that there are only a handful of laboratories that still carry out isolated perfused DVR experiments, the protocol for perfusing *in situ* vessels was adapted from this methodology (Burg 1972; Z. Zhang & Pallone 2004; K. K. Evans *et al*. 2015).

Interestingly, out of the laboratories that still perform the isolated DVR technique, they vary with regards to their vessel perfusion pressure and flow (Pallone 1994; O'Connor & Cowley 2012; Sendeski *et al*. 2012). Though there is no set method for determining DVR flow rate or pressure *in vivo*, it has been suggested that the physiological pressure is approximately 25 mmHg (Z. Zhang & Pallone 2004; Crawford *et al*. 2012) under normal conditions.

The labs of Pallone and colleagues (Pallone 1991; Pallone *et al*. 1994; Z. Zhang & Pallone 2004) and Sendeski *et al* (Sendeski *et al*. 2013; Sendeski *et al*. 2012) have used this approximation of pressure to conduct most of their isolated DVR experiments. However, Cowely *et al* (O'Connor & Cowley 2012) have used a different measurement and instead of measuring luminal pressure, they have taken into account luminal flow rate of DVR. Again, there is no accurate way for determining absolute luminal flow rate of vasa recta *in vivo*, however it has been suggested that it ranges from 5-20 nl/min (O'Connor & Cowley 2012; Holliger *et al*. 1983; Pallone *et al*. 1994). Interestingly, Pallone *et al* who carried out much of the very first isolated DVR research, has carried out experiments with flow rate instead of pressure (Pallone *et al*. 1994), which highlights the acknowledged interchangeable use of both these parameters for experimentation. The use of both measurements most probably stems from the perfusion model that which the isolated DVR was adapted (the isolated perfused tubule) which commonly uses flow rate instead of pressure, as tubular flow is more readily measured *in vivo* (Burg 1972) *via* micropuncture experiments.

Therefore, the aim of this initial study was to determine the relationship between luminal perfusion pressures and flow rates of *in situ* vasa recta. In addition,

investigate the effects of altering intraluminal flow and/or pressure on pericyte contractility.

To ascertain what relationship pressure had with flow, a reliable method for the measurement of flow rate in perfused vasa recta was required. To establish this, an approach published by O'Connor *et al* (O'Connor & Cowley 2012) was adapted for use in the live slice model. A pre-pulled glass capillary tube, see general methods for specific details, was filled with 1 µl filtered PSS previously bubbled in 95% O_2 / CO_2 (through 0.20 µM sterile syringe filter, Cole-Parmer, London, UK) and placed within a capillary tube holder of a manual micromanipulator (LBM-7 manual manipulator, Scientifica, Surrey, UK). After vasa recta puncture, a set pressure was applied using an attached sphygmomanometer. Perfusion of vasa recta continued until no further PSS was present in the pipette. The total volume of PSS (1 µl) was divided by the time taken for the perfusion to finish, to establish an approximate flow rate within perfused vasa recta.

To determine flow rate at a range of pressures, *in situ* vasa recta were perfused at a range of pressures, 0, 20, 25, 40, 60 80 and 100 mmHg. The time taken for 1 µl of PSS to clear the pipette at each pressure was used to approximate flow rate and was plotted against its corresponding pressure, as seen in figure 5.2.

Perfusion of vasa recta at 20 mmHg resulted in a perfusion rate of 18.325 ± 2.8 nl/min (n=6 (6)), figure 5.2. Perfusion pressures of 25, 40, 60, 80 and 100 mmHg resulted in perfusion rates of 21.67 ± 3.44, 31.35 ± 4.39, 56.37 ± 4.38, 102.64 ± 9.54 and 135.2 ± 3.76 nl/min, respectively (n=6 (6)). Corresponding pressure and flow rate values were plotted against each other to establish if luminal pressure of vasa recta had a linear relationship with luminal flow rate and if perfusion of single vasa recta within the live slice model was a valid model for further investigation, figure 5.2.

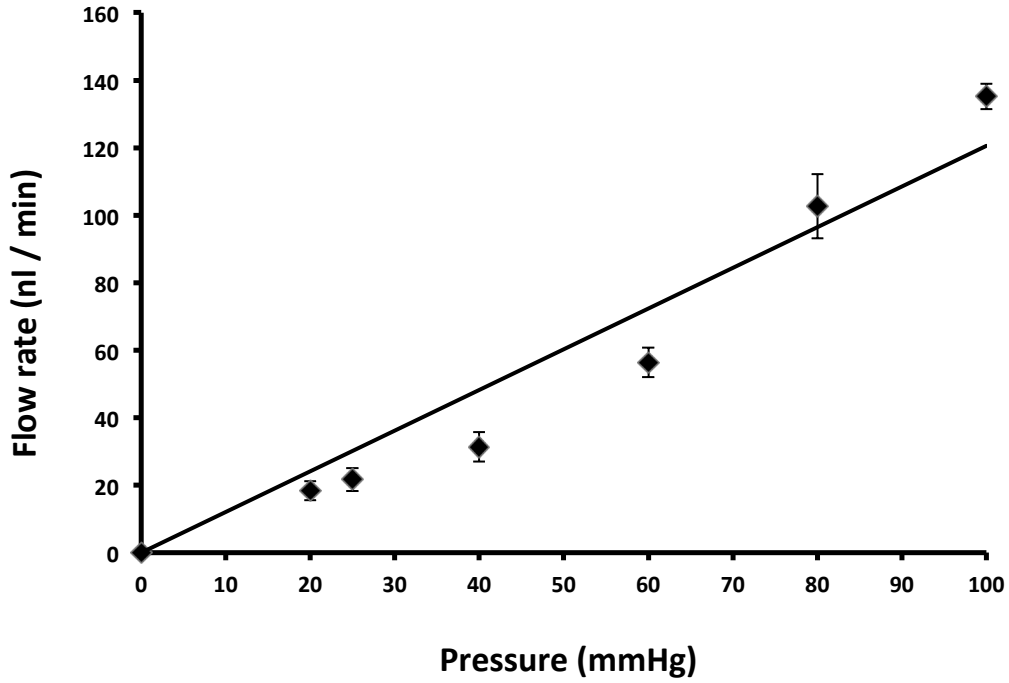

Figure 5.2 Increasing the luminal perfusion pressure effects flow rate of in situ vasa recta.

Individual vasa recta were perfused with PSS at varying pressures, 20-100 mmHg, to determine luminal perfusion rate at corresponding pressures. Values are mean ± SEM. n=6 (6).

5.3.1 Determining the effect perfusion pressure has on vessel tone.

As luminal perfusion is suggested to have a linear relationship with flow, the effect of luminal perfusion pressure on pericyte contractility was investigated.

Given what we know about pericyte physiology, it is reasonable to suggest that vasoactive substances that circulate within the vascular system are able to effect pericyte contractility through various molecular pathways (Pallone & Silldorff 2001). Therefore, would altering vessel flow rate impact vascular resistance due to its effect on pericyte contraction mediated through endothelial cell stress and pericyte feedback, thus suggest an autoregulatory mechanism between both cell types.

Early research in the 1980's suggested that increasing renal perfusion pressure would consequently increase vasa recta capillary pressure, therefore pressure would be passive and under control of upstream forces (Aukland 1980; Cowley 1997).

However, Zhang *et al* have challenged this notion using isolated DVR (Z. Zhang & Pallone 2004). Interestingly, the authors found that with an increased luminal pressure, intracellular endothelium calcium levels also increased. Moreover, they also discovered increased levels of NO production with the associated increase in pressure (Z. Zhang & Pallone 2004). This suggests that vasa recta are mechanosensitive and can respond to luminal pressure through calcium signalling and NO production to increase or decrease vessel tone, independent of regulation from arteriole pressure. It must be noted that an increased pressure in vasa recta must be initiated upstream *via* arteriole pressure therefore complete independent regulation is sceptical.

With this in mind, the aim of this study was to investigate the effect of increasing pressure on vasa recta diameter and to identify if pericytes are able to respond to altered luminal pressure.

In situ vasa recta were perfused at <5 mmHg and left to equilibrate for 10 minutes. Following equilibrium, luminal vasa recta pressure was increased to 20 mmHg and left for a further 10 minutes to stabilise. This was then increased incrementally in a stepwise fashion to pressures of 40, 60, 80 and 100 mmHg. Live video recording of the perfused vasa recta was carried throughout the experiment and vessel diameter analysed later offline (see methods for details).

Vasa recta diameter at 0-5 mmHg was considered as baseline; therefore any changes in diameter after increase of pressure were measured as a percentage change of baseline diameter. Perfused vasa recta diameter was measured at a pericyte site and non-pericyte site of a single vessel (figure 5.3).

Increasing the pressure from 0 to 20 mmHg within vasa recta resulted in a 3.73 ± 1.5% increase of diameter at pericyte sites while non-pericyte sites increased 1.8 ± 1.2% (n=8 (8), figure 5.3). The pressure increase did not result in a significant difference in vasa recta diameter at pericytes compared with that measured at non-pericyte sites.

Increasing the pressure from 20 to 40 mmHg resulted in an increase diameter at pericyte sites (9 ± 2.7 %) that was significantly greater than the increase of diameter measured at non-pericyte sites (2.92 ± 2.5%, n=8 (8), $P<0.01$), figure 5.3.

Increasing the luminal pressure in a stepwise manner from 40 to 100 mmHg resulted in an increase diameter at pericyte sites (14.12 ± 2.1, 15.25 ± 3.8 and 16.15 ± 4.2%, respectively) that was significantly greater than increase of diameter measured at non-pericyte sites (4.56 ± 3.1, 5.19 ± 3.6 and 6.54 ± 4.31%, respectively, n=8 (8), P<0.01), figure 5.3.

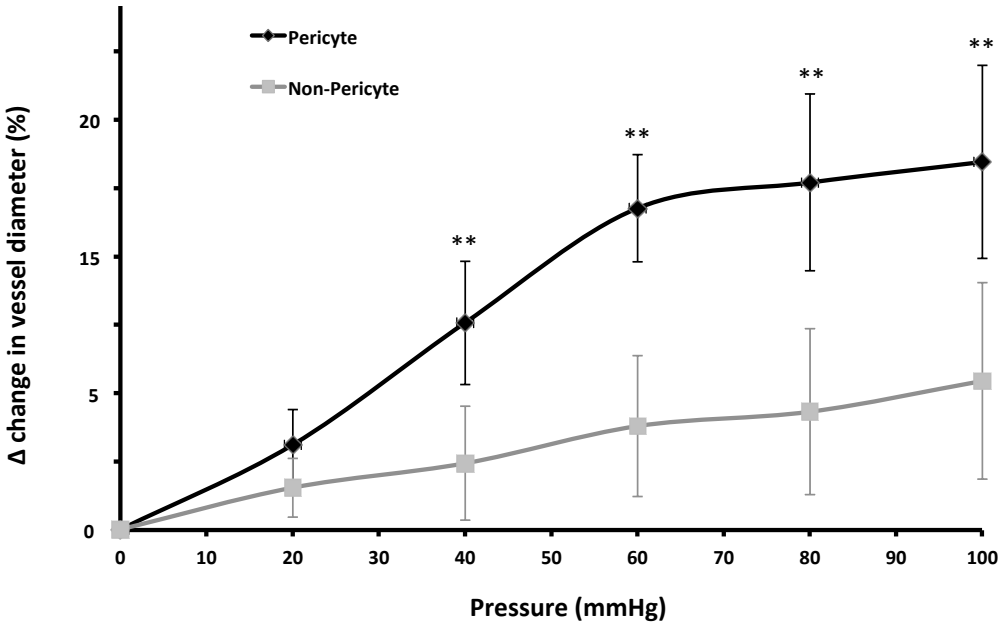

Figure 5.3 Increasing luminal perfusion flow increases diameter of *in situ* vasa recta. Increasing the perfusion flow of vasa recta in a stepwise manner resulted in a significantly greater increase in diameter of vasa recta at pericyte sites compared to that was measured at non-pericyte sites**.** Values are mean ± SEM. n=8 (8), ** P<0.01.

5.4 The effect of luminally perfused ANG II and ET-1 on *in situ* vasa recta diameter

With perfusion of *in situ* vasa recta being possible, vessel perfusion of vasoactive agents needed to be investigated to ascertain how accurate vasoactive responses were in comparison to already established models (Crawford *et al*. 2012; Z. Zhang *et al*. 2004). Perfusion of damaged or dead vessels would be pointless with respect to investigating pericyte-mediated control of vasa recta diameter therefore if perfusion

with a known vasoconstrictor produced no response, the model would be invalid or irrelevant to investigate further.

As the live slice model had already been investigated for its viability (Crawford *et al*. 2012), it was assumed that perfusion setup would have no effect on this. Therefore, a significant majority of the tissue would still be "alive".

Using the isolated DVR technique, Pallone *et al* have shown luminal perfused ANG II had no significant effect on vessel diameter until concentrations of 10 nM were reached (Pallone 1994). Interestingly, lower concentrations added to the surrounding bath solution, and not directly into the lumen, evoked a much more significant constriction of pericytes and consequently reduced vessel diameter (Pallone 1994). This is more than likely due to bath application of drug having a direct effect on pericytes whereas luminal perfusion relies on endothelial cell to pericyte communication. Nonetheless, the same group has shown luminal perfusion of a variety of vasoactive substances (PGE_2, ANG II and ET-1) are able to mediate pericyte-induced changes in DVR diameter, even after DVR were isolated and stripped of supporting tissue (Pallone 1991; Rhinehart & Pallone 2001a; Pallone 1994; Pallone & Silldorff 2001). Experiments performed using live kidney slices have shown similar results in that bath application of a variety of vasoactive compounds (ANG II, ET-1, NO donors and PGE_2) resulted in changes in vasa recta diameter due to the action of pericytes (Crawford *et al*. 2012). Taken together, it is reasonable to suggest that perfusion of vasa recta with vasoactive compounds within the live slice model should produce similar results to what has been previously observed both isolated and *in situ.*

In situ vasa recta were perfused with ANG II (100 nM) at 25 mmHg while tissue slices were constantly superfused with 95% O_2 / CO_2 PSS. Perfusion of ANG II resulted in a sustained constriction of vasa recta capillaries (Figure 5.4). Vasoconstriction was significantly greater at pericyte sites (39.21 ± 3.6%) compared with that measured at non-pericyte sites (10.96 ± 1.37%, n=9 (8), $P<0.001$), figure 5.4. The ANG II evoked constriction remained constant throughout perfusion and only reversed when perfusion was stopped after pipette removal. Due to the experimental nature of the perfusion setup, single pipette perfusion, solution change is not possible therefore unable to washout any drug that may remain within the vessel. This is discussed further in the discussion section of this chapter.

The initial concentration used in this experiment is taken from the primary studies by Crawford *et al* (Crawford *et al*. 2012) using the live slice model. As mentioned, Pallone *et al* did not notice any significant constriction until a concentration of 10 nM was luminally perfused (Pallone 1994), however did see a response when superfused abluminally with lower concentrations. Therefore, a range of ANG II concentrations (10-50 nM) would be perfused to ascertain the concentration dependent effect of ANG II on pericyte mediated of constriction of vasa recta.

In situ vasa recta were perfused with ANG II (10, 30 and 50 nM) at 25 mmHg while tissue slices were constantly superfused with 95% O_2 / CO_2 PSS. Perfusion resulted in a sustained constriction of vasa recta capillaries at all concentrations (Figure 5.4). Vasoconstriction was significantly greater at pericyte sites (17.98 ± 1.78, 19.90 ± 3.10 and 22.43 ± 2.13%, respectively) compared with that measured at non-pericyte sites (4.70 ± 1.90, 5.30 ± 3.10 and 7.39 ± 2.01%, respectively, n=9(8), P<0.001), figure 5.4. The ANG II evoked constriction at all concentrations remained constant throughout perfusion and only reversed when perfusion was stopped after pipette removal.

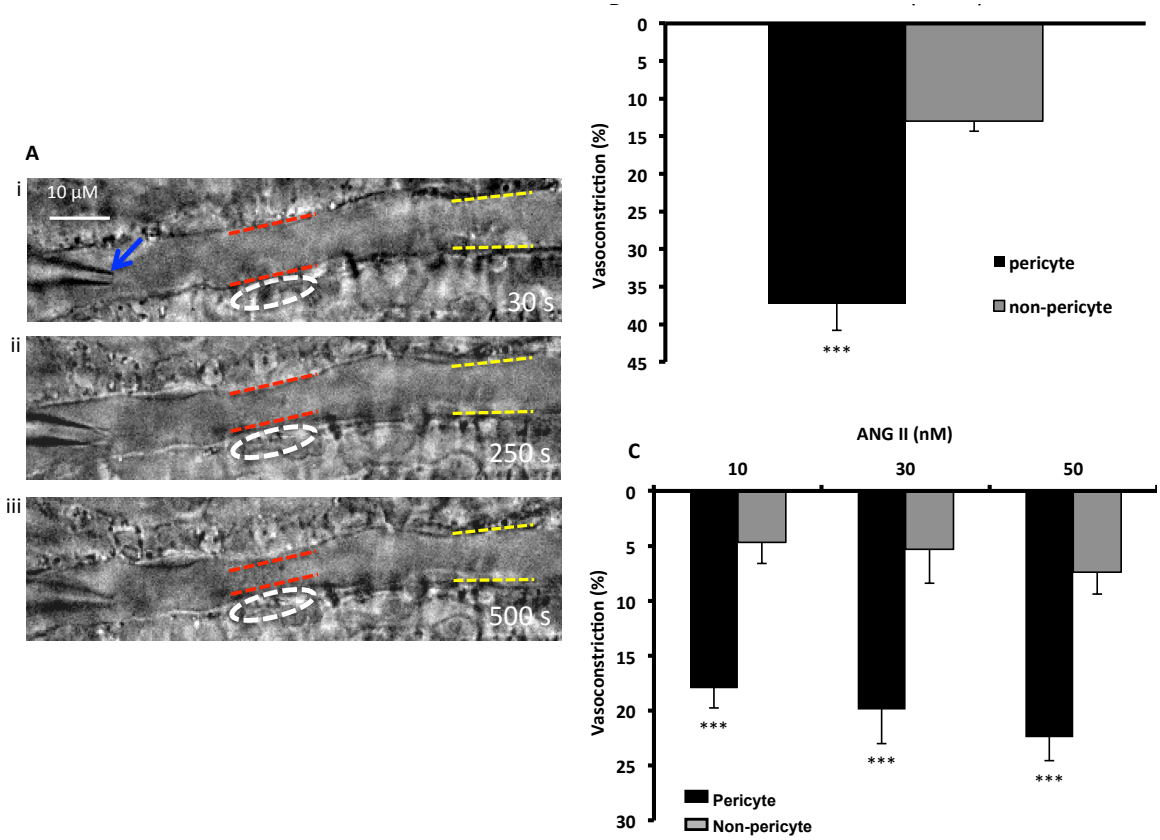

Figure 5.4 Luminal perfusion of ANG II induces pericyte-mediated constriction of *in situ* vasa recta. A: Typical field of view of vasa recta being perfused with ANG II (100 nM) is shown (i). Pericytes are located on capillary walls (white oval). Red and yellow dashed lines highlight the regions where vessel diameter was measured at pericyte and non-pericyte sites, respectively. Perfusion pipette highlighted by blue arrow. Perfusion of ANG II (100 nM) caused a reduction in vessel diameter at the pericyte site (ii) that continued and decreased over time (iii). B: Mean data for these experiments shows ANG II (100 nM) evoked a significantly greater constriction at pericyte sites (black bar) compared with non-pericyte sites (grey bar). C: Mean data for experiments using a range of ANG II concentrations (10, 30 and 50 nM) shows ANG II evoked a significantly greater constriction at pericyte sites (black bars) compared with non-pericyte sites (grey bars). Data are mean ± SEM, ***p<0.001; n= 9 (8).

To ascertain whether the pericyte-mediated change in vessel diameter occurred in response to other vasoactive mediators, vessels were perfused with ET-1. Superfusion of ET-1 in the live slice model has been shown to evoke pericyte-mediated vasoconstriction of in situ vasa recta by ~10% at 10 nM (Crawford *et al.* 2012). Perfusion of ET-1 in the isolated DVR technique has been show to produce

substantial constriction of vasa recta *via* pericytes, mediated through ET_A receptor activation, at ~65% at 10 nM (Silldorff *et al*. 1995).

In situ vasa recta were perfused with ET-1 (10 nM) at 25 mmHg while tissue slices were constantly superfused with 95% O_2 / CO_2 PSS. Perfusion resulted in a sustained constriction of vasa recta capillaries (Figure 5.5). Vasoconstriction was significantly greater at pericyte sites (37.26 ± 2.59%) compared with that measured at non-pericyte sites (5.47 ± 1.25%, n=7 (7), P<0.001) (Figure 5.5). The ET-1 evoked constriction remained constant throughout perfusion and only reversed when perfusion was stopped after pipette removal.

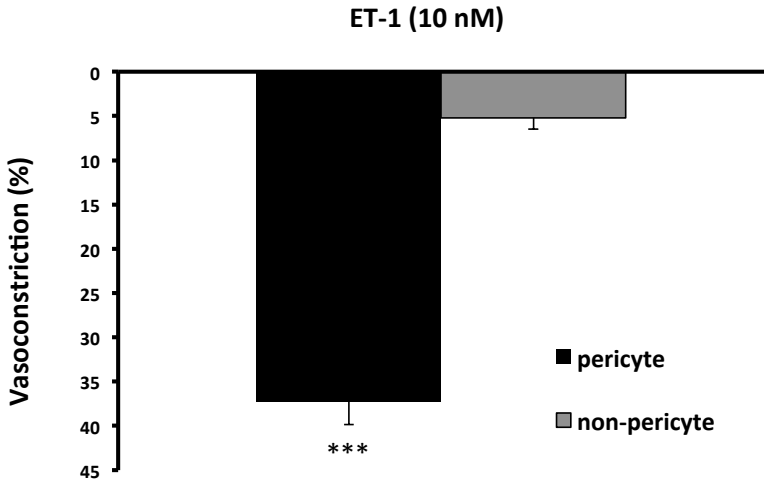

Figure 5.5 Luminal perfusion of ET-1 evokes pericyte-mediated constriction *of in situ* vasa recta. Luminal perfusion of ET-1 (10 nM) induced a significant vasoconstriction of in situ vasa recta at pericyte sites (black bars) compared with non-pericyte sites (grey bars). Data are mean ± SEM, ***p<0.001; n= 7 (7).

5.4.1 The effect of luminally perfused PGE_2 and SNAP on *in situ* vasa recta diameter

Given the fact it has been shown pericytes able to relax in response to endogenous and exogenous vasoactive dilators and hence vessel diameter increases (Crawford *et al*. 2012; Pallone 1994), the role for pericyte-mediated relaxation has been extensively investigated (Kennedy-Lydon *et al*. 2012; Pallone & Silldorff 2001; Pallone, Z. Zhang, *et al*. 2003). Renal pericytes are known to dilate and increase vasa recta diameter in response to NO and PGE_2 *in situ* (Crawford *et al*. 2012). Vasodilators have also been shown to attenuate ANG II-mediated constriction of vasa recta *in vitro* using the isolated DVR technique (Pallone 1994; Sendeski *et al*. 2013; O'Connor &

Cowley 2012). Interestingly, isolated perfused DVR have been shown to produce NO independently of exogenous stimuli (Rhinehart & Pallone 2001a). Using the isolated perfused DVR technique, Rhinehart and Pallone where able to show DVR increased production of NO when exposed to l-arginine but also produced NO when being perfused with physiological saline and left for several hours (Rhinehart & Pallone 2001b) suggesting a role for NO in the normal regulation of physiological pericyte tone.

Both NO and PGE_2 are endogenous vasodilators and as such S-nitroso-N-acetylpenicillamine (SNAP), a stable analogue of endogenous S-nitroso compounds, was used in experiments here to represent a NO donor and has previously been used *in vivo* and *in vitro* (Wilcox & Welch 2000; Crawford *et al*. 2012) and exogenous PGE_2 applied to mimic endogenous release. The aim of this study being to investigate the effect of luminal perfusion of vasodilators on vasa recta diameter and pericyte contractility.

In situ vasa recta were perfused with PGE_2 (10 μM) at 25 mmHg while tissue slices were constantly superfused with 95% O_2 / CO_2 PSS. Perfusion resulted in a sustained dilation of vasa recta capillaries (Figure 5.6). Vasa recta diameter was significantly greater at pericyte sites (9.52 ± 2.63%) compared with that measured at non-pericyte sites (1.6 ± 0.63%, n=8 (8), $P<0.01$) (Figure 5.6). The PGE_2 evoked dilation remained constant throughout perfusion and only reversed when perfusion was stopped after pipette removal.

In situ vasa recta where perfused with SNAP (100 μM) at 25 mmHg while tissue slices were constantly superfused with 95% O_2 / CO_2 PSS. Perfusion resulted in a sustained dilation of vasa recta capillaries (Figure 5.6). Vasa recta diameter was significantly greater at pericyte sites (10.18 ± 2.24%) compared to that measured at non-pericyte sites (3.14 ± 2.17%, n=8 (8), $P<0.01$) (Figure 5.6). The SNAP evoked dilation remained constant throughout perfusion and only reversed when perfusion was stopped after pipette removal.

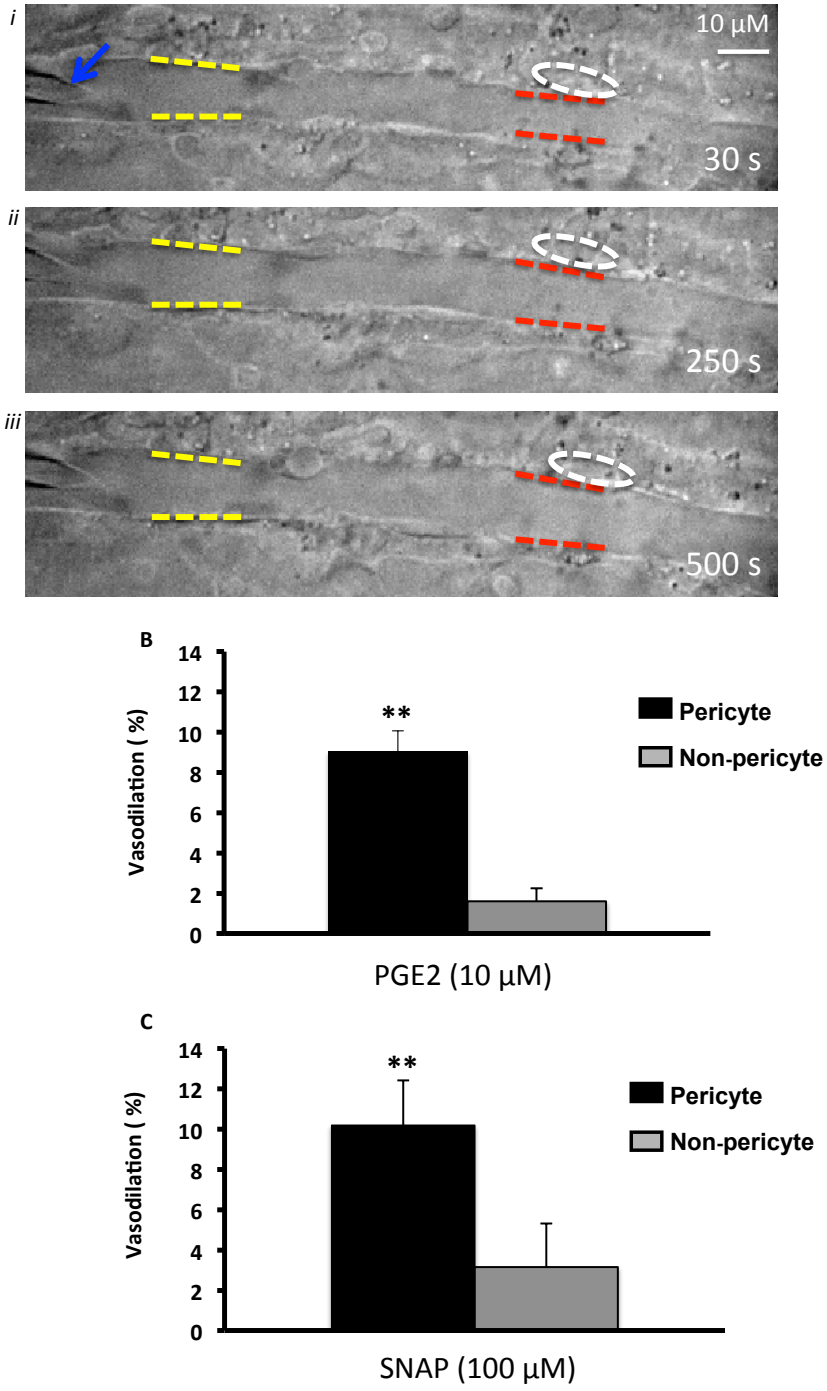

Figure 5.6 Luminal perfusion of PGE_2 and SNAP induces pericyte-mediated vasodilation of *in situ* vasa recta.

A: Typical field of view of vasa recta perfused with PGE_2 is shown (i). Pericytes are located on capillary walls (white oval). Red and yellow dashed lines highlight the regions where vessel diameter was measured at pericyte and non-pericyte sites, respectively. Perfusion pipette highlighted with blue arrow. Perfusion of PGE_2 (10 µM) caused an increase in vessel diameter at the pericyte site (aii) that continued throughout and increased over time (iii). B: Mean data for these experiments shows PGE_2 evoked a significantly greater dilation at pericyte sites (black bar) compared with non-pericyte sites (grey bar). C*:* Mean data for experiments of SNAP (100 µM) perfusion showing a significantly greater dilation at pericyte sites (black bars) compared with non-pericyte sites (grey bars). Data are mean ± SEM, **p<0.01; n= 8 (8).

5.5 The effect of luminally perfused CNIs on *in situ* vasa recta diameter

5.5.1 CsA perfusion

Having established that luminal perfusion of vasa recta with endogenous vasoactive agents resulted in similar responses to when agents were superfused, the model was then used to explore the role of CNIs on vasa recta diameter and the potential role pericytes might have in contributing towards CNI-induced nephrotoxicity and if CNI-mediated vasoconstriction is *via* their presence within the blood stream.

In situ vasa recta were perfused with CsA (3 μM, maximum clinically recommend trough concentration (360 ng/ml)) at 25 mmHg while tissue slices were constantly superfused with 95% O_2 / CO_2 PSS. Perfusion resulted in a sustained constriction of vasa recta capillaries (Figure 5.7). Vasoconstriction was significantly greater at pericyte sites (22.55 ± 1.85%) compared to that measured at non-pericyte sites (11.96 ± 2.10%, n=9 (8), P<0.01) (Figure 5.7). The CsA evoked constriction remained constant throughout perfusion and only reversed when perfusion was stopped after pipette removal.

For consistency and comparison, *in situ* vasa recta were perfused at the same concentrations used for superfusion experiments.

In situ vasa recta were perfused with CsA (1, 5 and 10 μM) at 25 mmHg, while tissue slices were constantly superfused with 95% O_2 / CO_2 PSS. Perfusion resulted in a sustained constriction of vasa recta capillaries at all concentrations (Figure 5.7). Vasoconstriction was significantly greater at pericyte sites (20.20 ± 3.80, 25.52 ± 2.91 and 33.04 ± 3.9%, respectively compared to that measured at non-pericyte sites (10.01 ± 2.09, 11.51 ± 1.02 and 10.97 ± 4.42%, respectively, n=9 (8), P<0.05) (Figure 5.7). The CsA evoked constriction at all concentrations remained constant throughout perfusion and only reversed when perfusion was stopped after pipette removal.

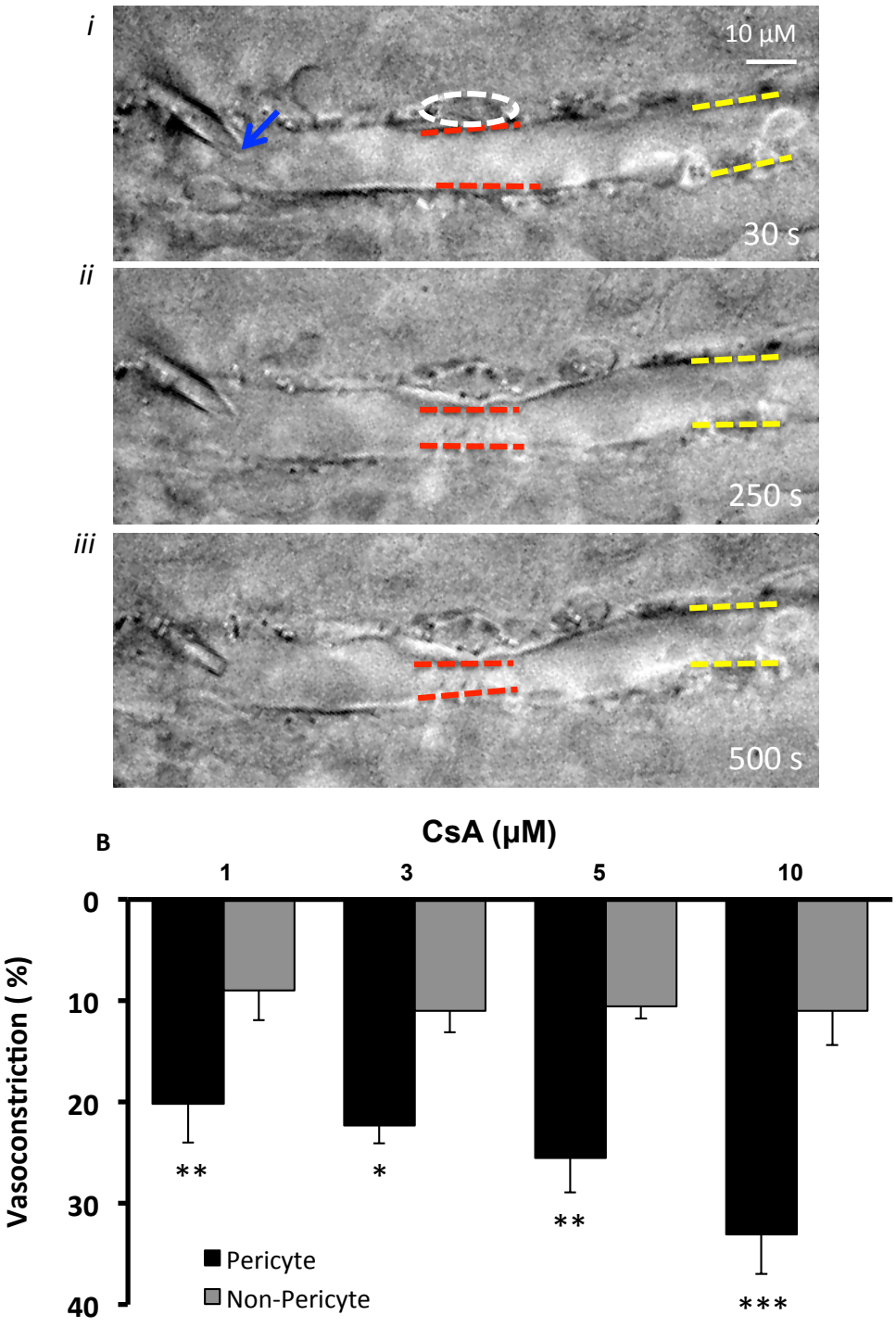

Figure 5.7 Luminal perfusion of CsA induces pericyte-mediated constriction of *in situ* vasa recta.

A: Typical field of view of vasa recta perfused with CsA is shown (i). Pericytes are located on capillary walls (white oval). Red and yellow dashed lines highlight the regions where vessel diameter was measured at pericyte and non-pericyte sites, respectively. Perfusion of CsA (3 µM) caused a reduction in vessel diameter at the pericyte site (ii) that continued throughout and decreased over time (iii). B*:* Mean data for experiments using a range of CsA concentrations (1, 3, 5 and 10 µM) shows CsA evoked a significantly greater constriction at pericyte sites (black bars) compared with non-pericyte sites (grey bars). Data are mean ± SEM, *p<0.05; n= 9 (8).

5.5.2 Comparing the effects of perfused CsA with superfused CsA on *in situ* vasa recta diameter

With all concentrations of perfused CsA evoking a significant vasoconstriction and suggesting a more substantial constriction compared to superfusion, pericyte constriction evoked using superfusion and perfusion were compared for each concentration of CsA.

Perfusion of CsA (1, 3, 5 and 10 µM) resulted in a significant vasoconstriction of DVR at pericyte sites (20.20 ± 3.80, 22.55 ± 1.85, 25.52 ± 2.91 and 33.04 ± 3.9%, respectively) compared to that measured at pericyte sites *via* superfusion of CsA (5.3 ± 0.99, 8.8 ± 1.03, 10.2 ± 0.81 and 12.7 ± 0.88%, respectively, **P<0.01, n= 7 (7), figure 5.8.

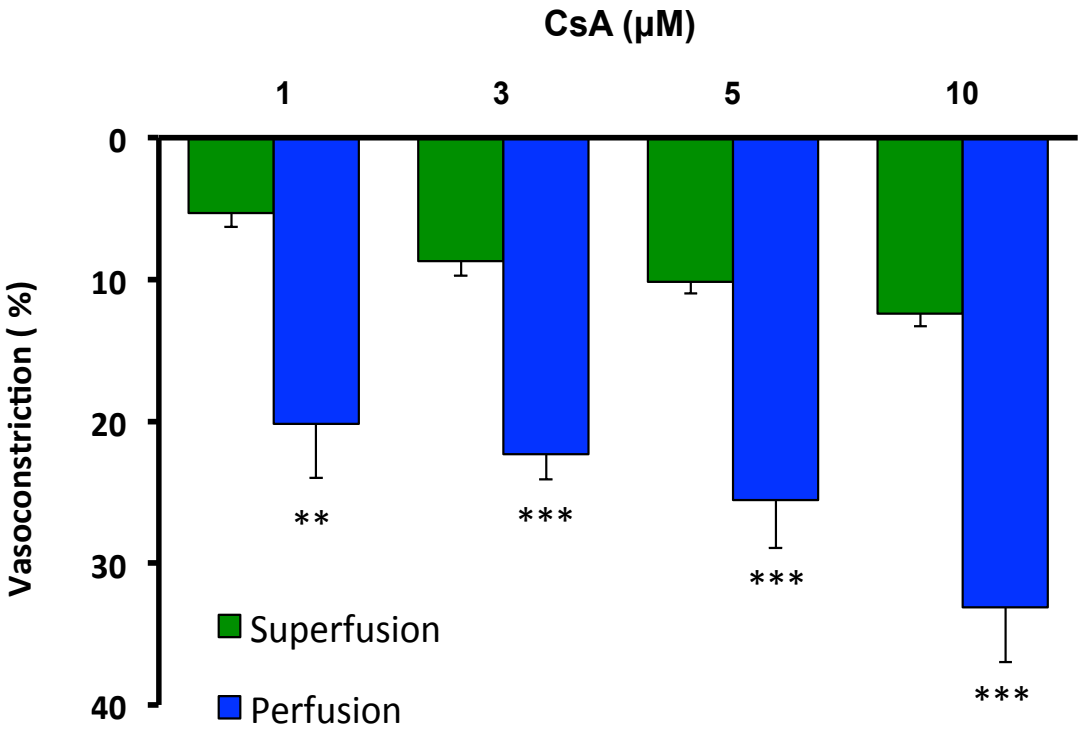

Figure 5.8 Luminal perfusion of CsA has an enhanced vasoconstrictive effect when compared to superfusion.

Bar graph shows mean data for the CsA-induced change in vessel diameter following luminal perfusion (blue bar) and bath superfusion (green bar) at pericyte sites. Data are means ±SEM, **P<0.01, n= 7 (7).

5.6 FK506 perfusion

Given data in previous chapters has demonstrated both CsA and FK506 induce changes in vessel diameter *via* their action pericytes, investigating FK506 perfusion would enable direct comparison against superfusion and aid in understanding endothelial cell to pericyte communication.

In situ vasa recta were perfused with FK506 (1 μM) at 25 mmHg while tissue slices were constantly superfused with 95% O_2 / CO_2 PSS. Perfusion resulted in a sustained constriction of vasa recta capillaries (Figure 5.9). Vasoconstriction was significantly greater at pericyte sites (29.82 ± 4.50%) compared to that measured at non-pericyte sites (6.96 ± 1.40%, n=9 (8), P<0.001) (Figure 5.9). The FK506 evoked constriction remained constant throughout perfusion and only reversed when perfusion was stopped after pipette removal.

As with CsA, to enable direct comparison between luminal perfusion and superfusion, *in situ* vasa recta were perfused at the same concentrations used for superfusion experiments.

In situ vasa recta were perfused with FK506 ($8x10^{-4}$, 0.05 and 0.1 μM) at 25 mmHg while tissue slices were constantly superfused with 95% O_2 / CO_2 PSS. Perfusion resulted in a sustained constriction of vasa recta capillaries at all concentrations (Figure 5.9). Vasoconstriction was significantly greater at pericyte sites (15.17 ± 2.50, 17.38 ± 3.70 and 21.88 ± 2.18%, respectively) compared to that measured at non-pericyte sites (7.15 ± 2.30, 10.94 ± 2.18 and 9.12 ± 1.70%, respectively, n=9 (8), P<0.05) (Figure 5.9). The FK506 evoked constriction at all concentrations remained constant throughout perfusion and only reversed when perfusion was stopped after pipette removal.

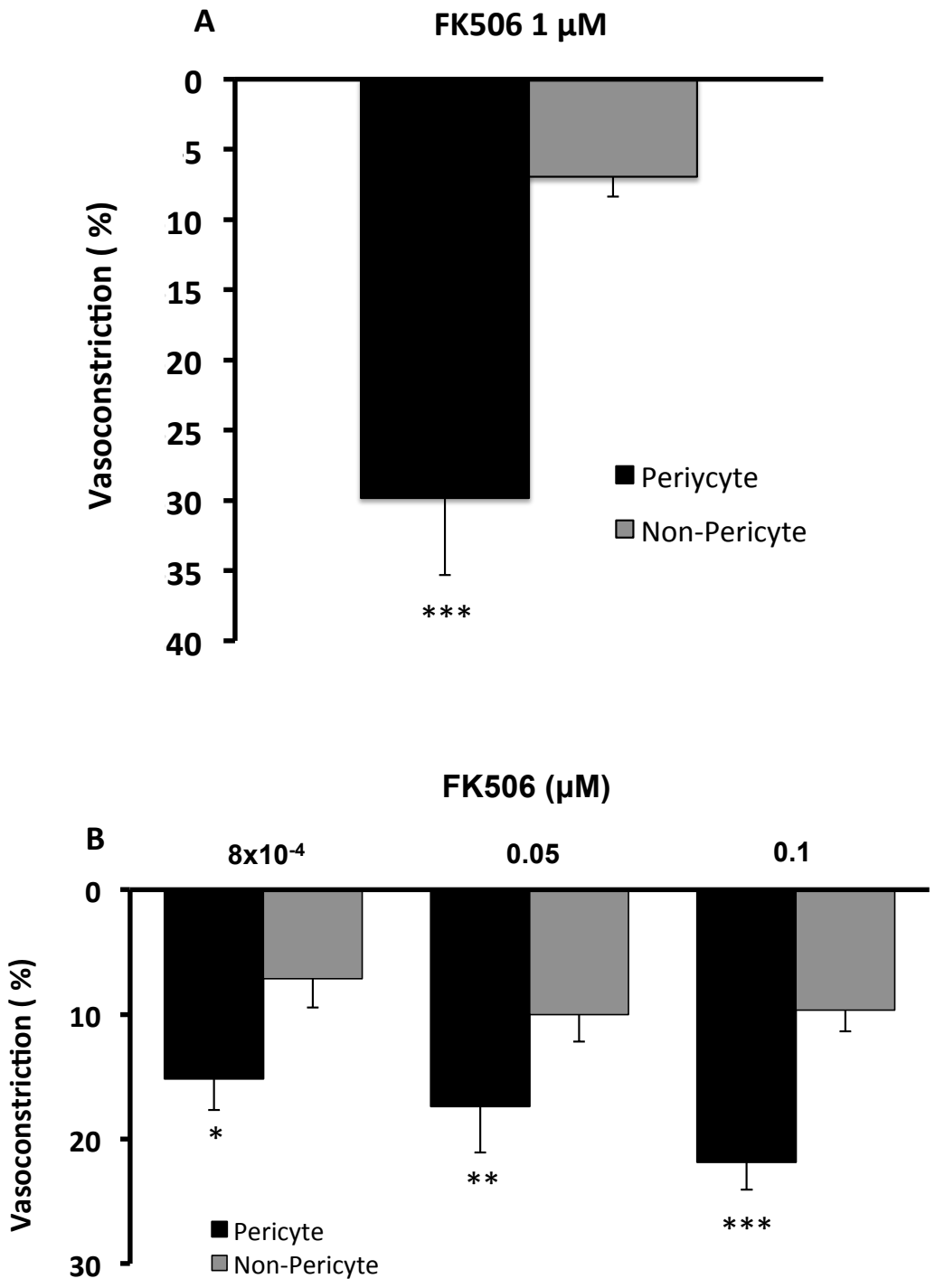

Figure 5.9 Luminal perfusion of FK506 induces pericyte-mediated constriction of *in situ* vasa recta.

A: Perfusion of FK506 (1 µM) evoked a significant reduction in vessel diameter at the pericyte sites (black bars) when compared to that measured at non-pericyte sites (grey bars). B: Mean data for experiments using a range of FK506 concentrations ($8x10^{-4,}$ 0.05 and 0.1µM) shows FK506 evoked a significantly greater constriction at pericyte sites (black bars) compared to that measured at non-pericyte sites (grey bars). Data are mean ± SEM, n= 9 (8), *p<0.05.

5.6.1 Comparing the effects of perfused FK506 with superfused FK506 on *in situ* vasa recta diameter

As was seen with CsA, all concentrations of FK506 (including the lowest clinical trough concentration) evoked a significant vasoconstriction of vasa recta pericytes. Therefore, comparing the pericyte-mediated vasoconstriction induced by perfusion with superfusion would highlight the physiological relevance perfusion of FK506 has on DVR. In addition, direct comparison of perfusion and superfusion would enable an understanding to the cell-to-cell signalling events depending on which site at which FK506 is exposed *i.e.* direct action on pericytes *via* superfusion or endothelial cell to pericyte communication *via* perfusion.

Perfusion of FK506 ($8x10^{-4}$, 0.05, 0.1 and 1 μM) resulted in a significant vasoconstriction of DVR at pericyte sites (15.17 ± 2.50, 17.38 ± 3.70 and 21.88 ± 2.18 and 29.82 ± 4.50%, respectively) compared to that measured at pericyte sites *via* superfusion of FK506 (4.87 ± 0.99, 8.03 ± 1.36, 9.77 ± 0.54, 11.34%, respectively, *P<0.05, n= 7 (7)), figure 5.10.

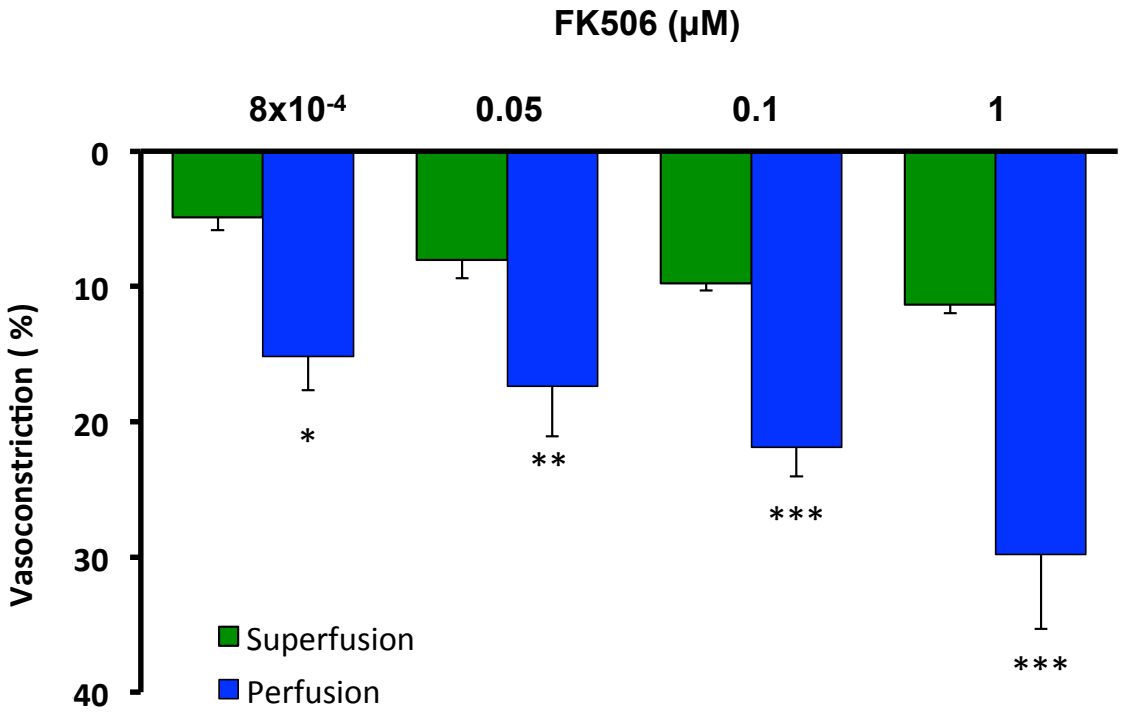

Figure 5.10 Luminal perfusion of FK506 has an enhanced vasoconstrictive effect when compared to superfusion.

Bar graph shows mean data for the FK506-induced change in vessel diameter following luminal perfusion (blue bar) and bath superfusion (green bar) at pericyte sites, Data are means ±SEM, *P<0.05, n= 8 (8).

5.7 Rapamycin perfusion

Rapamycin failed to evoke any significant vasoconstriction at pericytes of *in situ* vasa recta when superfused, thus the effect of luminally perfusing rapamycin was investigated to determine whether any changes in vessel diameter were evoked.

In situ vasa recta were perfused with rapamycin (1 μM) at 25 mmHg while tissue slices were constantly superfused with 95% O_2 / CO_2 PSS. Perfusion resulted in no significant constriction of vasa recta capillaries (Figure 5.11). When change in diameter was noted, it was not significantly greater at pericyte sites (0.42 ± 2.7%) compared to that measured at non-pericyte sites (1.9 ± 2.40%, n=8 (8); P>0.05) (Figure 5.11). Perfusion of rapamycin was stable throughout the entire experiment and no noticeable alterations in vasa recta diameter were observed.

For direct comparison against superfusion, rapamycin was perfused with matching concentrations.

As with superfusion observations, luminal perfusion of vasa recta with rapamycin failed to evoke any significant change in vasa recta diameter at any concentration tested. Perfusion of rapamycin (0.05 and 0.1 μM) resulted in no significant constriction of vasa recta capillaries (Figure 5.11). When change in diameter was noted, it was not significantly greater at pericyte sites (3.16 ± 1.01 and 4.4 ± 1.66%, respectively) compared to non-pericyte sites (2.9 ± 2.01 and 1.8 ± 2.06%, respectively, n=8 (8); P>0.05) (Figure 5.11).

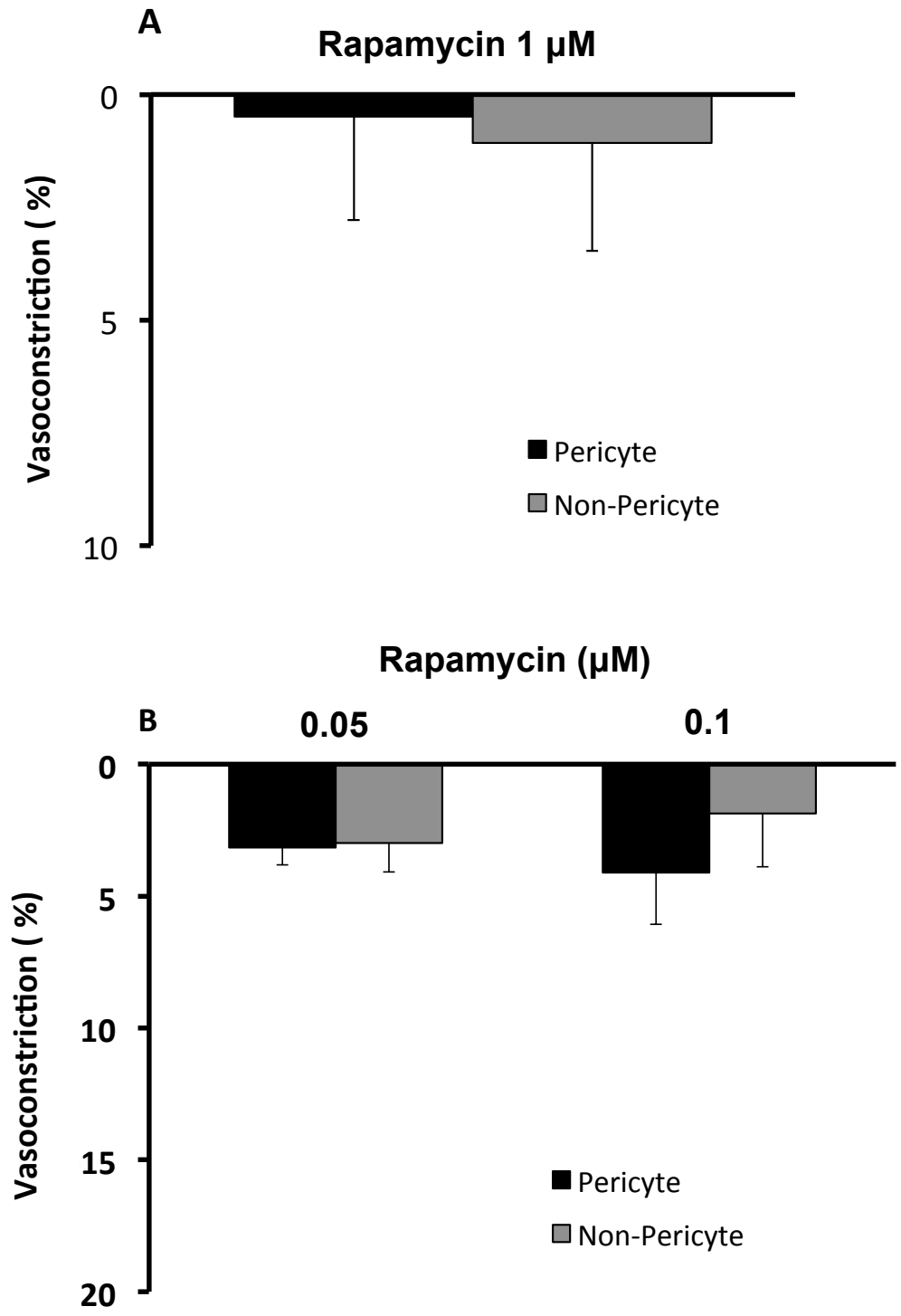

Figure 5.11 Luminal perfusion of rapamycin does not induce pericyte-mediated constriction of *in situ* vasa recta.

A: Perfusion of rapamycin (1 µM) did not evoke a significant reduction in vessel diameter at the pericyte sites (black bars) when compared to that measured at non-pericyte sites (grey bars). B: Mean data for experiments using a range of rapamycin concentrations (0.05 and 0.1µM) show rapamycin's inability to evoke greater constriction at pericyte sites (black bars) compared to that at non-pericyte sites (grey bars). Data are mean ± SEM, $p>0.05$, n= 9 (8).

5.7.1 Comparing the effects of perfused rapamycin with superfused rapamycin on *in situ* vasa recta

Perfusion of rapamycin (0.05, 0.1 and 1 μM) failed to evoke significant vasoconstriction of *in situ* vasa recta. Similarly, superfusion also failed to evoke any significant vasoconstriction.

The change in vasa recta diameter at pericyte sites through perfusion of rapamycin (0.42 ± 2.7, 3.16 ± 1.01 and 4.4 ± 1.66%, respectively) was not significantly different when compared to diameter measured at pericyte sites during superfusion of rapamycin (4.30 ± 2.5, 3.30 ± 0.87 and 4.98 ± 1.30%, respectively, P>0.05, n=7 (7)), figure 5.12.

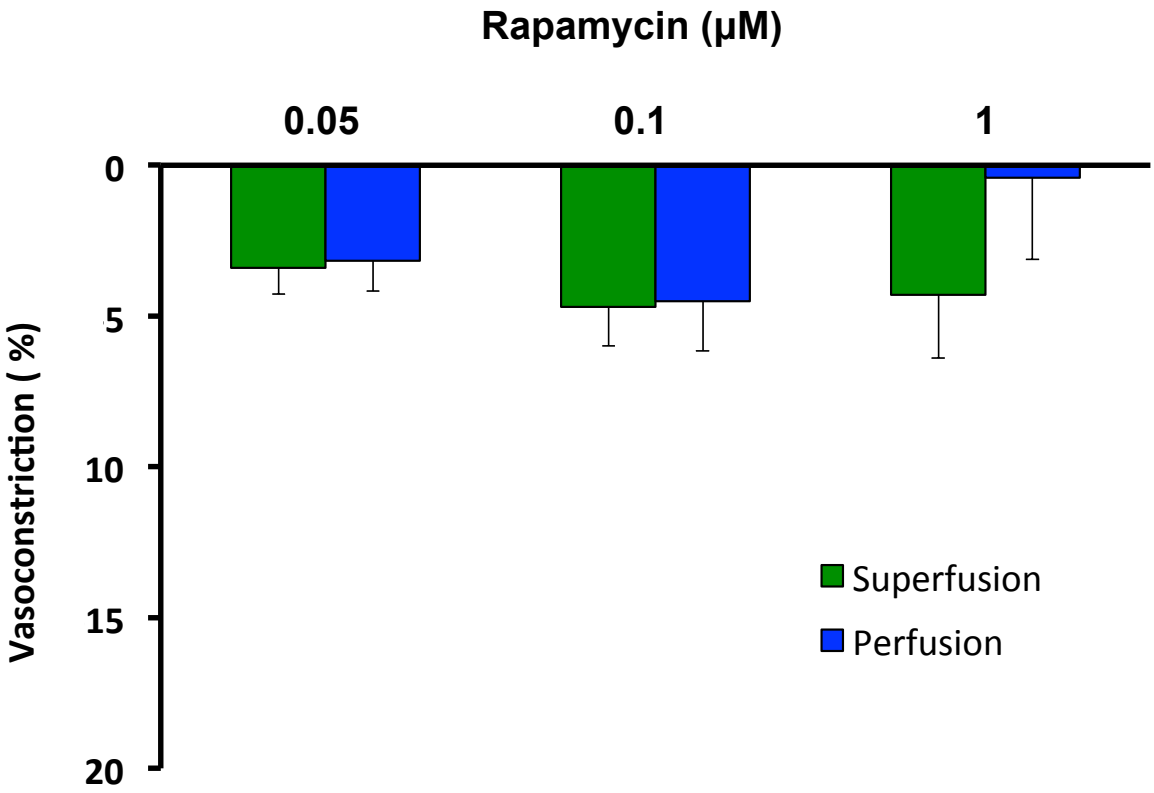

Figure 5.12 Luminal perfusion of rapamycin has no enhanced vasoconstrictive effect when compared to superfusion.

Bar graph shows mean data for the rapamycin-induced change in vessel diameter following luminal perfusion (blue bar) and bath superfusion (green bar) at pericyte sites, Data are means ±SEM, P> 0.05, n= 7 (7).

5.8 Discussion

The aim of this chapter was to develop a model for single vessel perfusion in the live kidney slice for investigating the cellular mechanisms involved when vasoactive agents and CNIs where luminally perfused in vasa recta.

The main findings of this investigation are the successful perfusion of *in situ* vasa recta capillaries in the live slice model and the results suggest luminal perfusion of vasoactive compounds caused more potent effects on vessel diameter than superfusion. Similarly, perfusion of CNIs evoked a substantial pericyte-mediated vasoconstriction of vasa recta that consequently reduces vessel diameter and is likely to impede MBF. These results, in combination with previous chapters, highlight the potential role of MBF in contribution to CNI-mediated nephrotoxicity. In addition, the results shown here merit further investigations into endothelial cell to pericyte communication for understanding the molecular mechanisms of luminally exposed vasoactive agents for further understanding the role of DVR in regulation of MBF. Taken together, targeting renal pericytes during CNI treatment could be a novel method for attenuation of CNI nephrotoxicity.

For the past two decades, use of the isolated perfused vasa recta technique has been fundamental in aiding the understanding of MBF and physiology of the renal pericyte. One of the first publications by Pallone *et al* (Pallone *et al*. 1994), described the method as an adaptation from isolated perfused tubule experiments carried out by Burg (Burg 1972). The two techniques are similar, as previously mentioned, and involve dissection and removal of any surrounding and supporting tissue in order to carry out free flow perfusion (Pallone *et al*. 1994; Burg 1972). Given the inaccessibility of the renal medullary architecture *in vivo*, this technique advanced our understanding of the complex and intricate pathways involved in blood flow circulation and renal osmotic changes.

However, as with most experimental scientific models, it is not perfect. Firstly, the technique is *in vitro*, therefore not as relevant or closely matched to *in vivo*. If it were possible to perform techniques similar to micropuncture studies in the vasculature of the medulla *in vivo* (Sakai *et al*. 1965), perfusion of DVR *in vivo* would be far superior compared to isolated techniques. Unfortunately, this is technically too demanding, even with recent technological advances. Isolation of the DVR involves mechanical stress inflicted upon the tissue; this not only increases the risk for physical damage

but also increases the risk of molecular damage including ROS generation, cell apoptosis and even receptor desensitisation due to shear stress inducing release of NO, ET and ATP (Beierwaltes 2013).

Secondly, removing the supporting structures of DVR including the renal medullary interstitial cells (RMIC) and surrounding interstitum, increases the risk for misinterpretation of results. For example, an agonist-induced vasoconstriction of isolated DVR might not equate to the same magnitude of constriction observed *in vivo* with supporting cells and structures intact, which play a part in vessel stability and acting as restricting structures. It must also be noted that these surrounding structures may also contribute towards pericyte-mediated vasoconstriction or vasodilation through release of paracrine mediators (Crawford *et al*. 2011). Renal pericytes are also known to play a crucial role in vessel stabilisation (Peppiatt-Wildman 2013) therefore possibly require information, growth factors for vessel regeneration for example, from surrounding cells to fully function and maintain endothelial cell to pericyte communication. RMIC are a known source of endogenous PGE_2 (Crawford *et al*. 2012), which has been shown to attenuate ANG II-mediated constriction of *in situ* vasa recta and cause dilation of vasa recta when applied alone (Crawford *et al*. 2012; Pallone 1994; Silldorff *et al*. 1995). Given these established mechanisms of vessel diameter regulation *in situ* following superfusion of agents it is or seems important to investigate the effect of luminal exposure to these agents to recapitulate the *in vivo* blood perfused setting.

Unlike in situ preparations, isolated perfused DVR do not have the localised signalling mechanisms derived from surrounding tissue which enables vessels to communicate with other surrounding tissue and specifically, unable to communicate with renal tubules. The idea of tubular-vascular cross-talk is still in its infancy, however given that the medullary microcirculation responds to minute changes in blood flow and osmolality *via* alternations in tubular flow rate, it is reasonable to suggest that small changes in communication between vessels and tubules may play a larger role in medullary circulation than once thought.

Vasoconstriction of DVR induced by ANG II during isolated perfusion experiments (Pallone 1994) was at a similar magnitude to that of *in situ* superfusion (Crawford *et al*. 2012), suggesting a similarity of contractile response. However, the pathways involved could be completely distinctive due to *in situ* superfusion utilising subsurface vessels, and therefore not having direct exposure to drugs at applied

concentrations due to drug-tissue diffusion and distribution *per se*, while isolated perfusion experiments have direct contact with ANG II from the abluminal surface (Pallone 1994). *In situ* perfusion relies on signals advancing from the luminal endothelial cells to pericytes residing on the abluminal wall of vasa recta and given that endothelial cells and pericytes are known to have peg and socket contacts (Armulik *et al*. 2005), the time taken for communication is not going to be as instantaneous as applying drug to the abluminal surface of vasa recta and direct contact with pericytes. This can be further seen using ET in isolated perfusion and *in situ* superfusion experiments. Pallone *et al*, using isolated perfusion, were able to show almost complete closure of DVR, >90%, when perfused with ET at 10 pM (Silldorff *et al*. 1995). Conversely, Crawford *et al*, using in situ superfusion, were only able to demonstrate a 10% vasoconstriction using 10 nM of ET (Crawford *et al*. 2012).

A study by Crawford *et al* highlighted the role for tubular-vascular crosstalk by inducing hypotonic shock in the live slice model (Crawford *et al*. 2012). This subsequently induced ATP-mediated vasodilation of vasa recta *via* pericytes, ATP vasoactivity is concentration dependent, and suggests a role for pericytes in preserving the cortico-medullary gradient and reducing localised ischemia (Peppiatt-Wildman 2013). Pericytes therefore are able to sense a change in extracellular nucleotides and respond by causing changes in vasa recta diameter and therefore potentially MBF. More recently, O'Connor and Cowley have similarly highlighted the importance of tubular-vascular crosstalk in their DVR with attached tubules preparation (O'Connor & Cowley 2012). The authors performed DVR perfusion, intact surrounding tubules, and demonstrated buffering of ANG II-mediated vasoconstriction of DVR, through NO release from medullary thick ascending limbs demonstrating direct tubular-vascular-crosstalk (O'Connor & Cowley 2012). Furthermore, the authors data also highlighted that reduced NO bioavailability enhances pericyte mediated vasoconstriction in response to ANG II (O'Connor & Cowley 2012).

Taken together, although the use of isolated perfused DVR was fundamental for our initial understanding of pericyte physiology and MBF regulation, it is clear from the increasing amount of evidence, that many factors involved in the physiological setting

of the renal medulla are neglected in this preparation that only allows investigation of a single isolated vessel.

The live kidney slice model aims to address the problems that are associated with isolated perfusion. Importantly, the tissue receives much less physical stress and damage when being prepared (Crawford *et al*. 2012), but also keeps the surrounding supporting structures intact and allows communication between cells from nearby locations (Crawford *et al*. 2012).

Although the live slice model has shown some interesting insights into possible renal insults from various nephrotoxic compounds (Kennedy-Lydon *et al*. 2012), the model has its limitations, which include investigation of acute injury only but more importantly, the lack of vessel perfusion. Through superfusion, the entire kidney slice is exposed to the compound of interest and subsequently does not exactly match what would be expected *in vivo*. This is particularly important for this investigation as CNIs are not circulated superficially and only exert their effect *via* the blood stream.

In addition, the model uses subsurface vessels; therefore the concentration at DVR investigated may not be which is applied to the bath for superfusion, therefore a hypothesis of drug concentration reaching the specific target area must be assumed (Kennedy-Lydon *et al*. 2012).

Ideally, perfusion of vessels within the live slice would enable a far more accurate representation of physiological settings, *via* an *in situ* model, and in addition, allow precise concentrations of drugs to reach the target area *via* perfusion of single vessels with concentrations required.

This chapter has demonstrated for the first time perfusion of individual *in situ* vasa recta in the live slice model. Results here have shown validation of the model, using what is available within the literature, and is possible to demonstrate reliability, similar to that of isolated perfusion and superfusion, to investigate renal pericytes and their contribution to alterations in MBF and renal injury. Interestingly, results using perfused ANG II have shown results similar to that of superfusion in terms of vasoconstriction. Perfusion of ANG II using isolated DVR resulted in very little contractile response until a much higher concentration was perfused, or remarkably, applied to the bath and acting abluminally (Pallone 1994). On the other hand, superfusion of ANG II had a significant contractile effect of pericytes when used at concentrations similar to isolated perfusion (Crawford *et al*. 2012). Perfusion of ANG II in the live slice model generated results similar to that of superfusion suggesting

ANG II can act at both pericytes and endothelial cells to mediate ANG II-evoked vasoconstriction, therefore multiple cellular pathways might contribute to the net contractile effect. This is further highlighted by the addition of ANG II to the bath of perfused isolated DVR which resulted in significant vasoconstriction compared to that of luminal perfusion (Pallone 1994).

On the contrary, when using ET-1, luminal perfusion *via* the live slice model generated results similar to that of isolated DVR perfusion. ET-1 perfusion of in situ vasa recta produced significant vasoconstriction, >40%, of vasa recta. Similarly, using isolated DVR, ET-1 evoked almost complete closure, >90%, of perfused DVR (Silldorff *et al*. 1995). Superfusion of ET-1 using the live slice induced significant vasoconstriction, ~10%, compared to that measured at non-pericyte sites but not at the magnitude of either *in situ* or isolated perfusion (Crawford *et al*. 2012). Interestingly, ET administration to healthy humans has been shown to reduce renal plasma flow by 25% and an increase in renal vascular resistance of 45% (Weitzberg *et al*. 1991) which would suggest that single, *in situ*, vessel perfusion corresponds to the physiologically seen events after ET administration.

Taken together, both sets of results show different magnitudes of response, depending on mode of drug application. However, *in situ* perfusion suggests bridging the gap between isolated perfusion and *in situ* superfusion, and emphasises the potential role of *in situ* perfusion of DVR for investigating medullary physiology. Moreover, *in situ* perfusion of vasodilatory substances resulted in significant vasodilation *via* pericytes. This suggests that *in situ* perfusion is a stable model to investigate endothelial cell and pericyte interactions as previous reports have shown that an increased perfusion rate of isolated perfused DVR is able to induce vasoconstriction *via* sheer stress and altered vasodilatory mechanisms (Z. Zhang & Pallone 2004) and illustrates the validation of *in situ* vasa recta perfusion to investigate alterations of vessel diameter and therefore MBF regulation.

Although *in situ* perfusion might more closely recapitulate the physiological setting for investigating physiological settings in the medulla, it is still not a perfect experimental model. Technical challenges are the requirement of an upright microscope, unlike isolated perfusion, which uses an inverted microscope (Sendeski *et al*. 2013), and use of precise manipulators to enable accurate single wall puncture of selected vessels. Single wall puncture allows for improved stable perfusion

compared to the easier to perform double wall puncture technique *in situ*. Double wall puncture results in multiple entry points within perfused vessels and perfusion is therefore less stable due to loss of vessel integrity and multiple puncture sites (Ishiguro & Steward 2011).

Importantly, using isolated perfused DVR enables a concentric microscopic pipette system to be established. The major advantage of this is perfusate exchange. Within the perfusion pipette of the concentric preparation, the user is able to exchange perfusion solution within a matter of minutes to investigate the effects of multiple solutions which unfortunately due to technical difficulties, cant be accomplished in the current *in situ* perfusion at this time. When perfusing *in situ* DVR, only a single perfusion pipette is applied therefore only one solution can be continuously perfused. However, during solution change using a concentric pipette, the luminal pressure has to be dropped to enable the changing of perfusate (Burg 1972) this has consequences which are discussed below. For example, although isolated perfusion enables a control solution to be followed by an experimental solution and back to control, the luminal pressure within the vessel is not constant and has to be dropped each time to enable solution exchange (Sendeski *et al*. 2013). Given that it has been shown luminal pressure changes effect vasa recta contractility (Z. Zhang & Pallone 2004), this not ideal for investigating drug solutions *via in situ* perfusion and hence not used in this study.

The perfusion of *in situ* vasa recta performed in this study therefore offers an enhanced physiological setting to investigate renal medullary physiology. By adapting isolated DVR perfusion with the *in situ* tissue model used by Crawford *et al*, the current model allows for single vessel perfusion of intact *in situ* tissue to recapitulate the more relevant physiological setting that would be observed *in vivo.* Although technically demanding, it would be possible to overcome the problem of fluid exchange within *in situ* perfusion. Unfortunately it is outwith the scope of this investigation, however would be an interest of this author to achieve an almost complete "*in vivo*" physiological setting.

The results from this chapter have also shown for the first time the effect of CNIs on luminally perfused vasa recta diameter and the possible role pericytes have in contributing to CNI-mediated nephrotoxicity. Results from previous chapters have shown that superfusion of CNIs are able to decrease vasa recta diameter, specifically

at pericytes, which could potently impede MBF *in vivo* and therefore have a damaging effect on overall renal function. In addition, perfusion of *in situ* vasa recta with CNIs has shown an enhanced vasoconstrictive effect over superfusion, which likely to be observed with *in vivo* exposure of CNIs. CsA perfusion resulted in > 30% decrease of vasa recta diameter, which using Pousiles law for an approximation of flow, would increase resistance to blood flow by ~5 fold and thus a ~70% decrease in blood flow (Peppiatt *et al*. 2006; Crawford *et al*. 2012). Given the extensive knowledge we already know about CNIs and total renal blood flow, it is interesting to note that very little research has been carried out on the microcirculation and as already mentioned, dysfunction of blood flow in the medullary microcirculation can precede that of cortical dysfunction (Mattson *et al*. 1993). Therefore, this previous area assumed not to be an influential part of the development of overall nephrotoxicity, is now questionable due to the understanding that MBF may play a larger role in RBF regulation than previously thought.

Perfusion of rapamycin failed to evoke any significant alterations of vasa recta diameter. This was similarly seen with superfusion, which corresponds suitably to clinical observations associated with rapamycin therapy (Kreis *et al*. 2000; Sehgal 2003; V. W. Lee & Chapman 2005). These results not only highlight the validity of *in situ* vessel perfusion experiments but also highlight the beneficial effects rapamycin may have over CNIs with regards to their reduced nephrotoxicity.

Unfortunately, the results from this chapter still fail to identify a single mechanism responsible for CNI nephrotoxicity. With what we know about CNIs, they are still poorly defined in terms of renal injury. How CNIs are able to induce pericyte-mediated vasoconstriction of vasa recta from luminal perfusion is still a question that remains unanswered. Nonetheless, in spite of this, it is well-known endothelial cell and pericyte communications exists, *via* specific channels or junctions and are important to identify for pursing pericyte regulation in disease states. Peg-socket contacts are membrane invaginations that extend from pericyte and endothelial cells to enable communication between the two cell types (Armulik *et al*. 2005). Peg contacts, tight, gap and adherence junctions have all been expressed as being present between pericytes and endothelial cells and may allow a variety of chemical signals to be transferred from one cell to another (Gerhardt & Betsholtz 2003; Armulik *et al*. 2005; Diaz-Flores *et al*. 2009). Interestingly, because pericyte processes often spread

to be in contact with several endothelial cells, they may integrate and coordinate neighbouring endothelial cell responses. This has been recently investigated by Zhang *et al* (Q. Zhang *et al*. 2006) using patch clamp electrophysiology. The author's results suggest that coupling between pericytes and endothelial cells is mediated mainly through open gap junctions (Q. Zhang *et al*. 2006). They also highlight the role of pericytes in membrane de/hyperpolarisation and "spreading" of electrical waves (Q. Zhang *et al*. 2006).

Interestingly, they have been able to show Lucifer yellow transfers between gap junctions in DVR and endothelial cells, Lucifer yellow is a 457 Dalton fluorescent marker which demonstrates small molecule communication between the two cells and can be further investigated to include cAMP, cGMP, Ca^{2+} and NO (Q. Zhang *et al*. 2006).

This suggests that perfusion of CNIs could have an effect on endothelial cell function, which has also previously been demonstrated *via* endothelial cell dysfunction, increased ROS generation, endothelial cell apoptosis and increased release of vasoconstrictors (Morris *et al*. 2000; Diederich *et al*. 1994; Navarro-Antolin *et al*. 2001; Naesens *et al*. 2009), and subsequently result in pericyte vasoconstriction of DVR, instigating the progression of renal medullary ischemia and development of nephrotoxicity.

Moreover, it is known that DVR pericytes produce superoxide (Z. Zhang *et al*. 2004), which may be conducted across myoendothelial junctions to limit NO bioavailability and because CNIs have been shown to inhibit NO production through endothelial dysfunction (Naesens *et al*. 2009; Oriji & Keiser 1999; Hamalainen *et al*. 2002; Lungu *et al*. 2004), the limited production and bioavailability of NO could be a possible mechanism involved in CNI-mediated vasoconstriction of vasa recta.

The results of this chapter have shown the validity of single vasa recta perfusion in live kidney slices and represents an experimental model for use in investigating the potential of vasoactive substances to influence vasa recta diameter and thus MBF. Luminal perfusion of CNIs was able to significantly reduce vessel diameter *via* their action at pericytes, likely through endothelial cell and pericyte communication, and expected to impede MBF and represents an innovative pathway for the development of CNI-induced nephrotoxicity.

6. Multiphoton imaging of the medullary microcirculation for investigating CNI nephrotoxicity

6.1 Introduction

An established complication of calcineurin inhibitor nephrotoxicity is the inability to directly measure the degree of injury above and beyond the established damage due to cellular mechanisms CNIs effect. Once instigated, CNI nephrotoxicity has historically been only identifiable after acute functional changes have been identified (Naesens *et al*. 2009; Tsechan 2002; Krejci *et al*. 2010; Pallet *et al*. 2011). The progression of nephrotoxicity is still poorly understood and given that there is no identifiable marker for progressive nephrotoxicity, regardless of cause, thus diagnosis is dependent on clinical measures such as altered serum creatinine levels and GFR (Fervenza *et al*. 2004; Pallet *et al*. 2011).

Previous chapters have noted the inaccessibility of the renal medulla *in vivo*, and using the live slice model, have demonstrated that CNIs act at medullary pericytes to alter vasa recta diameter and thus potentially reducing MBF. In order to better understand the underlying molecular and cellular events involved in CNI-mediated alterations of vasa recta diameter, multiphoton imaging of live kidney slices loaded with specific fluorophores in the presence of CNIs was carried out to ascertain how CNIs alter mitochondrial membrane potential and ROS production to induce pericyte-mediated constriction. The evidence for these investigations will be further discussed below.

6.1.2 Mechanisms of CNI nephrotoxicity

With the known combination of factors contributing towards CNI nephrotoxicity, an increasing amount of research is being focused on the molecular level in order to elucidate possible mechanisms involved to enable for earlier detection and prevention.

As previously highlighted, the CNI-mediated increase of vasoconstrictors originate from a variety of pathways including increased RAAS activation, increased ANG II and endothelin production and increased sympathetic nerve stimulation (Naesens *et al*. 2009; Abraham *et al*. 2012; Nishiyama *et al*. 1990; Morris *et al*. 2000). The decrease of vasodilators is thought to originate from endothelial dysfunction and decreased bioavailability of NO and PGE_2 (Morris *et al*. 2000; Eguchi *et al*. 2013; Amore *et al*. 1995; Hamalainen *et al*. 2002). These acute changes, coupled with cell apoptosis,

derived from a variety of pathways and activated caspases and increased cytokines release (Servais *et al*. 2008; Krejci *et al*. 2010; Tariq *et al*. 2000), collectively contribute to chronic CNI-mediated nephrotoxicity which manifests as a variety of disease states including glomerular sclerosis and interstial fibrosis (Kon *et al*. 1990; Thomas *et al*. 1998). Figure 6.0 highlights some of the known CNI-mediated acute and chronic nephrotoxic pathways.

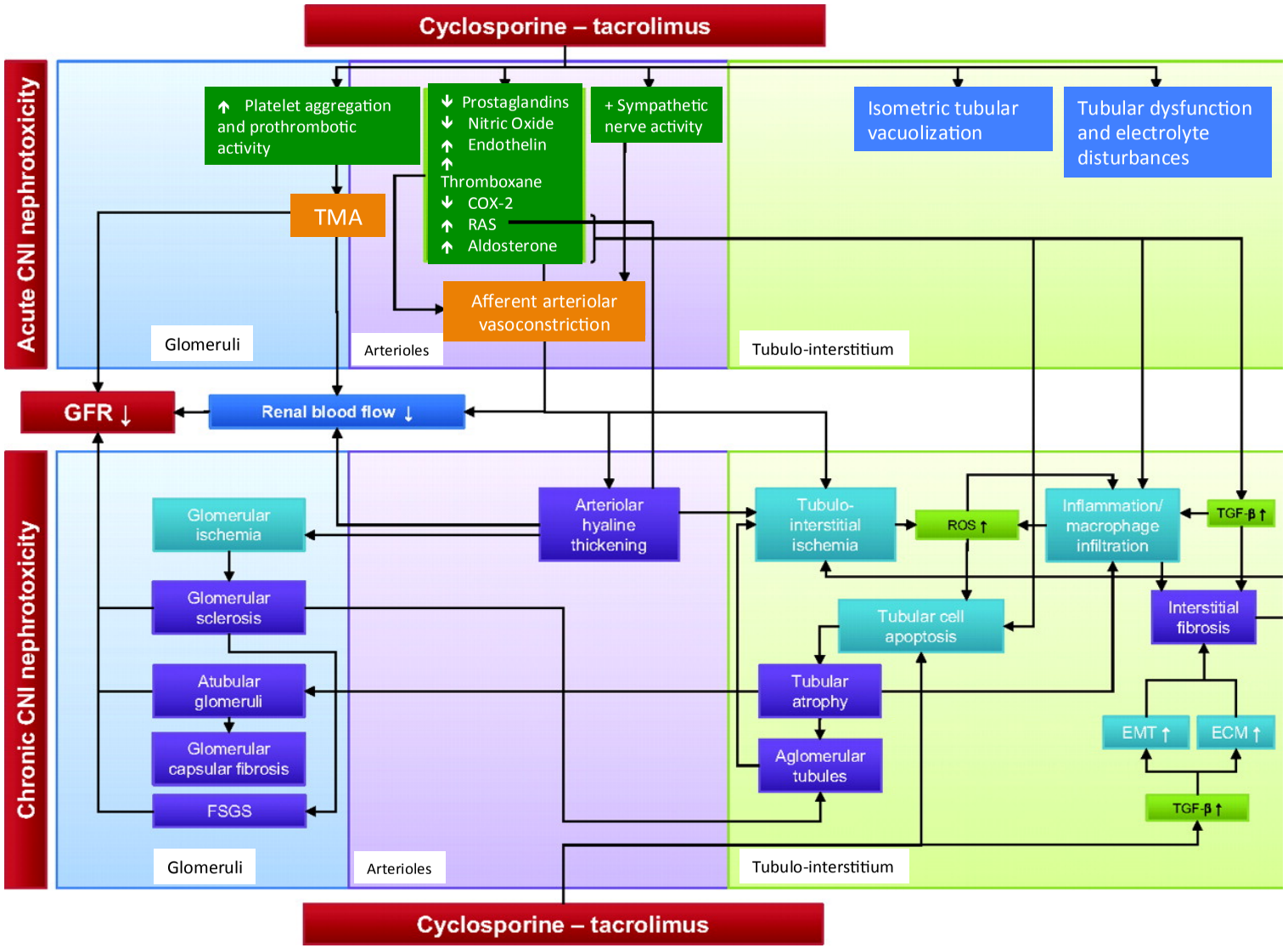

Figure 6.0 Proposed pathways of calcineurin inhibitor nephrotoxicity in glomerular, arterial and tubular compartments of the kidney. Abbreviations: CNI, calcineurin inhibitor; TMA, thrombotic microangiopathy; EMT, epithelial mesenchymal transition; ECM, extracellular matrix; GFR, glomerular filtration rate; FSFS, focal segmental glomerulosclerosis; ROS, reactive oxygen species (Adapted from Naesens et al. 2009)

Although it is thought that the acute changes are the most fundamental for development of CNI-mediated nephrotoxicity (Burdmann *et al*. 2003; M. D. Colombo *et al*. 2013; Bennett & Pulliam 1983; Naesens *et al*. 2009), we still poorly understand the mechanisms involved.

Given that calcineurin is ubiquitous within the body and is involved in a variety of physiological roles, other than just T-cell activation (Rusnak & Mertz 2000), it is possible that inhibition of this enzyme in one target organ might have detrimental effects in others. For example, calcineurin is thought to be involved in left ventricular hypertrophy upon load-induced hypertrophy of hypertensive patients (Lim *et al*. 2000). When calcineurin was attenuated *via* CsA, load induced cardiac hypertrophy was reduced in a concentration-dependent manner and also reduced histological findings of pressure-overload hypertrophy (Lim *et al*. 2000).

Preliminary evidence points to there being a role for mitochondrial dysfunction and ROS generation in the CNI-mediated nephrotoxicity detected experimentally and clinically (Perez de Hornedo *et al*. 2007; van der Toorn *et al*. 2007; Edwards *et al*. 2011; H.-W. Chen *et al*. 2002). The role foe these parameters will be discussed below.

6.1.3 Mitochondrial dysfunction

Mitochondria are complex membrane bound organelles, which are commonly referred to as the "powerhouse" of mammalian cells. They are responsible for the production of cellular adenosine triphosphate (ATP), through oxidative phosphorylation, as well as the regulation of cell growth, cell signalling, differentiation and cell death (McBride *et al*. 2006; Hall *et al*. 2009; Cossarizza *et al*. 1994; Kroemer *et al*. 2007; Ferrand-Drake *et al*. 1999). They are comprised of 5 specialised regions: the outer mitochondrial membrane (OMM), the intermembrane space, the inner mitochondrial membrane (IMM), the cristae and the matrix (Wojtczak & Zabłocki 2008).

The IMM is the main site of oxidative phosphorylation. In addition, the IMM is the site of electron flow through protein complexes of the respiratory chain, this coupled to the exit of protons to the intermembrane space is responsible for generation of the mitochondrial membrane potential ($\Delta\Psi m$) (Wojtczak & Zabłocki 2008). ATP production is generated by the flux of protons into the matrix through the ATP synthase enzyme on the IMM (Jackson *et al*. 2002).

Given the fundamental role mitochondria play in normal cell function, it is not surprising that dysfunction of such an imperative organelle would result in further complications at the cellular and organ level.

Interestingly, mitochondrial production of ROS is significant through its volume of production, just under 50% in the kidney, and contributes to oxidative damage of cells and membranes and retrograde cell redox signalling of nuclear alterations due to feedback of calcium dynamics and altered mitochondrial function (de Arriba *et al*. 2013; Perez de Hornedo *et al*. 2007). Mitochondrial ROS production is discussed in section 6.2.3.

Several groups utilising a variety of renal cell lines have recently demonstrated CNI-induced mitochondrial dysfunction. Arriba *et al* showed that CsA disarranged the IMM through cardiolipin oxidation (de Arriba *et al*. 2013). Cardiolipin is a membrane lipid responsible for structure and fluidity (Unsay *et al*. 2013) and oxidation of cardiolipin results in altered IMM fluidity and modified interactions with other membrane components including cholesterol and channel components (Unsay *et al*. 2013). Arriba *et al*'s data also demonstrated the effect of CsA on the OMM, the effect of which resulted in membrane permeabilisation and apoptosis. Apoptosis was a result of OMM permeabilisation and the contents of the intermembrane space (cytochrome C, endonuclease G and apoptosis inducing factor) travelling freely to the cytosol which induced unregulated damage of membranes and apoptosis (de Arriba *et al*. 2013).

Experiments performed in cultured endothelial cells revealed that CNIs are cytotoxic or cytoprotective at high or low concentrations, respectively (Caramelo *et al*. 2004). The biphasic response to CNIs in endothelial cells depends on the interaction of CNI with cyclophiln D (CyD) rather than with calcineurin. This was contradictory to previous studies that reported CNIs interaction with calcineurin being the most significant through systemic interactions (Naesens *et al*. 2009). Proximal tubules and endothelial cells are thought to adapt to the presence of CNI's, to limit cell damage. This is thought to be due to CsA-mediated increases in the mitochondrial concentration of CyD as well as the synthesis of chaperon molecules involved in CyD exportation to mitochondria, heat shock protein 70 (HSP70) (Ortiz *et al*. 2008). Studies performed in bacteria show that inhibition of HSP70 with geldanamycin increases endothelial toxicity of CsA *via* calcineurin inhibition (Cardenas *et al*. 1999).

Vascular endothelial growth factor (VEGF) is also thought to be a substantial factor in the cytoprotective effect of CsA (Alvarez-Arroyo *et al*. 2002). Studies performed in renal proximal tubule cells and animal models have shown endogenous VEGF protects against CsA toxicity both *in vitro* and *in vivo* (Slattery *et al*. 2005). Furthermore, proximal cells preconditioned with CsA have been shown to be resistant to FK506 toxicity, and vice versa (Ortiz *et al*. 2008).

The main effect CsA has on proximal tubule mitochondria specifically is thought to be inhibition of Ca^{2+} activation of CyD by the formation of a CsA–CyD complex, rather than CsA-calcineurin complex (Naesens *et al*. 2009; Ortiz *et al*. 2008; de Arriba *et al*. 2013). CyD, along with other proteins, form the mitochondrial permeability transition pore (MPTP), resulting in loss of ΔΨm (Schubert & Grimm 2004). Loss of ΔΨm is associated with cell apoptosis and ROS generation (Kroemer *et al*. 2007). Studies performed in animal models have demonstrated CsA binding to CyD prevents its binding to the adenine nucleotide translocator (ANT) and hence prevents MPTP activation due to the resulting increase in mitochondrial calcium concentrations (Nakagawa *et al*. 2005), this can be seen in figure 6.20. Acutely, this can protect against nephrotoxic compounds where toxicity is mediated by direct opening of the MPTP, CsA and Sanglifehrin for example (Halestrap *et al*. 2004) and highlights the unexpected clinical findings in patients treated with CsA to prevent graft rejection (Hortelano *et al*. 2000; Alvarez-Arroyo *et al*. 2002). However in a chronic setting, the lack of MPTP actively accelerates mitochondrial calcium uptake while maintaining oxidative phosphorylation (Ortiz *et al*. 2008). The progressive increase of intracellular calcium subsequently overcomes CsA binding to CyD, and the resulting MPTP opening becomes irreversible (Hortelano *et al*. 2000) with loss of mitochondrial potential and release of cytochrome c and other proapoptotic factors into the cytosol. The initial inhibition of MPTP by CsA is also observed with analogs able to bind cyclophiln but lack anti-calcineurinic activity (Readnower *et al*. 2011).

Taken together, it is becoming clear that mitochondrial dysfunction *via* direct or indirect insult from CNIs is a characteristic pathway for progression of CNI-mediated nephrotoxicity. Prevention of mitochondrial dysfunction could therefore be a novel mechanism for the delay of cell and organelle apoptosis, which would ultimately lead to graft and patient survival.

6.2 ROS generation

ROS are chemically reactive molecules derived from oxygen. They are generated as part of normal cell metabolism and have been well documented to have important roles in renal cell signalling and homeostasis (Wilcox 2002). ROS include the super oxide anion ($O_2^- \cdot$), hydrogen peroxide (H_2O_2), hydroxyl radical ($OH \cdot$) and singlet oxygen ($^1O_2$) (Kaelin 2005).

Unfortunately, ROS overproduction during cell stress can have a detrimental effect on cells and tissue and can result in oxidative damage of cellular structures including mitochondria, endoplasmic reticulum, plasma membranes and DNA (Cooke *et al*. 2003; Baud & Ardaillou 1986). ROS research is increasing with an exponential rate due to their common role in many pathological diseases. The kidney in particular, is a major source of ROS-generating oxidases (Bryan *et al*. 2009), therefore it is reasonable to suggest that ROS could be involved in a number of renal diseases.

6.2.1 Renal ROS

Production of ROS in the kidney, and its relation to disease, was first highlighted in the 1990's (Chakraborti *et al*. 1998; Brezis *et al*. 1991) specifically not long after NO's discovery as a signalling molecule (Arnold *et al*. 1977; Katsuki *et al*. 1977). It is thought that the enzyme NADPH oxidase (NOX) produces the majority of renal ROS, however 6 isoforms have been discovered in the last 20 years with NOX2 being the most comprehensively studied and NOX4 being the foremost isoform found in the kidney (Wilcox 2002). The specific roles of each NOX isoform are still poorly understood. Despite this, studies using wild type and salt sensitive rats have demonstrated that NADPH oxidase accounts for over half of all ROS production within the kidney (Taylor *et al*. 2006; Zou *et al*. 2001). Mitochondrial ROS production accounts for the remainder and will be discussed below (Wilcox 2002; Cowley *et al* 2015a). Production of ROS *via* NADPH and other sources can been seen in figure 6.1. Interestingly, the outer medulla has been shown to generate the greatest amount of ROS in the kidney (Cowley *et al* 2015a). Coincidently, this is also the area of the kidney with the greatest abundance of pericytes (Crawford *et al*. 2012; Pallone & Silldorff 2001; Pallone, Z. Z. Zhang, *et al*. 2003) and therefore ROS generation could play a major role in the vasoconstriction of vasa recta *via* pericytes, which have been

shown to constrict upon exposure to ROS (Z. Zhang & Pallone 2004; Z. Zhang *et al*. 2004).

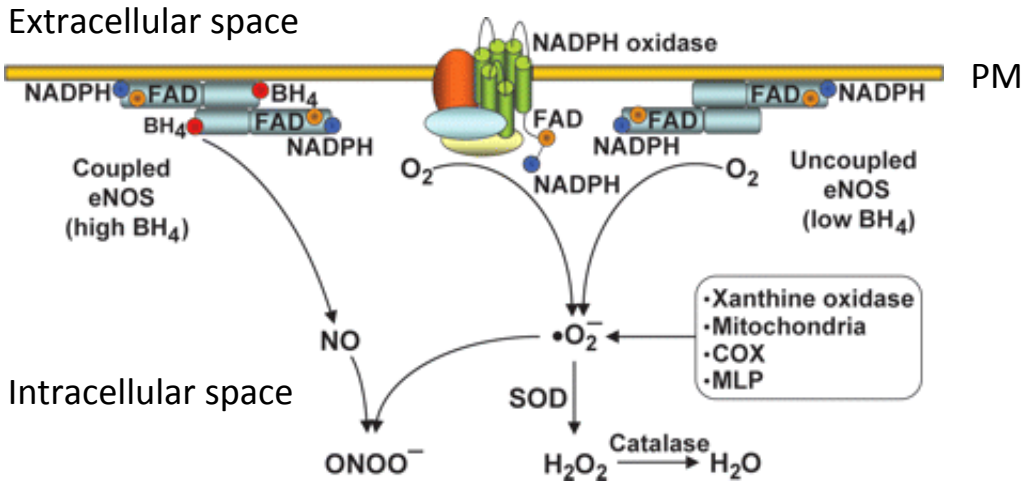

Figure 6.1 NADPH production of reactive oxygen species (ROS) in VSMC's

ROS production is increased, tetrahydrobiopterin (BH4) generation is reduced, and endothelial NO synthase (eNOS) produces superoxide ($\cdot O_2^-$). Excess generation of $\cdot O_2^-$ by different sources (NADPH oxidase, uncoupled eNOS, xanthine oxidase, myeloperoxidase, cyclooxygenase, mitochondria) will reduce NO bioavailability and convert NO into peroxynitrite ($ONOO^-$), which has detrimental effects. Reduced activity of superoxide dismutase (SOD) will also result in enhanced ROS accumulation in the vascular wall. COX, cyclooxygenase; FAD, flavin adenine dinucleotide; MLP, myeloperoxidase; NADPH, reduced nicotinamide adenine dinucleotide; XO, xanthine oxidase, PM; plasma membrane. Figure adapted from (Schiffrin 2008).

ROS induced renal damage is undoubtedly complex with various mechanisms and enzymes involved. A major pathway of ROS-induced renal decline relating to this study, is its ability to cause vascular smooth muscle cell (VSMC) vasoconstriction (Schnackenberg *et al*. 2000; Z. Zhang *et al*. 2004). A study by Schnackenbrg *et al* demonstrated the role for superoxide in mediating contractile responses of afferent arterioles *via* thromboxane A1 receptor activation (Schnackenberg *et al*. 2000). The results highlighted a role for ROS in vasoconstriction, as it inhibition augmented the agonist-induced contractile responses. Equally, a decrease in superoxide

bioavailability, *via* degradation, resulted in attenuated contraction. This suggests ROS may act directly through VSMCs to cause vasoconstriction. In addition, ROS has been shown to induce vasoconstriction through the juxtaglomerular apparatus (Wilcox & Welch 2000). Reabsorption of NaCl triggers tubuloglomerular feedback which simultaneously induces adenosine-induced vasoconstriction (D. Sun *et al*. 2001). Reduction of tubuloglomerular feedback through ROS degradation reduces the adenosine-mediated vasoconstrictive response in spontaneously hypertensive (SHR) rats (Wilcox & Welch 1998). SHR are well known to have increased production of superoxide in the kidney while also having reduced bioavailability of NO in the kidney (Paravicini & Touyz 2008). Collectively, evidence suggests that the production of ROS by juxtaglomerular apparatus leads to ROS-mediated vasoconstriction of afferent arterioles and thus NO can inhibit tubuloglomerular feedback.

6.2.2 CNI-induced ROS

CNIs are well documented to reduce the production of NO and PGE_2 through endothelial cell dysfunction (Morris *et al*. 2000; Perico *et al*. 1990; Diederich *et al*. 1994) however, their role in ROS production is less well characterised.

Both CsA and FK506 have been shown to up-regulate the expression of endothelial NOS (eNOS) in tumour cells lines (Navarro-Antolin *et al*. 1998) and vascular endothelial cells (LopezOngil *et al*. 1996). This would initially suggest a protective mechanism due to increased production of NO. However, the increased eNOS expression is mediated through the direct production of ROS *via* a negative feedback mechanism trying to overcome the excess production of ROS (LopezOngil *et al*. 1996; Navarro-Antolin *et al*. 1998). Given the fact that ROS and NO combine to form peroxynitrite, one of the most potent oxidants within the body (Wilcox & Welch 2000; Navarro-Antolin *et al*. 2001), increased expression of eNOS *via* CNIs can have detrimental effects on cell function.

As has been previously highlighted, treatment with CNIs induces the increased production of ANG II (Naesens *et al*. 2009). Interestingly, increased production of ANG II has also been linked with increased ROS production (Nishiyama *et al.* 2003). Nishiyama *et al* demonstrated the simultaneous increase of both ANG II and ROS with CsA treatment in animal models (Nishiyama *et al.* 2003). In this study, AT1 receptor inhibition resulted in a significant decrease in ROS production and savaging of ROS with tempol, a super oxide dismutase (SOD) mimetic, also produced a significant decrease in ROS (Nishiyama *et al.* 2003). This data highlights the role for AT1

receptor activation in CsA-induced ROS production but also the potential beneficial effect of including antioxidant therapy in patients treated with CNIs. Interestingly, their results not only highlighted a reduced ROS production, but also a reduced hypertensive and nephrotoxic effect, mediated through a reduced production of ANG II (Nishiyama *et al.* 2003).

Many antioxidants have however featured in clinical trials in the aim being to minimise the ROS damage induced by CNI therapy (Galletti *et al*. 2005; Nishiyama *et al* 2003; Jenkins *et al*. 2001). Vitamin E has been the most extensively studied, with results proving to be inconsistent. Wang *et al* were able to demonstrate the lipid peroxidation effects of CsA nephrotoxicity in animal studies. Peroxidation was initiated through ROS generation, however, supplementation of vitamin E attenuated both lipid peroxidation and ROS generation (Wang & Salahudeen 1995). In addition, Jenkins *et al* were able to demonstrate the protective effects of vitamin E against CsA nephrotoxicity *via* a variety of pathways (Jenkins *et al*. 2001). Their results indicated that vitamin E attenuates up regulation of COX I and II and TGF-β after CNI treatment. Both COX and TGF-β have been shown to be involved in CNI nephrotoxicity (de Vries *et al*. 2006). With vitamin E supplementation, Jenkins *et al* demonstrated the significant reduction of nephrotoxicity, hypertension and inflammatory mediators.

Conversely, it has recently been suggested that vitamin E's protective mechanism is not entirely through an antioxidant pathway. De Vries *et al* have shown that supplementation of vitamin E and C have the ability to reduce blood concentrations of CNIs (de Vries *et al*. 2006). The exact mechanism by which this occurs is still unclear however a suggestion of increased CYP metabolism has been put forward (Jenkins *et al*. 2001; de Vries *et al*. 2006).

Therefore, although initial antioxidant studies have shown promising results, the exact pathways involved in the antioxidant amelioration of some CNI side effects still remain elusive and may not be solely due to antioxidation reactions.

6.2.3 CNI-induced mitochondrial ROS

As mentioned previously, just under half of all remaining renal ROS is thought to derive from mitochondrial ROS. Mitochondrial ROS is generated *via* the electron transport chain in the IMM (Murphy 2009). Oxidative phosphorylation involves the passing of electrons from the generation of ATP. The process involves 5 main complexes and results in various sources of ROS. Figure 6.2 highlights the process of mitochondrial ROS production.

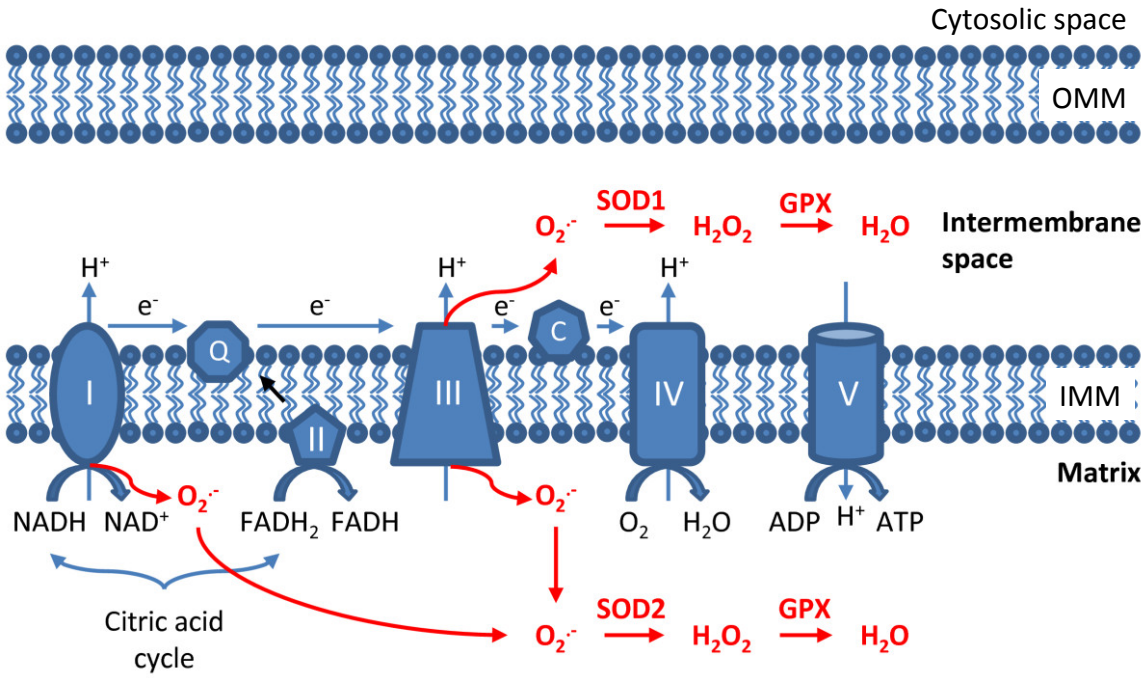

Figure 6.2 Production of mitochondrial ROS. Electrons (e^-) donated from NADH (complex 1) and $FADH_2$ (complex 2) pass through the electron transport chain and ultimately reduce O_2 to form H_2O at complex IV (cytochrome c oxidase). ROS are produced from the leakage of e^- to form superoxide ($O_2^{\cdot -}$) at complex I and complex III. $O_2^{\cdot -}$ is produced within the matrix at complex I, whereas at complex III, $O_2^{\cdot -}$ is released towards both the matrix and the intermembrane space. Once generated, $O_2^{\cdot -}$ is dismutated to H_2O_2 by superoxide dismutase 1 (SOD1) in the intermembrane space and by SOD2 in the matrix. Afterwards, H_2O_2 is fully reduced to water by glutathione peroxidase (GPX). Both $O_2^{\cdot -}$ and H_2O_2 produced in this process are considered as mitochondrial ROS. OMM, outer mitochondrial membrane; IMM, inner mitochondrial membrane. Adapted from (X. Li *et al*. 2013).

CNI-induced mitochondrial ROS is becoming increasingly documented, with the concern that this may be an important source of cellular damage induced by CNIs. Recently, Zhou *et al* demonstrated mitochondrial ROS production with CsA in an animal model (A. Y. Zhou & Ryeom 2014). The increased production of ROS was associated with tumor angiogenesis and endothelial cell proliferation and migration. Interestingly, increased mitochondrial ROS was also observed when mice were given a CsA analog that does not have calcineurin affinity, supporting the hypothesis of a

calcineurin-independent mechanism for detrimental ROS production (A. Y. Zhou & Ryeom 2014).

Additionally, de Arriba *et al*, using a renal tubule cell line, were able to highlight a specific mechanism for CNI-induced ROS production (de Arriba *et al*. 2013). CsA was shown to inhibit the activity of glutathione (endogenous antioxidant) while simultaneously increasing ROS. In addition, CsA was able to induce ΔΨm depolarisation through IMM and OMM modifications while allowing IMM contents (cytochrome C) to reach the cytosol (de Arriba *et al*. 2013). Intriguingly, the authors were able to illustrate MPTP formation with the treatment of CsA. Previously it has been thought CsA inhibits MPTP construction and can protect from cell apoptosis (Kroemer *et al*. 2007; Perez de Hornedo *et al*. 2007). Upon cell treatment with vitamin E, the authors concluded all detrimental effects were inhibited and suggests that mitochondrial ROS was responsible for renal tubule cell apoptosis (de Arriba *et al*. 2013).

Taken together, these two recent studies have shown the potential role of mitochondrial ROS for mediating toxicity further of other surrounding cells upstream.

The aim of this study was to investigate the role of mitochondrial dysfunction and ROS production in CNI-mediated vasoconstriction previously presented *via* the live slice model to possibly elucidate the mechanisms involved in pericyte mediated vasoconstriction and CNI nephrotoxicity.

6.3 Methods

Live kidney slices were prepared as previously described in chapter 2: General Methods.

To investigate possible mitochondrial membrane potential alterations, the cationic red fluorescent dye tetramethylrhodamine methyl ester (TMRM) was used. TMRM is readily sequestered in the negative charged interior of active mitochondria. The fluorescence signal is directly co-related to the ΔΨm of the IMM, therefore, a loss in membrane potential results in loss of fluorescence (Kroemer *et al*. 2007). TMRM was applied *via* superfusion, similar to DIC experiments, although the imaging bath was situated on a 2-photon microscope setup (see general methodology). Tissue slices were continually superfused with TMRM (1 μM) followed by a 10-minute wash with PSS to exclude unloaded TMRM from the bath prior to experimentation.

To determine the role of ROS in CNI-induced vasoconstriction, the superoxide fluorescent probe, dihydroethidum (DHE) was used. DHE is naturally blue in fluorescence, excited wavelength 518 nm, until it is oxidised to form ethidum, red in fluorescence, emission wavelength 605 nm. Once oxidised, DHE intercalates with cell DNA and stains the nucleus bright red. A 10-minute wash was also performed after dye loading to remove unloaded dye before experimentation.

To label other live structures including microvessels and tubules, tissue was simultaneously loaded with calcein (1 μg/ml). Calcein is a cell permanent dye used to determine cell viability by converting non-fluorescent calcein to green fluorescent calcein after acetoxymethyl ester hydrolysis by intracellular esterase's (Tenopoulou *et al*. 2007). Therefore, live viable cells omit green fluorescence at 488 nm. Slices were simultaneously loaded with calcein and either TMRM or DHE after which slices were washed with PSS prior to experimentation to remove any unloaded dye.

Live slices loaded with fluorophores were excited with a MiaTai laser set at 800nM and enabled light collection *via* PMTs attached to a 2-photon microscope fitted with a 665 nm long-pass dichroic mirror, to collect red signal, and 680 nm short-pass dichroic laser blocking filter to collect green signal.

For investigations of ΔΨm, kidney slices were superfused with oxygenated PSS for 30 minutes while 2-photon images where captured every 10 minutes to establish a baseline fluorescence signal. Slices were then exposed to CsA, FK506 or rapamycin for approximately 25 minutes and then subjected to a PSS wash to assess reversibility of any affect on fluorescent signal. Analysis of changes in fluorescence was similar to

that of changes in vessel diameter (General methodology). In short, each experiment was analysed using the free public domain software IMAGE J (NIH; http://rsb.info.nih.gov). For each experiment, several regions of interest (ROI) were chosen using the bright field microscope setting. Once chosen, tissue loading of dyes was assessed by measuring fluorescence intensity per ROI. This was essential prior to analysis as not all tissue loads fluorescent dyes equally. In addition, although the live slice preparation produces relatively parallel-sectioned tissues, images acquired are at a specific optical plane in the z plane and vessels do not always remain in focus, therefore fluorescence intensity may vary between subsurface.

After ROIs were chosen, the intensity signal at ROI locations was captured every five minutes for the duration of the experiment. An average of the first 3 measurements (30 minutes PSS wash after loading) was taken to represent the baseline fluorescent signal (*i.e.* 100%). All subsequent fluorescent measurements at ROIs were calculated as a percentage change of the corresponding baseline fluorescent signal.

6.3.1 Statistics

All data are presented as mean values ± SEM; *n* numbers are displayed as number of kidney slices, and were appropriate, (number of animals). All experiments were performed in at least six different animals. Statistical assessment was performed with GraphPad Prisim (v5.0f; GraphPad software, San Diego, CA, USA). When two groups were compared, a Student's t-test (two-tailed, paired or unpaired where appropriate) was used. A value of $P < 0.05$ was considered significant.

6.4 Results

6.4 Measuring mitochondrial membrane potential in the live kidney slices

Prior to initiating experiments to determine effects of CNIs on mitochondrial membrane potential, several control experiments were performed to determine whether if it was possible to monitor changes in TMRM signal in live kidney tissue. Carbonyl cyanide-*p*-trifluoromethoxyphenylhydrazone (FCCP) is a protonophore (H^+ ionophore) and uncoupler of oxidative phosphorylation in mitochondria (Gautier *et al*. 2012). It is capable of depolarizing plasma and mitochondrial membranes, therefore would be able to act as a positive control for membrane depolarization.

Superfusion (~1000 s) of FCCP (10 μM) resulted in a significant loss of TMRM signal (Figure 6.2). TMRM signal reduced over time after exposure to FCCP and failed to recover to baseline intensity after washout (Figure 6.3). 60 minutes after exposure to FCCP, TMRM signal fell to 14.5 ± 1.7% and was significantly lower in comparison to time matched PSS control (89.9 ± 4.3%, n=7 (8), P<0.001) (Figure 6.3). Calcein signal was unaffected with application of FCCP and remained constant during experimentation (Figure 6.3).

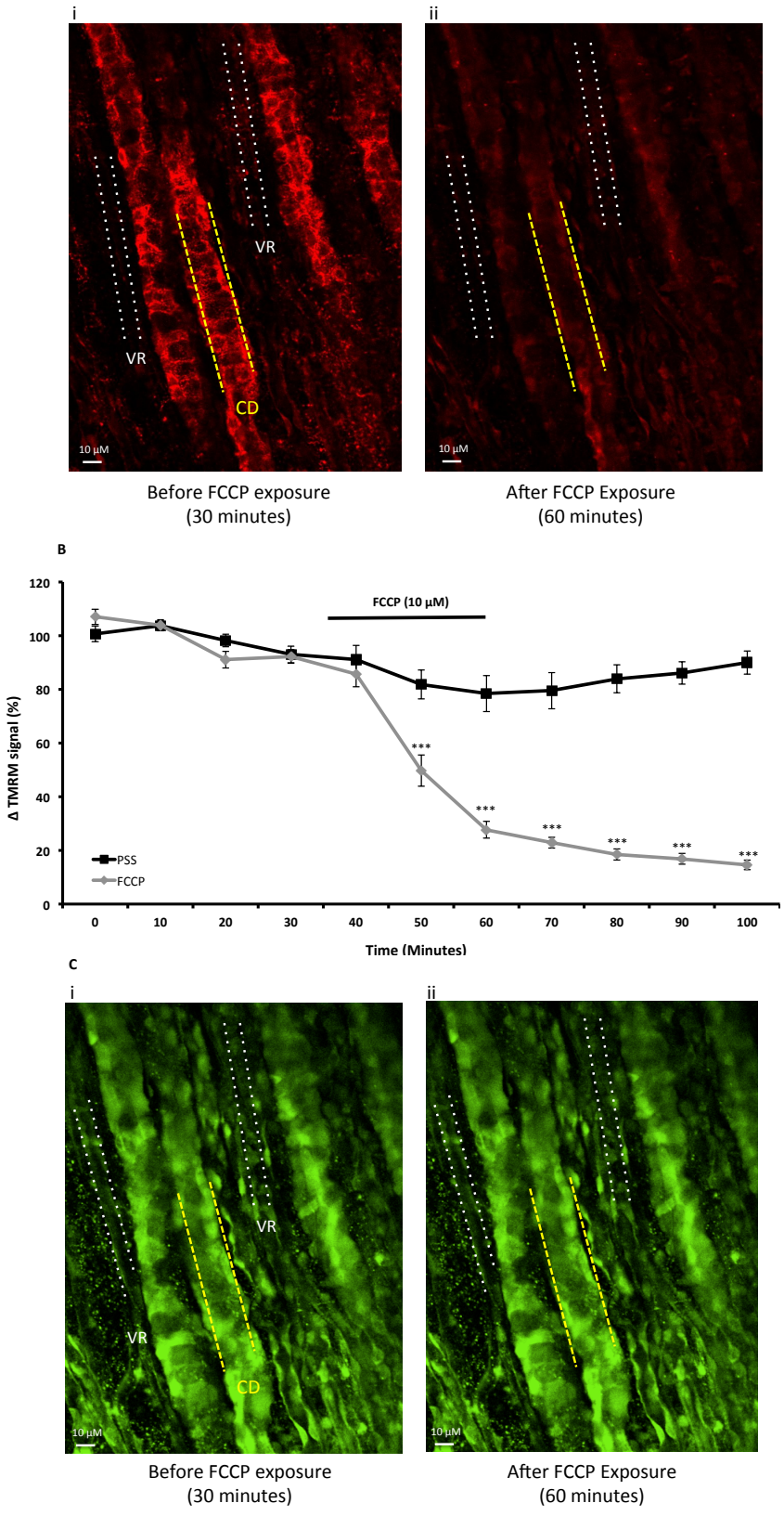

Figure 6.3 FCCP evokes a decrease in TMRM signal in medullary vasa recta and tubules. A: Representative images of TMRM fluorescence in the medulla before (i) and after (ii) exposure to FCCP. B: Representative graph shows the mean data for FCCP-mediated change in TMRM fluorescence over time compared to time matched PSS control. Mean fluorescence signal percentage measured in 10 tubule and 6 vessel ROIs in for trace over time in 8 slices from 8 animals. C: Representative images of calcein fluorescence in the medulla before (i) and after (ii) exposure to FCCP. VR, vasa recta; CD, collecting duct. Data are mean ± SEM, P<0.001, n=8 (8).

6.4.1 Effect of CNIs on mitochondrial membrane potential

After a positive control was established (FCCP depolarisation and oligomycin hyperpolarisation (data not shown), the effect of CNIs on TMRM signal was investigated to determine whether they induced a change in ΔΨm.

Superfusion (~1000 s) of CsA (10 μM) resulted in no significant loss of TMRM fluorescence (Figure 6.4). TMRM signal decreased over time after exposure to CsA however was not significantly different compared to time matched PSS controls (Figure 6.4). 60 minutes after exposure to CsA, TMRM fluorescence fell to 85.94 ± 4.3% and was not significantly lower in comparison to timed matched PSS controls (89.9 ± 4.3%, n=8 (7), (Figure 6.4). Calcein fluorescence was significantly greater after application of CsA compared to PSS control (Figure 6.4).

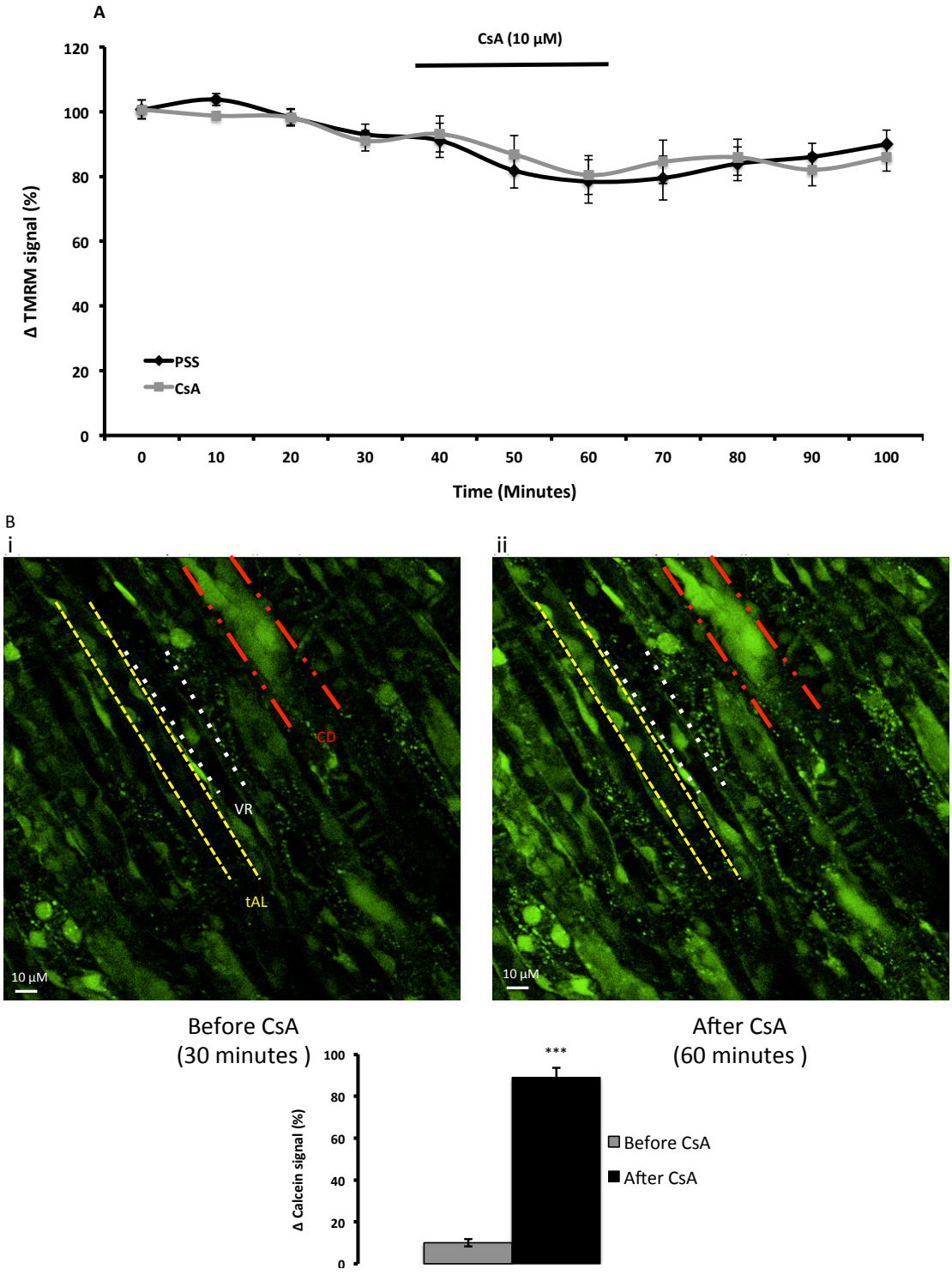

Figure 6.4 CsA does not evoke a change in TMRM fluorescence in medullary vasa recta and tubules. A: Representative trace shows mean data for CsA mediated change in TMRM fluorescence over time. Mean fluorescence signal percentage measured in 9 tubule and 6 vessel ROIs for trace over time in 8 slices from 7 animals. B: Representative images and mean data of calcein fluorescence in the medulla before (i) and after (ii) exposure to CsA. Inset; mean data for CsA induced increase of calcein fluorescence measured in in 9 tubule and 6 vessel ROIs. VR, vasa recta; CD, collecting duct; tAL, thin ascending limb. Data are mean ± SEM, P<0.001, n=8 (7).

Superfusion (~1000 s) of FK506 and rapamycin (3 and 1 μM, respectively) resulted in no significant loss of TMRM fluorescence (Figure 6.5). TMRM fluorescence reduced over time after exposure to FK506 and rapamycin, however both were not significantly different compared to time matched PSS controls (Figure 6.5). 60 minutes after exposure to FK506 and rapamycin, TMRM fluorescence fell to 90.94 ± 5.8% and 99.9 ± 3.3%, respectively, and was not significantly lower in comparison to time matched PSS control (91.9 ± 6.3%, n=8 (7), (Figure 6.5). Calcein fluorescence signal was significantly greater after application of FK506 and rapamycin compared to PSS control (Figure 6.5).

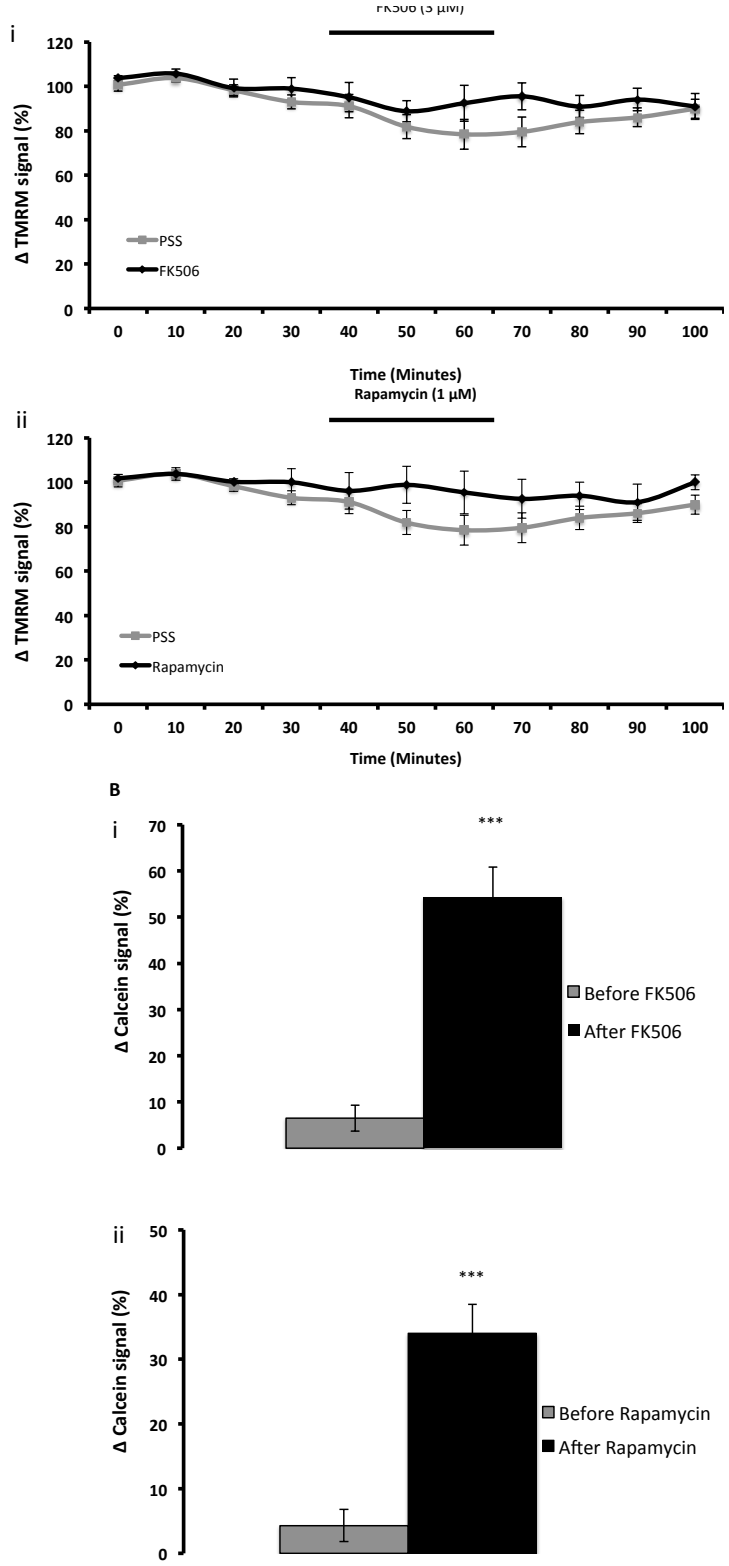

Figure 6.5 FK506 and rapamycin do not evoke a change in TMRM fluorescence in medullary vasa recta and tubules. A: Representative traces show the mean data for FK506 (i) and rapamycin (ii) mediated change in TMRM fluorescence over time fluorescence signal compared to time matched controls. B: Mean data of calcein fluorescence in the medulla before and after exposure to FK506 (i) and rapamycin (ii). Mean fluorescence signal percentage measured in 10 tubule and 8 vessel ROIs for trace over time in 8 slices from 7 animals. Data are mean ± SEM, $P<0.001$, n=8 (7).

6.4.2 Effect of CNIs on mitochondrial membrane permeability transition

Mitochondrial membrane transition (MMT), through the orientation of mitochondrial permeability transition pores (MPTP), is thought to be a key step in cell stress leading to apoptosis and necrosis (He & Lemasters 2002).

Given the fact CNIs failed to evoke depolarisation of mitochondria within the live slice model, combined with what is known about CNI prevention of MMT (Halestrap, Connern & Griffiths 1997; AL *et al*. 1996; Petronilli *et al*. 1994), MPTP formation was investigated.

Chenodeoxycholate (CDCA), an endogenous bile salt, has been proven to be a potent inducer of MPTP formation (Rolo *et al*. 2003) and would therefore act as a positive control to investigate the effect of whether CNIs block MPTP formation in the live slice model. TMRM fluorescence would represent the formation of MPTP with a reduction of TMRM signal suggesting MPTP formation and opening (Cho *et al*. 2014).

Superfusion (~1000 s) of CDCA (100 μM) resulted in a significant loss of TMRM fluorescence (Figure 6.6). TMRM fluorescence rapidly reduced over time after exposure to CDCA and failed to recover to baseline intensity after washout (Figure 6.6). 60 minutes after exposure to CDCA, TMRM fluorescence fell to 20.6 ± 2.02% and was significantly lower in comparison to time matched PSS controls (79.3 ± 5.92%, n=7 (8), $P<0.001$) (Figure 6.6) indicating CDCA-induced formation of MPTP which resulted in decrease of TMRM signal as expected. Calcein fluorescence was unaffected with application of CDCA and remained constant during superfusion.

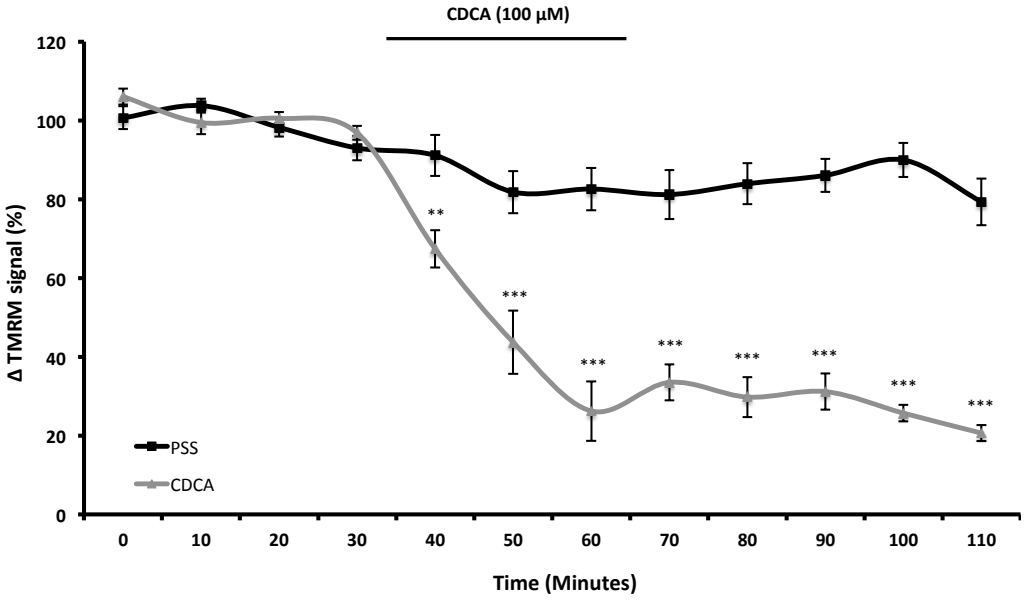

Figure 6.6 Chenodeoxycholate induces a decrease in TMRM fluorescence within the renal medulla. Representative trace shows the mean data for CDCA mediated change in TMRM fluorescence over time compared to time matched PSS control. Mean fluorescence signal percentage measured in 12 tubule and 10 vessel ROIs for trace over time in 8 slices from 8 animals. Data are mean ± SEM, ** P<0.01, n=8 (8).

In order to investigate the ability of CNIs to inhibit MPTP formation, CDCA superfusion in the presence of CNIs was performed and compared against CDCA superfusion alone.

Superfusion (~1000 s) of live tissue with both CDCA and CsA (100 & 10 μM, respectively) resulted in a significant retention of TMRM fluorescence (Figure 6.7). TMRM fluorescence was maintained throughout exposure to CDCA and CsA (Figure 6.7). 60 minutes after exposure to CDCA and CsA, TMRM fluorescence was preserved at 96.9 ± 4.7% and was significantly greater in comparison to time matched CDCA control (20.6 ± 2.02%, n=8 (7), P<0.001) (Figure 6.7). Calcein fluorescence signal was significantly greater after application of CsA and CDCA compared to CDCA control, P<0.01.

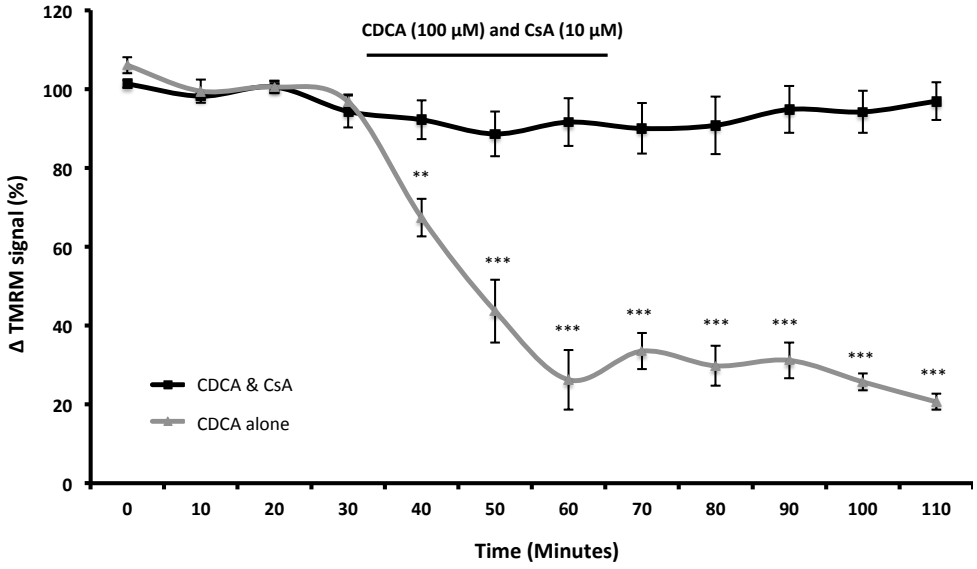

Figure 6.7 Cyclosporine prevents the chendeoxycholate-induced decrease in TMRM fluorescence. Representative trace shows the mean data for CsA inhibition of CDCA-induced loss of TMRM fluorescence compared to CDCA alone. Mean fluorescence signal percentage measured in 11 tubule and 19 vessel ROIs for trace over time in 8 slices from 7 animals Data are mean ± SEM, ** P<0.01, n=8 (7).

Superfusion (~1000 s) of CDCA (100 µM) in combination with either FK506 or rapamycin (3 and 1 µM, respectively) resulted in a loss of TMRM fluorescence (Figure 6.8). TMRM fluorescence reduced over time after exposure to CDCA and FK506 or rapamycin, however both were not significantly different compared to time matched CDCA controls. TMRM fluorescence did not recover after washout. 60 minutes after exposure to CDCA and FK506 or rapamycin, TMRM fluorescence fell 79.37 ± 4.2% and 75.93 ± 5.16%, respectively, and was not significantly lower in comparison to time matched CDCA control (79.37 ± 2.02%, n=8 (7), (Figure 6.8). Calcein fluorescence signal was significantly greater after application of CDCA and FK506 or rapamycin compared to CDCA control, P<0.01.

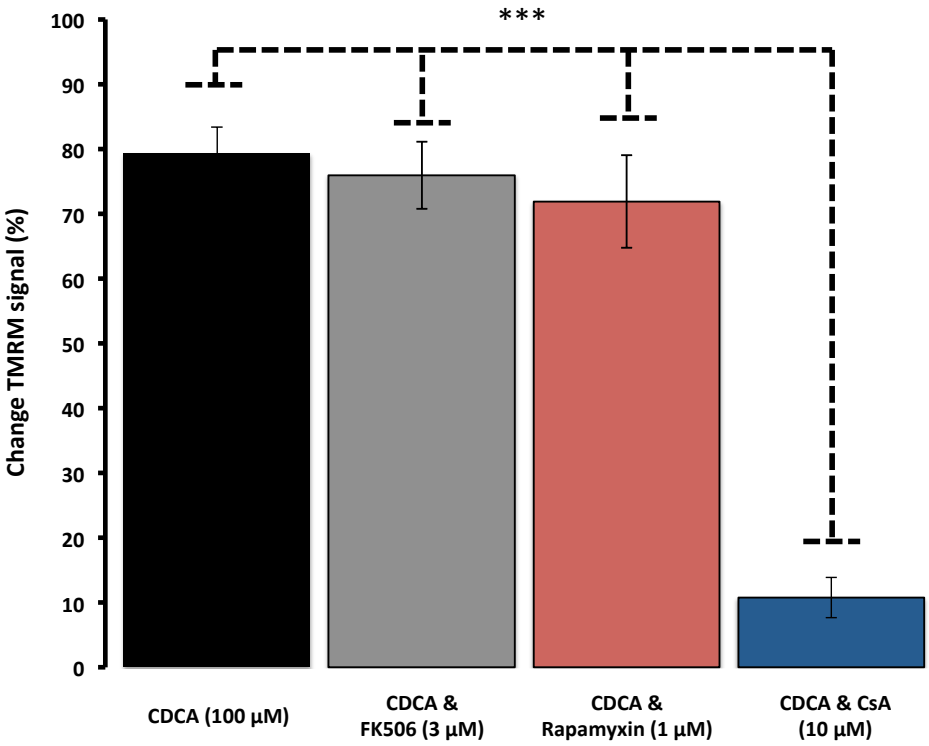

Figure 6.8 Tacrolimus and rapamycin do not prevent the chendeoxycholate-induced decrease in TMRM fluorescence in live kidney tissue. Bar graph shows the mean data for CDCA-induced loss of TMRM fluorescence alone and in combination with tacrolimus or rapamycin. Mean fluorescence signal percentage measured in 11 tubule and 11 vessel ROIs for trace over time in 8 slices from 7 animals. Data are mean ± SEM, $P<0.001$, n=8 (7).

6.5 Measuring production of ROS in live kidney slices

Given the fact CNIs failed to induce depolarisation of mitochondria and CsA inhibited the CDCA-mediated formation of MPTP suggesting the mechanism was due to CsA inhibition of MPTP formation that resulted in changes of ΔΨm, further investigation was necessary to elucidate possible mechanisms of CNI-induced pericyte vasoconstriction.

CNI-induced production of reactive oxygen species (ROS) is now becoming a more accepted aspect of CNI nephrotoxicity. It is well known that CNIs reduce the production and bioavailability of nitric oxide (NO) (Naesens *et al*. 2009; Oriji & Keiser 1999; Amore *et al*. 1995; Dusting *et al*. 1999), however the mechanisms involved in their production of ROS is still unclear. Mitochondrial ROS has been suggested with several groups confirming its production in cell lines (de Arriba *et al*. 2013; Perez de Hornedo *et al*. 2007; A. Y. Zhou & Ryeom 2014; Nishiyama *et al* 2003), while other groups have investigated its production *via* alternative cellular pathways including NADPH derived ROS production (Lopez-Ongil *et al*. 1998; Navarro-Antolin *et al*. n.d.; van der Toorn *et al*. 2007; H.W. Chen *et al*. 2002).
With this in mind, CNI-induced ROS production was investigated in the live kidney slice model.

MitoSOX red is a fluorescent dye specifically targeted to mitochondria in live cells. Once oxidised by superoxide, MitoSOX red produces red fluorescence, emits light at 605 nm, with excellent retention properties within the cell and minimal dye leakage (Carvalho da Costa *et al*. 2003; Perez de Hornedo *et al*. 2007).
Efforts to label live kidney tissue with MitoSOX failed and no fluorescence was detected in either control or H_2O_2 treated tissue. However, given that CNIs failed to depolarise mitochondria in the live slice model, which is thought to be a key step in mitochondrial ROS production (Murphy 2009) it was not surprising that CNIs failed to increases the level of MitoSOX fluorescence, although this has been previously observed in isolated cells (Perez de Hornedo *et al*. 2007; Carvalho da Costa *et al*. 2003).
Dihydroethidium (DHE) is an alternative probe for superoxide production (Zielonka *et al*. 2008). DHE is naturally blue in fluorescence, emits light at 518 nm, until it is oxidised after which it forms ethidum, red in fluorescence, emits light at 605 nm.

Once oxidised, DHE intercalates with cell DNA and stains the nucleus brilliant red (Zielonka *et al*. 2008).

To establish a protocol for detecting the CNI-mediated production of ROS in live tissue, slices were exposed to hydrogen peroxide (H_20_2) as a positive control and changes in fluorescence monitored.

Superfusion (~500 s) of H_20_2 (1 mM) resulted in a significant increase of DHE fluorescence (Figure 6.9). DHE fluorescence plateaued after exposure to H_20_2 and failed to return to baseline intensity after 30 minutes of washout (Figure 6.9). 60 minutes after exposure to H_20_2, DHE fluorescence increased to 190 ± 14.7% and was significantly greater in comparison to time matched PSS control (19.7 ± 5.6%, n=6 (7), P<0.001) (Figure 6.9). DHE fluorescence with PSS control was photobleached throughout experimentation and will be discussed further below in its own section. Calcein signal was unaffected with application of H_20_2 and remained constant during experimentation.

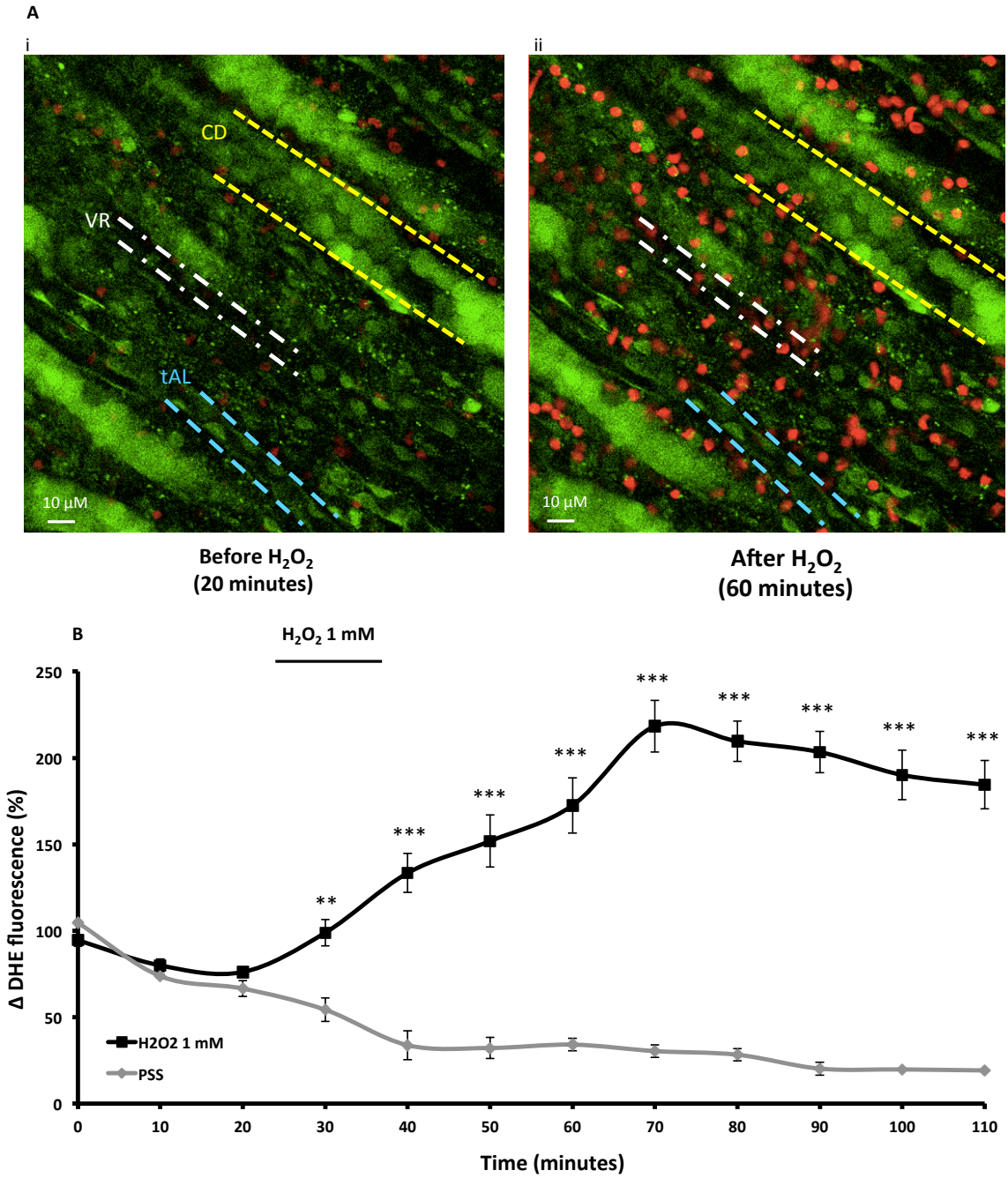

Figure 6.9 H_2O_2 evokes an increase in DHE fluorescence in medullary vasa recta and tubules. A: Representative images of DHE and calcein fluorescence in the medulla before (i) and after (ii) exposure to H_20_2. B: Representative trace show the mean data for H_20_2 mediated change in DHE fluorescence over time compared to time matched PSS controls. Mean fluorescence signal percentage measured in 9 tubule and 9 vessel ROIs for trace over time in 7 slices from 6 animals. VR, vasa recta; CD, collecting duct; tAL, thin ascending limb. Data are mean ± SEM, **P<0.01, n=7 (6).

Once oxidized, DHE forms oxyethidium and intercalates with DNA and is unable to exit the cell or return to its unoxidized form. Therefore, after excitation at preferentially 500 nM, emission fluorescence will be constant at an optimal wavelength of 580 nM.

During PSS timed controlled experiments of DHE fluorescence, it was noted that fluorescence signal dropped over time. Photobleaching is the term used for this loss in fluorescence and is from the irreversible decomposition of fluorescent molecules in the excited state because of the interaction they have with oxygen before emission (Patterson & Piston 2000). Photobleaching is irreversible and time dependent, therefore interpretation of fluorescence intensities, which decrease over time, can be problematic and lead to misinterpretation. In addition, DHE has been previously shown to undergo rapid photobleaching in a variety of cell types (Krishnamurthy *et al*. 1990; Zielonka *et al*. 2008; Kundu *et al*. 2009). To combat this, bleach correction can be applied to standardize fluorescence intensity over time (Patterson & Piston 2000).

Bleach correction involves the manipulation of the exponential decay of the fluorophore and its representative value at any given time (B. A. Smith & McConnell 1978).

Bleach corrector is a free plugin (FIJI: http://fiji.sc/Bleach_Correction) that utilizes the free public domain software IMAGE J. The plugin uses an exponential fitting method to determine the rate of decay of a series of images and reanalyze the image stack to take bleaching into consideration.

A time series control experiment was performed to carry out the degree of photobleaching and feasibility of bleach correction. A live kidney slice was loaded with DHE and after a 30 minute unloaded dye wash; DHE fluorescence was measured every ten minutes for up to two hours. Uncorrected DHE fluorescence was plotted against time (Figure 6.10). The series of images were then reanalyzed using the bleach corrector plugin and plotted against their respective time point (Figure 6.10).

Bleach correction resulted in a significant increase of DHE fluorescence intensity at all time intervals, n=6 (6), $P<0.001$.

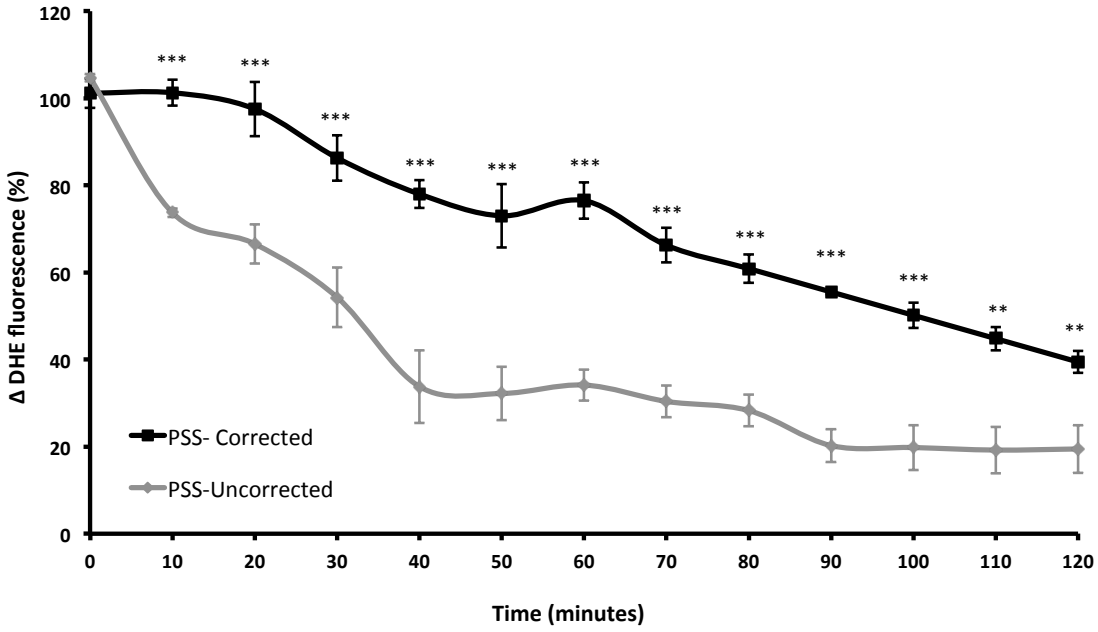

Figure 6.10 DHE photobleaching correction results in increased DHE fluorescence intensity. Representative trace for mean data of DHE fluorescence over time. Oxygenated PSS was superfused continuously while images captured every ten minutes. Correction of photobleach resulted in a significant increase of DHE fluorescence at all time intervals. Mean fluorescence signal percentage measured in 10 tubule and 10 vessel ROIs for trace over time in 6 slices from 6 animals. Data are mean ± SEM, **P<0.01, n=6 (6).

Although photobleaching correction was able to increase the DHE fluorescence, the resulting correction still resulted in ~50% decay of fluorescence over 2 hours. In addition, production of ROS results in an increase of DHE fluorescence therefore bleach correction would not be feasible. If a series of images taken from the production of ROS were analyzed for photobleaching, the resulting change of fluorescence would not take into account any increase in DHE fluorescence *via* the production of ROS. In light of this, the results produced in the rest of this chapter will not be corrected for photobleaching and left in their original form.

6.5.1 CNI-induced production of ROS

Given that H_2O_2-mediated ROS production in the live slice model could be monitored *via* changes in fluorescence, the effect of CNIs and production of ROS as measured *via* changes in DHE fluorescence was investigated.

CNIs are known to increase the production of superoxide (Perez de Hornedo *et al*. 2007; Navarro-Antolin *et al*. 2005.; Navarro-Antolin *et al*. 2001) and renal pericytes are known to constrict in response to ROS (Zou *et al*. 2001; Y.-F. Chen *et al*. 2003; Rhinehart & Pallone 2001b) therefore identification of CNI-induced superoxide production within the live kidney slice may identify a possible mechanism for CNI-induced vasoconstriction of vasa recta.

Superfusion (~1000 s) of CsA (3 μM) resulted in a significant increase of DHE fluorescence (Figure 6.11). DHE fluorescence continued to increase after exposure to CsA, however started to decrease 15 minutes after CsA application. Change in DHE fluorescence reached a maximum of 179.37 ± 13.2% after 15 minutes of CsA exposure and was significantly greater in comparison to time matched PSS controls (28.29 ± 3.6%, $P<0.001$, n=6 (6), (Figure 6.11). Calcein fluorescence signal was significantly greater after application of CsA compared to PSS control (Figure 6.11).

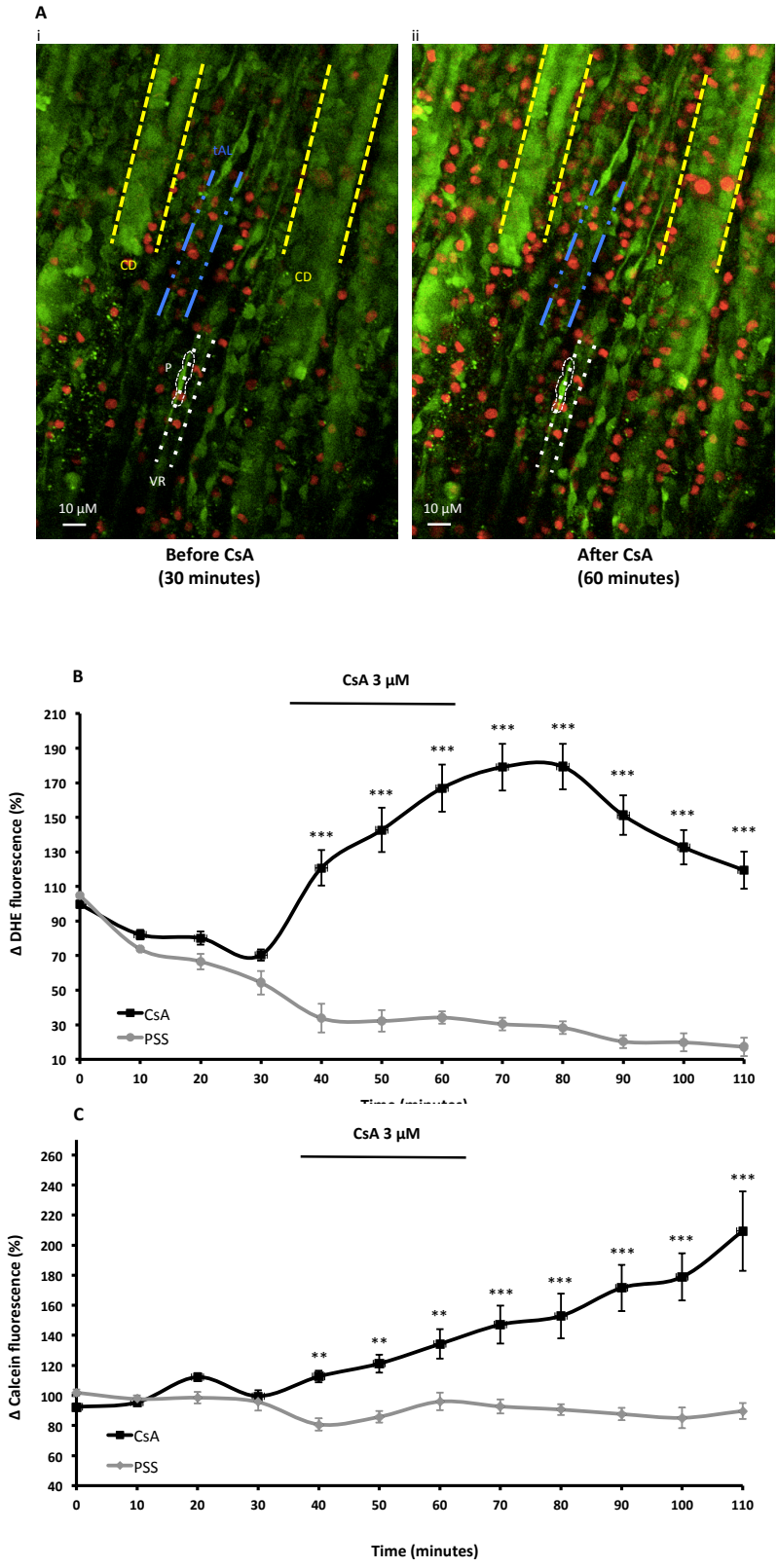

Figure 6.11 CsA evokes an increase in DHE fluorescence in medullary vasa recta and tubules. A: Representative images of DHE and calcein fluorescence in the medulla before (i) and after (ii) exposure to CsA. B: Representative trace shows the mean data for CsA mediated change in DHE fluorescence over time compared to time matched PSS control. C: Representative trace showing mean data for CsA induced change in calcein fluorescence over time compared to time matched PSS control. Mean fluorescence signal percentage measured in 11 tubule and 10 vessel ROIs for trace over time in 6 slices from 6 animals. VR, vasa recta; P, pericyte; CD, collecting duct; tAL, thin ascending limb. Data are mean ± SEM, **P<0.01, n=6 (6).

Superfusion (~1000 s) of FK506 (1 μM) resulted in a significant increase of DHE fluorescence. DHE fluorescence continued to increase after exposure to FK506, however started to decrease 10 minutes after FK506 application. Change in DHE fluorescence reached a maximum of 153.86 ± 15.6% after 10 minutes of FK506 exposure and was significantly greater in comparison to time matched PSS control, 28.29 ± 3.6%, $P<0.001$, n=6 (6), (Figure 6.12). Calcein fluorescence signal was significantly greater after application of FK506 compared to PSS control (Figure 6.12).

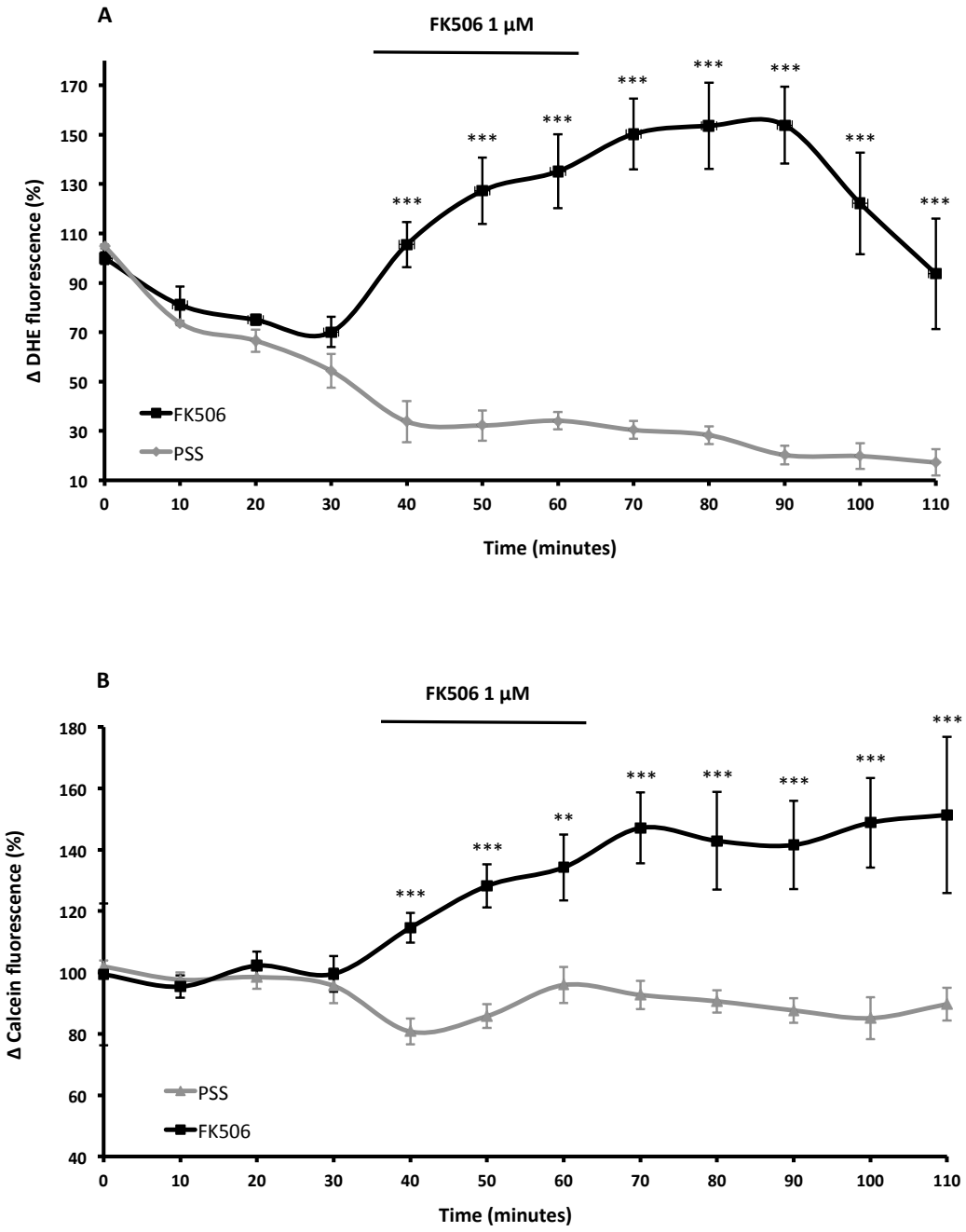

Figure 6.12 FK506 evokes an increase in DHE fluorescence in medullary vasa recta and tubules. A: Representative trace shows the mean data for FK506 mediated change in DHE fluorescence over time compared to time matched PSS control. B: Representative trace showing mean data for FK506 induced change in calcein fluorescence over time compared to time matched PSS control. Mean fluorescence signal percentage measured in 9 tubule and 8 vessel ROIs for trace over time in 6 slices from 6 animals. Data are mean ± SEM, **P<0.01, n=6 (6).

Rapamycin is not known for its production of ROS. In fact, several groups have shown its application to reduce ROS production in isolated cells (Shin *et al*. 2011; Tunon *et al*. 2003). However, clinical indications are showing its potential to be a nephrotoxic immunosuppressant possibly through ROS production (Dittrich *et al*. 2004; Marti & Frey 2005). Interestingly, rapamycin superfusion and isolated perfusion resulted in no significant vasoconstriction of vasa recta *via* pericytes. With this in mind, ROS production *via* rapamycin was investigated.

Superfusion (~1000 s) of rapamycin (1 μM) resulted in a significant increase of DHE fluorescence at certain time intervals (Figure 6.13). DHE fluorescence decreased before and after exposure to rapamycin. Application of rapamycin produced similar results to PSS in terms of DHE photobleaching experiments. At the end of experimentation, DHE fluorescence was reduced to 37.65 ± 9.32% after rapamycin exposure and was significantly greater in comparison to time matched PSS controls (17.21 ± 5.3%, $P<0.05$, n=6 (6), (Figure 6.13). Calcein fluorescence signal was significantly greater after application of rapamycin compared to PSS control (Figure 6.13).

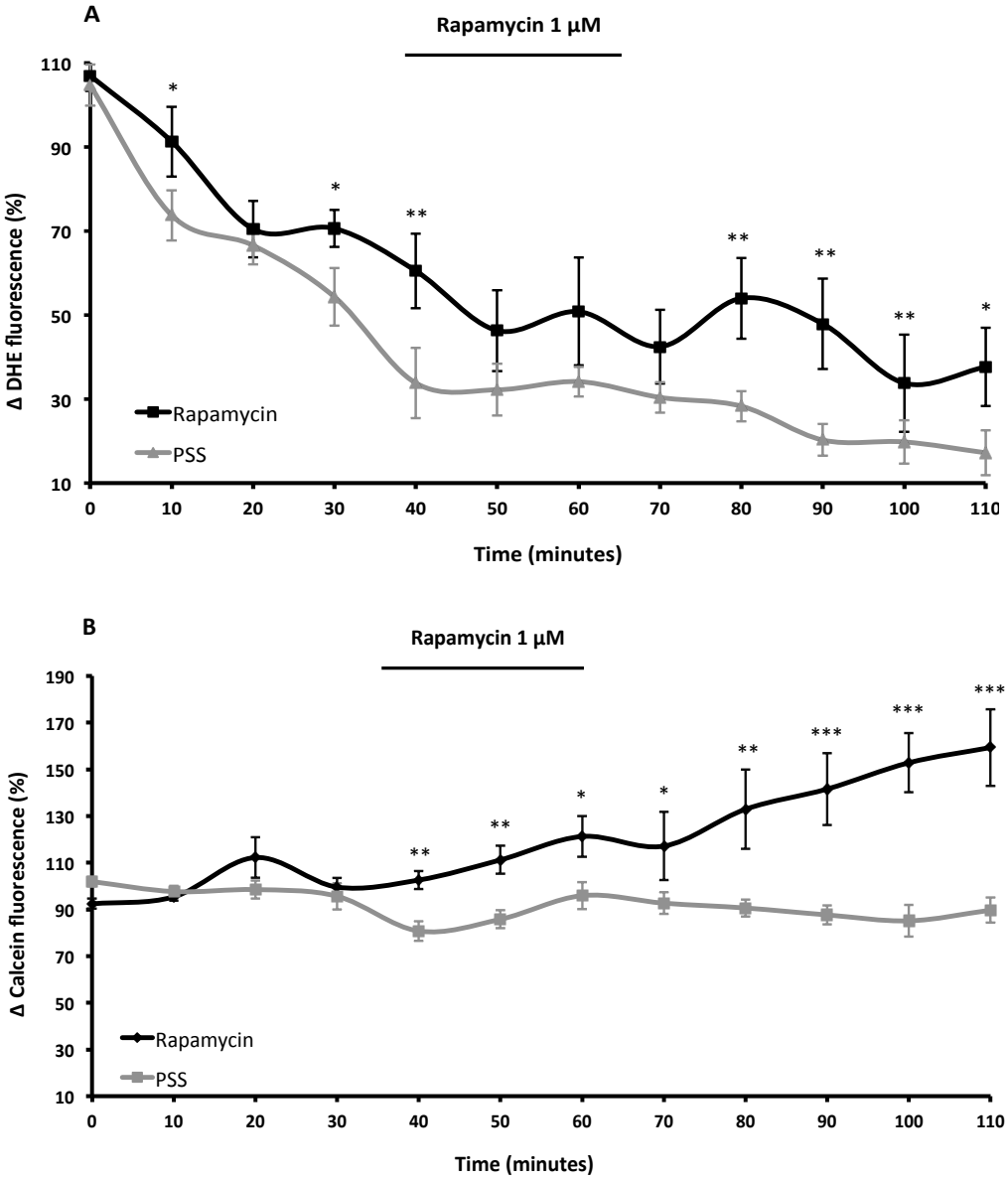

Figure 6.13 Rapamycin does not induce an increase in DHE fluorescence in medullary vasa recta and tubules. A: Representative trace shows the mean data for rapamycin-mediated change in DHE fluorescence over time compared to time matched PSS control. B: Representative trace showing mean data for rapamycin-induced change in calcein fluorescence over time compared to time matched PSS control. Mean fluorescence signal percentage measured in 8 tubule and 8 vessel ROIs for trace over time in 6 slices from 6 animals. Data are mean ± SEM, *P<0.05, n=6 (6).

Interestingly, both CNIs were able to increase DHE fluorescence indicating their ability to induce ROS. ROS production was measured from increases in DHE signal and measured within tubule and vessel ROIs. Due to the sporadic way ROS is detected *via* DHE and the time interval between images capture, it is difficult to determine whether ROS originated in vessels or tubules first.

However, it is possible to select random areas of interest that are vessel or tubule specific, measure the rate of DHE fluorescence, and therefore identify which structures produce ROS first and to an extent, what rate.

Analysis of time series experiments from which live slices where loaded with DHE and calcein and exposed to CsA or FK506 were carried out. Selection of tubules (collecting ducts and/or thick/thin ascending limbs) and blood vessels (vasa recta) were selected at random and regions of interest (ROI) drawn *via* ImageJ.

Superfusion (~1000 s) of CsA (3 μM) resulted in a significant increase of DHE fluorescence at vessel and tubule ROI's (Figure 6.14). DHE fluorescence increased at a significantly faster rate with significantly increased intensity at vessel ROI's compared to tubular ROI's. 10 minutes after CsA washout, DHE fluorescence of both vessel and tubule ROI's plateaued, which was significantly greater at vessel ROIs (161 ± 5.5%) compared to tubule ROIs (130 ± 5.2%, P<0.01, n=6 (6), figure 6.14. DHE fluorescence began to decline after maximum intensity, although rate of decline was not statistically different between each group.

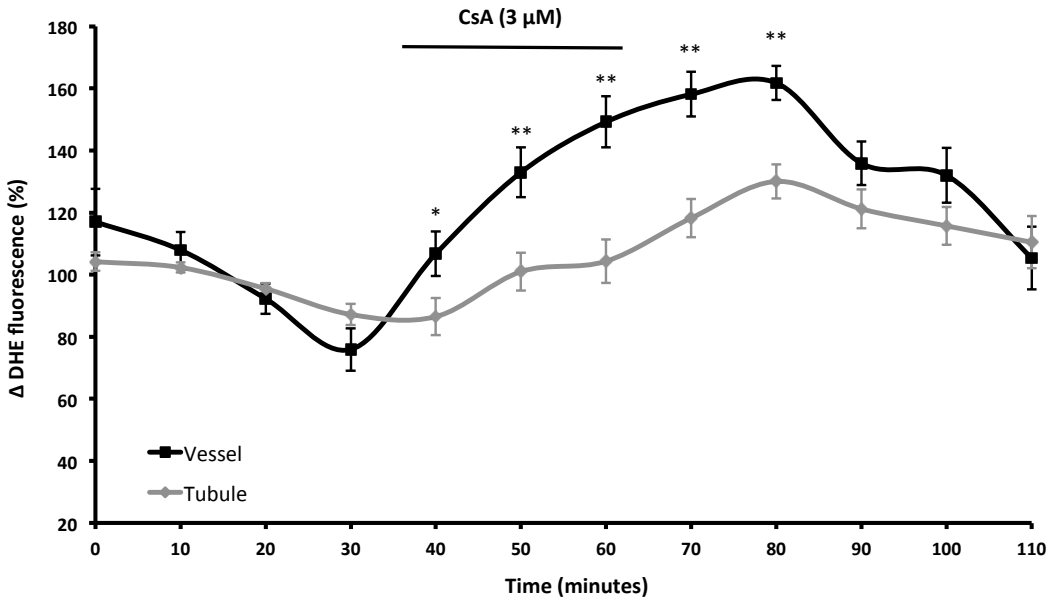

Figure 6.14 Medullary ROS production mediated *via* CsA is greater in vessels compared to tubules. Representative trace shows the mean data for CsA-mediated change in DHE fluorescence over time at vessel and tubule regions of interest. CsA application resulted in significantly greater ROS production in vessels compared to tubules. Mean fluorescence signal percentage measured in 7 tubule and 7 vessel ROIs for trace over time in 6 slices from 6 animals. Data is mean ± SEM, *P<0.05, n=6 (6).

Superfusion (~1000 s) of FK506 (1 μM) resulted in a significant increase of DHE fluorescence at vessel and tubule ROI's (Figure 6.15). DHE fluorescence increased at a significantly faster rate with significant increased intensity at vessel ROI's compared to tubular ROI's. Approximately 10 minutes after FK506 washout, DHE fluorescence of both vessel and tubule ROI's plateaued, which was significantly greater at vessel ROIs (121.7 ± 8.5%) compared to tubule ROI's (98.4 ± 4.8%, P<0.05, n=6 (6), figure 6.15. DHE fluorescence began to decline after maximum intensity, although rate of decline was not statistically different between each group.

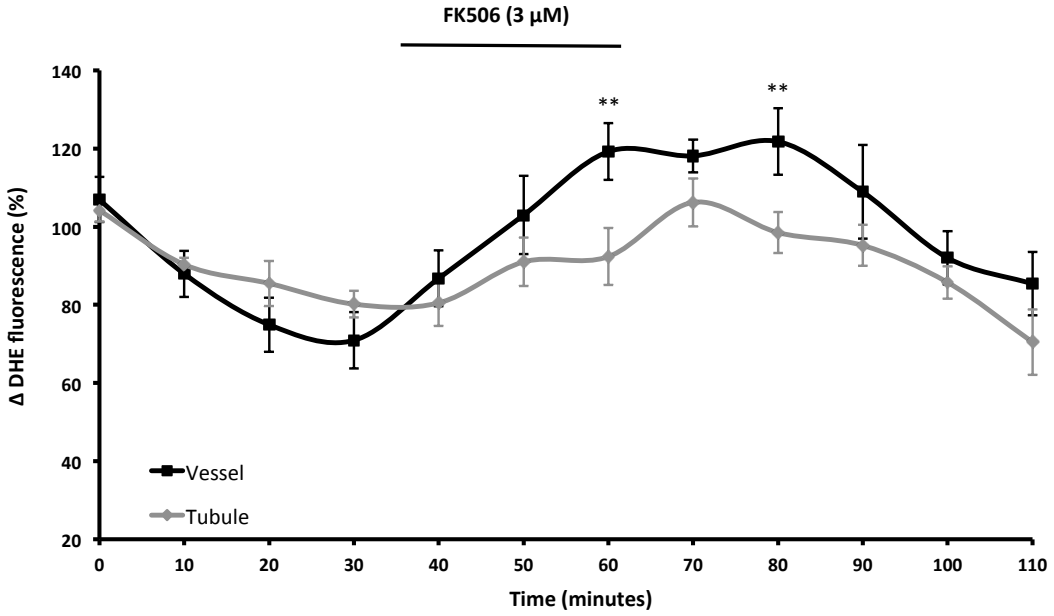

Figure 6.15 Medullary ROS production mediated *via* FK506 is greater in vessels compared to tubules. Representative trace shows the mean data for FK506 mediated change in DHE fluorescence over time at vessel and tubule regions of interest. FK506 application resulted in greater ROS production in vessels compared to tubules. Mean fluorescence signal percentage measured in 7 tubule and 7 vessel ROIs for trace over time in 6 slices from 6 animals. Data is mean ± SEM with, *P<0.05, n=6 (6).

6.6 Investigation of potential strategies to prevent CNI-induced ROS production

Given that it is well known that CNIs induce ROS production (Lopez-Ongil *et al*. 1998; A. Y. Zhou & Ryeom 2014; van der Toorn *et al*. 2007; de Arriba *et al*. 2013) and the detrimental role ROS play in the medullary microcirculation (Cowley *et al* 2015a; Wilcox 2002; Z. Zhang *et al*. 2004; Wilcox & Welch 2000), inhibiting their production may be a possible mechanism for attenuating CNI-induced nephrotoxicity.

As previously mentioned, over half of all ROS produced within the kidney originate from NADPH oxidase and its inhibition has already been shown to be beneficial in variety of disease states including diabetic nephropathy and hypertension (Asaba *et al*. 2005; Gill & Wilcox 2006). Remarkably, its role in CNI-nephrotoxicity is less well documented. Khanna *et al* were one of the first groups to demonstrate upregulation of NADPH in rats after treatment with CNIs and investigate its role in the aetiology of CNI-induced nephrotoxicity (Khanna & Pieper 2007). In addition, their experimental model utilised renal transplants further adding physiological relevance to the evidence that suggests NADPH oxidase might have and the role in CNI-mediated nephrotoxicity in renal transplant patients. Very few groups have further explored the role of NADPH in CNI nephrotoxicity.

Conversely, there is a plethora of studies focusing on scavenging of ROS induced by CNIs or its dismuation by SOD mimetics as a therapeutic strategy (Tunon *et al*. 2003; Lopez-Ongil *et al*. 1998; Navarro-Antolin *et al*. 2005; Damiano *et al*. 2013). Taken together, it is reasonable to suggest that not only targeting ROS degeneration, but also inhibiting its initial production would be a possible mechanism for attenuating CNI nephrotoxicity.

Apocynin is the best well-known NADPH oxidase inhibitor (Gill & Wilcox 2006). It has been shown to have anti-inflammatory properties and act as an antioxidant in endothelial cells and VSMCs (Stolk *et al*. 1994; Heumuller *et al*. 2008; C. O. Silva *et al*. 2015). Recently, Ciarcia *et al* have demonstrated the beneficial effect apocynin has on CsA-induced hypertension and nephrotoxicity (Ciarcia *et al*. 2015). Their results indicated apocynin was able to not only reduce production of ROS, but also restore the haemodynamic changes in the kidney that occurred with CsA administration. This suggests that ROS production, *via* NADPH oxidase, is involved in both nephrotoxicity and hypertension during CsA treatment.

Given the fact CNIs are able to induce ROS production and induce vasoconstriction of vasa recta, coupled to the fact pericytes are known to constrict after exposure to ROS, it is feasible to suggest ROS production may be involved in the mechanism of CNI-induce vasoconstriction of vasa recta. With this hypothesis in mind, apocynin was used to investigate its possible role of attenuating CNI-induced ROS production.

Superfusion of apocynin alone had not significant effect on DHE fluorescence. DHE photobleaching after exposure of apocynin was not significantly different (30.94 ± 5.87%) compared to timed matched controls of DHE alone (34.14 ± 2.72%, n=6 (6)).

Superfusion (~1000 s) of CsA (3 μM) and apocynin (10 μM) resulted in a significant decrease of DHE fluorescence compared to CsA alone (Figure 6.16). DHE fluorescence plateaued during exposure to CsA and apocynin however started to decrease after CsA and apocynin washout. Change in DHE fluorescence reached a maximum of 82.66 ± 13.6% and was significantly lower in comparison to CsA alone (179.05 ± 13.5%, P<0.001, n=6 (6), (Figure 6.16). Calcein fluorescence signal was not significantly different after application of CsA and apocynin (150 ± 9.87%) compared to CsA alone (164 ± 11.21%, n=6(6)).

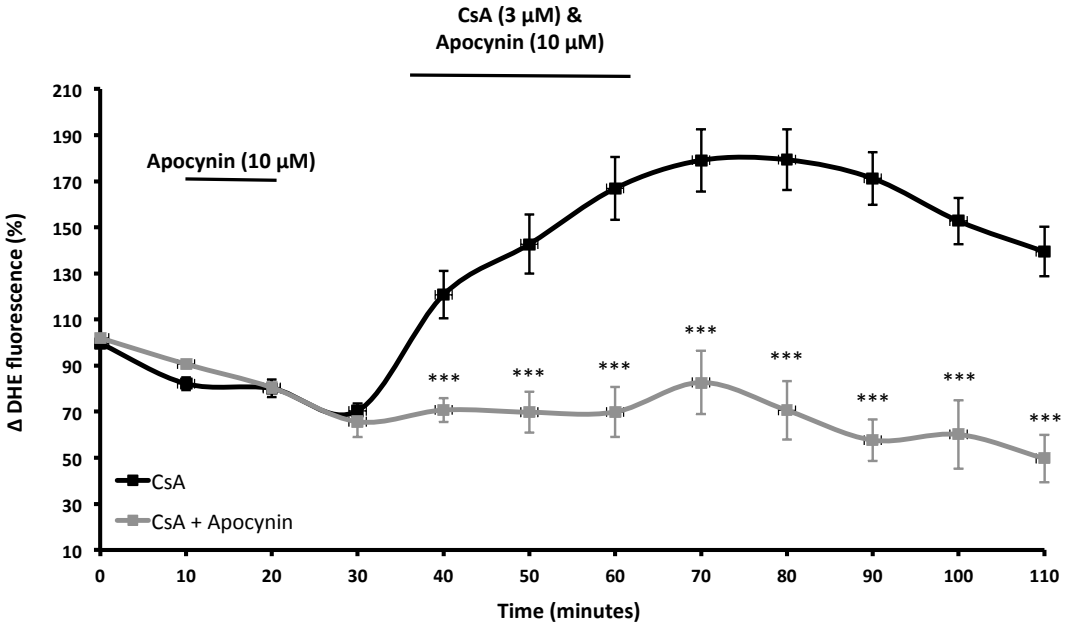

Figure 6.16 Apocynin significantly reduces CSA-induced ROS production.
Representative trace showing mean data for the change in DHE fluorescence in the presence of CsA alone and in combination with apocynin. Apocynin was able to significantly reduce DHE fluorescence induced *via* CsA therefore able to reduce ROS production. Mean fluorescence signal percentage measured in 9 tubule and 9 vessel ROIs for trace over time in 6 slices from 6 animals. Data are mean ± SEM, ***P<0.001, n=6 (6).

Superfusion (~1000 s) of FK506 (1 μM) and apocynin (10 μM) resulted in a significant decrease of DHE fluorescence compared to FK506 alone (Figure 6.17). DHE fluorescence stabilised during exposure however started to decrease after FK506 and apocynin washout. Change in DHE fluorescence reached a maximum of 91.90 ± 9.06% and was significantly lower in comparison to FK506 alone, time matched. (135.13 ± 14.9%, P<0.001, n=6 (6), (Figure 6.17). Calcein fluorescence signal was not significantly different after application of FK506 and apocynin (120 ± 8.54%) compared to FK506 alone (125 ± 4.49%, n=6(6)).

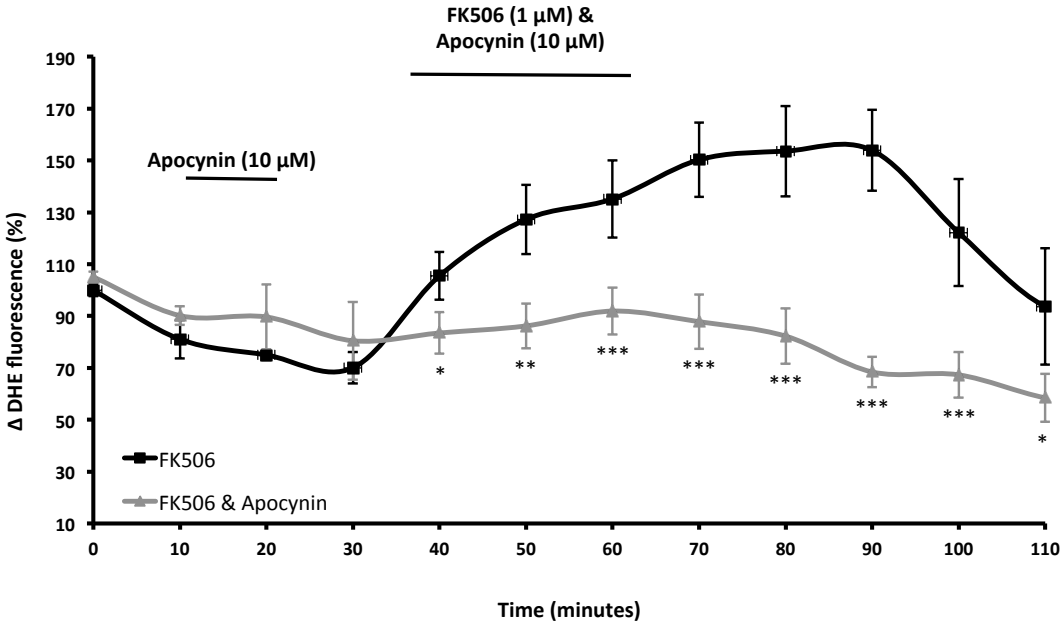

Figure 6.17 Apocynin significantly reduces FK506-induced ROS production.
Representative trace showing mean data for the change in DHE fluorescence in the presence of FK506 alone and in combination with apocynin. Apocynin was able to significantly reduce DHE fluorescence induced *via* FK506 therefore able to reduce ROS production. Mean fluorescence signal percentage measured in 7 tubule and 7 vessel ROIs for trace over time in 6 slices from 6 animals. Data are mean ± SEM, *P<0.05, n=6 (6).

Changes in fluorescence in tubules and vessels were investigated. There was no significant difference between fluorescence measured in both compartments, nor were there any significant differences in the temporal changes in fluorescence. Unlike experiments in which CsA and FK506 were applied alone, and changes in vessel fluorescence detected before changes in the tubule fluorescence, all changes in

fluorescence in tissue exposed to wither CsA/FK506 and apocynin occurred at the same time points in both vessels and tubules.

Superfusion (~1000 s) of rapamycin (1 μM) and apocynin (10 μM) resulted in no significant decrease of DHE fluorescence (50 ± 8.89%) compared to rapamycin alone (60.24 ± 9.39%, n=6(6)) (Figure 6.18). DHE fluorescence continued to decrease during exposure and after rapamycin and apocynin washout. Calcein fluorescence signal was not significantly different after application of rapamycin and apocynin (130 ± 8.32%) compared to rapamycin alone (125 ± 9.67%, n=6(6)).

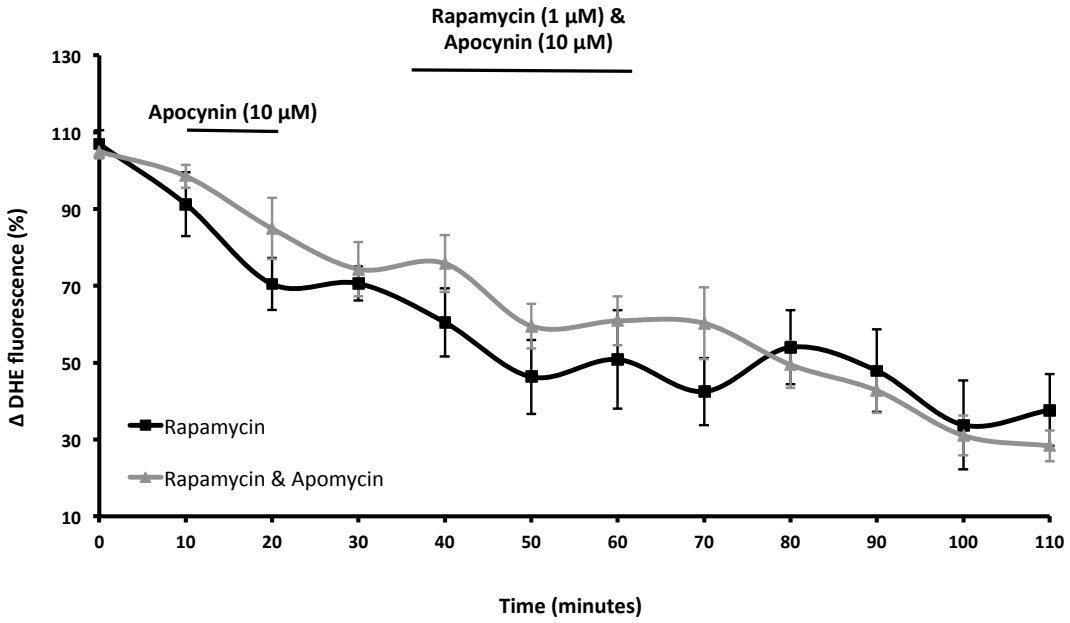

Figure 6.18 Apocynin has no effect on rapamycin-induced loss of DHE fluorescence. Representative trace showing mean data for the change in DHE fluorescence in the presence of rapamycin alone and in combination with apocynin. Apocynin had no effect on the reduction of DHE fluorescence *via* rapamycin superfusion. Mean fluorescence signal percentage measured in 7 tubule and 7 vessel ROIs for trace over time in 6 slices from 6 animals. Data are mean ± SEM, n=6 (6).

6.7 Discussion

The aim of this study was to use multiphoton microscopy to investigate possible mechanisms of CNI-induced vasoconstriction of vasa recta and the molecular events underlying development of CNI-induced nephrotoxicity. The results have shown that mitochondrial membrane potential of medullary vasa recta and tubules is unaffected by CNIs and rapamycin, but that mitochondrial permeability transition is inhibited by CsA but not by FK506 or rapamycin.

Reactive oxygen species production is induced in vasa recta and tubular compartments of the medulla in response to CNIs while rapamycin fails to induce ROS production. NADPH inhibition prevents the production of CNI-mediated ROS indicating CNIs mediate ROS production *via* NADPH oxidase.

Taken together, CNI-induced DVR vasoconstriction could possibly originate from the production of ROS, decreased bioavailability of NO, increased ET-1 production and ADP ribosyl cyclase production, all leading to increased vasoconstriction. Additionally, inhibition of CNI-induced ROS *via* NADPH inhibition could provide an alternative method for prevention of ROS production that could lead to CNI nephrotoxicity and graft dysfunction.

Multiphoton microscopy (MPM) is an alterative microscopy technique to fluorescence confocal microscopy, which enables clear advantages for three-dimensional imaging, particularly of live cells and intact tissue including slices and whole organs. MPM permits far greater tissue penetration along with less phototoxicity compared to conventional confocal imaging, therefore enables a distinct advantage for imaging of subsurface cellular structures (Hall *et al*. 2011).

MPM was a concept first described in the 1930's by Maria Goeppert-Mayer but not put into practical use some 30 years later (Göppert-Mayer 1931). In principle, MPM is based on the conception that 2 photons of lower energy than required for one photon (confocal) excitation can also excite a fluorophore simultaneously (Göppert-Mayer 1931). The longer length photons must arrive simultaneously at the focal plane and hence the wavelength of exciting photons is larger than emitted light (Williams *et al*. 2001). Therefore, each photon has approximately half the energy required to excite the fluorophore and results in reduced phototoxicity.

Both confocal and MPM require the use of lasers instead of fluorescence mercury lamps or LED's to excite fluorophores. MPM typically uses titanium: sapphire (Ti:S)

lasers which offer a far greater use of longer wavelength light and tunability (typically 700-1200 nanometres). MPM lasers also typically do not require water cooling like confocal laser sources, however are significantly more expensive, combined with the more expensive microscope setup, makes MPM a significant burden on laboratory funding. Confocal microscopy requires the use of a pinhole aperture to reduce out of focus light due to fluorescence being excited throughout the entire sample and thus only light close to the optical plane will be detected (Williams *et al*. 2001). Although a large proportion of sample will be excited, point illumination is achieved by the use of a pinhole aperture and reduces out of focus light. In turn, the pinhole aperture only enables a small fraction of light through from the focal plane and results in increased resolution and increased sample intensity (Nwaneshiudu *et al*. 2012).

Unlike confocal microscopy, MPM does not require a pinhole aperture. 2-photon excitation only produces fluorescence at the focal plane and therefore background fluorescence is not produced and no pinhole apertures are required (Williams *et al*. 2001). This distinct advantage enables only the focal plane to be imaged without possibility of background fluorescence compromising the signal. In addition, this reduced exposure minimises photobleaching and phototoxicity. Figure 6.19 demonstrates the degree of fluorescence from out of focus planes by confocal microscopy and fluorescence from the focal spot *via* multiphoton microscopy.

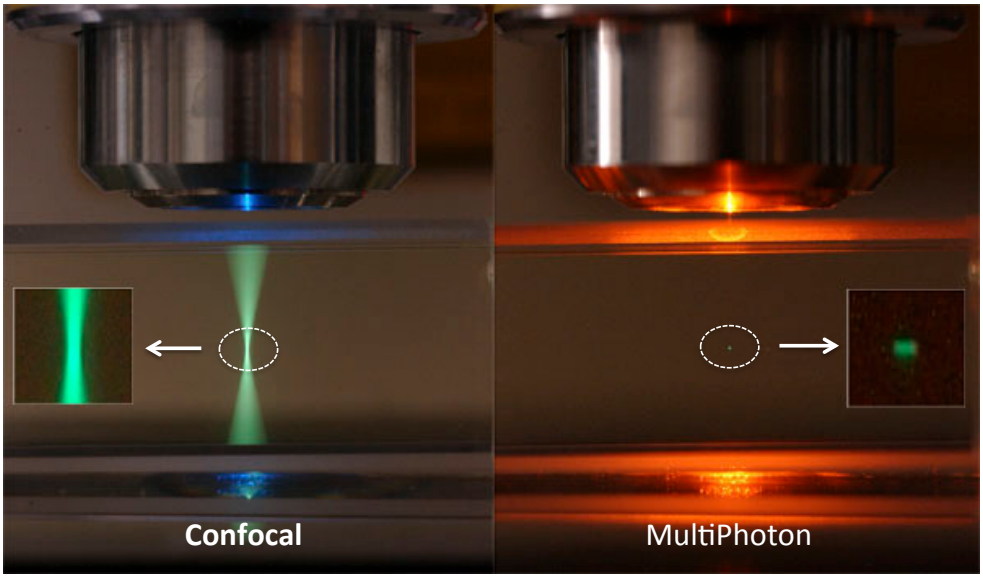

Figure 6.19 Visualisation of focal plane excitation in confocal and multiphoton microscopy. Confocal microscopy excites the fluorescence above and below the focal plane whereas multiphoton microscopy only excites fluorescence at the focal plane. Adapted from (Zipfel *et al*. 2003).

MPM has a distinct advantage on live cell imaging compared to confocal imaging due to reducing out of focus light, greater tissue penetration and reduced photobleaching. However, MPM is not without its limitations. Due to longer wavelengths being utilised (energy of a photon is inversely proportional to its wavelength, therefore 2 absorbed photons must equal a wavelength twice of that for confocal excitation (Williams *et al*. 2001), MPM actually results in a larger resolution spot. This increased resolution spot correlates to Abbe's law that states the resolution of a microscope is inversely proportional to the wavelength of light used (Heintzmann & Ficz 2006). Therefore, for any given fluorophore, 2-photon excitation uses approximately twice the wavelength of one-photon excitation and subsequently approximately half the resolution. This can result in poorer defined images of cellular structures and hampered image analysis.

Although MPM follows this principle, improved imaging technology has decreased the loss of resolution and is therefore not directly in relation to loss of half the resolution. It is now generally accepted that MPM resolution is no less compared to that of confocal microscopy because if a biological sample cannot be resolved using a confocal microscope, it similarly will not be resolved using a MP microscope.

As a whole, MPM offers a distinct advantage over conventional fluorescence microscopy for deeper 3-dimensional imaging of living tissue without the increased risks of photobleaching and phototoxicity.

These advantages have already helped us better understand the physiology of whole organs including the kidney. Hall *et al* have been able to use MPM on a isolated perfused kidney model to study the cell structure and physiology of a whole functional kidney (Hall *et al*. 2011). The study allowed visualisation of endogenous and exogenous fluorophores for investigations of renal function under certain pathological conditions. In addition, it also highlighted the importance of mitochondria structure and function during ischemia and reperfusion but also the production of ROS for mediating changes in renal function under oxidative stress. These changes are similarly seen in CNI-induced nephrotoxicity with altered mitochondrial function and increased ROS production (Buffoli *et al*. 2005; Perez de Hornedo *et al*. 2007; de Arriba *et al*. 2013; Weir *et al*. 1992), therefore it could be possible to identify similar pathways in their pathogenesis and help identify common targets for their prevention.

Using MPM within the live slice model enables a more detailed view of cellular changes of the medulla during chemical insult including CNIs and potentially helps identify therapeutic targets for prevention of nephrotoxicity.

The results from this chapter, in which MPM imaging of a variety of fluorophores was used to investigate CNI-mediated changes in cell function, suggest that CNIs do not alter mitochondrial membrane potential (ΔΨm) as an event leading to CNI-induced vasoconstriction. Pericyte-mediated vasoconstriction could not be measured using MPM due to the lack of brightfield microscopy resolution however changes in vessel diameter during superfusion of CNIs correspond to the timings of increased ROS production visualised during MPM microscopy. As discussed previously, ΔΨm is generated in the inner mitochondria membrane *via* electron flow through protein complexes of the respiratory chain, coupled to the exit of protons from the intermembrane space which generates the highly negative potential across the mitochondria membrane (McBride *et al*. 2006). Alterations in ΔΨm have been shown to alter mitochondrial function and are further discussed below.

Mitochondrial dysfunction has been shown to participate in the induction of apoptosis and possibly central to the apoptotic pathway of all living cells (Ly *et al*. 2003). Loss of ΔΨm may be an early event in apoptosis leading loss of oxidative phosphorylation and release of apoptogenic factors (Ly *et al*. 2003).

Changes in ΔΨm have been observed before any morphological adaptions (DNA fragmentation cell shrinking) in isolated embryonic cells suggesting that loss of ΔΨm may precede any changes in the apoptotic pathway (Vayssiere *et al*. 1994; Zamzami *et al*. 1995). However other studies demonstrated that ΔΨm is lost after apoptosis *via* DNA damage and apoptosis regulator BAX (Bax) translocation to mitochondria, and therefore is not useful for early identification of apoptosis (Cossarizza *et al*. 1994; Karpinich *et al*. 2002) and suggests the different rationale of ΔΨm being lost due to apoptosis and not *vice versa*. It therefore suggests that 2 pathways are thought to exist for linking changes of ΔΨm with apoptosis, however neither of the two have been independently confirmed.

Nonetheless, it is well regarded that mitochondrial dysfunction is central to cell apoptosis, whether it is a cause or effect is still debateable, and mitochondrial death undoubtedly results in cell and tissue apoptosis.

It has been previously shown that FCCP is capable of ΔΨm depolarisation in renal cell lines along with intact kidney tissue (Schnellmann *et al*. 1994; Hall *et al*. 2009)

therefore suitable as a positive control in the live kidney slice. Accordingly, administration of FCCP to live kidney slices significantly reduces ΔΨm and thus the live slice model was used to investigate the effects of CNIs on ΔΨm. Superfusion of CNIs failed to significantly alter ΔΨm therefore suggesting that mitochondrial (hyper) depolarisation is not involved in pericyte-mediated DVR vasoconstriction. Although changes in vessel diameter could not be directly measured using MPM *per se,* due to lack of brightfield images (MPM set-up with this particular model requires manual switching between DIC and MPM condensers) and bleaching of fluorophores, the acute changes in vessel diameter observed during superfusion correspond to the acute changes seen in MPM when changes in fluorescence was monitored.

Interestingly, CNIs have been shown to induce mitochondria depolarisation in renal cell lines. De arriba *et al*, Hornedo *et al* and Zhou *et al* have all been able to show CsA induced changes in mitochondrial membrane potential using TMRM or TMRE (analogue of TMRM) in renal cell lines (de Arriba *et al*. 2013; Perez de Hornedo *et al*. 2007; A. Y. Zhou & Ryeom 2014). However, the author's models have used confluent cells treated with CsA for 24 hours or more. Superfusion of CsA using the live kidney slice model ultimately exposes the tissue to CsA for up to 30 minutes.

Furthermore, it has been shown that acute exposure of CsA offers a protective role, preventing mitochondrial dysfunction induced by oxidised low-density lipoproteins in an *in vivo* skeletal muscle model *via* inhibition of MPTP opening (Merlini *et al*. 2008), hence offering a protective role against mitochondrial dysfunction. This has been further highlighted by Halestrap *et al* (Halestrap *et al*. 1997) who used CsA to prevent mitochondrial dysfunction in a heart ischemia/reperfusion *in vivo* model. Their results suggests that CsA binding to cyclophiln D (CsA's intracellular binding molecule) renders it incapable of effecting ΔΨm, cyclophiln D has been previously thought to be key in ΔΨm depolarisation through MPTP formation (Schubert & Grimm 2004; Nakagawa *et al*. 2005), figure 6.20.

Taken together, it is clear that CNI effects on ΔΨm are somewhat contradictory depending on which model used. Interestingly, it is now becoming clear that investigating ΔΨm as a component of cellular apoptosis is dependent on the cell system being used and evidence to date regarding whether changes in ΔΨm is a cause or effect of apoptosis varies depending on the experimental model (Ly *et al*. 2003). For example, rat embryonic cells induced to undergo acute apoptosis, *via* SV40 large antigen, show early signs of lowered ΔΨm and reduced mitochondrial respiration prior to apoptosis (H. H. Winkler & Lehninger 1968), while rat thymocytes treated

with dexamethasone, investigating chronic damage, have shown DNA fragmentation prior to ΔΨm depolarisation (Cossarizza *et al*. 1994).

CNI-induced mitochondrial dysfunction may or may not be an event in cellular apoptosis, however evidence in the literature suggesting that this link is a feature for several toxic compounds, but further research in this area is needed to clarify the relationship. Evidence here fails to implicate a role for ΔΨm in CNI-induced changes in cell function.

Interestingly, all immunosuppressant's investigated in this study where able to significantly increase the level of calcein fluorescence. Calcein-AM is a cell permanent dye used to label viable cells. Nonfluorescent calcein-AM is converted to fluorescent green calcein, emitted light at 518 nm, after acetoxymethyl ester hydrolysis by intracellular esterase's (Tenopoulou *et al*. 2007). Under normal conditions, calcein-AM has been shown to be a substrate for p-glycoprotein (P-GP) and multidrug resistance proteins (MDR) (Feller, Broxterman, *et al*. 1995; Feller, Kuiper, *et al*. 1995). Both groups of proteins are responsible for export of foreign compounds out of cells and used for prevention of cell toxicity. CsA, FK506 and rapamycin are all known to interact with MDR proteins therefore actively reduce the ability of P-GP and MDR to expel foreign material (Loh *et al*. 2008; Arceci *et al*. 1992). The data presented here demonstrates that all three immunosuppressant's are able to interact with P-GP and MDR function and results in increased calcein fluorescence after exposure due to decreased activity of MDR and P-GP. This has important clinical consequences as demonstrated by all three compounds having a narrow therapeutic range and requiring careful TDM with reduced drug combinations. Incorrect drug therapy could result in an increased inhibition of MDR and PGP resulting in increased systemic levels of immunosuppressant and increased risk of patient infection or allograft dysfunction. For example, it has been shown grapefruit juice inhibits the metabolism of CsA through inhibition of CYP 405 enzymes (Hollander *et al*. 1995) and may acutely increase the systemic and renal concentrations of CsA, putting patient and graft at risk of rejection.

Another source of mitochondrial dysfunction and depolarisation is through mitochondrial permeability transition (MPT). MPT involves the generation of MPT pores (MPTP) that allows the release particular mitochondrial apoptogenic factors including cytochrome C and apoptosis-inducting-factor (AIF) into the cytosol and is

often described as a sudden increase of membrane permeability of the mitochondrial membrane to solutes less than 1.5 kDa (Kroemer *et al*. 2007; McBride *et al*. 2006). MPTP regulation is thought to be dependent on intracellular calcium levels along with cyclophiln D binding however it remains uncertain what its exact physiological role is (Halestrap 2009). A proposed model of MPTP regulation is shown in figure 6.20.

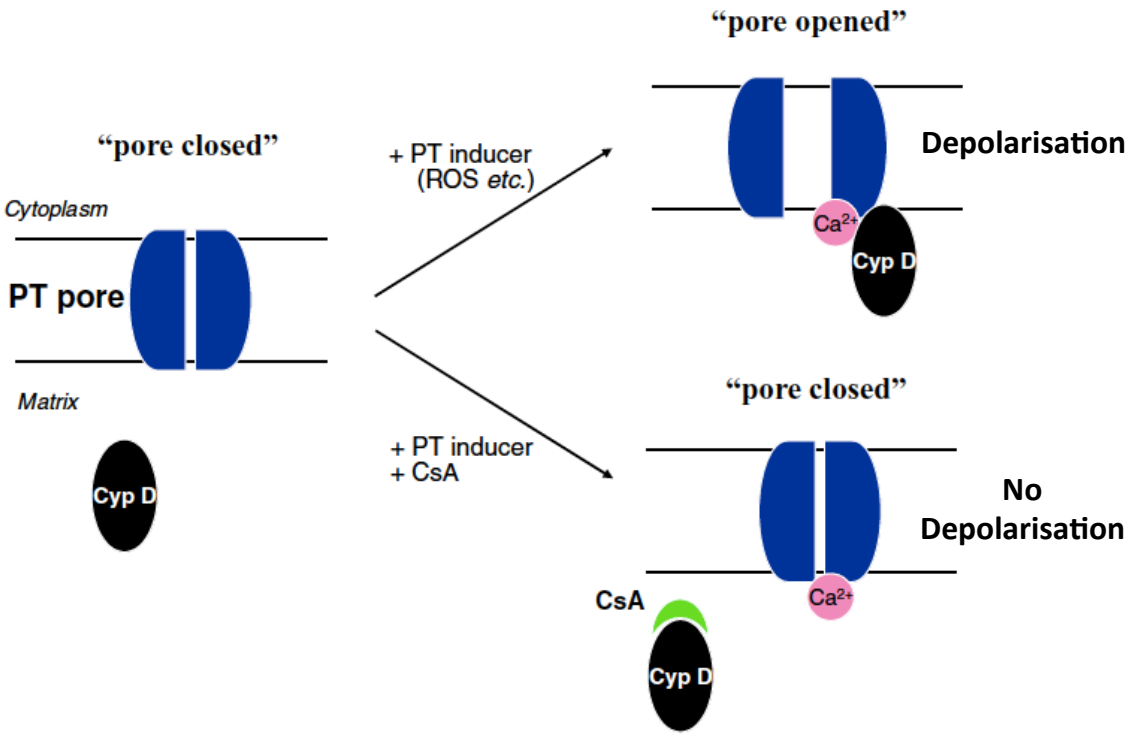

Figure 6.20 Proposed model of MPTP regulation. Cyclophiln D (Cyp D) is localized to the mitochondrial matrix, and the MPTP is closed. In the presence of permeability transition inducers, Cyp D is considered to bind to and induce a conformational change of a channel in the inner membrane, resulting in opening of the MPTP Cyclosporine A (CsA) binds to and inhibits Cyp D to prevent MPT pore opening. Adapted from (Tsujimoto & Shimizu 2007).

Once the MPTP is open, solutes and water enter the mitochondria resulting in swelling and rupture of the outer mitochondrial membrane and release of apoptotic factors (Kroemer 1997). Interestingly, $\Delta\Psi m$ is thought to be a regulator of MPTP opening and membrane depolarisation is thought to increase the chance of MPTP formation (Bernardi *et al*. 1992).

Results from this chapter using CDCA as a positive control for MPTP formation have suggested that CsA but not FK506 or rapamycin is able to inhibit MPTP opening and

protect from mitochondrial permeability transition.

Chenodeoxycholate (CDCA) is a naturally occurring bile salt with potent ability to induce MPTP formation without directly effecting ΔΨm (Rolo *et al*. 2003; Rolo *et al*. 2001). CDCA was able to significantly reduce TMRM fluorescence after application however in the presence of CsA, CDCA had no effect on TMRM signal. FK506 and rapamycin had no such inhibitory effect with CDCA.

The prevention of MPTP opening *via* CsA could potentially help explain its protective role in certain pathological conditions. As previously mentioned, CsA has been used to prevent mitochondrial dysfunction in a variety of *in vivo* disease models (Halestrap, *et al*. 1997; Merlini *et al*. 2008) and could be due to its interaction with cyclophiln D (Cyp D). As seen in figure 6.20, under normal conditions without the presence of CsA, Cyp D is a part of MPTP formation along with other pore forming proteins. In the presence of CsA, Cyp D is unable to form the MPTP.

It is generally thought that Cyp D is needed for MPTP formation and within the inner membrane, adenine nucleotide translocase (ANT) and Cyp D form the MPTP along with the outer membrane voltage-dependent anion channel (VDAC) to complete pore assembly (Kroemer *et al*. 2007). Inhibition of Cyp D and ANT prevents the formation of the pore and therefore stops mitochondrial transition to apoptosis. It must be noted that this model is still a working hypothesis and no definitive model has been published (Tsujimoto & Shimizu 2007). CsA normally binds to Cyp D to inhibit calcineurin translocation to the nuclease and activation of T cells, however as a secondary mechanism, CsA also inhibits Cyp D complexing to ANT and prevents MPTP formation. Tacrolimus and rapamycin do not bind to Cyp D therefore would not inhibit the formation of the MPTP. This is in fitting with the results produced here showing that tacrolimus and rapamycin fail to prevent the loss of TMRM fluorescence after CDCA exposure, which was in contrast with CsA, which prevented MPTP formation. The interaction on CNIs and rapamycin with intracellular proteins for MPTP regulation can be seen in figure 6.21.

The protective effect of MPTP inhibition has been shown in a variety of conditions including ischemic reperfusion and neurodegeneration (Brustovetsky & Dubinsky 2000; Matsumoto *et al*. 1999) however increasing evidence is suggesting that there are two forms of MPTP, CsA sensitive and CsA insensitive (Jung *et al*. 1997; He & Lemasters. 2001). CsA insensitive MPTP regulation is thought to be regulated through chaperone proteins and protein clusters formed from oxidative damage. CsA-insensitive MPTP opening results from an overload of protein clusters and reduced

number of chaperone proteins (García *et al*. 2007; He & Lemasters. 2001.; Jung *et al*. 1997). This is in contrast to data shown here with CsA inhibiting the formation of MPTP formation within medullary structures and FK506 and rapamycin unable to replicate similar results.

This secondary mechanism might be able to explain why some investigators are able to observe MPTP formation induced by CsA (Cho *et al*. 2014; Abdallah *et al*. 2011; de Arriba *et al*. 2013; A. Y. Zhou & Ryeom 2014) and ΔΨm depolarisation, however this mechanism does not support the protective role that CsA has been shown to have in numerous *in vivo* models of mitochondrial dysfunction.

Taken together, it is clear the literature dealing with MPT is complex and somewhat confusing. On one hand, many studies have shown the detrimental effect of MPTP formation leading to ΔΨm depolarisation and cell apoptosis (Kroemer *et al*. 2007; Halestrap *et al*. 2004; Rolo *et al*. 2003). Some of these studies have shown the beneficial effect of CsA and MPTP inhibition, resulting in stabilisation of mitochondria in a variety of pathological conditions (Nakagawa *et al*. 2005; Halestrap *et al*. 2004; Halestrap *et al* 1997; AL *et al*. 1996).

In the opposite category, there have been studies to show debatable existence of the MPTP and mitochondria dysfunction is only a result of calcium-sensitive phospholipases (Halestrap 2009), the augmented effect CsA has on MPTP opening and the destructive effect it has *via* mitochondrial dysfunction (Abdallah *et al*. 2011; Brustovetsky & Dubinsky 2000; He & Lemasters 2001.).

The results produced here indicate CNI-induced vasoconstriction *via* pericytes is most likely not mediated *via* mitochondrial depolarisation or *via* the opening of MPTP. CsA failed to (hyper) depolarise the ΔΨm but inhibited MPTP formation therefore suggests stable mitochondria throughout CsA exposure. Tacrolimus and rapamycin also failed to (hyper) depolarise the ΔΨm however they also failed to inhibit MPTP opening. This is due to FK506 and rapamycin not having the same intracellular binding protein as CsA, Cyp D. Instead, FK506 and rapamycin bind to FKB12, which has been shown to have no effect on MPTP (Friberg *et al*. 1998; Groenewoud & Zwartkruis 2013). Although unable to inhibit MPTP opening *via* an exogenous source, studies suggests they are unable to induce MPTP formation endogenously *via* calcium signalling (Ferrand-Drake *et al*. 1999; Elmore *et al*. 2001; Bernardi & Petronilli 1996). Therefore, FK506 induced vasoconstriction of vasa recta is also unlikely to be mediated *via* mitochondrial dysfunction, while rapamycin is also

unlikely to alter mitochondrial function.

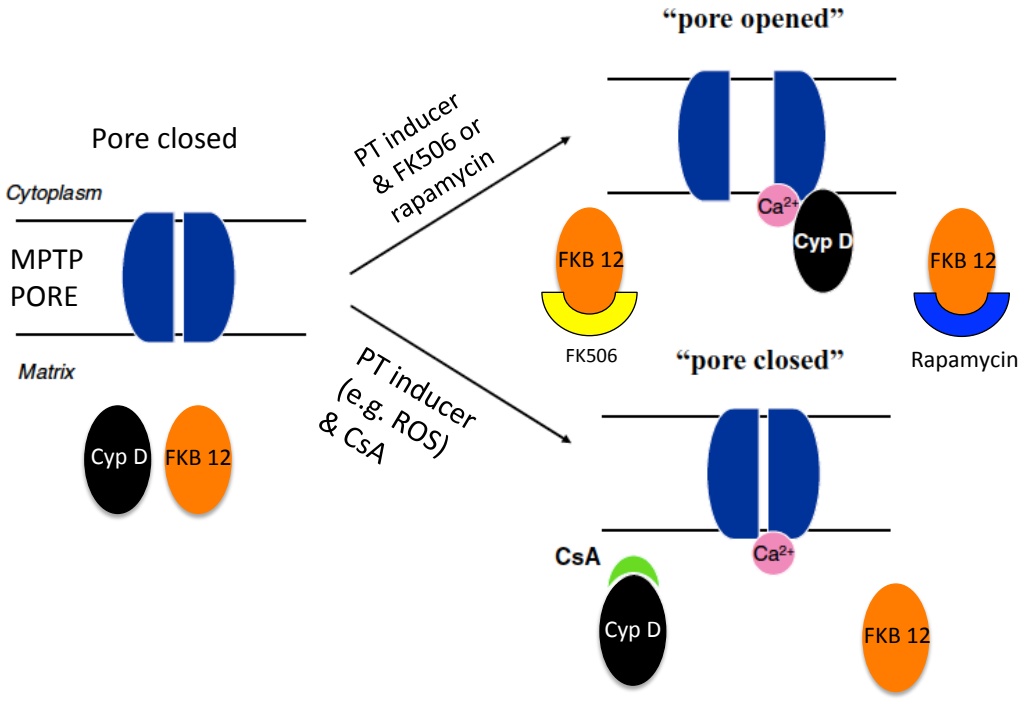

Figure 6.21 CNI and rapamycin interactions with intracellular proteins for MPTP regulation. Cyclophiln D (Cyp D) and FK506 binding protein (FKB 12) are localized to the mitochondrial matrix and under normal conditions and the MPTP is closed. In the presence of permeability transition inducers, Cyp D is considered to bind to and induce a conformational change of a channel in the inner membrane, resulting in opening of the MPTP. Cyclosporine A (CsA) binds to and inhibits Cyp D to prevent MPT pore opening. In the presence of FK506 or rapamycin, Cyp D is able to induce a conformational change due to FK506 and rapamycin both binding to FKB 12. Adapted from (Tsujimoto & Shimizu 2007).

Data presented here has shown both CNIs are capable of inducing ROS within the renal medulla while rapamycin has no such effect. Dihydroethidum (DHE) is a naturally blue fluorescent probe, emits light at 518 nm, when it is located within the cytosol however once oxidised by superoxide, it intercalates with cell DNA and exhibits a bright red fluorescence, and emits light at 605 nm. Although not technically a specific superoxide probe, DHE is able to freely permeate cell membranes and often used as a read out of increased superoxide production (Owusu-Ansah *et al*. 2008).

Within the kidney, there are two major sources of ROS: NADPH oxidase (NOX) and mitochondria. NOX accounts for just over half of all renal ROS production while mitochondria supply the reminder (Taylor *et al*. 2006; Cowley, M. Abe, Mori, O'Connor, Ohsaki & Zheleznova 2015a). Given the fact CNIs were unable to alter ΔΨm, a major step in production of mitochondrial ROS (Murphy 2009), it is fair to postulate that mitochondria are unlikely to be sources of superoxide or ROS. This was unable to be investigated due to poor loading of MtioSox in live kidney tissue therefore the majority of the discussion will be focused on NOX ROS production.

NADPH oxidases are a family of ROS producing enzymes consisting of seven isoforms: NOX1, NOX2, NOX3, NOX4, NOX5, Doux1 and Duox2 (Kawahara *et al*. 2007). Under normal conditions, NADPH derived ROS play important roles in many cellular signalling pathways and defences including regulation of ion channels, gene expression and cell growth (Kaelin 2005; Sedeek *et al*. 2010). However under stress, cells overproduce ROS, which can lead to lipid peroxidation and membrane damage (Murphy 2009) and have been linked to several renal diseases including ischemia reperfusion, allograft rejection and glomerulonephritis (Baud & Ardaillou 1986). NADPH oxidase is well expressed within the kidney with NOX1 and 4 being the dominant isoforms (Nistala *et al*. 2008). There is a prominent expression of NOX 1 and 4 in renal vessels, glomeruli, thick ascending loop of Henle, distal tubules, collecting ducts and macula densa (Gill & Wilcox 2006).

It is now well established that ROS production has a role to play in CNI-induced nephrotoxicity, however to what extent, is still unknown. Both CsA and FK506 have been shown to up-regulate eNOS in cultured endothelial cells and would initially suggest a protective role through the subsequent production of NO and vasodilation (LopezOngil *et al*. 1996; Navarro-Antolin *et al*. 1998). However this upregulation of eNOS proceeds the initial production of ROS as the cells try to overcome excess production of ROS and decreased bioavailability of NO. NO rapidly reacts with ROS to form peroxynitrite, an alternative source of ROS, which ultimately reduces NO bioavailability, reduces vasodilation and promotes platelet aggregation and leukocyte aggregation (Muller & Morawietz 2009). As discussed previously in chapter 1, CNI-induced ROS production has also been shown to be involved in ANG II-mediated hypertension. Nishiyama *et al* and Chander *et al* have both shown that treatment with CNIs increase the production of ANG II and subsequent increased levels of circulating ROS (Nishiyama, *et al*. 2004). Authors found that Inhibiting ANG II signalling with specific AT1 receptor antagonists resulted in a reduction in the level of ROS

production, significant reduction in hypertension and overall nephrotoxicity was attenuated. In addition, CNI-induced ROS production has been shown to increase independent of ANG II production (Jennings *et al*. 2007; de Arriba *et al*. 2013). This suggests CNIs are capable of ROS production through various pathways and makes identification of specific therapeutic targets even more challenging.

Importantly, ROS production was not induced *via* rapamycin, which correlates to current literature and clinical observations that demonstrate rapamycin's inability to induce ROS production in cell lines but also in human transplant settings (Arceci *et al*. 1992; Tunon *et al*. 2003; Shin *et al*. 2011; MacDonald 2003). Given the fact rapamycin failed to induce pericyte-mediated vasoconstriction and also failed to induce ROS production whereas both CNIs had the opposite effect, it could be suggested that ROS signalling may be involved in CNI-mediated vasoconstriction and potentially CNI-induced nephrotoxicity, as has been demonstrated in animal models with increased free radical production correlating to nephrotoxicity (A. Y. Zhou & Ryeom 2014).

ROS production within the cortex has already been shown to be influential in the regulation of tubuloglomerular feedback (Wilcox & Welch 2000) and the response of vasa recta to ischemia (Z. Zhang *et al*. 2004; Cowley *et al*. 2015a). Importantly, pericytes have been shown to constrict vasa recta in response to ROS but also pericyte-mediated constriction was inhibited *via* SOD or ROS scavengers (Z. Zhang *et al*. 2004; Cowley, M. Abe, Mori, O'Connor, Ohsaki & Zheleznova 2015a; Crawford *et al*. 2012). Taken together, evidence suggests renal pericyte are able react to surrounding NO and ROS levels and modulate medullary blood vessels in response to ischemia and toxic insult. With CNIs able to produce superoxide within the medulla, it is reasonable to suggest that CNI-mediated vasoconstriction of vasa recta could be mediated through ROS signalling and decreased bioavailability of NO.

Interestingly, new research has demonstrated the beneficial effects of inhibiting ROS production induced by CNIs. One particular study by Ciarcia *et al* used the specific NADPH oxidase inhibitor, apocynin, to reduce all haemodynamic changes seen with CsA administration along with a reduction of ROS production and increase in NO bioavailability (Ciarcia *et al*. 2015). Importantly, this was carried out *in vivo* using animal models, highlighting the physiological relevance ROS inhibition may have in the human setting. Despite the fact NADPH oxidase is thought to be responsible for over 50% of renal ROS production (Gill & Wilcox 2006; Cowley *et al* 2015a), this approach to attenuate ROS has been poorly investigated, with the majority of

research focusing on reduction of ROS rather than preventing its production. Damiano *et al* used a recombinant manganese SOD in CsA treated rats to significantly reduce the ROS-mediated haemodynamic alterations induced *via* CsA and also demonstrate the attenuated renal morphological lesions seen with CsA (Damiano *et al*. 2013). Their data suggests that ROS is somewhat responsible for both the reduction of renal blood flow (acute nephrotoxicity) but also the morphological changes downstream of altered RBF seen after CNI therapy (chronic nephrotoxicity).

Wang *et al* highlighted the role of lipid peroxidation in response to ROS generation after CNI administration (Wang & Salahudeen 1995). The data suggested that CNIs are able to increase significant levels of atherosclerosis in transplant recipients and the source of ROS could stem from cytochrome P-450 (CYP 450) metabolism of CNIs producing the hydroxyl radical. CYP 450 activation induces superoxide production (Freeman & Crapo 1982), therefore metabolism of CNIs would result an excess production of ROS through direct (eNOS and mitochondrial ROS) and indirect (CYP 450 metabolism and increased ANG II) mechanisms. Importantly, the author's data also demonstrated the significant attenuation of ROS and associated renal injury after the use of vitamin E for ROS scavenging, again suggesting a role of ROS production in CNI nephrotoxicity.

The results produced in this chapter have highlighted the use of an NADPH oxidase inhibitor for prevention of CNI renal damage. Apocynin was able to significantly attenuate the CNI-induced production of ROS, more specifically, superoxide, which has been shown to effect the renal medullary microcirculation (Zou *et al*. 2001; Taylor *et al*. 2006; Cowley *et al* 2015a) and constrict vasa recta *via* pericytes (Z. Zhang *et al*. 2004), which is in fitting with data presented in this chapter. NADPH oxidase has been shown to be expressed on retinal pericytes (Mustapha *et al*. 2010) and NADPH oxidase derived ROS is responsible for increased pericyte apoptosis and can be attenuated using apocynin in diabetic retinopathy (Mustapha *et al*. 2010), evidence that further emphasises a link between ROS and pericyte-mediated vessel constriction.

As mentioned in the results section of this chapter, changes in DHE fluorescence occurred initially in the vascular compartment and were significantly greater than changes measured in the tubules. This indicates the vascular compartment is more sensitive to changes in local ROS and is in fitting with observations in which CsA and FK506 resulted in changes in vessel diameter. Localised changes in blood flow would

thus impact upon tubular function, which is in fitting with clinical observations of altered GFR before alterations in tubular function.

Taken together, along with results produced in this chapter, it is clear that ROS are involved in CNI nephrotoxicity. Given that ROS are capable of inducing pericyte-mediated vasoconstriction and prevention of ROS *via* apocynin, an NADPH oxidase inhibitor, attenuates the haemodynamic changes induced by CNIs, it is not unreasonable to suggests targeting NADPH inhibition therapeutically would be an excellent strategy for the reduction of pericyte-mediated vasoconstriction of ensuing CNI nephrotoxicity.

7. General discussion, conclusions, and future work

The calcineurin inhibitors cyclosporine A and tacrolimus have been at the forefront of solid organ transplantation for the past thirty years. Their introduction at the time revolutionised allograft function and 1-year graft survival post-transplantation rates are now at over 90% (Haynes *et al*. 2013). Their use however has been hampered by their unwanted side effects including hypertension, glucose intolerance and nephrotoxicity. The incidence of CNI-induced nephrotoxicity is 30% (1 year after renal transplant) following onset of treatment (Nankivell *et al*. 2003) and has been shown in 100% of patients 10 years post transplant (Nankivell *et al*. 2004). Interestingly, the mechanisms underlying CNI-induced nephrotoxicity are still poorly defined, with a combination of factors including increased vasoconstriction, reduced vasodilation and sympathetic nerve activation all thought to play a part in renal decline.

This study set out to investigate the effects of CNIs on the renal medullary microcirculation, of which there is little research, and primarily their effects on renal pericytes. Given that CNIs are already known to reduce renal cortical blood flow as measured by changes in GFR and this evidence together with an established role for pericytes as renal medullary blood flow regulators, the effect CNIs have on medullary blood flow is yet to be investigated and may enhance our understanding of the cellular mechanism underlying the pathogenesis of CNI-induced nephrotoxicity.

In this thesis, data presented in chapter 3 shows for the first time the contractile effect CNIs have on renal medullary pericytes. The reduction in diameter of vasa recta *via* pericytes is most likely to impede medullary blood flow, given that using Poiseuille's law as an estimate of changes in blood flow (BF) assumes laminar flow, a 10% decrease in diameter would result in an 1.5 fold increase in vessel resistance (Crawford *et al*. 2012). Furthermore, the mTOR inhibitor, rapamycin, failed to induce any significant changes in vasa recta diameter, which is in fitting with clinical observations that suggest a reduction in the extent and manifestations of rapamycin associated nephrotoxicity.

The majority of research that has been conducted on CNI-induced nephrotoxicity, with respect to renal blood flow, has concentrated on the larger afferent and efferent arterioles of the glomerulus (Naesens *et al*. 2009). Very little information regarding any renal microvasculature modifications is available. Not surprisingly, this might

reflect the previous understanding of how medullary flow was thought to be regulated. Upstream regulation *via* afferent and/or efferent vasoconstriction/dilation was recognised as the main pathway for medullary blood flow alterations (R. G. R. Evans *et al*. 2004), all changes in capillary blood flow being assumed to be passive. However, in recent years, the role of pericyte cells in regulation of medullary blood flow has received a significant amount of attention. Pallone and colleges carried out much of the early research, which suggested pericytes were able to adapt to surrounding conditions and/or endogenous stimuli to regulate vasa recta diameter independent of arteriole flow (Pallone & Silldorff 2001). In addition, given that MBF accounts for less than 1% of total renal blood flow and yet its regulation is essential for maintenance of the cortico-meduallry gradients and delivery of oxygen and nutrients (Kennedy-Lydon *et al*. 2012), it is not perhaps surprising that regulation of this highly specialized region would not be passive and is tightly regulated.

It is well known that CNIs induce increased vasoconstriction and reduced vasodilation of the renal vasculature through alteration in the bioavailability of a variety of endogenous compounds. These include an increase of ANG II, ET and thromboxane, and a decrease of NO, PGE_2 and COX-2 expression (Naesens *et al*. 2009). Interestingly, all the aforementioned compounds have also been shown to constrict or dilate vasa recta *via* pericytes (Crawford *et al*. 2012; Crawford *et al*. 2013; Rhinehart & Pallone 2001b; Pallone 1994; Silldorff *et al*. 2002). In addition, it has been shown that dysregulation of medullary blood flow can actually precede any changes seen in cortical flow (Mattson *et al*. 1992). Yagil was able to demonstrate the detrimental effects CsA has on post-transplant kidneys, concentrating on total renal blood flow. The author used post-ischemic kidneys injected with FITC-labelled ϒ-globulin in rats and fluorescence microscopy readings at papilla to estimate erythrocyte velocity as a readout of vasa recta blood flow and highlighted the significant reduction of both renal cortical and medullary flow after CsA administration (Yagil 1990).

Taken as a whole, evidence presented here in combination with data yielded from previous studies indicate CNIs may have a more profound effect on medullary blood flow than previously thought and may even be an initial step in the progression of nephrotoxicity.

Data presented in chapter 4 concentrated on investigating the effect of combining antihypertensives with CNIs on CNI-mediated contraction of vasa recta based on

clinical evidence showing that over 90% of post operative renal transplant patients will develop some form of hypertension (First *et al*. 1994; Textor *et al*. 1994).

The data regarding the specific mechanism underlying the pathogenesis of CNI-induced hypertension varies, some clinicians will suggest only the vasculature is involved will others only identify sympathetic nerve activation as responsible, as being compliant due to its action on vessels (Hoorn *et al*. 2012). Interestingly, Hoorn *et al* have identified a form of salt-sensitive hypertension after CNI treatment that was mediated through NCC in the distal convoluted tubule (Hoorn *et al*. 2011), indicating a tubular contribution to CNI-mediated hypertension. Since the risk factors for hypertension after renal transplantation include both donor and recipient elements it is almost impossible to identify a single cause and thus the precise pathogenesis is highly complex.

Regardless of the causal mechanisms, it is now known CNI-induced hypertension can be controlled pharmacologically with a wide variety of antihypertensive agents. Angiotensin II receptor inhibitors (ARIs) have been used to treat CNI-induced hypertension since it was first discovered that CsA is able to increase circulating ANG II concentrations. Although many trials have investigated ARIs for their ability to prevent CNI-induced hypertension, their relative efficiency in doing so is still unclear. Inigo *et al* demonstrated the insignificant effect losartan had on improving GFR in transplant patients, although slightly reducing blood pressure (Iñigo *et al*. 2001) while Rastghalam *et al* postulated that complete blockade of ANG II was of no use at all for prevention of hypertension and CNI-mediated nephrotoxicity (Rastghalam *et al*. 2014). The results in this chapter suggest CNI-induced vasoconstriction of vasa recta in not mediated through ANG II acting at AT-1 receptors since losartan failed to inhibit pericyte constriction of either CsA or FK506. Interestingly, ANG II has been shown to significantly induce pericyte vasoconstriction of vasa recta *in vitro* and *in situ* (Pallone 1994; Crawford *et al*. 2012) and losartan has been shown to successfully inhibit *in vitro* and *in situ* pericyte vasoconstriction mediated *via* ANG II in these studies (Rhinehart *et al*. 2003; Crawford *et al*. 2012). As seen in figure 1.8 of the general introduction, ANG II has direct and indirect mechanisms of vasoconstriction within the kidney and taken together, it can be postulated that although production of ANG II is increased after CNI treatment, its effects on medullary blood flow may not be direct and pericyte mediated vasoconstriction could be through an alternative pathway, ANG II mediated ROS production, endothelin production or decreased bioavailability of NO for example.

Although ANG II receptor inhibition failed to prevent CNI-induced vasoconstriction in this study, a variety of other antihypertensive agents were more successful. Hydrochlorothiazide (HCT) was able to significantly reduce CNI-mediated pericyte-evoked constriction of vasa recta. Typically used for oedema treatment and hypertension, HCT has now been suggested to prevent CNI-induced hypertension. The initial data for this hypothesis was adapted from Hoorn *et al* who demonstrated a direct upregulation of NCC in the distal tubule of animals after treatment with FK506 (Hoorn *et al*. 2011). Subsequently the induced salt-sensitive hypertension in mice was attenuated by NCC inhibition. HCT is a NCC inhibitor; therefore using HCT would prevent NCC activation and result in an attenuated salt- sensitive hypertensive response after CNI administration. How HCT is able to directly attenuate CNI-induced vasoconstriction *via* pericytes in the medulla is still unclear, however HCT has been shown to have direct vasodilatory effects on a variety of blood vessels (A. D. A. Hughes 2004; Pickkers *et al*. 1998) and even inhibit intracellular calcium signalling in isolated cells which is essential for contraction (SandstrÃ m 1993). Together, these results suggest HCT acts to relax VSMC's leading to vasodilation. Although not SMC themselves, pericytes have similar contractile properties to SMC and express similar components of the contractile machinery (Shepro & Morel 1993) and even similar levels of cyclic GMP (an enzyme in high concentrations of VSMCs used for dilation) (Joyce *et al*. 1984).

Intriguingly, it has been shown that increased sodium and water uptake in the medullary thick ascending limbs of Henle increases the production of medullary ROS (Cowley *et al* 2015a) therefore HCT-mediated inhibition of this excess reabsorption, through the NCC, could prevent the production of ROS and attenuate the potential ROS-mediated vasoconstriction of vasa recta by pericytes in the presence of CNIs. Crawford *et al* were able to use a hypotonic insult within the live kidney slice to produce an ATP-mediated vasodilation of vasa recta (Crawford *et al*. 2012). Using HCT at high concentrations (500 μM) has been shown to induce hypotonic shock in isolated tubules (Lajeunesse & Brunette 1991) therefore possibly result in a hypotonic shock of tubular epithelial cells and subsequently release ATP, thus further highlights the role of tubulovascular crosstalk and how signaling molecules, NO and ATP from the above examples, from nearby structures could mediate local adaptions of blood flow in response to particular stress stimuli.

The results from chapter 4 also suggest a role of calcium signaling in CNI-mediated vasoconstriction. Diltiazem and isradipine are both calcium channel antagonists and although different in molecular structures and channel efficacy, they both primarily inhibit voltage-dependent calcium channel activation. Both diltiazem and isradipine were able to inhibit CNI-induced vasoconstriction of vasa recta and further helps identify a molecular mechanism underlying CNI-mediated constriction and suggest for their use against the prevention of CNI-induced hypertension. However, this observation is not new, calcium channel blockers (CCBs) have been used to treat CNI-induced hypertension (Rahn *et al*. 1999) and confirmed *via* the major randomized study by Midtvedt *et al* who revealed their superior antihypertensive property compared to ACE inhibitors (Midtvedt *et al*. 2001) and interestingly, the beneficial use of specifically diltiazem and isradipine for CNI-induced hypertension has also been confirmed by other studies (Ingsathit *et al*. 2006; Xue *et al*. 2010; Bursztyn *et al*. 1997; van den Dorpel *et al*. 1994; Becker *et al*. 1996; van Riemsdijk *et al*. 2000).

Further highlighting the role of calcium inhibition for prevention of hypertension, vasa recta constriction has been show to be mediated through voltage gated calcium entry. Using fluorescence and electrophysiological techniques, Zhang *et al* were able to demonstrate that pericyte contractility is controlled through variations of membrane potential and voltage-gated calcium entry into pericytes (Z. Zhang *et al*. 2002). In addition, the authors were also able to show the inhibitory and vasodilatory effects diltiazem had on agonist-induced vasoconstriction and preconstricted vasa recta, respectively. This undoubtedly emphasizes the role of calcium signaling in pericyte constriction but also strongly suggests a mechanism for CCB inhibition of CNI-mediated vasoconstriction. This hypothesis is further supported by the notion of increased calcium signaling in VSMCs after treatment with CsA (Avdonin *et al*. 1999; Grzesk *et al*. 2012; Meyer-Lehnert *et al*. 1993). Although calcium channel inhibition did not completely abolish the vasoconstrictive effects of CNIs, CCBs do not inhibit the regulation of intracellular calcium signaling. Rises in intracellular calcium have been shown to constrict pericytes independent of extracellular calcium entry (Borysova *et al*. 2013; Shepro & Morel 1993; Q. Zhang *et al*. 2006; Z. Zhang *et al*. 2002) therefore offers a possible mechanism for contraction independent of calcium entry.

The combined results of chapter 4 therefore parallel clinical observations regarding CNIs and antihypertensives. Although the exact mechanisms for protective pathways are unclear, specifically the contribution of NCC-mediated inhibition of pericyte contraction, data here further highlights that a better understanding of the medulla microcirculation and future studies to this end can only enhance our knowledge of all possible mechanisms involved in CNI-mediated nephrotoxicity and can help identify novel inform strategies for the prevention of CNI nephrotoxicity.

One of the intentions of this thesis was to develop an *in situ* perfusion model for the use within the live kidney slice to better simulate the blood perfused mode of drug delivery to the inner medulla. Data presented in chapter 5 includes data yielded following setup and validation of this model and further investigates the effects of perfusing vasa recta with CNIs to offer a potentially enhanced understanding of CNIs and MBF. The results indicate that when perfused, CNIs have an enhanced contractile effect, their role in regulation of vasa recta *via* their action at pericytes is enhanced compared to superfusion, and as such are likely to contribute to CNI-mediated medullary ischemia and nephrotoxicity. The results from this chapter suggest an endothelial cell to pericyte signal transduction pathway is involved in mediating the contractile effects seen in response to both perfusion of CsA and FK506. Interestingly, the communication between endothelial cells and pericytes has already been explored. Recently, Zhang *et al* suggested a role of DVR endothelium as an electrical syncytium (Q. Zhang *et al*. 2006). Their results suggest that depolarizing or hyperpolarising waves are spread between cells to regulate vasomotin *in vivo* and that DVR gap junctions facilitate passage of signaling molecules (cAMP, Ca^{2+} and NO for example) between endothelial cells and pericytes to alter vessel diameter by their action as endothelium-dependent (hyper) depolarising agents. Furthermore, superoxide is produced by pericytes and therefore may be directed across myoendothelial junctions to limit the bioavailability of NO (Z. Zhang *et al*. 2004) further highlighting a role of ROS for pericyte mediated vasoconstriction.

Several studies have already identified the expression of tight, gap and adherence junctions between pericytes and endothelial cells (Cuevas *et al*. 1984; Tilton *et al*.

1979; Gerhardt *et al*. 2000; Gerhardt & Betsholtz 2003). This evidence, coupled to the fact calcium signaling has already been established between pericytes and endothelial cells (Z. Zhang *et al*. 2002; Borysova *et al*. 2013; Rhinehart *et al*. 2003), strongly suggests that communication between these two linking cells is through a variety of complex pathways. Furthermore, it has also been demonstrated that communication between these cells can be independent of each other but interestingly, also communicate under certain stimuli to affect the regulation of other cells. This was highlighted by Zhang *et al* who were able to stimulate vasa recta pericytes to induce an escalation of NO production from endothelial cells that were down stream from the pericyte itself and not necessarily in contact with the pericyte cell body or processes (Q. Zhang *et al*. 2006). In addition, Peppiatt *et al* were able to demonstrate pericyte to pericyte communication in retina (Peppiatt *et al*. 2006) highlighting the complex signaling mechanisms that pericytes have developed. Whilst it is known that CNIs are known to constrict the larger afferent arterioles of the glomerulus (although no specific mechanism has been defined), the data presented here demonstrates for the first time the ability of CNIs to induce vasoconstriction of vasa recta *via* pericytes when luminally perfused. This could have detrimental effects with regards to allograft dysfunction since pericytes have an essential role in the regulation of MBF (Pallone, Z. Zhang, *et al*. 2003) and pericyte-mediated contraction may play a role in medullary ischemia. With a transplanted kidney already being subjected to possible hours of ischemia, then subsequently exposed to ischemia reperfusion, an already established mechanism known to underlie transplant dysfunction (Regner & Roman 2012; Mittal & Kohli 2014), the further CNI-mediated contraction of vasa recta may lead to chronic medullary ischemia in an already borderline hypoxic region of the kidney. Thus the importance of correct regulation of blood flow in the medulla is fundamental in maintaining function in transplanted kidneys.

Interestingly, during allograft transplant, ROS are known to increase during both ischemia and reperfusion and play a central role on the pathophysiology of allograft dysfunction (Raedschelders *et al*. 2012). Given the fact CNIs are also known to produce ROS during allograft transplant (A. Y. Zhou & Ryeom 2014; Nishiyama, *et al*. 1998) and that the medullary microcirculation is particularly susceptible to changes in ROS production (Cowley *et al* 2015a; Wilcox 2002), investigating this

pathway for a possible mechanism underlying CNI-induced vasoconstriction would highlight a significant area in which the attenuation or prevention of CNI-induced vasoconstriction and nephrotoxicity might be further explored.

Chapter 5 of this thesis investigates specific molecular mechanisms of CNI-induced vasoconstriction. Using multiphoton microscopy to delineate changes in molecular events highlighted the importance of NADPH oxidase in the generation of medullary ROS following treatment of live tissue with CNIs. Furthermore, data here suggests the use of specific NADPH inhibitors could potentially offer a defensive role against CNI-mediated oxidative damage and chronic nephrotoxicity.
It is now known in the literature that CNIs are able to induce cellular and morphological changes of mitochondria to bring about larger upscale organelle and tissue damage. De Arribia *et al* have suggested a central role for mitochondria damage in CsA-mediated nephrotoxicity. Their hypothesis includes an increase of mitochondrial ROS production leading to cytochrome C release and cellular apoptosis, formation of pores in the outer mitochondrial membrane, again, leading to cytochrome C release and altered mitochondrial energy dynamics which could possibly lead to mitochondrial fission and apoptosis (de Arriba *et al*. 2013). Their hypothesis has been some what confirmed by other groups who have similarly demonstrated mitochondrial ROS production *via* CsA (Perez de Hornedo *et al*. 2007; van der Toorn *et al*. 2007) and also pore formation (Brustovetsky & Dubinsky 2000; Friberg *et al*. 1998) but both so far fail to determine CsA-induced mitochondrial fission leading to apoptosis thus the precise mechanisms remain unclear. The results of this chapter have also unfortunately failed to confirm any of these findings. The live kidney slice was unable to be loaded with the mitochondrial specific ROS dye MitoSOX therefore, although CNI's may have increased mitochondrial ROS, it could not be detected. In addition, CNIs failed to (hyper) depolarize the mitochondrial membrane, which has been previously highlighted as a preceding requirement before an increase in ROS production (McBride *et al*. 2006; Murphy 2009). Interestingly, depolarization has also been indicated as an after effect of ROS production in isolated cells rather than a precursor event (de Arriba *et al*. 2013; Perez de Hornedo *et al*. 2007), therefore it is somewhat unclear to what extent mitochondria membrane potential plays in mitochondrial ROS production in

CsA-mediated toxicity. Intriguingly, this chapter has emphasized the role of cyclophiln D in the formation of the mitochondrial permeability transition pore required for mitochondrial transition upon insult. CsA was able to inhibit pore formation induced by chenodeoxycholate and thus preventing mitochondrial membrane depolarisation, hypothetically through CsA-Cyp-D binding, while tacrolimus and rapamycin failed to inhibit pore formation. This suggests a conceivable role for CsA in the protection of mitochondria damage by preventing mitochondria transition to apoptosis after insult. This theory has already been confirmed in multiple studies for myocardial ischemia reperfusion injury (Piot *et al*. 2008; Raedschelders *et al*. 2012; Abdallah *et al*. 2011; Halestrap *et al*. 2004) and demonstrates the protective role CsA can have under certain conditions.

Nonetheless, CsA and FK506 are known to induce ROS production and based on the results of this chapter, it is feasible to suggest they are able to induce an increase of medullary ROS *via* other non-mitochondrial pathways. Medullary ROS have been suggested to partake in a variety of roles including regulation of MBF, sodium homeostasis and hypertension (Cowley *et al* 2015a). In addition, it has also been demonstrated that DVR pericytes are able to induce ROS as well as constrict in response to ROS (Rhinehart & Pallone 2001b; Edwards *et al*. 2011; O'Connor & Cowley 2012; Cowley *et al* 2015a). Taken together, for the first time, it is feasible to suggest that CNI therapy could cause medullary ROS production, as well as cortical ROS, which acts to constrict vasa recta *via* pericytes and contribute towards hypertension and nephrotoxicity. This offers a novel possible mechanism contributing towards CNI nephrotoxicity and sheds a new light in understanding the role dysregulation of MBF may have in this destructive condition.

This chapter also demonstrates the potential protective effect NADPH oxidase inhibition has on attenuation of CNI-mediated production of ROS and associated nephrotoxicity. Currently, the majority of the literature regarding CNI-induced ROS involves its production in the cortical region of the kidney and focuses on ROS scavenging. Very little, if any, focuses on the role of medullary ROS and preventing its production rather than post-hoc scavenging. Given that NADPH oxidase accounts for over 50% of ROS production in the kidney (Cowley *et al* 2015b) and typically, prevention of production may be more efficient that scavenging, it seems logical to target the site of production of the biggest source of ROS with the hope of

attenuating its production and reducing the onset of oxidative damage. Interestingly, it has been shown that CNIs increase NADPH expression and activity within the kidney after renal transplant (Khanna & Pieper 2007) inevitably increasing ROS production. Furthermore, Ciarcia *et al* used a specific NADPH inhibitor, apocynin, to completely ameliorate the acute hemodynamic and chronic morphological changes seen with CsA in rats which is in fitting with data provide here (Ciarcia *et al*. 2015). Moreover, this chapter has also highlighted medullary blood vessels as the initial sources of ROS suggesting vasa have a more influential role in the progression of nephrotoxicity than first perceived. For example, Buffoli *et al* have used a polyphenol to restore morphological fibrotic changes in the cortex induced by CsA, however medullary fibrosis, especially around vasa recta, was still evident suggesting prolonged irreversible damage (Buffoli *et al*. 2005). The results from this chapter further demonstrates the ability of apocynin to inhibit CNI-induced ROS production within the medulla, and highlights its potential role n the attenuation of medullary ROS production and reduced risk for the development of CNI-induced nephrotoxicity. A schematic diagram for possible mechanisms involved in CNI-induced pericyte-evoked constriction of vasa recta can be seen in figure 7.0.

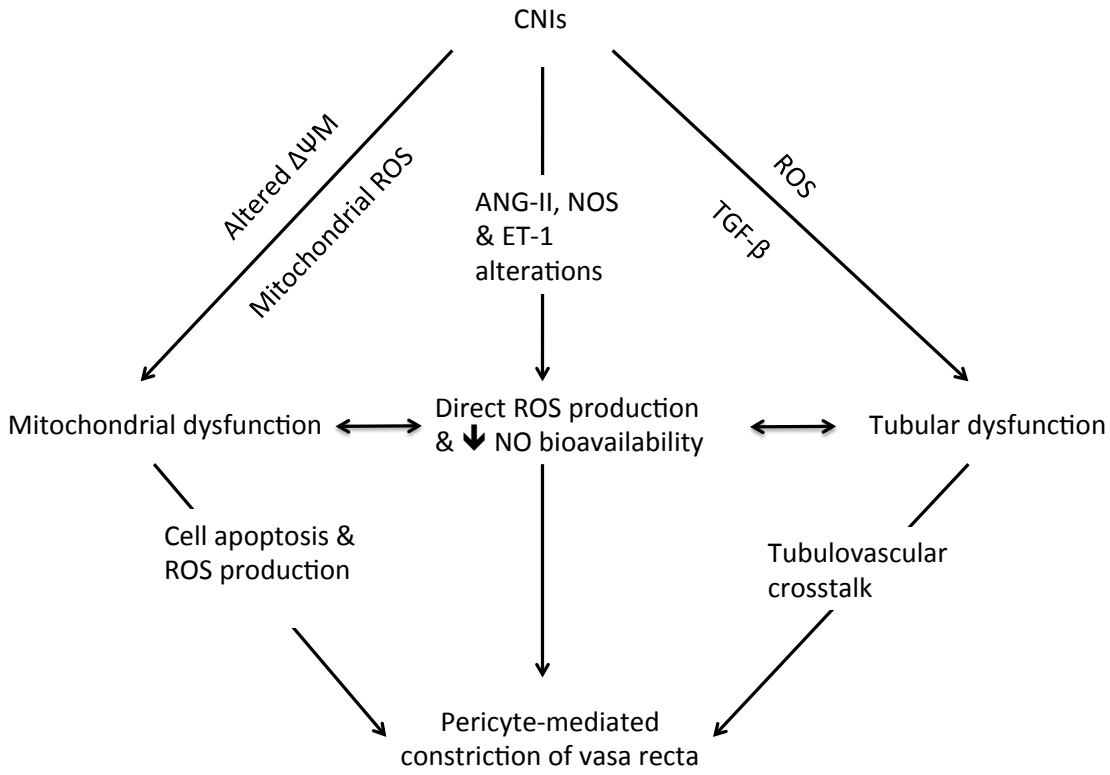

Figure 7.0 Schematic diagram highlighting possible pathways involved in CNI-mediated pericyte-evoked constriction of vasa recta. Summary of possible pathways involved in CNI-mediated constriction of vasa recta *via* pericytes. CNIs, calcineurin inhibitors; ROS, reactive oxygen species; TGF-β, transforming growth factor; ET-1, endothelin 1; NO, nitric oxide; ΔΨM, mitochondrial membrane potential.

7.1 Limitations and future work

Although this thesis has demonstrated for the first time the ability of CNIs to induce ROS generation, which is linked to vasa recta constriction *via* pericytes, the work carried out is not without its limitations.

Firstly, while pericyte vasoconstriction reduced vasa recta diameter, it cannot be directly associated with reduced MBF. The live kidney slice preparation is unable to measure flow therefore any reduction in diameter is assumed to result in reduced flow and not is directly measured *per se*. However, given that CNI-mediated changes in vessel diameter in the cortex, which can directly alter flow, it is reasonable to assume similar mechanisms exist in the medulla and are mediated by contraction of pericytes rather than VSMC's.

Secondly, perfusion of *in situ* single vasa recta has increased our understanding the role tubulovascular crosstalk has in regulation of MBF and communication between structures. However, the perfusion in this thesis did not allow perfusate exchange and therefore does not directly replicate *in vivo* physiological conditions. Future work would enable a perfusate exchange system to be established, although this is highly dependent on equipment and technical expertise but would support a similar system seen with isolated perfusion that enables researchers to carry out perfusate exchange. Excitingly, the technical equipment required could possibly investigate the decreased flow measurement as mentioned above through similar analytical techniques used for isolated perfused tubule experiments. Particular isolated perfusion experiments allow the perfusate to be collected after perfusion through hollow structures. If the same technique were carried over to the live slice model, collection of perfusate could be analysed to identify alterations in sodium or other ion concentrations to identify possible endothelial cell to pericyte interactions under normal physiological conditions. However, under pericyte vasoconstriction from an exogenous bath application of vasoconstrictor for example, the collected perfusate could be compared to the control conditions to help identify possible alterations of salt concentrations or even signalling molecules that could be important in endothelial cell and pericyte communication.

As highlighted in the discussion section of chapter 4, it was suggested that a high K^+ membrane depolarisation experiment, following application of CNI and CCB, should be carried out to assess reversibility of Ca^{2+} inhabitation and ability of isradipine and diltiazem to be washed out of the experimental setup. The membrane depolarisation of K^+ after CCB wash would highlight a possible mechanism for pericyte-mediated vasoconstriction of DVR in response to CNI's, and suggest CNI's are able to directly affect either pericyte membrane potential or through EC membrane potential which could hypothetically induce pericyte depolarisation through gap and hetrocellular gap junctions. Previously, Zhang *et al* have highlighted the use of a high K^+ bath solution to induce membrane depolarisation of pericytes in their isolated perfused DVR technique (Z. Zhang *et al*. 2002) however due to the nature of the isolated technique, it is unclear to which site depolarisation commences, either EC's or pericytes. Nonetheless, the authors where able to demonstrate the inhabitation of depolarisation through use of diltiazem (Z. Zhang *et al*. 2002). Although not presented in the author's manuscript, personal correspondence with the authors have stated the

inhibition was reversible with CCB's and could be washed out after several experiments. This was highlighted due to the fact isolated perfused DVR can be used for more than one experiment due to the washable nature of the setup and timely manor these types of experiments take.

Future experiments in the live slice model with a high K^+ solution after CNI and CCB exposure would highlight a possible mechanism for CNI-induced vasoconstriction *via* pericytes and could be further investigated with perfusion in combination with Ca^{2+} fluorescent probes and imaging techniques to establish the site of membrane depolarisation. Identifying the initial site of depolarisation, most likely through EC's if perfusion was used, could help pinpoint a possible mechanism for CNI-mediated pericyte vasoconstriction and novel therapeutic strategies for the prevention of reduced RMBF and acute nephrotoxicity after CNI therapy.

The multiphoton data presented here highlights the role ROS may potentially have in regulation of MBF during CNI therapy. Although not directly measurable, the increased production of ethidium fluorescence suggests that an increase of superoxide may be responsible for pericyte vasoconstriction. This could be further investigated using functional DIC experiments with apocynin to ascertain the degree ROS play in pericyte vasoconstriction.

Additionally, using MPM with *in situ* perfusion of vasa recta opens a wide variety of experiments to investigate the molecular mechanism involved in CNI-induced vasoconstriction. For example, experiments using calcium imaging, researchers could confirm the role of pericyte/endothelium interactions after CNI perfusion to help identify temporal calcium signalling and how this correlates to changes in vessel diameter. Moreover, to what degree calcium signal propagations affect surrounding tissues like collecting ducts and ascending limbs could be investigated to include CNI-mediated tubulovascular cross talk. This would offer further insight and may help identify potential novel mechanisms for combating progression of CNI nephrotoxicity.

Although the use of the SD rat model for investigations into acute renal injury has been well documented and even used to this day (Bach 2013), the effects of CNI's on small animal renal function are less well understood. For example, administration of CNI's to animal models in similar doses received by patients, on a weight basis, produces significantly lower incidences of acute or chronic renal dysfunction (Yang *et al* 2010) and can only be enhanced with extremely high concentrations of CNIs or a

low salt diet to exacerbate the nephrotoxic effects (Coffman 1991). Studies have demonstrated that there is substantial variation between species, strains and sex in response to CsA and development of nephrotoxicity. Interestingly, the use of rat and mouse models for investigating human disease settings has always been speculative. For example, in experiments where the exact same application can be applied to animals and humans (skin tests), only around 60% of abnormalities correlate between the two. Interestingly, only around 70% of side effects for CNI's are found between rodent species (Hartung 2008). Therefore it is clear that species differences are not only important for human interpretation but also for members of the same animal family. This is highlighted by early animal studies for investigation into CNI toxicity with little or no evidence of nephrotoxic side effects (Whiting *et al*. 1985). This oversight clearly demonstrated the need for alternative investigative models for nephrotoxicity and even to this day, valuable models such as single cell line studies are often overlooked with investigators proceeding straight to *in vivo* models (Whiting *et al*. 1982).

Although this study utilised SD tissue slices for interpretation of the effects CNI's have on renal pericytes, it has been previously shown that renal DVR pericytes from humans and rats have similar contractile responses after exposure to vasoconstrictors (Sendeski *et al*. 2012). Ideally, human tissue would be ideal to investigate such effects of CNI's however is outwith the scope of this study and intriguingly, it has been shown that SD histology of CNI nephrotoxicity is similar to that of the human setting with similar histological lesions being observed and no other species studied at present overs any particular advantage to replicating the human setting in response to CNI's (Whiting *et al*. 1982).

Although animal models have been useful in highlighting the possible mechanisms of CNI induced vasoconstriction and development of nephrotoxicity, they fail to replicate the pharmacokinetic and pharmacodynamics humans have, as well as different tolerances for the drugs themselves.

With advances in molecular biology and development of new single cell lines, it could be postulated that identification of single mechanisms that are crucial for CNI nephrotoxicity may help alleviate the underlying causes of renal cell dysfunction and identify novel therapeutic strategies.

8. References

Abdallah, Y. *et al*., 2011. Interplay between Ca2+ cycling and mitochondrial permeability transition pores promotes reperfusion-induced injury of cardiac myocytes. *Journal of cellular and molecular medicine*, 15(11), pp.2478–2485.

Abraham, F. *et al*., 2012. Angiotensin II activates the calcineurin/NFAT signaling pathway and induces cyclooxygenase-2 expression in rat endometrial stromal cells. S. R. Singh, ed. *PLoS ONE*, 7(5), pp.e37750–e37750.

AL, N. *et al*., 1996. Cyclosporin A delays mitochondrial depolarization induced by N-methyl-D-aspartate in cortical neurons: evidence of the mitochondrial permeability transition. *Neuroscience*, 75(4), pp.993–997.

Alvarez-Arroyo, M.V. *et al*., 2002. Cyclophilin-mediated pathways in the effect of cyclosporin A on endothelial cells: role of vascular endothelial growth factor. *Circulation research*, 91(3), pp.202–209.

Amore, A. *et al*., 1995. A Possible Role for Nitric-Oxide in Modulating the Functional Cyclosporine Toxicity by Arginine. *Kidney international*, 47(6), pp.1507–1514.

Andoh, T.F. *et al*., 1996. Synergistic effects of cyclosporine and rapamycin in a chronic nephrotoxicity model. *Transplantation*, 62(3), pp.311–316.

Aparicio, L.S. *et al*., 2013. Hypertension: The Neglected Complication of Transplantation. *ISRN Hypertension*, 2013, p.10.

Arceci, R.J., Stieglitz, K. & Bierer, B.E., 1992. Immunosuppressants FK506 and rapamycin function as reversal agents of the multidrug resistance phenotype. *Blood*, 80(6), pp.1528–1536.

Armstrong, V.W. & Oellerich, M., 2001. New developments in the immunosuppressive drug monitoring of cyclosporine, tacrolimus, and azathioprine. *Clinical Biochemistry*, 34(1), pp.9–16.

Armulik, A., Abramsson, A. & Betsholtz, C., 2005. Endothelial/pericyte interactions. *Circulation research*, 97(6), pp.512–523.

Arnold, W.P. *et al*., 1977. Nitric oxide activates guanylate cyclase and increases guanosine 3“:5-”cyclic monophosphate levels in various tissue preparations. *Proceedings of the National Academy of Sciences of the United States of America*, 74(8), pp.3203–3207.

Asaba, K. *et al*., 2005. Effects of NADPH oxidase inhibitor in diabetic nephropathy. *Kidney international*, 67(5), pp.1890–1898.

Assmann, T., Homey, B. & Ruzicka, T., 2001. Topical tacrolimus for the treatment of inflammatory skin diseases. *Expert Opinion on Pharmacotherapy*, 2(7), pp.1167–1175.

Aukland, K., 1980. Methods for measuring renal blood flow: total flow and regional distribution. *Annual review of physiology*, 42, pp.543–555.

Avdonin, P.V. *et al*., 1999. Cyclosporine A up-regulates angiotensin II receptors and

calcium responses in human vascular smooth muscle cells. *Kidney international*, 55(6), pp.2407–2414.

Åsberg, A., Christensen, H. & Hartmann, A., 1999. Pharmacokinetic interactions between microemulsion formulated cyclosporine A and diltiazem in renal transplant recipients. *European journal of Transplantation*, 88(23), pp.220

Baboolal, K., 2003. A phase III prospective, randomized study to evaluate concentration-controlled sirolimus (rapamune) with cyclosporine dose minimization or elimination at six months in de novo renal allograft recipients. *Transplantation*, 75(8), pp.1404–1408.

Bach, P., 2013. *Nephrotoxicity: In Vitro to In Vivo Animals to Man*,

Bach, P.H. & Lock, E.A. eds., 1987. *Nephrotoxicity in the experimental and clinical situation*, Dordrecht: Springer Netherlands.

Bakker, R.C. *et al*., 2004. Chronic cyclosporine nephrotoxicity in renal transplantation. *Transplantation Reviews*, 18(1), pp.54–64.

Ballou, L.M. & Lin, R.Z., 2008. Rapamycin and mTOR kinase inhibitors. *Journal of chemical biology*, 1(1-4), pp.27–36.

Bandopadhyay, R.R. *et al*., 2001. Contractile proteins in pericytes at the blood-brain and blood-retinal barriers. *Journal of Neurocytology*, 30(1), pp.35–44.

Bankir, L. & Derouffignac, C., 1985. Urinary Concentrating Ability - Insights From Comparative Anatomy. The American Journal Of Physiology, 249(6), Pp.R643–R666.

Barany, P. *et al*., 2001. Effect of 6 weeks of vitamin E administration on renal haemodynamic alterations following a single dose of neoral in healthy volunteers. *Nephrology, dialysis, transplantation : official publication of the European Dialysis and Transplant Association - European Renal Association*, 16(3), pp.580–584.

Barbarino, J.M. *et al*., 2013. PharmGKB summary: cyclosporine and tacrolimus pathways. *Pharmacogenetics and Genomics*, 23(10), pp.563–585.

Baroletti, S.A. *et al*., 2003. Calcium Channel Blockers as the Treatment of Choice for Hypertension in Renal Transplant Recipients: Fact or Fiction. *Pharmacotherapy: The Journal of Human Pharmacology and Drug Therapy*, 23(6), pp.788–801.

Barros, E.J. *et al*., 1987. Glomerular hemodynamics and hormonal participation on cyclosporine nephrotoxicity. *Kidney international*, 32(1), pp.19–25.

Baud, L. & Ardaillou, R., 1986. Reactive oxygen species: production and role in the kidney. *American journal of physiology. Renal physiology*, 251(5), pp.F765–F776.

Baumgärtl, H. *et al*., 1972. The oxygen supply of the dog kidney: measurements of intrarenal pO 2 . *Microvascular research*, 4(3), pp.247–257.

Becker, G. *et al*., 1996. Diltiazem minimizes tubular damage due to FK506-mediated nephrotoxicity following ischemia and reperfusion in rats. *transplant immunology 1996*, 4(1), pp.68–71.

Beierwaltes, W.H., 2013. Endothelial dysfunction in the outer medullary vasa recta as a key to contRAASt media-induced nephropathy. *American journal of physiology. Renal physiology*, 304(1), pp.F31–F32.

Bennett, W.M., 1997. Drug interactions and consequences of sodium restriction. *American Journal of Clinical Nutrition*, 65(2), pp.S678–S681.

Bennett, W.M. & Pulliam, J.P., 1983. Cyclosporine nephrotoxicity. *Annals of internal medicine*, 99(6), pp.851–854.

Bennett, W.M. *et al*., 1996. Chronic cyclosporine nephropathy: The Achilles' heel of immunosuppressive therapy. *Kidney international*, 50(4), pp.1089–1100.

Bergers, G., 2005. The role of pericytes in blood-vessel formation and maintenance. *Neuro-oncology*, 7(4), pp.452–464.

Bernardi, P. & Petronilli, V., 1996. The permeability transition pore as a mitochondrial calcium release channel: A critical appraisal. *Journal of Bioenergetics and Biomembranes*, 28(2), pp.131–138.

Bernardi, P. *et al*., 1992. Modulation of the mitochondrial permeability transition pore. Effect of protons and divalent cations. *Journal of Biological Chemistry*, 267(5), pp.2934–2939.

Berti, F., 2013. *The Prostaglandin System: Endoperoxides, Prostacyclin, and Thromboxanes*,

Blankenstein, K. *et al*., 2014. Acute inhibition of calcineurin using cyclosporine activates renal salt transporters (892.31). *The FASEB Journal*, 28(1 Supplement).

Bobadilla, N.A. & Gamba, G., 2007. New insights into the pathophysiology of cyclosporine nephrotoxicity: a role of aldosterone. *American journal of physiology. Renal physiology*, 293(1), pp.F2–9.

Boers, M. *et al*., 1992. Cyclosporine Nephrotoxicity in Rheumatoid-Arthritis - No Effect of Short-Term Misoprostol Treatment. *Journal of Rheumatology*, 19(4), pp.534–537.

Bohle, A. *et al*., 1982. Juxtaglomerular Apparatus of the Human-Kidney - Correlation Between Structure and Function. *Kidney international*, 12, pp.S18–S23.

Bonventre, J.V. & Yang, L., 2011. Cellular pathophysiology of ischemic acute kidney injury. *The Journal of Clinical Investigation*, 121(11), pp.4210–4221.

Border, W.A. & Noble, N.A., 1994. Transforming growth factor beta in tissue fibrosis. *New England Journal of Medicine*, 331(19), pp.1286–1292.

Borysova, L. *et al*., 2013. How calcium signals in myocytes and pericytes are integrated across in situ microvascular networks and control microvascular tone(). *Cell Calcium*, 54(3), pp.163–174.

Bracho-Valdes, I. *et al*., 2011. mTORC1- and mTORC2-interacting proteins keep their multifunctional partners focused. *IUBMB life*, 63(10), pp.896–914.

Brezis, M. & ROSEN, S., 1995. Hypoxia of the renal medulla--its implications for

disease. *New England Journal of Medicine*, 332(10), pp.647–655.

Brezis, M. *et al*., 1991. Role of nitric oxide in renal medullary oxygenation. Studies in isolated and intact rat kidneys. *Journal of Clinical Investigation*, 88(2), pp.390–395.

Brook, N.R. *et al*., 2005. Cyclosporine and rapamycin act in a synergistic and dose-dependent manner in a model of immunosuppressant-induced kidney damage. *Transplantation Proceedings*, 37(2), pp.837–838.

Brustovetsky, N. & Dubinsky, J.M., 2000. Limitations of cyclosporin A inhibition of the permeability transition in CNS mitochondria. *The Journal of neuroscience : the official journal of the Society for Neuroscience*, 20(22), pp.8229–8237.

Bryan, N.S., Bian, K. & Murad, F., 2009. Discovery of the nitric oxide signaling pathway and targets for drug development. *Frontiers in bioscience (Landmark edition)*, 14, pp.1–18.

Buffoli, B. *et al*., 2005. Provinol Prevents CsA-induced Nephrotoxicity by Reducing Reactive Oxygen Species, iNOS, and NF-kB Expression. *Journal of Histochemistry and Cytochemistry*, 53(12), pp.1459–1468.

Burdmann, E.A. *et al*., 2003. Cyclosporine nephrotoxicity. *Seminars in Nephrology*, 23(5), pp.465–476.

Burdmann, E.A. *et al*., 1995. Prevention of experimental cyclosporin-induced interstitial fibrosis by losartan and enalapril. *The American journal of physiology*, 269(4 Pt 2), pp.F491–F499.

Burdyga, T. & Borysova, L., 2014. Calcium Signalling in Pericytes. *Journal of vascular research*.

Burg, M.B., 1972. Perfusion of Isolated Renal Tubules. *Yale Journal of Biology and Medicine*, 45(3-4), pp.321–&.

Bursztyn, M. *et al*., 1997. Isradipine for the prevention of cyclosporine-induced hypertension in allogeneic bone marrow transplant recipients: a randomized, double-blind study. *Transplantation*, 63(7), pp.1034–1036.

Calne, R.Y. *et al*., 1978. Cyclosporin-a in Patients Receiving Renal-Allografts From Cadaver Donors. *Lancet*, 2(8104), pp.1323–1327.

Calne, R.Y. *et al*., 1989. Rapamycin for Immunosuppression in Organ Allografting. *Lancet*, 2(8656), pp.227–227.

Campistol, J.M. *et al*., 1999. Losartan decreases plasma levels of TGF-beta1 in transplant patients with chronic allograft nephropathy. *Kidney international*, 56(2), pp.714–719.

Cao, Y. *et al*., 2013. Pericyte coverage of differentiated vessels inside tumor vasculature is an independent unfavorable prognostic factor for patients with clear cell renal cell carcinoma. *Cancer*, 119(2), pp.313–324.

Caramelo, C. *et al*., 2004. Cyclosporin A toxicity, and more: vascular endothelial growth factor (VEGF) steps forward. *Nephrology, dialysis, transplantation : official*

publication of the European Dialysis and Transplant Association - European Renal Association, 19(2), pp.285–288.

Cardenas, M.E. *et al*., 1999. Antifungal activities of antineoplastic agents: Saccharomyces cerevisiae as a model system to study drug action. *Clinical microbiology reviews*, 12(4), pp.583–611.

Caruso, R.A. *et al*., 2009. UltRAAStructural Descriptions of Pericyte/endothelium Peg-socket Interdigitations in the Microvasculature of Human Gastric Carcinomas. *Anticancer Research*, 29(1), pp.449–453.

Carvalho da Costa, M. *et al*., 2003. Cyclosporin A tubular effects contribute to nephrotoxicity: role for Ca2+ and Mg2+ ions. *Nephrology, dialysis, transplantation : official publication of the European Dialysis and Transplant Association - European Renal Association*, 18(11), pp.2262–2268.

Cascorbi, I., 2013. P-glycoprotein (MDR1/ABCB1). In *Pharmacogenomics of Human Drug Transporters*. John Wiley & Sons, Inc., pp. 271–293.

Cavarape, A. *et al*., 1998. Contribution of endothelin receptors in renal microvessels in acute cyclosporine-mediated vasoconstriction in rats. *Kidney international*, 53(4), pp.963–969.

Chakraborti, T. *et al*., 1998. Targets of oxidative stress in cardiovascular system. *Molecular and cellular biochemistry*, 187(1-2), pp.1–10.

Chander, V. & Chopra, K., 2005. Effect of molsidomine and L-arginine in cyclosporine nephrotoxicity: role of nitric oxide. *Toxicology*, 207(3), pp.463–474.

Chander, V. *et al*., 2004. Amelioration of cyclosporine nephrotoxicity by irbesartan, A selective AT1 receptor antagonist. *Renal failure*, 26(5), pp.467–477.

Chapman, J.R.J., 2011. Chronic calcineurin inhibitor nephrotoxicity-lest we forget. *American Journal of Transplantation*, 11(4), pp.693–697.

Charney, D.A., Bhaskaran, M. & Molmenti, E., 2009. Calcineurin inhibitor toxicity in a renal transplant recipient. *NDT Plus*, 2(2), pp.175–176.

Charuk, J., Wong, P.Y. & Reithmeier, R., 1995. Differential Interaction Of Human Renal P-Glycoprotein With Various Metabolites And Analogs Of Cyclosporine-A. The American Journal Of Physiology, 269(1), Pp.F31–F39.

Chen, H.-W. *et al*., 2002. Cyclosporine A regulate oxidative stress-induced apoptosis in cardiomyocytes: mechanisms *via* ROS generation, iNOS and Hsp70. *British Journal of Pharmacology*, 137(6), pp.771–781.

Chen, Y.-F., Cowley, A.W.J. & Zou, A.-P., 2003. Increased H(2)O(2) counteracts the vasodilator and natriuretic effects of superoxide dismutation by tempol in renal medulla. *American Journal of Physiology - Regulatory, Integrative and Comparative Physiology*, 285(4), pp.R827–33.

Cheng, C.-H. *et al*., 2008. Possible Mechanism by Which Rapamycin Increases Cyclosporine Nephrotoxicity. *Transplantation Proceedings*, 40(7), pp.3–3.

Cho, S.W. *et al*., 2014. Dual Modulation of the Mitochondrial Permeability Transition

Pore and Redox Signaling Synergistically Promotes Cardiomyocyte Differentiation From Pluripotent Stem Cells. *Journal of the American Heart Association*, 3(2), pp.–e000693.

Ciarcia, R. *et al*., 2015. The protective effect of Apocynin on Cyclosporine A-induced hypertension and nephrotoxicity in rats. *Journal of cellular biochemistry*.

Coffman, T., 1991. Animal Models of Cyclosporine Nephrotoxicity. In M. Hatano, ed. *Nephrology*. Springer Berlin Heidelberg, pp. 555–563.

Colas, B. *et al*., 2000. Direct vascular actions of methyclothiazide and indapamide in aorta of spontaneously hypertensive rats. *Fundamental & Clinical Pharmacology*, 14(4), pp.363–368.

Collins, B.S. *et al*., 1992. Reversible Cyclosporine Arteriolopathy. *Transplantation*, 54(4), pp.732–734.

Colombo, D. & Ammirati, E., 2011. Cyclosporine in transplantation - a history of converging timelines. *Journal of biological regulators and homeostatic agents*, 25(4), pp.493–504.

Colombo, M.D., Perego, R. & Bellia, G., 2013. Cyclosporine-Associated Nephrotoxicity. *Open Journal of Nephrology*.

Cooke, M.S. *et al*., 2003. Oxidative DNA damage: mechanisms, mutation, and disease. *Faseb Journal*, 17(10), pp.1195–1214.

Cossarizza, A. *et al*., 1994. Mitochondrial modifications during rat thymocyte apoptosis: a study at the single cell level. *Experimental Cell Research*, 214(1), pp.323–330.

Courtoy, P.J. & Boyles, J., 1983. Fibronectin in the Microvasculature - Localization in the Pericyte Endothelial Interstitium. *Journal of UltRAAStructure Research*, 83(3), pp.258–273.

Cowley, A.W., 1997. Role of the renal medulla in volume and arterial pressure regulation. *American Journal of Physiology - Regulatory, Integrative and Comparative Physiology*, 273(1), pp.R1–R15.

Cowley, A.W. *et al*., 1995. The Renal Medulla and Hypertension. *Hypertension*, 25(4), pp.663–673.

Cowley, A.W., Abe, M., Mori, T., O'Connor, P.M., Ohsaki, Y. & Zheleznova, N.N., 2015a. Reactive oxygen species as important determinants of medullary flow, sodium excretion, and hypertension. *American journal of physiology. Renal physiology*, 308(3), pp.F179–F197.

Cowley, A.W.J., Abe, M., Mori, T., O'Connor, P.M., Ohsaki, Y. & Zheleznova, N.N., 2015b. Reactive oxygen species as important determinants of medullary flow, sodium excretion, and hypertension. *American journal of physiology. Renal physiology*, 308(3), pp.F179–97.

Crawford, C. *et al*., 2012. An intact kidney slice model to investigate vasa recta properties and function in situ. *Nephron. Physiology*, 120(3), pp.p17–31.

Crawford, C. *et al*., 2011. Extracellular nucleotides affect pericyte-mediated regulation of rat in situ vasa recta diameter. *Acta physiologica (Oxford, England)*, 202(3), pp.241–251.

Crawford, C. *et al*., 2013. Sympathetic nerve-derived ATP regulates renal medullary vasa recta diameter *via* pericyte cells: a role for regulating medullary blood flow? *Frontiers in Physiology*, 4, pp.307–307.

Cuevas, P. *et al*., 1984. Pericyte endothelial gap junctions in human cerebral capillaries. *Anatomy and Embryology*, 170(2), pp.155–159.

Cuhaci, B. *Et al*., 1999. Transforming Growth Factor-β Levels In Human Allograft Chronic Fibrosis Correlate With Rate Of Decline In Renal Function1. Transplantation, 68(6), P.785.

Curtis, J.J. *et al*., 1993. Captopril-induced fall in glomerular filtration rate in cyclosporine-treated hypertensive patients. *Journal of the American Society of Nephrology*, 3(9), pp.1570–1574.

Curtis, J.J. *et al*., 1988. Hypertension in Cyclosporine-Treated Renal-Transplant Recipients Is Sodium-Dependent. *American Journal of Medicine*, 85(2), pp.134–138.

d'Ardenne, A.J.A. *et al*., 1986. Cyclosporin and renal graft histology. *Journal of Clinical Pathology*, 39(2), pp.145–151.

Dalkara, T., Gursoy-Ozdemir, Y. & Yemisci, M., 2011. Brain microvascular pericytes in health and disease. *Acta neuropathologica*, 122(1), pp.1–9.

Damiano, S. *et al*., 2013. A new recombinant MnSOD prevents the Cyclosporine A-induced renal impairment. *Nephrology, dialysis, transplantation : official publication of the European Dialysis and Transplant Association - European Renal Association*, 28(8), pp.2066–2072.

Damiano, S.S. *et al*., 2010. Regulation of sodium transporters in the kidney during cyclosporine treatment. *Journal of nephrology*, 23 Suppl 16, pp.S191–S198.

Davis, L.S. *et al*., 1994. Effects of selective endothelin antagonists on the hemodynamic response to cyclosporin A. *Journal of the American Society of Nephrology*, 4(7), pp.1448–1454.

de Arriba, G. *et al*., 2013. Cyclosporine A-induced apoptosis in renal tubular cells is related to oxidative damage and mitochondrial fission. *Toxicology Letters*, 218(1), pp.30–38.

de Nucci, G. *et al*., 1988. Pressor effects of circulating endothelin are limited by its removal in the pulmonary circulation and by the release of prostacyclin and endothelium-derived relaxing factor. *Proceedings of the National Academy of Sciences of the United States of America*, 85(24), pp.9797–9800.

de Vries, A.P.J. *et al*., 2006. Supplementation with anti-oxidants Vitamin C and E decreases cyclosporine A trough-levels in renal transplant recipients. *Nephrology, dialysis, transplantation : official publication of the European Dialysis and Transplant Association - European Renal Association*, 21(1), pp.231–232.

Deppe, C.E. *et al*., 1997. Effect of cyclosporine A on Na+/K(+)-ATPase, Na+/K+/2Cl- cotransporter, and H+/K(+)-ATPase in MDCK cells and two subtypes, C7 and C11. *Experimental Nephrology*, 5(6), pp.471–480.

Diaz-Flores, L. *et al*., 2009. Pericytes. Morphofunction, interactions and pathology in a quiescent and activated mesenchymal cell niche. *Histology and histopathology*, 24(7), pp.909–969.

Dickhout, J.G., Mori, T. & Cowley, A.W.J., 2002. Tubulovascular nitric oxide crosstalk: buffering of angiotensin II-induced medullary vasoconstriction. *Circulation research*, 91(6), pp.487–493.

Diederich, D. *et al*., 1994. Cyclosporine produces endothelial dysfunction by increased production of superoxide. *Hypertension*, 23(6 Pt 2), pp.957–961.

Dieperink, H. *et al*., 1985. Glomerulotubular Function in Cyclosporine-Treated Rats - a Lithium Clearance, Occlusion Time Transit-Time and Micropuncture Study. *Proceedings of the European Dialysis and Transplant Association*, 21, pp.853–859.

DiJoseph, J.F. *et al*., 1996. Therapeutic blood levels of sirolimus (rapamycin) in the allografted rat. *Transplantation*, 62(8), pp.1109–1112.

Dittrich, E. *et al*., 2004. Rapamycin-associated post-transplantation glomerulonephritis and its remission after reintroduction of calcineurin-inhibitor therapy. *Transplant International*, 17(4), pp.215–220.

Djamali, A., 2007. Oxidative stress as a common pathway to chronic tubulointerstitial injury in kidney allografts. *American journal of physiology. Renal physiology*, 293(2), pp.F445–F455.

Dore-Duffy, P. & Cleary, K., 2011. Morphology and properties of pericytes. *The Blood-Brain and Other Neural Barriers*.

Dorm, G.W. & Becker, M.W., 1993. Thromboxane-A2 Stimulated Signal Transduction in Vascular Smooth-Muscle. *Journal of Pharmacology and Experimental Therapeutics*, 265(1), pp.447–456.

Duarte, J.D. & Cooper-DeHoff, R.M., 2010. Mechanisms for blood pressure lowering and metabolic effects of thiazide and thiazide-like diuretics. *Expert review of cardiovascular therapy*, 8(6), pp.793–802.

Dudley, C., 2001. Sustained improvement of renal graft function for two years in hypertensive renal transplant recipients treated with nifedipine as compared to lisinopril. Transplantation 2001, 72, 1787. K. Midtvedt, A. Hartmann, A. Foss, P. Fauchald, K. P. Nordal, K. Rootwelt, and H. Holdaas - Treatment of posttransplant hypertension; ace is trumped? *Transplantation*, 72(11), pp.1728–1729.

Dusting, G.J. *et al*., 1999. Cyclosporin A and tacrolimus (FK506) suppress expression of inducible nitric oxide synthase in vitro by different mechanisms. *British Journal of Pharmacology*, 128(2), pp.337–344.

Eaton, D. & Pooler, J., 2009. *Vander's Renal Physiology, 7th Edition*, McGraw-Hill Education.

Edwards, A., Cao, C. & Pallone, T.L., 2011. Cellular mechanisms underlying nitric

oxide-induced vasodilation of descending vasa recta. *American Journal of Physiology: Renal, Fluid & Electrolyte Physiology (Abstracts)*, 300(2), pp.F441–F456.

Eguchi, R. *et al*., 2013. FK506 induces endothelial dysfunction through attenuation of Akt and ERK1/2 independently of calcineurin inhibition and the caspase pathway. *Cellular Signalling*, 25(9), pp.1731–1738.

Ekberg, H. *et al*., 2010. Cyclosporine, tacrolimus and sirolimus retain their distinct toxicity profiles despite low doses in the Symphony study. *Nephrology, dialysis, transplantation : official publication of the European Dialysis and Transplant Association - European Renal Association*, 25(6), pp.2004–2010.

Ekberg, H. *et al*., 2007. Reduced exposure to calcineurin inhibitors in renal transplantation. *New England Journal of Medicine*, 357(25), pp.2562–2575.

Ekser, B., Cooper, D.K.C. & Tector, A.J., 2015. The need for xenotransplantation as a source of organs and cells for clinical transplantation. *International journal of surgery (London, England)*.

Elmore, S.P. *et al*., 2001. The mitochondrial permeability transition initiates autophagy in rat hepatocytes. *The FASEB Journal*, 15(12), pp.2286–2287.

Elzinga, L.W., Rosen, S. & Bennett, W.M., 1993. Dissociation Of Glomerular-Filtration Rate From Tubulointerstitial Fibrosis In Experimental Chronic Cyclosporine Nephropathy - Role Of Sodium-Intake. Journal Of The American Society Of Nephrology, 4(2), Pp.214–221.

English, J. *et al*., 1987. Cyclosporine-induced acute renal dysfunction in the rat. Evidence of arteriolar vasoconstriction with preservation of tubular function. *Transplantation*, 44(1), pp.135–141.

Ericzon, B.G. *et al*., 1992. The Effect of Fk506 Treatment on Pancreaticoduodenal Allotransplantation in the Primate. *Transplantation*, 53(6), pp.1184–1189.

Evans, K.K., Nawata, C.M. & Pannabecker, T.L., 2015. Isolation and perfusion of rat inner medullary vasa recta. *American journal of physiology. Renal physiology*, p.ajprenal.00214.2015.

Evans, R.G. *et al*., 2008. Intrarenal oxygenation: unique challenges and the biophysical basis of homeostasis. *American journal of physiology. Renal physiology*, 295(5), pp.F1259–F1270.

Evans, R.G.R. *et al*., 2004. Mechanisms underlying the differential control of blood flow in the renal medulla and cortex. *Journal of Hypertension*, 22(8), pp.1439–1451.

Fahr, A., 1993a. Cyclosporin clinical pharmacokinetics. *Clinical Pharmacokinetics*, 24(6), pp.472–495.

Fahr, A., 1993b. Cyclosporine Clinical Pharmacokinetics. *Clinical Pharmacokinetics*, 24(6), pp.472–495.

Faulkner, J.L. *et al*., 2005. Origin of Interstitial Fibroblasts in an Accelerated Model of Angiotensin II-Induced Renal Fibrosis. *The American Journal of Pathology*, 167(5),

pp.1193–1205.

Feldman, G. *et al*., 2007. Role for TGF-beta in cyclosporine-induced modulation of renal epithelial barrier function. *Journal of the American Society of Nephrology*, 18(6), pp.1662–1671.

Feller, N., Broxterman, H.J., *et al*., 1995. ATP-dependent efflux of calcein by the multidrug resistance protein (MRP): no inhibition by intracellular glutathione depletion. *FEBS Letters*, 368(2), pp.385–388.

Feller, N., Kuiper, C.M., *et al*., 1995. Functional detection of MDR1/P170 and MRP/P190-mediated multidrug resistance in tumour cells by flow cytometry. *British journal of cancer*, 72(3), pp.543–549.

Ferrand-Drake, M., Friberg, H. & Wieloch, T., 1999. Mitochondrial permeability transition induced DNA-fragmentation in the rat hippocampus following hypoglycemia. *Neuroscience*, 90(4), pp.1325–1338.

Fervenza, F.C. *et al*., 2004. Acute rapamycin nephrotoxicity in native kidneys of patients with chronic glomerulopathies. *Nephrology, dialysis, transplantation : official publication of the European Dialysis and Transplant Association - European Renal Association*, 19(5), pp.1288–1292.

Fioretto, P. *et al*., 2011. Tacrolimus and cyclosporine nephrotoxicity in native kidneys of pancreas transplant recipients. *Clinical Journal of the American Society of Nephrology*, 6(1), pp.101–106.

First, M.R., Neylan, J.F. & ROCHER, L.L., 1994. Hypertension after renal transplantation. *Journal of the American ….*

Fischer, G. *et al*., 1989. Cyclophilin and Peptidyl-Prolyl Cis-Trans IsomeRAASe Are Probably Identical Proteins. *Nature*, 337(6206), pp.476–478.

Flanagan, W.M. *et al*., 1991. Nuclear-Association of a T-Cell Transcription Factor Blocked by Fk-506 and Cyclosporine-A. *Nature*, 352(6338), pp.803–807.

Fligny, C.C. & Duffield, J.S.J., 2013. Activation of pericytes: recent insights into kidney fibrosis and microvascular rarefaction. *Current Opinion in Rheumatology*, 25(1), pp.78–86.

Fogo, A. *et al*., 1990. Severe Endothelial Injury in a Renal-Transplant Patient Receiving Cyclosporine. *Transplantation*, 49(6), pp.1190–1192.

Forslund, T. *et al*., 1995. Hypertension in cyclosporin A-treated patients is independent of circulating endothelin levels. *Journal of internal medicine*, 238(1), pp.71–75.

Frapier, J.M. *et al*., 2001. Cyclosporin A increases basal intracellular calcium and calcium responses to endothelin and vasopressin in human coronary myocytes. *FEBS Letters*, 493(1), pp.57–62.

Freeman, B.A. & Crapo, J.D., 1982. Biology of disease: free radicals and tissue injury. *Laboratory investigation; a journal of technical methods and pathology*, 47(5), pp.412–426.

Friberg, H. *et al*., 1998. Cyclosporin A, but not FK 506, protects mitochondria and neurons against hypoglycemic damage and implicates the mitochondrial permeability transition in cell death. *The Journal of neuroscience : the official journal of the Society for Neuroscience*, 18(14), pp.5151–5159.

Friis, U.G., Jensen, B.L. & Skott, O., 2006. Cyclosporine A increases renin release from single juxtaglomerular cells in a calcium-dependent manner. *The FASEB Journal*, 20(4), p.A343.

Frishman, W.H., 2007. Calcium channel blockers: differences between subclasses. *American journal of cardiovascular drugs : drugs, devices, and other interventions*, 7 Suppl 1, pp.17–23.

Fry, B.C. *et al*., 2014. Impact of renal medullary three-dimensional architecture on oxygen transport. *American journal of physiology. Renal physiology*, 307(3), pp.F263–F272.

Fukata, Y., Amano, M. & Kaibuchi, K., 2001. Rho-Rho-kinase pathway in smooth muscle contraction and cytoskeletal reorganization of non-muscle cells. *Trends in Pharmacological Sciences*, 22(1), pp.32–39.

Fung, J.J. *et al*., 1990. Overview of FK506 in transplantation. *Clinical transplants*, pp.115–121.

Galletti, P. *et al*., 2005. Diverse effects of natural antioxidants on cyclosporin cytotoxicity in rat renal tubular cells. *Nephrology, dialysis, transplantation : official publication of the European Dialysis and Transplant Association - European Renal Association*, 20(8), pp.1551–1558.

García, N. *et al*., 2007. On the Opening of an Insensitive Cyclosporin A Non-specific Pore by Phenylarsine Plus Mersalyl. *Cell Biochemistry and Biophysics*, 49(2), pp.84–90.

Garlicki, M. *et al*., 2006. Conversion from cyclosporine to tacrolimus improves renal function and lipid profile after cardiac transplantation. *Annals of transplantation : quarterly of the Polish Transplantation Society*, 11(1), pp.24–27.

Gaston, R.S., 2009. Chronic calcineurin inhibitor nephrotoxicity: reflections on an evolving paradigm. *Clinical Journal of the American Society of Nephrology*, 4(12), pp.2029–2034.

Gaston, R.S., Julian, B.A. & CURTIS, J.J., 1994. Posttransplant erythrocytosis: an enigma revisited. *American Journal of Kidney Diseases*, 24(1), pp.1–11.

Gattone, V., 2009. Kidney Structure and Function. *Microscopy and Microanalysis*, 15(S2), pp.74–75.

Gautier, C. *et al*., 2012. Regulation of mitochondrial permeability transition pore by PINK1. *Molecular Neurodegeneration*, 7(1), p.22.

Gerhardt, H. & Betsholtz, C., 2003. Endothelial-pericyte interactions in angiogenesis. *Cell and tissue research*, 314(1), pp.15–23.

Gerhardt, H., Wolburg, H. & Redies, C., 2000. N-cadherin mediates pericytic-endothelial interaction during brain angiogenesis in the chicken. *Developmental*

dynamics : an official publication of the American Association of Anatomists, 218(3), pp.472–479.

Gill, P.S. & Wilcox, C.S., 2006. NADPH oxidases in the kidney. *Antioxidants & redox signaling*, 8(9-10), pp.1597–1607.

Gokce, M. *et al*., 2012. Cilostazol and Diltiazem Attenuate Cyclosporine-Induced Nephrotoxicity in Rats. *Transplantation Proceedings*, 44(6), pp.1738–1742.

Gordjani, N. *et al*., 2000. Cyclosporin-A-induced effects on the free Ca2+ concentration in LLC-PK1-cells and their mechanisms. *Pflugers Archiv : European journal of physiology*, 439(5), pp.627–633.

Göppert-Mayer, M., 1931. Über Elementarakte mit zwei Quantensprüngen. *Annalen der Physik*, 401(3), pp.273–294.

Grace, A.A. *et al*., 1987. Cyclosporine A enhances platelet aggregation. *Kidney international*, 32(6), pp.889–895.

Graef, I.A. *et al*., 2001. Signals Transduced by Ca2+/Calcineurin and NFATc3/c4 Pattern the Developing Vasculature. *Cell*, 105(7), pp.863–875.

Groenewoud, M.J. & Zwartkruis, F.J.T., 2013. Rheb and mammalian target of rapamycin in mitochondrial homoeostasis. *Open Biology*, 3(12), pp.130185–130185.

Groningen, M.C.M.R.-V. *et al*., 2006. Molecular comparison of calcineurin inhibitor-induced fibrogenic responses in protocol renal transplant biopsies. *Journal of the American Society of Nephrology*, 17(3), pp.881–888.

Group, E.M.T., 1983. Cyclosporin In Cadaveric Renal Transplantation: One-Year Follow-Up Of A Multicentre Trial. Lancet, 322(8357), Pp.986–989.

Grzesk, G. *et al*., 2012. Calcium blockers inhibit cyclosporine A-induced hyperreactivity of vascular smooth muscle cells. *Molecular medicine reports*, 5(6), pp.1469–1474.

Haas, M. *et al*., 2004. Isometric tubular epithelial vacuolization in renal allograft biopsy specimens of patients receiving low-dose intravenous immunoalobulin for a positive crossmatch. *Transplantation*, 78(4), pp.549–556.

Halestrap, A.P., 2009. What is the mitochondrial permeability transition pore? *Journal of molecular and cellular cardiology*, 46(6), pp.821–831.

Halestrap, A.P., Clarke, S.J. & Javadov, S.A., 2004. Mitochondrial permeability transition pore opening during myocardial reperfusion--a target for cardioprotection. *Cardiovascular Research*, 61(3), pp.372–385.

Halestrap, A.P., Connern, C.P. & Griffiths, E.J., 1997. Cyclosporin A binding to mitochondrial cyclophilin inhibits the permeability transition pore and protects hearts from ischaemia/reperfusion injury. *Detection of Mitochondrial ….*

Halestrap, A.P., Connern, C.P., Griffiths, E.J., *et al*., 1997. Cyclosporin A binding in mitochondrial cyclophilin inhibits the permeability transition pore and protects hearts from ischaemia/reperfusion injury. *Molecular and cellular biochemistry*,

174(1-2), pp.167–172.

Hall, A.M. *et al*., 2009. Multiphoton Imaging Reveals Differences in Mitochondrial Function between Nephron Segments. *Journal of the American Society of Nephrology : JASN*, 20(6), pp.1293–1302.

Hall, A.M.A. *et al*., 2011. Multiphoton imaging of the functioning kidney. *Journal of the American Society of Nephrology*, 22(7), pp.1297–1304.

Hamalainen, M., Lahti, A. & Moilanen, E., 2002. Calcineurin inhibitors, cyclosporin A and tacrolimus inhibit expression of inducible nitric oxide synthase in colon epithelial and macrophage cell lines. *European journal of pharmacology*, 448(2-3), pp.239–244.

Hamilton, N.B., Attwell, D. & Hall, C.N., 2010. Pericyte-mediated regulation of capillary diameter: a component of neurovascular coupling in health and disease. *Frontiers in neuroenergetics*, 2.

Hammes, H.P. *et al*., 2004. Angiopoietin-2 causes pericyte dropout in the normal retina - Evidence for involvement in diabetic retinopathy. *Diabetes*, 53(4), pp.1104–1110.

Hannedouche, T.P. *et al*., 1996. Angiotensin converting enzyme inhibition and chronic cyclosporine-induced renal dysfunction in type 1 diabetes. *Nephrology, dialysis, transplantation : official publication of the European Dialysis and Transplant Association - European Renal Association*, 11(4), pp.673–678.

Hansell, P., 1992. Evaluation of Methods for Estimating Renal Medullary Blood-Flow. *Renal Physiology and Biochemistry*, 15(5), pp.217–230.

Hansen, J.M. *et al*., 1996. Effects of the prostacyclin analogue iloprost on cyclosporin-induced renal hypoperfusion in stable renal transplant recipients. *Nephrology, dialysis, transplantation : official publication of the European Dialysis and Transplant Association - European Renal Association*, 11(2), pp.340–346.

Harding, M.W. *et al*., 1989. A receptor for the immunosuppressant FK506 is a cis-trans peptidyl-prolyl isomeRAASe. *Nature*, 341(6244), pp.758–760.

Harrison-Bernard, L.M., 2009. The renal renin-angiotensin system. *AJP: Advances in Physiology Education*, 33(4), pp.270–274.

Hartung, T., 2008. Thoughts on limitations of animal models. *LIMPE Seminars "Experimental Models in Parkinson's Disease"23-25 September 2007, Sardinia, Italy*, 14, Supplement 2 IS -, pp.S81–S83.

Hauser, I.A. *et al*., 2005. ABCB1 genotype of the donor but not of the recipient is a major risk factor for cyclosporine-related nephrotoxicity after renal transplantation. *Journal of the American Society of Nephrology*, 16(5), pp.1501–1511.

Haynes, R. *et al*., 2013. Campath, calcineurin inhibitor reduction and chronic allograft nephropathy (3C) study: background, rationale, and study protocol. *Transplantation research*, 2(1), p.7.

He, L. & Lemasters, J.J., 2002. Regulated and unregulated mitochondrial permeability

transition pores: a new paradigm of pore structure and function? *FEBS Letters*, 512(1-3), pp.1–7.

He, L. & Lemasters, J.J., Regulated and unregulated mitochondrial permeability transition pores: a new paradigm of pore structure and function? *FEBS Letters*, 512(1–3), pp.1–7.

Healy, E. *et al*., 1998. Apoptosis and necrosis: Mechanisms of cell death induced by cyclosporine A in a renal proximal tubular cell line. *Kidney international*, 54(6), pp.1955–1966.

Hebert, M.F. *et al*., 2003. Association between ABCB1 (multidrug resistance transporter) genotype and post-liver transplantation renal dysfunction in patients receiving calcineurin inhibitors. *Pharmacogenetics and Genomics*, 13(11), p.661.

Heering, P. & Grabensee, B., 1991. Influence of ciclosporin A on renal tubular function after kidney transplantation. *Nephron*, 59(1), pp.66–70.

Heering, P. *et al*., 1998. Distal tubular acidosis induced by FK506. *Clinical transplantation*, 12(5), pp.465–471.

Heering, P.J., Klein-Vehne, N. & Fehsel, K., 2004. Decreased mineralocorticoid receptor expression in blood cells of kidney transplant recipients undergoing immunosuppressive treatment: cost efficient determination by quantitative PCR. *Journal of Clinical Pathology*, 57(1), pp.33–36.

Heintzmann, R. & Ficz, G., 2006. Breaking the resolution limit in light microscopy. *Briefings in functional genomics & proteomics*, 5(4), pp.289–301.

Hesselink, D.A. *et al*., 2003. Genetic polymorphisms of the CYP3A4, CYP3A5, and MDR-1 genes and pharmacokinetics of the calcineurin inhibitors cyclosporine and tacrolimus. *Clinical pharmacology and therapeutics*, 74(3), pp.245–254.

Heumuller, S. *et al*., 2008. Apocynin is not an inhibitor of vascular NADPH oxidases but an antioxidant. *Hypertension*, 51(2), pp.211–217.

Hiremath, S. *et al*., 2007. Renin angiotensin system blockade in kidney transplantation: a systematic review of the evidence. *American Journal of Transplantation*, 7(10), pp.2350–2360.

Hocherl, K. *et al*., 2002. Cyclosporine A suppresses cyclooxygenase-2 expression in the rat kidney. *Journal of the American Society of Nephrology*, 13(10), pp.2427–2436.

Hohage, H. *et al*., 1996. Influence of cyclosporine A and FK506 on 24 h blood pressure monitoring in kidney transplant recipients. *Clinical nephrology*, 45(5), pp.342–344.

Hollander, A.A. *et al*., 1995. The effect of grapefruit juice on cyclosporine and prednisone metabolism in transplant patients. *Clinical pharmacology and therapeutics*, 57(3), pp.318–324.

Holliger, C. *et al*., 1983. Direct determination of vasa recta blood flow in the rat renal papilla. *Circulation research*, 53(3), pp.401–413.

Holzmacher, R. *et al*., 2005. Low serum magnesium is associated with decreased graft survival in patients with chronic cyclosporin nephrotoxicity. *Nephrology, dialysis, transplantation : official publication of the European Dialysis and Transplant Association - European Renal Association*, 20(7), pp.1456–1462.

Hooks, M.A., 1994. Tacrolimus, a New Immunosuppressant - a Review of the Literature. *Annals of Pharmacotherapy*, 28(4), pp.501–511.

Hoorn, E.J. *et al*., 2011. The calcineurin inhibitor tacrolimus activates the renal sodium chloride cotransporter to cause hypertension. *Nature Medicine*, 17(10), pp.1304–1309.

Hoorn, E.J., Walsh, S.B., McCormick, J.A., *et al*., 2012. Pathogenesis of calcineurin inhibitor-induced hypertension. *Journal of nephrology*, 25(3), pp.269–275.

Hoorn, E.J., Walsh, S.B., Unwin, R.J., *et al*., 2012. Hypertension after kidney transplantation: calcineurin inhibitors increase salt-sensitivity. *Journal of Hypertension*, 30(4), pp.832–834.

Hoorn, E.J.E., van der Lubbe, N.N. & Zietse, R.R., 2009. The renal WNK kinase pathway: a new link to hypertension. *Nephrology, dialysis, transplantation : official publication of the European Dialysis and Transplant Association - European Renal Association*, 24(4), pp.1074–1077.

Hortelano, S. *et al*., 2000. Potentiation by nitric oxide of cyclosporin a and FK506-induced apoptosis in renal proximal tubule cells. *Journal of the American Society of Nephrology*, 11(12), pp.2315–2323.

Hoskova, L. *et al*., 2014. Tacrolimus-induced hypertension and nephrotoxicity in Fawn-Hooded rats are attenuated by dual inhibition of renin-angiotensin system. *Hypertension research : official journal of the Japanese Society of Hypertension*, 37(8), pp.724–732.

Hughes, A.D.A., 2004. How do thiazide and thiazide-like diuretics lower blood pressure? *Journal of the Renin-Angiotensin-Aldosterone System*, 5(4), pp.155–160.

Hughes, C.C.W., 2008. Endothelial-stromal interactions in angiogenesis. *Current opinion in hematology*, 15(3), pp.204–209.

Humphreys, B.D. *et al*., 2010. Fate tracing reveals the pericyte and not epithelial origin of myofibroblasts in kidney fibrosis. *The American Journal of Pathology*, 176(1), pp.85–97.

Iijima, K. *et al*., 2000. Immunohistochemical analysis of renin activity in chronic cyclosporine nephropathy in childhood nephrotic syndrome. *Journal of the American Society of Nephrology*, 11(12), pp.2265–2271.

Ikeda, E. *et al*., 1997. Tacrolimus-rapamycin combination therapy for experimental autoimmune uveoretinitis. *Japanese Journal of Ophthalmology*, 41(6), pp.396–402.

Ingsathit, A. *et al*., 2006. Co-administration of diltiazem and cyclosporine for kidney transplant recipients: a four year follow-up study. *Journal of the Medical Association of Thailand = Chotmaihet thangphaet*, 89 Suppl 2, pp.S235–41.

Iñigo, P. *et al*., 2001. Effects of losartan and amlodipine on intrarenal hemodynamics

and TGF-beta(1) plasma levels in a crossover trial in renal transplant recipients. *Journal of the American Society of Nephrology*, 12(4), pp.822–827.

Ishiguro, H. & Steward, M.C., 2011. Microperfusion and micropuncture analysis of ductal secretion. *The Pancreapedia …*.

Israni, A. *et al*., 2002. Conversion to tacrolimus for the treatment of cyclosporine-associated nephrotoxicity in heart transplant recipients. *American Journal of Kidney Diseases*, 39(3), pp.–E16.

Jackson, M.J. *et al*., 2002. Antioxidants, reactive oxygen and nitrogen species, gene induction and mitochondrial function. *Molecular Aspects of Medicine*, 23(1-3), pp.209–285.

Jain, S., Bicknell, G.R. & Nicholson, M.L., 2000. Tacrolimus has less fibrogenic potential than cyclosporin A in a model of renal ischaemia-reperfusion injury. *British Journal of Surgery*, 87(11), pp.1563–1568.

Jamison, R.L. & Kriz, W., 1982. *Urinary concentrating mechanism*, Oxford University Press.

Jeanmart, H. *et al*., 2002. Comparative study of cyclosporine and tacrolimus vs newer Immunosuppressants mycophenolate mofetil and rapamycin on coronary endothelial function. *Journal of Heart and Lung Transplantation*, 21(9), pp.990–998.

Jenkins, J.K. *et al*., 2001. Vitamin E inhibits renal mRNA expression of COX II, HO I, TGFbeta, and osteopontin in the rat model of cyclosporine nephrotoxicity. *Transplantation*, 71(2), pp.331–334.

Jennings, P. *et al*., 2007. Cyclosporine A induces senescence in renal tubular epithelial cells. *American journal of physiology. Renal physiology*, 293(3), pp.F831–F838.

Jette, L. *et al*., 1996. Cyclosporin A treatment induces overexpression of P-glycoprotein in the kidney and other tissues. *The American journal of physiology*, 270(5), pp.F756–F765.

Jimeno, A. *et al*., 2006. Pharmacodynamic-guided, modified continuous reassessment method (mCRM)-based, dose finding study of rapamycin in adult patients with solid tumors. *Journal of Clinical Oncology*, 24(18), pp.125S–125S.

Joffres, M. *et al*., 2013. Hypertension prevalence, awareness, treatment and control in national surveys from England, the USA and Canada, and correlation with stroke and ischaemic heart disease mortality: a cross-sectional study. *BMJ open*, 3(8), p.e003423.

Jonas, S. *et al*., 1996. Conversion to tacrolimus after liver transplantation. *Transplant International*, 9(1), pp.23–31.

Joyce, N.C., DeCamilli, P. & BOYLES, J., 1984. Pericytes, like vascular smooth muscle cells, are immunocytochemically positive for cyclic GMP-dependent protein kinase. *Microvascular research*, 28(2), pp.206–219.

Jung, D.W., Bradshaw, P.C. & Pfeiffer, D.R., 1997. Properties of a cyclosporin-insensitive permeability transition pore in yeast mitochondria. *Journal of*

Biological Chemistry, 272(34), pp.21104–21112.

Kaelin, W.G.J., 2005. ROS: really involved in oxygen sensing. *Cell metabolism*, 1(6), pp.357–358.

Kahan, B.D., 2003. Two-year results of multicenter phase III trials on the effect of the addition of sirolimus to cyclosporine-based immunosuppressive regimens in renal transplantation. *Transplantation Proceedings*, 35(3 Suppl), pp.37S–51S.

Karliova, M. *et al*., 2000. Interaction of Hypericum perforatum (St. John's wort) with cyclosporin A metabolism in a patient after liver transplantation. *Journal of Hepatology*, 33(5), pp.853–855.

Karpinich, N.O. *et al*., 2002. The course of etoposide-induced apoptosis from damage to DNA and p53 activation to mitochondrial release of cytochrome c. *Journal of Biological Chemistry*, 277(19), pp.16547–16552.

Katsuki, S. *et al*., 1977. Stimulation of guanylate cyclase by sodium nitroprusside, nitroglycerin and nitric oxide in various tissue preparations and comparison to the effects of sodium azide and hydroxylamine. *Journal of cyclic nucleotide research*, 3(1), pp.23–35.

Katz, A.M., 1986. Pharmacology and mechanisms of action of calcium-channel blockers. *Journal of clinical hypertension*, 2(3 Suppl), pp.28S–37S.

Kaufman, J. *et al*., 1991. Community-acquired acute renal failure. *American Journal of Kidney Diseases*, 17(2), pp.191–198.

Kawahara, T., Quinn, M.T. & Lambeth, J.D., 2007. Molecular evolution of the reactive oxygen-generating NADPH oxidase (Nox/Duox) family of enzymes. *BMC Evolutionary Biology*, 7, pp.109–109.

Kawamura, H. *et al*., 2002. Endothelin-induced changes in the physiology of retinal pericytes. *Investigative Ophthalmology & Visual Science*, 43(3), pp.882–888.

Kaye, D. *et al*., 1993. Cyclosporine therapy after cardiac transplantation causes hypertension and renal vasoconstriction without sympathetic activation. *Circulation*, 88(3), pp.1101–1109.

Kennedy-Lydon, T.M. *et al*., 2012. Renal pericytes: regulators of medullary blood flow. *Acta physiologica (Oxford, England)*.

Khanna, A.K. & Pieper, G.M., 2007. NADPH oxidase subunits (NOX-1, p22phox, Rac-1) and tacrolimus-induced nephrotoxicity in a rat renal transplant model. *Nephrology, dialysis, transplantation : official publication of the European Dialysis and Transplant Association - European Renal Association*, 22(2), pp.376–385.

Kida, Y.Y. & Duffield, J.S.J., 2011. Pivotal role of pericytes in kidney fibrosis. *Clinical and Experimental Pharmacology and Physiology*, 38(7), pp.467–473.

Kino, T. *et al*., 1987. FK-506, a novel immunosuppressant isolated from a Streptomyces. II. Immunosuppressive effect of FK-506 in vitro. *Journal of Antibiotics*, 40(9), pp.1256–1265.

Klein, I. *et al*., 2002. Different effects of tacrolimus and cyclosporine on renal

hemodynamics and blood pressure in healthy subjects. *Transplantation*, 73(5), pp.732–736.

Klintmalm, G. *et al*., 1993. Use of Prograf (Fk-506) as Rescue Therapy for Refractory Rejection After Liver-Transplantation. *Transplantation Proceedings*, 25(1), pp.679–688.

Klintmalm, G., Iwatsuki, S. & Starzl, T.E., 1981. Nephrotoxicity Of Cyclosporin A In Liver And Kidney-Transplant Patients. Lancet, 1(8218), Pp.470–471.

Kneen, M.M.M. *et al*., 1999. Imaging of renal medullary interstitial cells in situ by confocal fluorescence microscopy. *Anatomy and Embryology*, 200(1), pp.117–121.

Kobashigawa, J.A. *et al*., 2006. Tacrolimus with mycophenolate mofetil (MMF) or sirolimus vs. Cyclosporine with MMF in cardiac transplant patients: 1-year report. *American Journal of Transplantation*, 6(6), pp.1377–1386.

Koeppen, B.M. & Stanton, B.A., 2013a. 2 - Structure and Function of the Kidneys. In B. M. K. A. Stanton, ed. *Renal Physiology (Fifth Edition)*. Renal Physiology (Fifth Edition). Philadelphia: Mosby, pp. 15–26.

Koeppen, B.M. & Stanton, B.A., 2013b. 3 - Glomerular Filtration and Renal Blood Flow. In B. M. K. A. Stanton, ed. *Renal Physiology (Fifth Edition)*. Renal Physiology (Fifth Edition). Philadelphia: Mosby, pp. 27–43.

Koeppen, B.M. & Stanton, B.A., 2013c. 5 - Regulation of Body Fluid Osmolality: Regulation of Water Balance. In B. M. K. A. Stanton, ed. *Renal Physiology (Fifth Edition)*. Renal Physiology (Fifth Edition). Philadelphia: Mosby, pp. 73–92.

Koeppen, B.M. & Stanton, B.A., 2013d. 6 - Regulation of Extracellular Fluid Volume and Nacl Balance. In B. M. K. A. Stanton, ed. *Renal Physiology (Fifth Edition)*. Renal Physiology (Fifth Edition). Philadelphia: Mosby, pp. 93–114.

Koeppen, B.M. & Stanton, B.A., 2013e. 9 - Regulation of Calcium and Phosphate Homeostasis. In B. M. K. A. Stanton, ed. *Renal Physiology (Fifth Edition)*. Renal Physiology (Fifth Edition). Philadelphia: Mosby, pp. 153–166.

Koesters, R. *et al*., 2010. Tubular overexpression of transforming growth factor-beta1 induces autophagy and fibrosis but not mesenchymal transition of renal epithelial cells. *The American Journal of Pathology*, 177(2), pp.632–643.

Kon, V. *et al*., 1990. Role of Endothelin in Cyclosporine-Induced Glomerular Dysfunction. *Kidney international*, 37(6), pp.1487–1491.

Kopp, J.B.J. & Klotman, P.E.P., 1990. Cellular and molecular mechanisms of cyclosporin nephrotoxicity. *Journal of the American Society of Nephrology*, 1(2), pp.162–179.

Kothari, J. *et al*., 2004. Diltiazem use in tacrolimus-treated renal transplant recipients. *Journal of Clinical Pharmacy and Therapeutics*, 29(5), pp.425–430.

Kou, R., Greif, D. & Michel, T., 2002A. Dephosphorylation Of Endothelial Nitric-Oxide Synthase By Vascular Endothelial Growth Factor: Implications For The Vascular Responses To Cyclosporin A. Journal Of Biological Chemistry, 277(33), Pp.29669–29673.

Kou, R.Q., Greif, D. & Michel, T., 2002b. Dephosphorylation of endothelial nitric-oxide synthase by vascular endothelial growth factor - Implications for the vascular responses to cyclosporin A. *Journal of Biological Chemistry*, 277(33), pp.29669–29673.

Kovarik, J.M. *et al*., 2005. Pharmacokinetic interaction between verapamil and everolimus in healthy subjects. *British Journal of Clinical Pharmacology*, 60(4), pp.434–437.

Krause, T. *et al*., 2011. Management of hypertension: summary of NICE guidance. *British Medical Journal*, 343(aug25 2), pp.d4891–d4891.

Kreis, H. *et al*., 2000. Sirolimus in association with mycophenolate mofetil induction for the prevention of acute graft rejection in renal allograft recipients. *Transplantation*, 69(7), pp.1252–1260.

Krejci, K. *et al*., 2010. Calcineurin inhibitor-induced renal allograft nephrotoxicity. *Biomedical Papers*, 154(4), pp.297–306.

Krishnamurthy, G. *et al*., 1990. A photochemical method to map ethidium bromide binding sites on DNA: application to a bent DNA fragment. *Biochemistry*, 29(4), pp.981–988.

Kriz, W., 1981. Structural Organization of the Renal Medulla - Comparative and Functional-Aspects. *The American journal of physiology*, 241(1), pp.R3–R16.

Kroemer, G., 1997. The proto-oncogene Bcl-2 and its role in regulating apoptosis. *Nature Medicine*, 3(6), pp.614–620.

Kroemer, G., Galluzzi, L. & Brenner, C., 2007. Mitochondrial Membrane Permeabilization in Cell Death. *Physiological Reviews*, 87(1), pp.99–163.

Kumana, C.R. *et al*., 2003. Diltiazem co-treatment in renal transplant patients receiving microemulsion cyclosporin. *British Journal of Clinical Pharmacology*, 56(6), pp.670–678.

Kundu, K. *et al*., 2009. Hydrocyanines: a class of fluorescent sensors that can image reactive oxygen species in cell culture, tissue, and in vivo. *Angewandte Chemie (International ed. in English)*, 48(2), pp.299–303.

Kung, L. *et al*., 2001. Tissue distribution of calcineurin and its sensitivity to inhibition by cyclosporine. *American Journal of Transplantation*, 1(4), pp.325–333.

Kurtz, A., Dellabruna, R. & Kuhn, K., 1988. Cyclosporine A Enhances Renin Secretion And Production In Isolated Juxtaglomerular Cells. Kidney International, 33(5), Pp.947–953.

Ladefoged, S.D. & Andersen, C.B., 1994. Calcium channel blockers in kidney transplantation. *Clinical transplantation*, 8(2 Pt 1), pp.128–133.

Laftavi, M.R. *et al*., 2010. Sirolimus-Induced Isometric Tubular Vacuolization: A New Sirolimus Histopathologic Manifestation. *Transplantation Proceedings*, 42(7), pp.4–4.

Lajeunesse, D. & Brunette, M.G., 1991. The hypocalciuric effect of thiazides:

subcellular localization of the action. *Pflugers Archiv : European journal of physiology*, 417(5), pp.454–462.

Lajeunesse, D., Bouhtiauy, I. & Brunette, M.G., 1994. Parathyroid hormone and hydrochlorothiazide increase calcium transport by the luminal membrane of rabbit distal nephron segments through different pathways. *Endocrinology*, 134(1), pp.35–41.

Landis, E.M., 1933. Factors Controlling the Movement of Fluid Through the Human Capillary Wall. *Yale Journal of Biology and Medicine*, 5(3), pp.201–225.

Lanese, D.M. & Conger, J.D., 1993. Effects of endothelin receptor antagonist on cyclosporine-induced vasoconstriction in isolated rat renal arterioles. *Journal of Clinical Investigation*, 91(5), pp.2144–2149.

Laskow, D.A. *et al*., 1988. Cyclosporine impairs the renal response to volume depletion. *Transplantation Proceedings*, 20(3 Suppl 3), pp.568–571.

Lassila, M., 2002. Interaction of cyclosporine A and the renin-angiotensin system; new perspectives. *Current drug metabolism*, 3(1), pp.61–71.

Lassila, M. *et al*., 2000. Comparison of enalapril and valsartan in cyclosporine A-induced hypertension and nephrotoxicity in spontaneously hypertensive rats on high-sodium diet. *British Journal of Pharmacology*, 130(6), pp.1339–1347.

Lassila, M. *et al*., 2001. Vascular changes in cyclosporine A-induced hypertension and nephrotoxicity in spontaneously hypertensive rats on high-sodium diet. *Journal of physiology and pharmacology : an official journal of the Polish Physiological Society*, 52(1), pp.21–38.

Lebranchu, Y., Thierry, A. & Toupance, O., 2009. Efficacy on renal function of early conversion from cyclosporine to sirolimus 3 months after renal transplantation: concept study. *… of Transplantation*.

Lee, C.-T. *et al*., 2002. Cyclosporine A-induced hypercalciuria in calbindin-D28k knockout and wild-type mice. *Kidney international*, 62(6), pp.2055–2061.

Lee, C.H. & Kim, G.-H., 2007. Electrolyte and Acid-base disturbances induced by clacineurin inhibitors. *Electrolytes & Blood Pressure*, 5(2), pp.126–130.

Lee, D.B., 1997. Cyclosporine and the renin-angiotensin axis. *Kidney international*, 52(1), pp.248–260.

Lee, S.H. *et al*., 2005. Attenuation of interstitial inflammation and fibrosis by recombinant human erythropoietin in chronic cyclosporine nephropathy. *American journal of nephrology*, 25(1), pp.64–76.

Lee, V.W.V. & Chapman, J.R.J., 2005. Sirolimus: its role in nephrology. *Nephrology*, 10(6), pp.606–614.

Lemley, K.V. *et al*., 1986. The Shape of Renal Vasa Recta Capillaries and Its Effect on Calculation of Single Capillary Blood-Flow. *Microvascular research*, 32(1), pp.1–20.

Lewis, E.J. *et al*., 1993. The effect of angiotensin-converting-enzyme inhibition on

diabetic nephropathy. The Collaborative Study Group. *New England Journal of Medicine*, 329(20), pp.1456–1462.

Li, L. *et al*., 2010. Autophagy Is a Component of Epithelial Cell Fate in Obstructive Uropathy. *American Journal of Pathology*, 176(4), pp.1767–1778.

Li, X. *et al*., 2013. Targeting mitochondrial reactive oxygen species as novel therapy for inflammatory diseases and cancers. *Journal of hematology & oncology*, 6, p.19.

Lim, H.W. *et al*., 2000. Calcineurin expression, activation, and function in cardiac pressure-overload hypertrophy. *Circulation*, 101(20), pp.2431–2437.

Lin, H.Y. *et al*., 1989. Cyclosporine-Induced Hyperuricemia and Gout. *New England Journal of Medicine*, 321(5), pp.287–292.

Lin, S.-L. *et al*., 2008. Pericytes and Perivascular Fibroblasts Are the Primary Source of Collagen-Producing Cells in Obstructive Fibrosis of the Kidney. *American Journal of Pathology*, 173(6), pp.1617–1627.

Lin, S.-L. *et al*., 2011. Targeting endothelium-pericyte cross talk by inhibiting VEGF receptor signaling attenuates kidney microvascular rarefaction and fibrosis. *American Journal of Pathology*, 178(2), pp.911–923.

Ling, S.Y. *et al*., 2013. Pharmacokinetics of voclosporin in renal impairment and hepatic impairment. *The Journal of Clinical Pharmacology*, 53(12), pp.1303–1312.

Liptak, P.P. & Ivanyi, B.B., 2006. Primer: Histopathology of calcineurin-inhibitor toxicity in renal allografts. *Nature Clinical Practice Nephrology*, 2(7), pp.398–404.

Lisik, W. *et al*., 2007. Statins benefit outcomes of renal transplant recipients on a sirolimus-cyclosporine regimen. *Transplantation Proceedings*, 39(10), pp.3086–3092.

Liu, E.H. *et al*., 2007. T cell-directed therapies: lessons learned and future prospects. *Nature Immunology*, 8(1), pp.25–30.

Liu, Y.H., 2004. Epithelial to mesenchymal transition in renal fibrogenesis: Pathologic significance, molecular mechanism, and therapeutic intervention. *Journal of the American Society of Nephrology*, 15(1), pp.1–12.

Loh, P.T. *et al*., 2008. Significant impact of gene polymorphisms on tacrolimus but not cyclosporine dosing in Asian renal transplant recipients. *Transplantation Proceedings*, 40(5), pp.1690–1695.

Longoni, B. *et al*., 2001. Apoptosis and adaptive responses to oxidative stress in human endothelial cells exposed to cyclosporin A correlate with BCL-2 expression levels. *Faseb Journal*, 15(3), pp.731–740.

Lopez-Ongil, S. *et al*., 1998. Role of reactive oxygen species in the signalling cascade of cyclosporine A-mediated up-regulation of eNOS in vascular endothelial cells. *British Journal of Pharmacology*, 124(3), pp.447–454.

LopezOngil, S. *et al*., 1996. Regulation of endothelial NO synthase expression by cyclosporin A in bovine aortic endothelial cells. *American journal of physiology. Heart and circulatory physiology*, 271(3), pp.H1072–H1078.

Lote, C.J., 1994. *Principles of renal physiology*, New York : Chapman & Hall.

Lucey, M.R. *et al*., 2005. A comparison of tacrolimus and cyclosporine in liver transplantation: effects on renal function and cardiovascular risk status. *American Journal of Transplantation*, 5(5), pp.1111–1119.

Lungu, A.O. *et al*., 2004. Cyclosporin A inhibits flow-mediated activation of endothelial nitric-oxide synthase by altering cholesterol content in caveolae. *Journal of Biological Chemistry*, 279(47), pp.48794–48800.

Luntz, S.P. *et al*., 2005. HEGPOL: randomized, placebo controlled, multicenter, double-blind clinical trial to investigate hepatoprotective effects of glycine in the postoperative phase of liver transplantation (ISRCTN69350312). *BMC Surgery*, 5, pp.18–18.

Ly, J.D., Grubb, D.R. & Lawen, A., 2003. The mitochondrial membrane potential (Δψm) in apoptosis; an update. *Apoptosis*, 8(2), pp.115–128.

MacDonald, A.S., 2003. Rapamycin in combination with cyclosporine or tacrolimus in liver, pancreas, and kidney transplantation. *Transplantation Proceedings*, 35(3 Suppl), pp.201S–208S.

MacDonald, A.S. & Grp, R.G.S., 2001. A worldwide, phase III, randomized, controlled, safety and efficacy study of a sirolimus/cyclosporine regimen for prevention of acute rejection in recipients of primary mismatched renal allografts. *Transplantation*, 71(2), pp.271–280.

Majid, D.S., Godfrey, M. & Omoro, S.A., 1997. Pressure natriuresis and autoregulation of inner medullary blood flow in canine kidney. *Hypertension*, 29(1 Pt 2), pp.210–215.

Mangray, M. & Vella, J.P., 2011. Hypertension After Kidney Transplant. *American Journal of Kidney Diseases*, 57(2), pp.331–341.

Markowitz, G.S. & Perazella, M.A., 2005. Drug-induced renal failure: a focus on tubulointerstitial disease. *Clinica Chimica Acta*, 351(1-2), pp.31–47.

Marti, H.P. & Frey, F.J., 2005. Nephrotoxicity of rapamycin: an emerging problem in clinical medicine. *Nephrology, dialysis, transplantation : official publication of the European Dialysis and Transplant Association - European Renal Association*, 20(1), pp.13–15.

Marumo, T. *et al*., 1995. Cyclosporin A inhibits nitric oxide synthase induction in vascular smooth muscle cells. *Hypertension*, 25(4 Pt 2), pp.764–768.

Maschio, G. *et al*., 1996. Effect of the angiotensin-converting-enzyme inhibitor benazepril on the progression of chronic renal insufficiency. The Angiotensin-Converting-Enzyme Inhibition in Progressive Renal Insufficiency Study Group. *New England Journal of Medicine*, 334(15), pp.939–945.

Matas, A.J. *et al*., 2015. OPTN/SRTR 2013 Annual Data Report: Kidney. *American Journal of Transplantation*, 15(S2), pp.1–34.

Matsumoto, S. *et al*., 1999. Blockade of the mitochondrial permeability transition pore diminishes infarct size in the rat after transient middle cerebral artery occlusion.,

19(7), pp.736–741.

Mattson, D.L. *et al*., 1993. Relationship Between Renal Perfusion-Pressure and Blood-Flow in Different Regions of the Kidney. *The American journal of physiology*, 264(3), pp.R578–R583.

Mattson, D.L., ROMAN, R.J. & COWLEY, A.W., 1992. Role of nitric oxide in renal papillary blood flow and sodium excretion. *Hypertension*, 19(6 Pt 2), pp.766–769.

McAlister, V.C. *et al*., 2000. Sirolimus-tacrolimus combination immunosuppression. *Lancet*, 355(9201), pp.376–377.

McBride, H.M., Neuspiel, M. & Wasiak, S., 2006. Mitochondria: more than just a powerhouse. *Current Biology*, 16(14), pp.R551–60.

Mejia, J.C., Basu, A. & Shapiro, R., 2014. Chapter 17 - Calcineurin Inhibitors. In P. J. M. J. Knechtle, ed. *Kidney Transplantation–Principles and Practice (Seventh Edition)*. Kidney Transplantation–Principles and Practice (Seventh Edition). Philadelphia (PA): Content Repository Only!, pp. 231–249.

Melnikov, S. *et al*., 2011. Cyclosporine metabolic side effects: association with the WNK4 system. *European Journal of Clinical Investigation*, 41(10), pp.1113–1120.

Merlini, L. *et al*., 2008. Cyclosporin A corrects mitochondrial dysfunction and muscle apoptosis in patients with collagen VI myopathies. *Proceedings of the National Academy of Sciences*, 105(13), pp.5225–5229.

Mervaala, E. *et al*., 1999. Effects of ACE inhibition on cyclosporine A-induced hypertension and nephrotoxicity in spontaneously hypertensive rats on a high-sodium diet. *Blood Pressure*, 8(1), pp.49–56.

Mescher, A., 2013. *Junqueira's Basic Histology: Text and Atlas, Thirteenth Edition*, McGraw Hill Professional.

Meyer-Lehnert, H. *et al*., 1993. Cellular signaling by cyclosporine A in contractile cells: interactions with atrial natriuretic peptide. *The clinical investigator*, 71(2), pp.153–160.

Midtvedt, K. & Hartmann, A., 2002a. Hypertension after kidney transplantation: are treatment guidelines emerging? *Nephrology, dialysis, transplantation : official publication of the European Dialysis and Transplant Association - European Renal Association*, 17(7), pp.1166–1169.

Midtvedt, K. & Hartmann, A., 2002b. Hypertension after kidney transplantation: are treatment guidelines emerging? *Nephrology, dialysis, transplantation : official publication of the European Dialysis and Transplant Association - European Renal Association*, 17(7), pp.1166–1169.

Midtvedt, K., Hartmann, A., Foss, A., *et al*., 2001. Sustained improvement of renal graft function for two years in hypertensive renal transplant recipients treated with nifedipine as compared to lisinopril. *Transplantation*, 72(11), pp.1787–1792.

Midtvedt, K., Hartmann, A., Holdaas, H., *et al*., 2001. Efficacy of nifedipine or lisinopril in the treatment of hypertension after renal transplantation: a double-blind randomised comparative trial. *Clinical transplantation*, 15(6), pp.426–431.

Mihatsch, M.J. *et al*., 1992. Giant Mitochondria in Zero-Hour Transplant Biopsies. *UltRAAStructural Pathology*, 16(3), pp.277–282.

Mihatsch, M.J. *et al*., 1985. Morphological patterns in cyclosporine-treated renal transplant recipients. *Transplantation Proceedings*, 17(4 Suppl 1), pp.101–116.

Mihatsch, M.J. *et al*., 1986. Morphology of Cyclosporine Nephrotoxicity in the Rat. *Clinical nephrology*, 25, pp.S2–S8.

Mihatsch, M.J. *et al*., 1998. The side-effects of ciclosporine-A and tacrolimus. *Clinical nephrology*, 49(6), pp.356–363.

Mink, D. *et al*., 1984. Interendothelial junctions in kidney vessels. *Cell and tissue research*, 236(3), pp.567–576.

Mittal, T. & Kohli, H.S., 2014. Post renal transplant acute kidney injury. *Indian Journal of Transplantation*.

Modena, F.M. *et al*., 1991. Progression of Kidney-Disease in Chronic Renal-Transplant Rejection. *Transplantation*, 52(2), pp.239–244.

Moes, A.D. *et al*., 2014. Calcineurin inhibitors and hypertension: a role for pharmacogenetics? *Pharmacogenomics*, 15(9), pp.1243–1251.

Moran, M. *et al*., 1990. Prevention of Acute Graft-Rejection by the Prostaglandin-E1 Analog Misoprostol in Renal-Transplant Recipients Treated with Cyclosporine and Prednisone. *New England Journal of Medicine*, 322(17), pp.1183–1188.

Morelon, E.E. *et al*., 2001. Sirolimus: a new promising immunosuppressive drug. Towards a rationale for its use in renal transplantation. *Nephrology, dialysis, transplantation : official publication of the European Dialysis and Transplant Association - European Renal Association*, 16(1), pp.18–20.

Morozumi, K. *et al*., 1992. Studies on Morphological Outcome of Cyclosporine-Associated Arteriolopathy After Discontinuation of Cyclosporine in Renal-Allografts. *Clinical nephrology*, 38(1), pp.1–8.

Morris, S. *et al*., 2000. Endothelial dysfunction in renal transplant recipients maintained on cyclosporine. *Kidney international*, 57(3), pp.1100–1106.

Muller, G. & Morawietz, H., 2009. Nitric oxide, NAD(P)H oxidase, and atherosclerosis. *Antioxidants & redox signaling*, 11(7), pp.1711–1731.

Murphy, M.P., 2009. How mitochondria produce reactive oxygen species. *Biochemical Journal*, 417(Pt 1), pp.1–13.

Murray, B.M., Paller, M.S. & Ferris, T.F., 1985. Effect Of Cyclosporine Administration On Renal Hemodynamics In Conscious Rats. Kidney International, 28(5), Pp.767–774.

Mustapha, N.M. *et al*., 2010. NADPH Oxidase versus Mitochondria-Derived ROS in Glucose-Induced Apoptosis of Pericytes in Early Diabetic Retinopathy. *Journal of Ophthalmology*, 2010, p.10.

Myers, B.D. *et al*., 1984. Cyclosporine-associated chronic nephropathy. *New England*

Journal of Medicine, 311(11), pp.699–705.

Na, 2002. Tacrolimus interaction. *Reactions Weekly*, &NA;(906), p.11.

Naesens, M. *et al*., 2004. Bartter"s and Gitelman"s syndromes: from gene to clinic. *Nephron. Physiology*, 96(3), pp.p65–p78.

Naesens, M. *et al*., 2007. Tacrolimus exposure and evolution of renal allograft histology in the first year after transplantation. *American Journal of Transplantation*, 7(9), pp.2114–2123.

Naesens, M.M., Kuypers, D.R.J.D. & Sarwal, M.M., 2009. Calcineurin inhibitor nephrotoxicity. *Clinical Journal of the American Society of Nephrology*, 4(2), pp.481–508.

Nakagawa, T. *et al*., 2005. Cyclophilin D-dependent mitochondrial permeability transition regulates some necrotic but not apoptotic cell death. *Nature*, 434(7033), pp.652–658.

Nakahama, H., 1990. Stimulatory effect of cyclosporine A on endothelin secretion by a cultured renal epithelial cell line, LLC-PK1 cells. *European journal of pharmacology*, 180(1), pp.191–192.

Nankivell, B.J. *et al*., 2003. The natural history of chronic allograft nephropathy. *New England Journal of Medicine*, 349(24), pp.2326–2333.

Nankivell, B.J., Borrows, R.J., Fung, C., *et al*., 2004. Evolution and pathophysiology of renal-transplant glomerulosclerosis. *Transplantation*, 78(3), pp.461–468.

Nankivell, B.J., Chapman, J.R., *et al*., 2004. Oral cyclosporine but not tacrolimus reduces renal transplant blood flow. *Transplantation*, 77(9), pp.1457–1459.

Nankivell, B.J.B., Borrows, R.J.R., Fung, C.L.S.C., *et al*., 2004. Calcineurin inhibitor nephrotoxicity: longitudinal assessment by protocol histology. *Transplantation*, 78(4), pp.557–565.

Nash, K., Hafeez, A. & Hou, S., 2002. Hospital-acquired renal insufficiency. *American Journal of Kidney Diseases*, 39(5), pp.930–936.

Navar, L.G. *et al*., 1996. Paracrine regulation of the renal microcirculation. *Physiological Reviews*, 76(2), pp.425–536.

Navar, L.G. *et al*., 2011. *The Renal Microcirculation*, Hoboken, NJ, USA: John Wiley & Sons, Inc.

Navarro-Antolin, J. *et al*., 1998. CsA and FK506 up-regulate eNOS expression: role of reactive oxygen species and AP-1. *Kidney international. Supplement*, 68, pp.S20–4.

Navarro-Antolin, J. *et al*., CsA and FK506 up-regulate eNOS expression: Role of reactive oxygen species and AP-1. *Kidney international*, 54(S68), pp.S20–S24.

Navarro-Antolin, J. *et al*., 2001. Formation of peroxynitrite in vascular endothelial cells exposed to cyclosporine A. *Faseb Journal*, 15(7), pp.1291–1293.

Navarro-Antolin, J., Rey-Campos, J. & LAMAS, S., 2000. Transcriptional induction of

endothelial nitric oxide gene by cyclosporine A - A role for activator protein-1. *Journal of Biological Chemistry*, 275(5), pp.3075–3080.

Nehls, V. & Drenckhahn, D., 1991. Heterogeneity Of Microvascular Pericytes For Smooth-Muscle Type Alpha-Actin. Journal Of Cell Biology, 113(1), Pp.147–154.

Nishiyama, A., Kobori, H., Fukui, T., Zhang, G.-X., Yao, L., Rahman, M., Hitomi, H., Kiyomoto, H., Shokoji, T., Kimura, S., Kohno, M. & Abe, Y., 2003. Physiology of the renal medullary microcirculation. *American journal of physiology. Renal physiology*, 284(2), pp.F253–F266.

Nishiyama, A., Kobori, H., Fukui, T., Zhang, G.X., Yao, L., Rahman, M., Hitomi, H., Kiyomoto, H., Shokoji, T., Kimura, S., Kohno, M. & Abe, Y., 2003. Role of angiotensin II and reactive oxygen species in cyclosporine A-dependent hypertension. *Hypertension*, 42(4), pp.754–760.

Nistala, R., Whaley-Connell, A. & Sowers, J.R., 2008. Redox control of renal function and hypertension. *Antioxidants & redox signaling*, 10(12), pp.2047–2089.

Nolin, T.D. & Himmelfarb, J., 2010. Mechanisms of drug-induced nephrotoxicity. *Handbook of experimental pharmacology*, (196), pp.111–130.

Noris, M. & Remuzzi, G., 2010. Thrombotic Microangiopathy After Kidney Transplantation. *American Journal of Transplantation*, 10(7), pp.1517–1523.

Nwaneshiudu, A. *et al*., 2012. Introduction to confocal microscopy., 132(12), p.e3.

O'Connell, S. *et al*., 2012. Sirolimus Enhances Cyclosporine A-Induced Cytotoxicity in Human Renal Glomerular Mesangial Cells. *Journal of Transplantation*, 2012, pp.1–9.

O'Connor, P.M. & Cowley, A.W.J., 2012. Medullary Thick Ascending Limb Buffer Vasoconstriction of Renal Outer-Medullary Vasa Recta in Salt-Resistant But Not Salt-Sensitive Rats. *Hypertension*, 60(4), pp.965–.

Ochaia, T. *et al*., 1987. Effect of a New Immunosuppressive Agent, Fk-506, on Heterotopic Cardiac Allotransplantation in the Rat. *Transplantation Proceedings*, 19(1), pp.1284–1286.

Olyaei, A.J.A., de Mattos, A.M.A. & Bennett, W.M.W., 2001. Nephrotoxicity of immunosuppressive drugs: new insight and preventive strategies. *Current Opinion in Critical Care*, 7(6), pp.384–389.

Opelz, G., Wujciak, T. & Ritz, E., 1997. The association of chronic kidney graft failure with recipient blood pressure. *Journal of the American Society of Nephrology*, 8, pp.A3240–A3240.

Oriji, G.K. & Keiser, H.R., 1999. Nitric oxide in cyclosporine A-induced hypertension: Role of protein kinase C. *American Journal of Hypertension*, 12(11), pp.1091–1097.

Oriji, G.K. & Schanz, N., Nitric oxide in CsA-induced hypertension: role of β - adrenoceptor antagonist and thromboxane A2. *Prostaglandins, Leukotrienes and Essential Fatty Acids (PLEFA)*, 65(5–6), pp.259–263.

Ortiz, A., Tejedor, A. & Caramelo, C., 2008. *Nephrotoxicity*, Hoboken, NJ, USA: John Wiley & Sons, Inc.

Owusu-Ansah, E., Yavari, A. & Banerjee, U., 2008. A protocol for _in vivo_ detection of reactive oxygen species.

Óskarsson, H.J., Hofmeyer, T.G. & Olivari, M.T., 1997. Cyclosporine Impairs the Ability of Human Platelets to Mediate Vasodilation. *Hypertension*, 29(6), pp.1314–1321.

Özen, I. *et al*., 2014. Brain pericytes acquire a microglial phenotype after stroke. *Acta neuropathologica*, 128(3), pp.381–396.

Paller, M.S., 1988. Effects of the Prostaglandin-E1 Analog Misoprostol on Cyclosporine Nephrotoxicity. *Transplantation*, 45(6), pp.1126–1131.

Pallet, N., Djamali, A. & Legendre, C., 2011. Challenges in diagnosing acute calcineurin-inhibitor induced nephrotoxicity: From toxicogenomics to emerging biomarkers. *Pharmacological Research*, 64(1), pp.6–6.

Pallone, T.L., 1991. Effect of Sodium-Chloride Gradients on Water Flux in Rat Descending Vasa Recta. *Journal of Clinical Investigation*, 87(1), pp.12–19.

Pallone, T.L., 1994. Vasoconstriction of outer medullary vasa recta by angiotensin II is modulated by prostaglandin E2. *The American journal of physiology*, 266(6 Pt 2), pp.F850–F857.

Pallone, T.L. & Cao, C., 2007. *Renal cortical and medullary microcirculations: Structure and function*, The Kidney: Physiology and Pathophysiology.

Pallone, T.L. & Silldorff, E.P., 2001. Pericyte Regulation of Renal Medullary Blood Flow. *Nephron Experimental Nephrology*, 9(3), pp.165–170.

Pallone, T.L. *et al*., 1994. Transport of sodium and urea in outer medullary descending vasa recta. *Journal of Clinical Investigation*, 93(1), pp.212–222.

Pallone, T.L., Edwards, A. & Mattson, D.L., 2012. Renal medullary circulation. *Comprehensive Physiology*, 2(1), pp.97–140.

Pallone, T.L., ROBERTSON, C.R. & Jamison, R.L., 1990. Renal medullary microcirculation. *Physiological Reviews*.

Pallone, T.L., Turner, M.R., *et al*., 2003. Countercurrent exchange in the renal medulla. *American Journal of Physiology - Regulatory, Integrative and Comparative Physiology*, 284(5), pp.R1153–R1175.

Pallone, T.L.T., Zhang, Z.Z. & Rhinehart, K.K., 2003. Physiology of the renal medullary microcirculation. *American Journal of Physiology: Renal, Fluid & Electrolyte Physiology (Abstracts)*, 284(2), pp.F253–F266.

Palmer, B.F., 2002. Current concepts: Renal dysfunction complicating the treatment of hypertension. *New England Journal of Medicine*, 347(16), pp.1256–1261.

Pannabecker, T.L. & Dantzler, W.H., 2004. Three-dimensional lateral and vertical relationships of inner medullary loops of Henle and collecting ducts. *American journal of physiology. Renal physiology*, 287(4), pp.F767–F774.

Papp, K. *et al*., 2008. Efficacy of ISA247 in plaque psoriasis: a randomised, multicentre, double-blind, placebo-controlled phase III study. *The Lancet*.

Paravicini, T.M. & Touyz, R.M., 2008. NADPH oxidases, reactive oxygen species, and hypertension: clinical implications and therapeutic possibilities. *Diabetes care*, 31 Suppl 2, pp.S170–80.

Park, F. *et al*., 1997. Evidence for the presence of smooth muscle α-actin within pericytes of the renal medulla. *American Journal of Physiology - Regulatory, Integrative and Comparative Physiology*, 273(5), pp.R1742–R1748.

Park, J.W. *et al*., 2011. Rho Kinase Inhibition by Fasudil Attenuates Cyclosporine-Induced Kidney Injury. *Journal of Pharmacology and Experimental Therapeutics*, 338(1), pp.271–279.

Parra, T. *et al*., 1998. Cyclosporine A nephrotoxicity: role of thromboxane and reactive oxygen species. *The Journal of laboratory and clinical medicine*, 131(1), pp.63–70.

Paslaru, L. *et al*., 2000. Cyclosporin A induces an atypical heat shock response. *Biochemical and Biophysical Research Communications*, 269(2), pp.464–469.

Patterson, G.H. & Piston, D.W., 2000. Photobleaching in two-photon excitation microscopy. *Biophysical Journal*, 78(4), pp.2159–2162.

Peppiatt, C.M. *et al*., 2006. Bidirectional control of CNS capillary diameter by pericytes. *Nature*, 443(7112), pp.700–704.

Peppiatt-Wildman, C.M., 2013. The evolving role of renal pericytes. *California and western medicine*, 22(1), pp.10–16.

Peppiatt-Wildman, C.M. *et al*., 2013. A pivotal role for pericytes in non-steroidal anti-inflammatory drug-induced toxicity. *The FASEB Journal*, 27(1_MeetingAbstracts), p.111017.

Perazella, M.A., 2005. Drug-induced nephropathy: an update. 4(4), pp.689–706.

Perez de Hornedo, J. *et al*., 2007. (Cyclosporin A causes oxidative stress and mitochondrial dysfunction in renal tubular cells). *Nefrologia : publicacion oficial de la Sociedad Espanola Nefrologia*, 27(5), pp.565–573.

Perico, N. *et al*., 1996. Cyclosporine induces glomerulosclerosis: three-dimensional definition of the lesions in a rat model of renal transplant. *Kidney international*, 49(5), pp.1283–1288.

Perico, N., DADAN, J. & Remuzzi, G., 1990. Endothelin Mediates the Renal Vasoconstriction Induced by Cyclosporine in the Rat. *Journal of the American Society of Nephrology*, 1(1), pp.76–83.

Petronilli, V. *et al*., 1994. Regulation of the permeability transition pore, a voltage-dependent mitochondrial channel inhibited by cyclosporin A. *... et Biophysica Acta (BBA ...*.

Piao, S.G. *et al*., 2014. Combined Treatment of Tacrolimus and Everolimus Increases Oxidative Stress by Pharmacological Interactions. *Transplantation*, Publish Ahead of Print, p.1.

Picard, N. *et al*., 2007. Metabolism of sirolimus in the presence or absence of cyclosporine by genotyped human liver microsomes and recombinant cytochromes P450 3A4 and 3A5. *Drug Metabolism and Disposition*, 35(3), pp.350–355.

Pichler, R.H. *et al*., 1995. Pathogenesis of cyclosporine nephropathy: roles of angiotensin II and osteopontin. *Journal of the American Society of Nephrology*, 6(4), pp.1186–1196.

Pickkers, P. *et al*., 1998. Thiazide-induced vasodilation in humans is mediated by potassium channel activation. *Hypertension*, 32(6), pp.1071–1076.

Piot, C. *et al*., 2008. Effect of Cyclosporine on Reperfusion Injury in Acute Myocardial Infarction. *New England Journal of Medicine*, 359(5), pp.473–481.

Pisoni, R., Ruggenenti, P. & Remuzzi, G., 2001. Drug-induced thrombotic microangiopathy - Incidence, prevention and management. *Drug safety : an international journal of medical toxicology and drug experience*, 24(7), pp.491–501.

Podder, H. *et al*., 2001. Pharmacokinetic interactions augment toxicities of sirolimus/cyclosporine combinations. *Journal of the American Society of Nephrology*, 12(5), pp.1059–1071.

Powles, R.L. *Et al*., 1978. Cyclosporin A For The Treatment Of Graft-Versus-Host Disease In Man. Lancet, 312(8104), Pp.1327–1331.

Pugliese, F. & Ciabattoni, G., 1984. The role of prostaglandins in the control of renal function: renal effects of nonsteroidal anti-inflammatory drugs. *Clinical and experimental rheumatology*, 2(4), pp.345–352.

Qiu, X.-Y. *et al*., 2008. Association of MDR1, CYP3A4*18B, and CYP3A5*3 polymorphisms with cyclosporine pharmacokinetics in Chinese renal transplant recipients. *European journal of clinical pharmacology*, 64(11), pp.1069–1084.

Raedschelders, K., Ansley, D.M. & Chen, D.D.Y., 2012. The cellular and molecular origin of reactive oxygen species generation during myocardial ischemia and reperfusion. *Pharmacology & therapeutics*, 133(2), pp.230–255.

Rahn, K.H. *et al*., 1999. Effect of nitrendipine on renal function in renal-transplant patients treated with cyclosporin: a randomised trial. *Lancet*, 354(9188), pp.1415–1420.

Ramirez, C. *et al*., 2000. Role of intrarenal endothelin 1, endothelin 3, and angiotensin II expression in chronic cyclosporin A nephrotoxicity in rats. *Experimental Nephrology*, 8(3), pp.161–172.

Randhawa, P.S., Starzl, T.E. & Demetris, A.J., 1997. Tacrolimus (FK506)-Associated Renal Pathology. *Advances in anatomic pathology*, 4(4), pp.265–276.

Rao, A., Luo, C. & Hogan, P.G., 1997. Transcription factors of the NFAT family: regulation and function. *Annual review of immunology*, 15, pp.707–747.

RAAStghalam, R. *et al*., 2014. Angiotensin Type-1 Receptor Blockade May Not Protect Kidney against Cisplatin-Induced Nephrotoxicity in Rats. *ISRN Nephrology*, 2014,

p.7.

Readnower, R.D. *et al*., 2011. Post-injury administration of the mitochondrial permeability transition pore inhibitor, NIM811, is neuroprotective and improves cognition after traumatic brain injury in rats. *Journal of neurotrauma*, 28(9), pp.1845–1853.

Regner, K.R.K. & Roman, R.J.R., 2012. Role of medullary blood flow in the pathogenesis of renal ischemia-reperfusion injury. *Current opinion in nephrology and hypertension*, 21(1), pp.33–38.

Remuzzi, G., 1994. Renal pathophysiology. *Current opinion in nephrology and hypertension*, 3(4), p.431.

Remuzzi, G. *et al*., 2005. The role of renin-angiotensin-aldosterone system in the progression of chronic kidney disease. *Kidney international. Supplement*, (99), pp.S57–65.

Rhinehart, K. & Pallone, T.L., 2001a. Nitric oxide (NO) generation by isolated descending vasa recta. *Faseb Journal*, 15(4), pp.A146–A146.

Rhinehart, K. *et al*., 2003. ANG II AT2 receptor modulates AT1 receptor-mediated descending vasa recta endothelial Ca2+ signaling. *American journal of physiology. Heart and circulatory physiology*, 284(3), pp.H779–H789.

Rhinehart, K.L. & Pallone, T.L., 2001b. Nitric oxide generation by isolated descending vasa recta. *American journal of physiology. Heart and circulatory physiology*, 281(1), pp.H316–H324.

Richards, N.T., Poston, L. & Hilton, P.J., 1989. Cyclosporine A inhibits relaxation but does not induce vasoconstriction in human subcutaneous resistance vessels. *Journal of Hypertension*, 7(1), pp.1–3.

Robert J Alpern, D.W.S.S.C.H.G.H.G., 2008. *Seldin and Giebischs the Kidney*, Elsevier.

Rolo, A.P. *et al*., 2003. Chenodeoxycholate induction of mitochondrial permeability transition pore is associated with increased membrane fluidity and cytochrome c release: protective role of carvedilol. *Mitochondrion*, 2(4), pp.305–311.

Rolo, A.P. *et al*., 2001. Chenodeoxycholate is a potent inducer of the permeability transition pore in rat liver mitochondria. *Bioscience reports*, 21(1), pp.73–80.

Roman, R.J. *et al*., 1988. Pressure-Diuresis in Volume-Expanded Rats - Cortical and Medullary Hemodynamics. *Hypertension*, 12(2), pp.168–176.

Rossert, J., 2001. Drug-induced acute interstitial nephritis. *Kidney international*, 60(2), pp.804–817.

Roullet, J.B. *et al*., 1994. Vascular mechanisms of cyclosporin-induced hypertension in the rat. *Journal of Clinical Investigation*, 93(5), pp.2244–2250.

Ruester, C. & Wolf, G., 2006. Renin-angiotensin-aldosterone system and progression of renal disease. *Journal of the American Society of Nephrology*, 17(11), pp.2985–2991.

Ruggenenti, P., Noris, M. & Remuzzi, G., 2001. Thrombotic microangiopathy, hemolytic uremic syndrome, and thrombotic thrombocytopenic purpura. *Kidney international*, 60(3), pp.831–846.

Rusnak, F. & Mertz, P., 2000. Calcineurin: Form and function. *Physiological Reviews*, 80(4), pp.1483–1521.

Russell, N.K.I., Knight, S.R. & Morris, P.J., 2008. Chapter 16 - Cyclosporine. In P. J. M. J. Knechtle, ed. *Kidney Transplantation (Sixth Edition)*. Kidney Transplantation (Sixth Edition). Philadelphia: W.B. Saunders, pp. 234–258.

Rüster, C. & Wolf, G., 2006. Renin-Angiotensin-Aldosterone System and Progression of Renal Disease. *Journal of the American Society of Nephrology*, 17(11), pp.2985–2991.

Ryffel, B. *et al*., 1986. Pge2 Reduces Nephrotoxicity and Immunosuppression of Cyclosporine in Rats. *Clinical nephrology*, 25, pp.S95–S99.

Sabatini, D.M. *et al*., 1994. RAFT1: A mammalian protein that binds to FKBP12 in a rapamycin-dependent fashion and is homologous to yeast TORs. *Cell*, 78(1), pp.35–43.

Saeki, T. *et al*., 1993. Human P-glycoprotein transports cyclosporin A and FK506. *Journal of Biological Chemistry*, 268(9), pp.6077–6080.

Sakai, F., Jamison, R.L. & Berliner, R.W., 1965. A method for exposing the rat renal medulla in vivo: micropuncture of the collecting duct. *The American journal of physiology*, 209(3), pp.663–668.

SandstrÃ m, P.E., 1993. Inhibition by hydrochlorothiazide of insulin release and calcium influx in mouse pancreatic beta-cells. *British Journal of Pharmacology*, 110(4), pp.1359–1362.

Sanjana, V.M. *et al*., 1976. An examination of transcapillary water flux in renal inner medulla. *The American journal of physiology*, 231(2), pp.313–318.

Sanjana, V.M. *et al*., 1975. Hydraulic and Oncotic Pressure Measurements in Inner Medulla of Mammalian Kidney. *The American journal of physiology*, 228(6), pp.1921–1926.

Sánchez-Lozada, L.G. *et al*., 2005. Mild hyperuricemia induces vasoconstriction and maintains glomerular hypertension in normal and remnant kidney rats. *Kidney international*, 67(1), pp.237–247.

Schetz, M. *et al*., 2005. Drug-induced acute kidney injury. *Current Opinion in Critical Care*, 11(6), pp.555–565.

Schiff, J., Cole, E. & Cantarovich, M., 2007. Therapeutic monitoring of calcineurin inhibitors for the nephrologist. *Clinical Journal of the American Society of Nephrology*, 2(2), pp.374–384.

Schiffrin, E.L., 2008. Oxidative stress, nitric oxide synthase, and superoxide dismutase: a matter of imbalance underlies endothelial dysfunction in the human coronary circulation. *Hypertension*, 51(1), pp.31–32.

Schnackenberg, C.G., Welch, W.J. & Wilcox, C.S., 2000. TP receptor-mediated vasoconstriction in microperfused afferent arterioles: roles of O(2)(-) and NO. *American journal of physiology. Renal physiology*, 279(2), pp.F302–F308.

Schnellmann, R.G., Yang, X. & Carrick, J.B., 1994. Arachidonic acid release in renal proximal tubule cell injuries and death. *Journal of biochemical toxicology*, 9(4), pp.211–217.

Schoolwerth, A.C. *et al*., 2001. Renal considerations in angiotensin converting enzyme inhibitor therapy - A statement for healthcare professionals from the council on the kidney in cardiovascular disease and the council for high blood pressure research of the American Heart Association. *Circulation*, 104(16), pp.1985–1991.

Schrimpf, C. & Duffield, J.S., 2011. Mechanisms of fibrosis: the role of the pericyte. *Current opinion in nephrology and hypertension*, 20(3), pp.297–305.

Schubert, A. & Grimm, S., 2004. Cyclophilin D, a component of the permeability transition-pore, is an apoptosis repressor. *Cancer research*, 64(1), pp.85–93.

Schwartz, G.J. & Al-Awqati, Q., 2005. Role of hensin in mediating the adaptation of the cortical collecting duct to metabolic acidosis. *Current opinion in nephrology and hypertension*, 14(4), pp.383–388.

Sedeek, M. *et al*., 2010. Critical role of Nox4-based NADPH oxidase in glucose-induced oxidative stress in the kidney: implications in type 2 diabetic nephropathy. *American journal of physiology. Renal physiology*, 299(6), pp.F1348–58.

Sehgal, S.N., 2003. Sirolimus: its discovery, biological properties, and mechanism of action. *Transplantation Proceedings*, 35(3 Suppl), pp.7S–14S.

Selzner, N. *et al*., 2010. The immunosuppressive pipeline: Meeting unmet needs in liver transplantation. *Liver Transplantation*, 16(12), pp.1359–1372.

Sendeski, M.M. *et al*., 2013. Functional characterization of isolated, perfused outermedullary descending human vasa recta. *Skandinavisches Archiv Fur Physiologie*, 208(1), pp.50–56.

Sendeski, M.M. *et al*., 2012. Iodinated contRAASt media cause endothelial damage leading to vasoconstriction of human and rat vasa recta. *American journal of physiology. Renal physiology*, 303(12), pp.F1592–F1598.

Sennesal, J. *et al*., 1995. Comparison of Perindopril and Amlodipine in Cyclosporine-Treated Renal-Allograft Recipients. *Hypertension*, 26(3), pp.436–444.

Servais, H. *et al*., 2008. Renal cell apoptosis induced by nephrotoxic drugs: cellular and molecular mechanisms and potential approaches to modulation. *Apoptosis*, 13(1), pp.11–32.

Shapiro, R. *et al*., 1991. FK 506 in clinical kidney transplantation. *Transplantation Proceedings*, 23(6), pp.3065–3067.

Sharma, A. *et al*., 2010. Calcineurin inhibitor toxicity in renal allografts: morphologic clues from protocol biopsies. *Indian Journal of Pathology and Microbiology*, 53(4), pp.651–657.

Shepro, D. & Morel, N.M., 1993. Pericyte physiology. *Faseb Journal*, 7(11), pp.1031–1038.

Shiba, N. *et al*., 2004. Analysis of survivors more than 10 years after heart transplantation in the cyclosporine era: Stanford experience. *Journal of Heart and Lung Transplantation*, 23(2), pp.155–164.

Shin, Y.J. *et al*., 2011. Rapamycin reduces reactive oxygen species in cultured human corneal endothelial cells. *Current eye research*, 36(12), pp.1116–1122.

Sieber, M. & Baumgraass, R., 2009. Novel inhibitors of the calcineurin/NFATc hub - alternatives to CsA and FK506? *Cell Communication and Signaling*, 7, pp.25–25.

Siekierka, J.J. *Et al*., 1989. A Cytosolic Binding-Protein For The Immunosuppressant Fk506 Has Peptidyl-Prolyl IsomeRAASe Activity But Is Distinct From Cyclophilin. Nature, 341(6244), Pp.755–757.

Sigal, N.H. *et al*., 1991. Is cyclophilin involved in the immunosuppressive and nephrotoxic mechanism of action of cyclosporin A? *The Journal of experimental medicine*, 173(3), pp.619–628.

Silldorff, E.P. & Pallone, T.L., 2001. Adenosine signaling in outer medullary descending vasa recta. *American Journal of Physiology - Regulatory, Integrative and Comparative Physiology*, 280(3), pp.R854–R861.

Silldorff, E.P., Hilbun, L.R. & Pallone, T.L., 2002. Angiotensin II constriction of rat vasa recta is partially thromboxane dependent. *Hypertension*, 40(4), pp.541–546.

Silldorff, E.P., Yang, S. & Pallone, T.L., 1995. Prostaglandin E2 abrogates endothelin-induced vasoconstriction in renal outer medullary descending vasa recta of the rat. *Journal of Clinical Investigation*, 95(6), pp.2734–2740.

Silva, C.O. *et al*., 2015. Apocynin decreases AGEs-induced stimulation of NF-kappaB protein expression in vascular smooth muscle cells from GK rats. *Pharmaceutical biology*, 53(4), pp.488–493.

Silva, F.G., 2004. Chemical-induced nephropathy: a review of the renal tubulointerstitial lesions in humans. *Toxicologic Pathology*, 32 Suppl 2, pp.71–84.

Sims, D.E., 2000. Diversity within pericytes. *Clinical and Experimental Pharmacology and Physiology*, 27(10), pp.842–846.

Skalli, O. *et al*., 1989. Alpha-smooth muscle actin, a differentiation marker of smooth muscle cells, is present in microfilamentous bundles of pericytes. *The journal of histochemistry and cytochemistry : official journal of the Histochemistry Society*, 37(3), pp.315–321.

Slattery, C. *et al*., 2005. Cyclosporine A-induced renal fibrosis - A role for epithelial-mesenchymal transition. *American Journal of Pathology*, 167(2), pp.395–407.

Smith, B.A. & McConnell, H.M., 1978. Determination of molecular motion in membranes using periodic pattern photobleaching. *Proceedings of the National Academy of Sciences of the United States of America*, 75(6), pp.2759–2763.

Smith, S.R. *et al*., 1993. Chronic Thromboxane Synthase Inhibition with Cgs-12970 in

Human Cyclosporine Nephrotoxicity. *Transplantation*, 56(6), pp.1422–1426.

Smith, S.W., Chand, S. & Savage, C.O.S., 2012. Biology of the renal pericyte. *Nephrology, dialysis, transplantation : official publication of the European Dialysis and Transplant Association - European Renal Association*, 27(6), pp.2149–2155.

Spurney, R.F. *et al*., 1990. Thromboxane receptor blockade improves cyclosporine nephrotoxicity in rats. *Prostaglandins*, 39(2), pp.135–146.

Staatz, D.C.E. & Tett, S.E., 2004. Clinical Pharmacokinetics and Pharmacodynamics of Tacrolimus in Solid Organ Transplantation. *Clinical Pharmacokinetics*, 43(10), pp.623–653.

Stahl, R.A. *et al*., 1986. Hyperchloremic metabolic acidosis with high serum potassium in renal transplant recipients: a cyclosporine A associated side effect. *Clinical nephrology*, 25(5), pp.245–248.

Starzl, T.E. *et al*., 1989. Fk-506 for Liver, Kidney, and Pancreas Transplantation. *Lancet*, 2(8670), pp.1000–1004.

Stolk, J. *et al*., 1994. Characteristics of the inhibition of NADPH oxidase activation in neutrophils by apocynin, a methoxy-substituted catechol. *American journal of respiratory cell and molecular biology*, 11(1), pp.95–102.

Stroes, E. *et al*., 1997. Cyclosporin A increases nitric oxide activity in vivo. *Hypertension*, 29(2), pp.570–575.

Su, Q. *et al*., 1995. Distribution and activity of calcineurin in rat tissues. Evidence for post-transcriptional regulation of testis-specific calcineurin B. *European journal of biochemistry / FEBS*, 230(2), pp.469–474.

Sugimoto, T. *et al*., 2001. Endothelin-1 induces cyclooxygenase-2 expression via nuclear factor of activated T-cell transcription factor in glomerular mesangial cells. *Journal of the American Society of Nephrology*, 12(7), pp.1359–1368.

Sun, B.K. *et al*., 2005. Blockade of angiotensin II with losartan attenuates transforming growth factor-beta1 inducible gene-h3 (betaig-h3) expression in a model of chronic cyclosporine nephrotoxicity. *Nephron Experimental Nephrology*, 99(1), pp.e9–16.

Sun, D. *et al*., 2001. Mediation of tubuloglomerular feedback by adenosine: evidence from mice lacking adenosine 1 receptors. *Proceedings of the National Academy of Sciences of the United States of America*, 98(17), pp.9983–9988.

Suzuki, K. *et al*., 2003. Pathologic evidence of microvascular rarefaction in the brain of renal hypertensive rats. *Journal of Stroke and Cerebrovascular Diseases*, 12(1), pp.8–16.

Swaisland, A.J., 1991. The pharmacokinetics of co-administered lisinopril and hydrochlorothiazide. *Journal of Human Hypertension*, 5 Suppl 2, pp.69–71.

Takahashi, N., Hayano, T. & Suzuki, M., 1989. Peptidyl-Prolyl Cis-Trans IsomeRAASe Is The Cyclosporin-A-Binding Protein Cyclophilin. Nature, 337(6206), Pp.473–475.

Takeda, Y. *et al*., 1999. Mechanisms of FK 506-induced hypertension in the rat.

Hypertension, 33(1), pp.130–136.

Tariq, M. *et al*., 2000. Effect of lithium on cyclosporin induced nephrotoxicity in rats. *Renal failure*, 22(5), pp.545–560.

Tasnim, F. & Zink, D., 2012. Cross talk between primary human renal tubular cells and endothelial cells in cocultures. *American journal of physiology. Renal physiology*, 302(8), pp.F1055–62.

Taylor, N.E. *et al*., 2006. NADPH oxidase in the renal medulla causes oxidative stress and contributes to salt-sensitive hypertension in Dahl S rats. *Hypertension*, 47(4), pp.692–698.

Tell, von, D., Armulik, A. & Betsholtz, C., 2006. Pericytes and vascular stability. *Experimental Cell Research*, 312(5), pp.623–629.

Tenopoulou, M. *et al*., 2007. Does the calcein-AM method assay the total cellular "labile iron pool" or only a fraction of it? *Biochemical Journal*, 403(Pt 2), pp.261–266.

Textor, S.C. *et al*., 1994. Cyclosporine-induced hypertension after transplantation. *Mayo Clinic Proceedings*, 69(12), pp.1182–1193.

Textor, S.C. *et al*., 2000. Posttransplantation hypertension related to calcineurin inhibitors. *Liver Transplantation*, 6(5), pp.521–530.

Thiery, J.P. & Sleeman, J.P., 2006. Complex networks orchestrate epithelial–mesenchymal transitions. 7(2), pp.131–142.

Thomas, S.E. *et al*., 1998. Accelerated apoptosis characterizes cyclosporine-associated interstitial fibrosis. *Kidney international*, 53(4), pp.897–908.

Thurau, K. & Deetjen, P., 1962. Die Diurese bei arteriellen Drucksteigerungen. *Pflüger's Archiv für die gesamte Physiologie des Menschen und der Tiere*, 274(6), pp.567–580.

Tilton, R.G., Kilo, C. & Williamson, J.R., 1979. Pericyte-endothelial relationships in cardiac and skeletal muscle capillaries. *Microvascular research*, 18(3), pp.325–335.

Tomasiak, M. *et al*., 2007. Cyclosporine enhances platelet procoagulant activity. *Nephrology, dialysis, transplantation : official publication of the European Dialysis and Transplant Association - European Renal Association*, 22(6), pp.1750–1756.

Toschi, A. *et al*., 2009. Regulation of mTORC1 and mTORC2 complex assembly by phosphatidic acid: competition with rapamycin. *Molecular and cellular biology*, 29(6), pp.1411–1420.

Tsechan, 2002. Nephrotoxicity of immunosuppressive agents in renal transplantation. *Hong Kong Journal of Nephrology*, 4(2), pp.8–8.

Tsujimoto, Y. & Shimizu, S., 2007. Role of the mitochondrial membrane permeability transition in cell death. *Apoptosis*, 12(5), pp.835–840.

Tumlin, J.A. & Sands, J.M., 1993. Nephron Segment-Specific Inhibition of Na+/K+-

Atpase Activity by Cyclosporine-A. *Kidney international*, 43(1), pp.246–251.

Tunon, M.J. *et al*., 2003. Effects of FK506 and rapamycin on generation of reactive oxygen species, nitric oxide production and nuclear factor kappa B activation in rat hepatocytes. *Biochemical pharmacology*, 66(3), pp.439–445.

Tziomalos, K. *et al*., 2013. Hydrochlorothiazide vs. chlorthalidone as the optimal diuretic for the management of hypertension. *Current pharmaceutical design*, 19(21), pp.3766–3772.

Uetrecht, J., 2009. *Adverse Drug Reactions* J. Uetrecht, ed., Berlin, Heidelberg: Springer Science & Business Media.

Unsay, J.D. *et al*., 2013. Cardiolipin effects on membrane structure and dynamics. *Langmuir : the ACS journal of surfaces and colloids*, 29(51), pp.15878–15887.

Utecht, K.N., Hiles, J.J. & Kolesar, J., 2006. Effects of genetic polymorphisms on the pharmacokinetics of calcineurin inhibitors. *American journal of health-system pharmacy : AJHP : official journal of the American Society of Health-System Pharmacists*, 63(23), pp.2340–2348.

van den Dorpel, M.A. *et al*., 1994. Effect of isradipine on cyclosporin A-related hypertension. *Blood pressure. Supplement*, 1, pp.50–53.

van der Toorn, M. *et al*., 2007. Cyclosporin A-induced oxidative stress is not the consequence of an increase in mitochondrial membrane potential. *FEBS Journal*, 274(12), pp.3003–3012.

van Riemsdijk, I.C. *et al*., 2000. Addition of isradipine (Lomir) results in a better renal function after kidney transplantation: a double-blind, randomized, placebo-controlled, multi-center study. *Transplantation*, 70(1), pp.122–126.

Vates, G.E. *et al*., 2010. Pericyte constriction after stroke: the jury is still out. *Nature Medicine*, 16(9), pp.959–959.

Vayssiere, J.L. *et al*., 1994. Commitment to apoptosis is associated with changes in mitochondrial biogenesis and activity in cell lines conditionally immortalized with simian virus 40. *Proceedings of the National Academy of Sciences of the United States of America*, 91(24), pp.11752–11756.

Vaziri, N.D. *et al*., Depressed renal and vascular nitric oxide synthase expression in cyclosporine-induced hypertension. *Kidney international*, 54(2), pp.482–491.

Vergoulas, G., Antihypertensive agents and renal transplantation. *Hippokratia*, 11(1), pp.3–12.

Vezza, R. *et al*., 1993. Prostaglandin E2 potentiates platelet aggregation by priming protein kinase C. *Blood*, 82(9), pp.2704–2713.

Vieira, J.M. *et al*., 1999. Cyclosporine-induced interstitial fibrosis and arteriolar TGF-beta expression with preserved renal blood flow. *Transplantation*, 68(11), pp.1746–1753.

Vincenti, F. *et al*., 2007. Results of an international, randomized trial comparing glucose metabolism disorders and outcome with cyclosporine versus tacrolimus.

American Journal of Transplantation, 7(6), pp.1506–1514.

Vlahakos, D.V. *et al*., 1991. Enalapril-associated anemia in renal transplant recipients treated for hypertension. *American Journal of Kidney Diseases*, 17(2), pp.199–205.

Voss, B.L. *et al*., 1988. Cyclosporine suppression of endothelial prostacyclin generation. A possible mechanism for nephrotoxicity. *Transplantation*, 45(4), pp.793–796.

Vu, M.D. *et al*., 1997. Tacrolimus (FK506) and sirolimus (rapamycin) in combination are not antagonistic but produce extended graft survival in cardiac transplantation in the rat. *Transplantation*, 64(12), pp.1853–1856.

Wallemacq, P.E. & Reding, R., 1993. Fk506 (Tacrolimus), A Novel Immunosuppressant In Organ-Transplantation - Clinical, Biomedical, And Analytical Aspects. Clinical Chemistry, 39(11), Pp.2219–2228.

Wang, C. & SALAHUDEEN, A.K., 1995. Lipid peroxidation accompanies cyclosporine nephrotoxicity: effects of vitamin E. *Kidney international*, 47(3), pp.927–934.

Wang, C.Y. & Salahudeen, A.K., 1995. Lipid-Peroxidation Accompanies Cyclosporine Nephrotoxicity - Effects Of Vitamin-E. Kidney International, 47(3), Pp.927–934.

Watarai, Y. *et al*., 2004. Effect of tacrolimus and cyclosporine on renal microcirculation and nitric oxide production. *Transplantation Proceedings*, 36(7), pp.2130–2132.

Watkins, P.B., 1990. The role of cytochromes P-450 in cyclosporine metabolism. *Journal of the American Academy of Dermatology*, 23(6 Pt 2), pp.1301–9– discussion 1309–11.

Webster, A.C. *et al*., 2005. Tacrolimus versus ciclosporin as primary immunosuppression for kidney transplant recipients: meta-analysis and meta-regression of randomised trial data. *British Medical Journal*, 331(7520), pp.810–.

Weir, M.R. & Lerma, E.V., 2014. *Kidney Transplantation* M. R. Weir & E. V. Lerma, eds., New York, NY: Springer Science & Business Media.

Weir, M.R., KLASSEN, D.K. & BURDICK, J.F., 1992. A Pilot-Study to Assess the Ability of an Orally Available Selective Thromboxane Synthase Inhibitor to Improve Renal-Function in Cyclosporine-Treated Renal-Transplant Recipients. *Journal of the American Society of Nephrology*, 2(8), pp.1285–1290.

Weitzberg, E., Ahlborg, G. & Lundberg, J.M., 1991. Long-lasting vasoconstriction and efficient regional extraction of endothelin-1 in human splanchnic and renal tissues. *Biochemical and Biophysical Research Communications*, 180(3), pp.1298–1303.

Whiting, P.H. et al., 1982. Experimental cyclosporin A nephrotoxicity. *British journal of experimental pathology*, 63(1), pp.88–94.

Whiting, P.H., Thomson, A.W. & Simpson, J.G., 1985. Cyclosporine: toxicity, metabolism, and drug interactions--implications from animal studies. *Transplantation Proceedings*, 17(4 Suppl 1), pp.134–144.

Wilcox, C.S., 2002. Reactive oxygen species: roles in blood pressure and kidney function. *Current Hypertension Reports*, 4(2), pp.160–166.

Wilcox, C.S. & Welch, W.J., 2000. Interaction between nitric oxide and oxygen radicals in regulation of tubuloglomerular feedback. *Acta physiologica Scandinavica*, 168(1), pp.119–124.

Wilcox, C.S. & Welch, W.J., 1998. Macula densa nitric oxide synthase: expression, regulation, and function. *Kidney international. Supplement*, 67, pp.S53–7.

Williams, R.M., Zipfel, W.R. & Webb, W.W., 2001. Multiphoton microscopy in biological research. *Current Opinion in Chemical Biology*, 5(5), pp.603–608.

Wilson, P.D. & Hartz, P.A., 1991. Mechanisms of cyclosporine A toxicity in defined cultures of renal tubule epithelia: a role for cysteine proteases. *Cell biology international reports*, 15(12), pp.1243–1258.

Winkler, H.H. & Lehninger, A.L., 1968. The atractyloside-sensitive nucleotide binding site in a membrane preparation from rat liver mitochondria. *Journal of Biological Chemistry*, 243(11), pp.3000–3008.

Winkler, M. *et al*., 1994. Plasma vs whole blood for therapeutic drug monitoring of patients receiving FK 506 for immunosuppression. *Clinical Chemistry*, 40(12), pp.2247–2253.

Wojtczak, L. & Zabłocki, K., 2008. Basic Mitochondrial Physiology in Cell Viability and Death. In *Nephrotoxicity*. John Wiley & Sons, Inc., pp. 1–35.

Wolf, G., 2006. Renal injury due to renin-angiotensin-aldosterone system activation of the transforming growth factor-beta pathway. *Kidney international*, 70(11), pp.1914–1919.

Wolf, G., Killen, P.D. & Neilson, E.G., 1990. Cyclosporin A stimulates transcription and procollagen secretion in tubulointerstitial fibroblasts and proximal tubular cells. *Journal of the American Society of Nephrology*, 1(6), pp.918–922.

Xiao, Z. *et al*., 2013. Mechanisms of Cyclosporine-Induced Renal Cell Apoptosis: A Systematic Review. *American journal of nephrology*, 37(1), pp.30–40.

Xue, W. *et al*., 2010. The effects of diltiazem in renal transplantation patients treated with cyclosporine A. *Journal of Biomedical Research*, 24(4), pp.317–323.

Yagil, Y., 1990. Acute effect of cyclosporin on inner medullary blood flow in normal and postischemic rat kidney. *The American journal of physiology*, 258(5 Pt 2), pp.F1139–44.

Yamagishi, S. & Imaizumi, T., 2005. Pericyte biology and diseases. *International journal of tissue reactions*, 27(3), pp.125–135.

Yamauchi, H. *et al*., 1998. Time-dependent cyclosporine A-induced nephrotoxicity in rats. *Clinical and Experimental Pharmacology and Physiology*, 25(6), pp.435–440.

Yoshida, M., Suzuki, A. & Itoh, T., 1994. Mechanisms of vasoconstriction induced by endothelin-1 in smooth muscle of rabbit mesenteric artery. *The Journal of Physiology*, 477 (Pt 2)(Pt 2), pp.253–265.

Young, L.S. *et al*., 1996. Methods of renal blood flow measurement. *Urological Research*, 24(3), pp.149–160.

Zachariah, P.K.P., Messerli, F.H.F. & Mroczek, W.W., 1993. Low-dose bisoprolol/hydrochlorothiazide: an option in first-line, antihypertensive treatment. *Clinical Therapeutics*, 15(5), pp.779–787.

Zager, R.A., 1997. Pathogenetic mechanisms in nephrotoxic acute renal failure. *Seminars in Nephrology*, 17(1), pp.3–14.

Zamzami, N. *et al*., 1995. Reduction in mitochondrial potential constitutes an early irreversible step of programmed lymphocyte death in vivo. *The Journal of experimental medicine*, 181(5), pp.1661–1672.

Zhang, Q. *et al*., 2006. Descending vasa recta endothelium is an electrical syncytium. *American Journal of Physiology - Regulatory, Integrative and Comparative Physiology*, 291(6), pp.R1688–R1699.

Zhang, X.Z. *et al*., 2001. L-arginine supplementation in young renal allograft recipients with chronic transplant dysfunction. *Clinical nephrology*, 55(6), pp.453–459.

Zhang, Z. & Pallone, T.L., 2004. Response of descending vasa recta to luminal pressure. *American journal of physiology. Renal physiology*, 287(3), pp.F535–F542.

Zhang, Z. *et al*., 2004. ANG II signaling in vasa recta pericytes by PKC and reactive oxygen species. *American journal of physiology. Heart and circulatory physiology*, 287(2), pp.H773–H781.

Zhang, Z., Payne, K. & Pallone, T.L., 2014. Syncytial communication in descending vasa recta includes myoendothelial coupling. *American journal of physiology. Renal physiology*, 307(1), pp.F41–52.

Zhang, Z., Rhinehart, K. & Pallone, T.L., 2002. Membrane potential controls calcium entry into descending vasa recta pericytes. *American Journal of Physiology - Regulatory, Integrative and Comparative Physiology*, 283(4), pp.R949–R957.

Zhong, Z.Z. *et al*., 1998. Cyclosporin A increases hypoxia and free radical production in rat kidneys: prevention by dietary glycine. *The American journal of physiology*, 275(4), pp.F595–F604.

Zhong, Z.Z. *et al*., 1999. Dietary glycine and renal denervation prevents cyclosporin A-induced hydroxyl radical production in rat kidney. *Molecular Pharmacology*, 56(3), pp.455–463.

Zhou, A.Y. & Ryeom, S., 2014. Cyclosporin a promotes tumor angiogenesis in a calcineurin-independent manner by increasing mitochondrial reactive oxygen species. *Molecular Cancer Research*, 12(11), pp.1663–1676.

Zhou, S.-F., Liu, J.-P. & Chowbay, B., 2009. Polymorphism of human cytochrome P450 enzymes and its clinical impact. *Drug metabolism reviews*, 41(2), pp.89–295.

Zhu, Z. *et al*., 2005. Thiazide-like diuretics attenuate agonist-induced vasoconstriction by calcium desensitization linked to Rho kinase. *Hypertension*, 45(2), pp.233–239.

Zielonka, J., Vasquez-Vivar, J. & Kalyanaraman, B., 2008. Detection of 2-

hydroxyethidium in cellular systems: a unique marker product of superoxide and hydroethidine. *Nature protocols*, 3(1), pp.8–21.

Zimmerhackl, B.L., Robertson, C.R. & Jamison, R.L., 1987. The Medullary Microcirculation. Kidney International, 31(2), Pp.641–647.

Zipfel, W.R., Williams, R.M. & Webb, W.W., 2003. Nonlinear magic: multiphoton microscopy in the biosciences. 21(11), pp.1369–1377.

Zou, A.P., Li, N. & Cowley, A.W.J., 2001. Production and actions of superoxide in the renal medulla. *Hypertension*, 37(2 Pt 2), pp.547–553.

Appendix 1: Publications arising from this thesis.

Abstracts:

Kelly, Mark, Crawford, Carol, Loo, Ruey Leng, Delaney, Michael, Farmer, Chris and Wildman, Scott S.P. and Peppiatt-Wildman, Claire M. (2013) *Live kidney slices present a novel method for delineating the mechanisms of calcineurin inhibitor-mediated nephrotoxicity.* Journal of the Federation of American Scoieties for Experimental Biology, 27 (646.8). ISSN 0892-6638. **See poster 1**

Kelly, M, Wildman, S. & Peppiatt-Wildman, C. *Contractile pericytes and calcineurin inhibitor-mediated nephrotoxicity* (2014). ISN's Forefronts Symposium of 2014, Charleston, SC, USA, March 6-9. **See poster 2**

Mark C. Kelly, Carol Crawford, Scott S.P. Wildman, Claire M. Peppiatt-Wildman Contractile Pericytes May Contribute to Calcineurin Inhibitor-Mediated Nephrotoxicity Journal of the Federation of American Societies for Experimental Biology, 28 (637.7). ISSN 0268-1285.

Kelly, M, Wildman, S. & Peppiatt-Wildman, C., 2015. Luminal Perfusion of in situ Vasa Recta Capillaries with Calcineurin Inhibitors Enhances Pericyte-mediated Vasoconstriction. *The FASEB Journal*, 29 (1 Supplement). **See poster 3**

Appendix 2: Other publications and presentations

Publications:

Wildman, S.S., Kelly, M.C., Leech, H.K., Duckett, J.R.A., Stevens, P.E., & Peppiatt-Wildman, C.M. (2013) Embracing translation: avant-garde urinary system research in Kent. Science Omega Review UK, DOI:10.13140/RG.2.1.5137.7121

Crawford, C. Wildman SS, Kelly MC, Kennedy-Lydon TM, Peppiatt-Wildman CM, 2013. Sympathetic nerve-derived ATP regulates renal medullary vasa recta diameter via

pericyte cells: a role for regulating medullary blood flow? *Frontiers in Physiology*, 4, pp.307–307.

Kelley, S.P., Coutneidge, H.R., Birch, R.E., Contreras-Sanz, A., Kelly, M.C., Durodie J., Peppiatt-Wildman, C.M., Farmer, C.K., Delaney, P., Mallone-Lee, J., Harber, M.A., Wildman, S.S.P. (2014) Urinary ATP and visualization of intracellular bacteria: a superior diagnostic marker for recurrent UTI in renal transplant recipients? SpringerPlus Medicine. 3, 200 (p1-7).

Kelley SP, Walsh J, Kelly MC, Muhdar S, Adel-Aziz M, Barrett ID, Wildman SS (2014) Inhibition of native 5-HT3 receptor-evoked contractions in Guinea pig and mouse ileum by antimalarial drugs. Eur J Pharmacol 2014

Presentations:

Calcineurin inhibitors in renal transplants: past and future.
EKUHT, at European Dialysis And Transplant Nurses Association, EDTNA, October 2013, Ashford, Kent.

Contractile pericytes and calcineurin inhibitor-mediated nephrotoxicity
International Society of Nephrology Forefront conference 2014, Charleston, South Carolina.

Poster 1

279

646.8

Live kidney slices present a novel method for delineating the mechanisms of calcineurin inhibitor-mediated nephrotoxicity.

Mark Kelly[1], Carol Crawford[1], Ruey-Leng Loo[1], Michael Delaney[2], Chris Farmer[2], Scott SP Wildman[1], Claire M Peppiatt-Wildman[1]

[1]Medway School of Pharmacy, Universities of Kent and Greenwich, Chatham, Kent, United Kingdom. [2]Renal Unit, East Kent Hospitals University NHS Foundation Trust, Canterbury, Kent, Untied Kingdom

Introduction

- Cyclosporine A (CsA) and Tacrolimus (FK-506) are calcineurin inhibitor immunosuppressant's (CNIs) used to i) prevent allograft rejection in solid organ transplantation and ii) in the treatment of rheumatoid arthritis.
- CNI's are known to have nephrotoxic side effects, which hinders long-term renal function and patient survival post organ transplantation.
- The precise mechanisms of CNI-induced nephrotoxicity remain unknown, contributing factors include endothelial cell dysfunction, reduced release of vasodilators, increased production of vasoconstrictors and increased production of reaction oxygen species.
- Rapamycin is another immunosuppressant used clinically and exhibits reduced nephrotoxicity
- Contractile pericytes cells reside along descending vasa recta capillaries and respond to a variety of both endogenous and exogenous compounds to regulate vessel diameter and thus medullary blood flow (MBF) [1]
- Using the live kidney slice model pioneered in our lab [1], we have investigated whether CNIs act specifically at vasa recta pericytes to modulate MBF?
- A reduction in MBF may results in regional ischemia that would would exacerbate additional tubular nephrotoxicity associated with these agents.

Methods

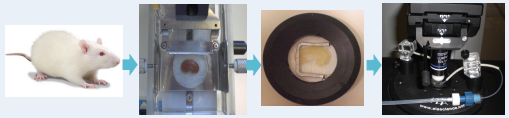

- Whole kidneys were isolated from ≈250 g male Sprague Dawley rats and 200 µm serial slices were collected as previously described [1].
- Slices were secured in a bath using a platinum "harp" and continually superfused with PSS, bubbled with O_2/CO_2.
- Video imaging techniques were utilised to collect DIC images of pericytes on vasa recta and were analysed off-line using ImageJ software. Data were compared using a paired Student's t-test and unpaired t-test where appropriate.

Results

1. CsA and FK-506 act at pericytes to regulate vasa recta diameter

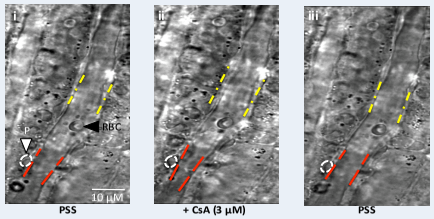

Figure 1. DIC imaging of pericyte-mediated constriction of *in situ* vasa recta capillaries by CsA (3 µM). Images of vasa recta taken from a time series experiment in which live kidney slices were exposed to CsA. i) shows a typical field of view of vasa recta under control conditions (PSS), the pericyte is highlighted (white oval). ii) shows vasa recta constrict at pericyte sites during exposure to CsA and, iii) shows vasa recta diameter returns toward original diameter when CsA is removed. Vessel diameter was measured every 5 s throughout the experiment at a pericyte site (red lines) and a corresponding non-pericyte site (yellow lines)

Results

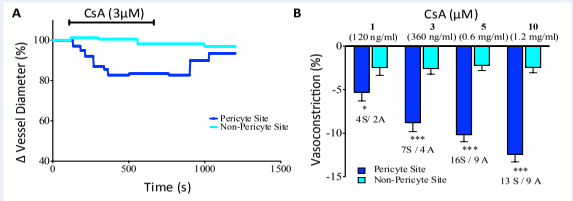

Figure 2. The effect of CsA on vasa recta diameter.
A) a representative trace of CsA (3µM) superfusion , showing change in vessel diameter over time at pericyte site (blue line) and corresponding non-pericyte site (aqua line). B) bar graph showing mean data for the CsA-induced change in vessel diameter at pericyte (blue bar) and non-pericyte sites (aqua bar). Cyclosporine (1-10 µM) caused a significantly greater constriction at pericyte sites compared to non-pericyte sites (mean±SEM, *P<0.05, S=Slices, A=Animals).

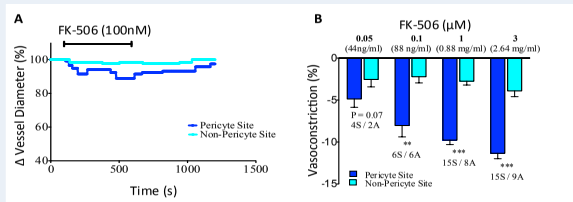

Figure 3. The effect of FK-506 on vasa recta diameter.
A) a representative trace of the FK-506- (100 nM) induced change in vessel diameter at a pericyte site (blue line) and non-pericyte site (aqua line). B) bar graph showing mean data for the FK-506-induced change in vessel diameter at pericyte sites (blue bar) and non-pericyte sites (aqua bar). FK-506 caused a significantly greater constriction at pericyte sites compared to non-pericyte sites (mean±SEM, *P<0.05, S=Slices, A=Animals).

2.Lorsartan has no effect on CNI-induced pericyte vasoconstriction

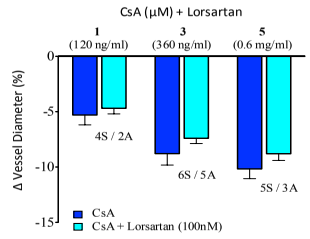

Figure 4. CsA-induced constriction of vasa recta is not significantly attenuated by the AT_1 receptor antagonist losartan. Bar graph showing the mean % change in vasa recta diameter at pericytes when slices were superfused with CsA alone at varying concentrations (1, 3 and 5 µM; blue bars) and in the presence of losartan (100 nM; aqua bars) Data are mean±SEM, S=Slices, A=Animals. No significant attenuation of the CsA-induced change in vessel diameter was observed when losartan was present indicating the CsA-induced vasoconstriction of vasa recta by pericytes is not mediated via AT_1 receptors

Results

3. Rapamycin has no contractile effect at pericyte sites

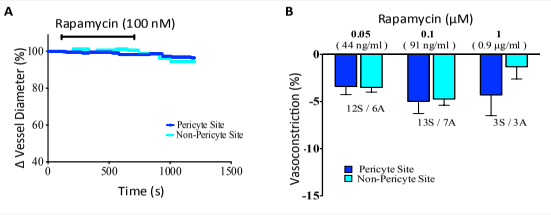

Figure 5. The effect of rapamycin on vasa recta diameter
A) shows a representative trace of the rapamycin (100nM)-induced change in vessel diameter at both pericyte sites (blue line) and non-pericyte sites (aqua line). B) bar graph showing mean data for the rapamycin-induced change in vessel diameter at pericyte sites (blue bar) and non-pericyte sites (aqua bar). Rapamycin at all concentrations tested failed to evoke a significantly greater constriction of vasa recta at pericyte sites than at non-pericyte sites. Data are mean±SEM, S=slices, A=animals.

4. CsA & FK-506 have no significant effect of tubule diameter

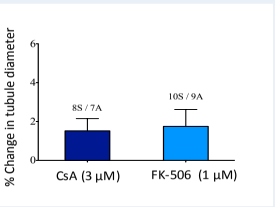

Figure 6. CsA and FK-506 did not evoke any significant change in tubule diameter. Superfusion of live kidney slices with CsA (3 µM, blue bar) and FK-506 (1 µM, aqua bar) failed to evoke any significant changes in tubule diameter (< 2%) for the duration of the experiment in which changes in vessel diameter were measured. This indicates that tubular swelling did not occur and is therefore not contributing to the changes in vessel diameter measured. Data are mean±SEM, S=Slices, A=Animals.

Conclusions

- CsA & FK-506 caused a significantly greater constriction of vasa recta at pericyte sites compared with non-pericyte sites.
- The CsA-induced constriction of vasa recta at pericyte sites was not via AT_1 receptors.
- Rapamycin, a less potent nephrotoxic immunosuppressant, failed to evoked a significant constriction of vasa recta at pericyte sites.
- CsA & FK-506 did not evoke tubule swelling, further confirming the mechanism of vasoconstriction to be pericyte-mediated.
- CsA and FK-506-evoked reduction in MBF (as a result of decreased vasa recta diameter) and the resultant localized ischemia may represent a novel mechanism of nephrotoxicity by these agents.

References

[1] Crawford C, Kennedy-Lydon TM, Sprott, C, Desai T, Munday J, Unwin RJ, Wildman SSP, Peppiatt-Wildman CM. An intact kidney slice model to investigate vasa recta properties and function *in situ*. *Nephrol Physiol.* In press.

This work was funded by The Medical Research Council and University of Kent, UK

Poster 2

280

Contractile Pericytes may Contribute to Calcineurin Inhibitor-Mediated Nephrotoxicity

Mark Kelly[1], Michael Delaney[2], Chris Farmer[2], Scott SP Wildman[1], Claire M Peppiatt-Wildman[1]

[1]Medway School of Pharmacy, Universities of Kent and Greenwich, Chatham, Kent, United Kingdom. [2]Renal Unit, East Kent Hospitals University NHS Foundation Trust, Canterbury, Kent, Unitied Kingdom.

Introduction

- Cyclosporine A (CsA) and Tacrolimus (FK-506) are calcineurin inhibitor immunosuppressants (CNIs), used to i) prevent allograft rejection in solid organ transplantation, and ii) in the treatment of rheumatoid arthritis.
- CNIs are known to have nephrotoxic side effects, which hinder long-term renal function and patient survival post organ transplantation.
- The precise mechanisms of CNI-induced nephrotoxicity remain unknown; contributing factors include endothelial cell dysfunction, reduced release of vasodilators, increased production of vasoconstrictors, and increased production of reactive oxygen species.
- Rapamycin is another immunosuppressant used clinically, and exhibits reduced clinical nephrotoxicity.
- Contractile pericyte cells reside along descending vasa recta capillaries and respond to a variety of both endogenous and exogenous compounds to regulate vessel diameter and thus medullary blood flow (MBF) [1].
- Using the live kidney slice model pioneered in our lab [1], we have investigated whether CNIs act specifically at vasa recta pericytes to modulate MBF.
- A reduction in MBF may result in regional ischemia that would would exacerbate additional tubular nephrotoxicity associated with these agents.

Methods

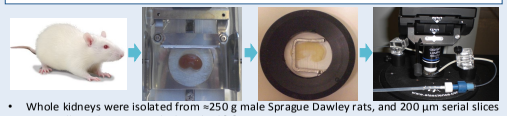

- Whole kidneys were isolated from ≈250 g male Sprague Dawley rats, and 200 µm serial slices were collected as previously described [1].
- Slices were secured in a bath using a platinum "harp" and continually superfused with PSS, bubbled with O_2/CO_2.
- Video imaging techniques were utilised to collect DIC images of pericytes on vasa recta and were analysed off-line using ImageJ software. Data were compared using a paired Student's t-test and unpaired t-test where appropriate.

Results

1. CsA and FK-506 act at pericytes to regulate vasa recta diameter

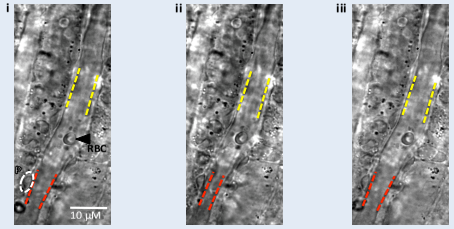

Figure 1. DIC imaging of pericyte-mediated constriction of *in situ* vasa recta capillaries by CsA [3 µM]. Images of vasa recta taken from a time series experiment in which live kidney slices were exposed to CsA. i) shows a typical field of view of vasa recta under control conditions (PSS), the pericyte is highlighted (white oval, P). ii) shows vasa recta constrict at pericyte sites during exposure to CsA and, iii) shows vasa recta diameter returns toward original diameter when CsA is removed. Vessel diameter was measured every 5 s throughout the experiment at a pericyte site (red lines) and a corresponding non-pericyte site (yellow lines).

Results

2. Cyclosporine (CsA) induces pericyte-mediated vasoconstriction of vasa recta

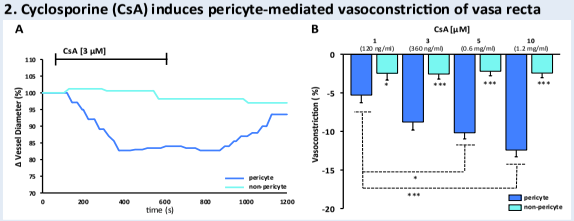

Figure 2. The effect of CsA on vasa recta diameter.
A) a representative trace of CsA [3µM] superfusion, shows a change in vessel diameter over time at pericyte site (blue line) and corresponding non-pericyte site (aqua line). B) bar graph shows mean data for the CsA-induced change in vessel diameter at pericyte (blue bar) and non-pericyte sites (aqua bar). Cyclosporine [1-10 µM] caused a significantly greater constriction at pericyte sites compared to non-pericyte sites (mean±SEM, *P<0.05, **P<0.01, *** P<0.001).

3. Tacrolimus (FK506) induces pericyte-mediated vasoconstriction

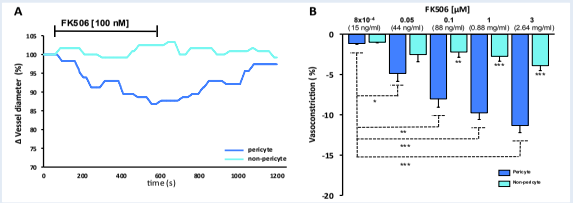

Figure 3. The effect of FK-506 on vasa recta diameter.
A) a representative trace of the FK-506- (100 nM) induced change in vessel diameter at a pericyte site (blue line) and non-pericyte site (aqua line). B) bar graph shows mean data for the FK-506-induced change in vessel diameter at pericyte sites (blue bar) and non-pericyte sites (aqua bar). FK-506 caused a significantly greater constriction at pericyte sites compared to non-pericyte sites (mean±SEM, *P<0.05, **P<0.01, *** P<0.001).

4. Diltiazem attenuates CsA-induced vasoconstriction of vasa recta

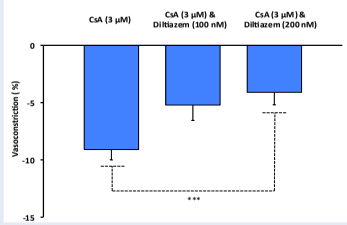

Figure 4. Diltiazem attenuates CsA-induced vasoconstriction of vasa recta.
Bar graph shows mean data for % change in vasa recta diameter at pericytes when slices were superfused with CsA alone, 3 µM, and in the presence of Diltiazem (100-200 nM). No change in vessel diameter was measured at non-pericyte sites. Data are mean ±SEM. ***P<0.001.

Results

5. Rapamycin enhances the CsA-mediated constriction of vasa recta

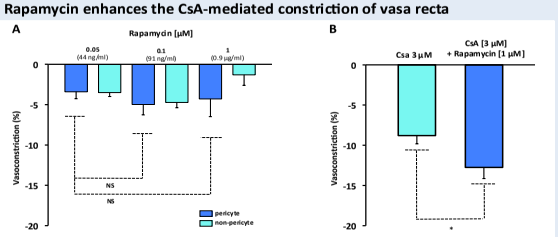

Figure 5. The effect of rapamycin on vasa recta diameter
A) Bar graph shows mean data for the rapamycin-induced change in vessel diameter at pericyte sites (blue bar) and non-pericyte sites (aqua bar). Rapamycin, at all concentrations tested, failed to evoke a significantly greater constriction of vasa recta at pericyte sites than at non-pericyte sites. B) Bar graph shows mean data for % change in vessel diameter in response to CsA [3 µM] and rapamycin [1 µM]. Application of CsA and rapamycin in combination caused a significantly greater constriction of vasa recta at pericyte sites than when CsA was applied alone. Data are mean±SEM, *P<0.05.

6. Hydrochlorothiazide (HCT) attenuates the FK-506-induced vasoconstriction

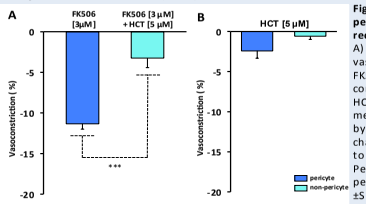

Figure 6. HCT significantly attenuated the pericyte-mediated constriction of vasa recta evoked by FK506.
A) Bar graph showing mean constriction of vasa recta via pericytes in response to FK506 [3 µM] alone (blue bar) and in combination with HCT [5 µM] (aqua bar). HCT significantly attenuated the pericyte-mediated constriction of vasa recta evoked by FK506. B) Bar graph shows no significant change in vasa recta diameter in response to application of HCT [5 µM] alone. Pericyte-site sites (blue bar) and non-pericyte sites (aqua bar). Data are mean ±SEM,*P<0.05, ***P<0.001.

Conclusions

- CsA & FK-506 caused a significantly greater constriction of vasa recta at pericyte sites compared with non-pericyte sites. .
- Rapamycin, a less potent nephrotoxic immunosuppressant, failed to evoked a significant constriction of vasa recta at pericyte sites alone, however rapamycin enhanced CsA-induced vasoconstriction.
- HCT, a thiazide diuretic, significantly attenuated FK506-induced vasoconstriction at pericyte sites, while Diltiazem, a calcium channel blocker, significantly attenuated CsA-induced vasoconstriction.
- CsA and FK-506-evoked reduction of descending vasa recta diameter, (and thus MBF), and the resultant localized ischemia may represent a novel mechanism of nephrotoxicity by these agents.

References

[1] Crawford C, Kennedy-Lydon TM, Sprott, C, Desai T, Munday J, Unwin RJ, Wildman SSP, Peppiatt-Wildman CM. An intact kidney slice model to investigate vasa recta properties and function *in situ*. *Neph Physiol.* 2012;120(3):17-31.

MRC Medical Research Council Leading science for better health

This work was funded by The Medical Research Council and University of Kent, UK

Poster 3

281

Imaging of Luminal Perfused Vasa Recta Capillaries Enhances Understanding of Pericyte-Mediated Control of Medullary Blood Flow

Mark Kelly[1], Gary Mabbutt[1], Scott SP Wildman[1], Claire M Peppiatt-Wildman[1]

[1]Medway School of Pharmacy, Universities of Kent and Greenwich, Chatham, Kent, United Kingdom.

Introduction

- Renal medullary blood flow is one of the most inaccessible microcirculatory systems to accurately measure or image *in vivo* .
- Therefore it has been been previously hypothesised that renal medullary blood flow was at the control of the arteries and pre-capillary arterioles and it was the pressure generated from these structures that drove medullary perfusion and changes in osmotic gradients.
- *In vitro* studies using the isolated perfused descending vasa recta (DVR) technique have proposed local systemic factors including endothelins (ET), nitric oxide (NO) and angiotensin (ANG-II) may be involved in local regulation of blood flow.
- Contractile pericyte cells reside along descending vasa recta capillaries and respond to a variety of both endogenous and exogenous compounds to regulate vessel diameter and thus medullary blood flow (MBF) .
- Using the live kidney slice model pioneered in our lab, we have developed this model further to include luminal perfusion which enables an enhanced physiological setting to visualize *in situ* DVR and whether pericytes specifically act on vasa recta to modulate MBF.
- A reduction in MBF may result in regional ischemia that would would exacerbate additional tubular nephrotoxicity associated with these agents.

Methods

- Whole kidneys were isolated from ~ 250 g male Sprague Dawley rats, and 200 µm serial slices were collected as previously described.
- Slices were secured in a bath using a platinum "harp" and continually superfused with PSS, bubbled with O_2/CO_2.
- Vasa recta where perfused using glass pipettes, ID ~4-6µM, at varying pressures and flow
- Video imaging techniques were utilised to collect DIC images of pericytes on vasa recta and were analysed off-line using ImageJ software. Data were compared using a paired Student's t-test and unpaired t-test where appropriate.

Results

1. Effect of ANG II perfusion on *in situ* vasa recta

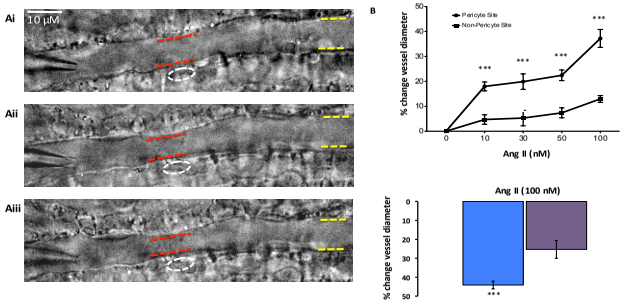

Figure 1. Luminal perfusion of *in situ* vasa recta with Ang II evoked pericyte-mediated vasoconstriction.
Ai-Aiii: DIC images of vasa recta taken from a time series experiment in which live kidney slices were perfused with Ang II (50 nM). Vessel diameter was measured every 5 s throughout the experiment at a pericyte site (red lines) and a corresponding non-pericyte site (yellow lines). Pericyte is highlighted (white oval). **B**: Mean data of perfused Ang II shows significant change in vessel diameter at pericyte site compared to non-pericyte sites. **C: :** Bar graph shows mean data for the ANG II-induced change in vessel diameter following luminal perfusion (blue bar) and bath superfusion (purple bar) at pericyte sites, no significant change in diameter was measured at non-pericyte sites. n>8 slices, > 8 animals. Values are means ± SEM, *** P<0.001

2. Determining the effect perfusion pressure has on flow rate and vessel contractility

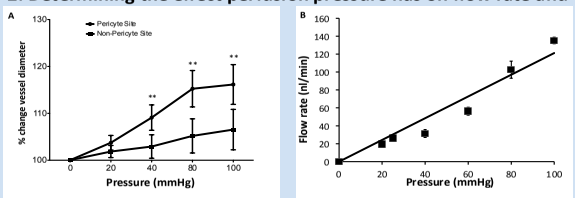

Figure 2. Altering the lunimal perfusion pressure effects flow rate and pericyte-mediated vasoconstriction.
A: Increasing pressure of perfused *in situ* vasa recta, 0-100 mmHg, produced a greater % vessel diameter at pericyte sites compared to non-pericyte sites. **B:** Individual vasa recta were perfused with PSS at varying pressures, 20-100 mmHg, to determine luminal perfusion rate. n = 8 slices, = 8 animals. Values are means ± SEM, **P<0.01.

Results

3. Luminal perfusion of *in situ* vasa recta with ET-1 induced an enhanced pericyte-mediated constriction when compared with superfusion-mediated changes in vessel diameter.

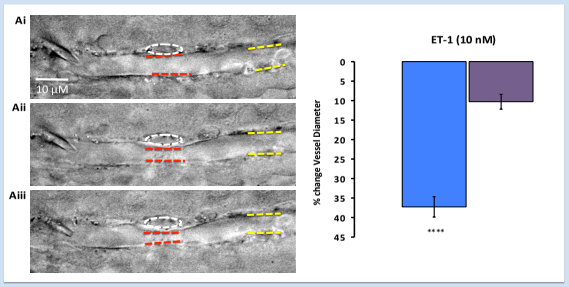

Figure 3. The effect of perfused ET-1 on *in situ* vasa recta diameter.
Ai-Aiii: DIC images of vasa recta taken from a time series experiment in which live kidney slices were perfused with ET-1 (10 nM). Vessel diameter was measured every 5 s throughout the experiment at a pericyte site (red lines) and a corresponding non-pericyte site (yellow lines). Pericyte is highlighted (white oval). **B:** Bar graph shows mean data for the ET-1-induced change in vessel diameter following luminal perfusion (blue bar) and bath superfusion (purple bar) at pericyte sites, no significant change in diameter was measured at non-pericyte sites. n = 8 slices, = 8 animals. Values are means ± SEM, **** P<0.0001

4. Luminal perfusion of *in situ* vasa recta with Prostaglandin E2 (PGE_2) and S-Nitroso-N-acetylpenicillamine (SNAP) induced similar pericyte-mediated vasodilation when compared to superfusion-mediated changes in vessel diameter.

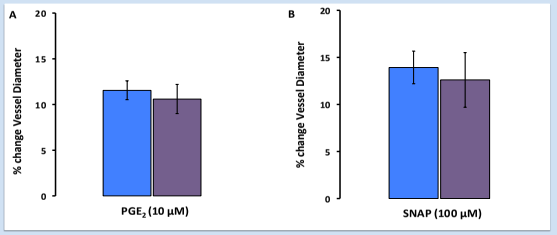

Figure 4: Luminal perfusion of *in situ* vasa recta with PGE_2 and SNAP induced pericyte-mediated dilation of vasa recta similar to that of superfusion. Bar graphs A and B show mean data for the PGE_2 and SNAP- induced change in vessel diameter respectively. Data shown is for changes in vessel diameter at pericyte sites following luminal perfusion (blue bar) and bath superfusion (purplebar), respectively, no significant change was observed at non-pericyte sites. n = 8 slices, = 8 animals Values are means ± SEM.

Conclusions

- **Increase of luminal pressure has a significant effect on vessel diameter of *in situ* vasa recta specifically at pericytes.**
- **Perfusion of single *in situ* vasa recta with ANG II & ET-1 evoked significant pericyte-mediated constriction of vessels.**
- **Perfusion of PGE_2 and SNAP evoked significant pericyte-mediated dilation of vessels which was similarly seen in superfusion.**
- ***In situ* perfusion of single vasa recta, via the live kidney slice model, offers for the first time almost complete physiological conditions to investigate pericytes as regulators of renal medullary blood flow.**

MRC Medical Research Council Leading science for better health

This work was funded by The Medical Research Council and University of Kent, UK